SOLARNET
Radiative transfer

Mats Carlsson
Institute of Theoretical Astrophysics
University of Oslo

- Basic concepts
- Formal solution
  - Numerical integration, scattering problem, lambda iteration, shooting, finite difference methods, Feautrier's method, accelerated lambda iteration, convergence acceleration
- non-LTE
  - Linearization, rate equations, Scharmer operator, local operator
- 3D
  - Long characteristics, short characteristics
- Energy equation
  - ODF, multi-group opacities

Examples

- Contribution & response functions
- non-Statistical equilibrium
- 3D simulations from convection zone to corona
- 3D radiative transfer
- IRIS
- Mg II diagnostics

- MULTI non-LTE code
- working with IRIS data
- public release of 3D models

- Hands on Session, radiative transfer
  - Na-D, Mg-b, Ca-H, Hinode BFI continua
  - getting input data - building atomic models
  - non-LTE effects for abundance determinations of stars
  - 3D column-by-column with MULTI
- Hands on Session, IRIS

Basic concepts

Basic definitions

I_ν Intensity. $\mathrm{erg\ cm^{-2}s^{-1}sr^{-1}Hz^{-1}}$

η_ν Emissivity

χ_ν Opacity

Intensity gives the amount of energy per unit area perpendicular to the ray in a given direction per unit time per solid angle and per frequency bin. The intensity is constant with distance in the absence of emission and absorption/scattering processes.

Emissivity gives the addition of energy to the ray through emission processes.

Opacity gives the removal of energy from the ray through absorption and scattering processes.

Transfer equation

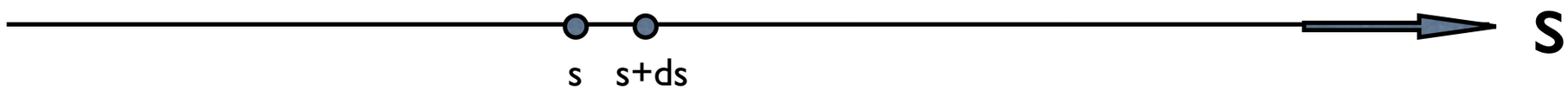

$$dI_\nu = -\chi_\nu I_\nu ds + \eta_\nu ds$$

Coronal approximation: $\chi_\nu = 0$

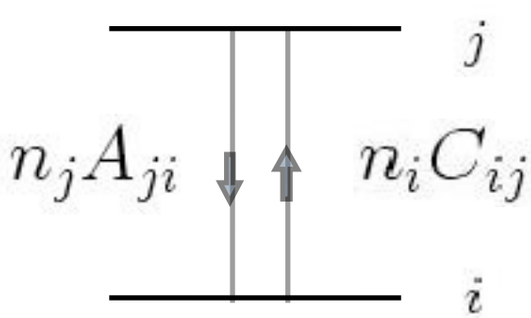

$$\eta_\nu = \frac{h\nu}{4\pi} n_j A_{ji}$$

$$n_j A_{ji} = n_i C_{ij}$$

Emissivity and rates set by local conditions.

Transfer equation

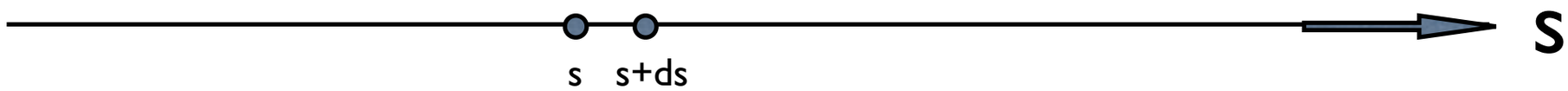

$$dI_\nu = -\chi_\nu I_\nu ds + \eta_\nu ds$$

Opacity non-zero case

$$d\tau_\nu \equiv \chi_\nu ds \quad S_\nu \equiv \frac{\eta_\nu}{\chi_\nu}$$

$$\frac{dI_\nu}{d\tau_\nu} = S_\nu - I_\nu$$

Transfer equation

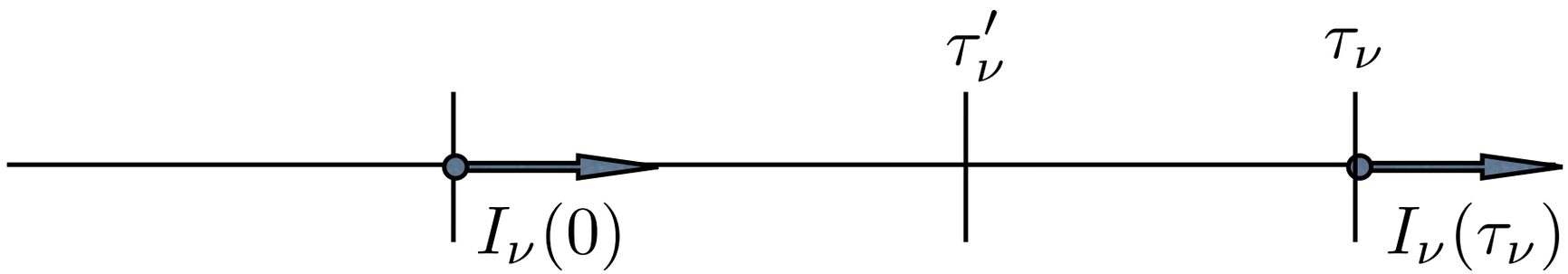

$$I_\nu(\tau_\nu) = I_\nu(0)e^{-\tau_\nu} + \int_0^{\tau_\nu} S_\nu(\tau'_\nu)e^{-(\tau_\nu - \tau'_\nu)}d\tau'_\nu$$

Homogeneous slab, small optical depth:

$$I_\nu(\tau_\nu) = I_\nu(0) + \tau_\nu(S_\nu - I_\nu(0))$$

Intensity (wavelength dependent!) is then an interpolation between the incoming intensity and the source function and thus always between the two. For I(0)>S we get an absorption line, for I(0)<S we get an emission line.

Homogeneous slab

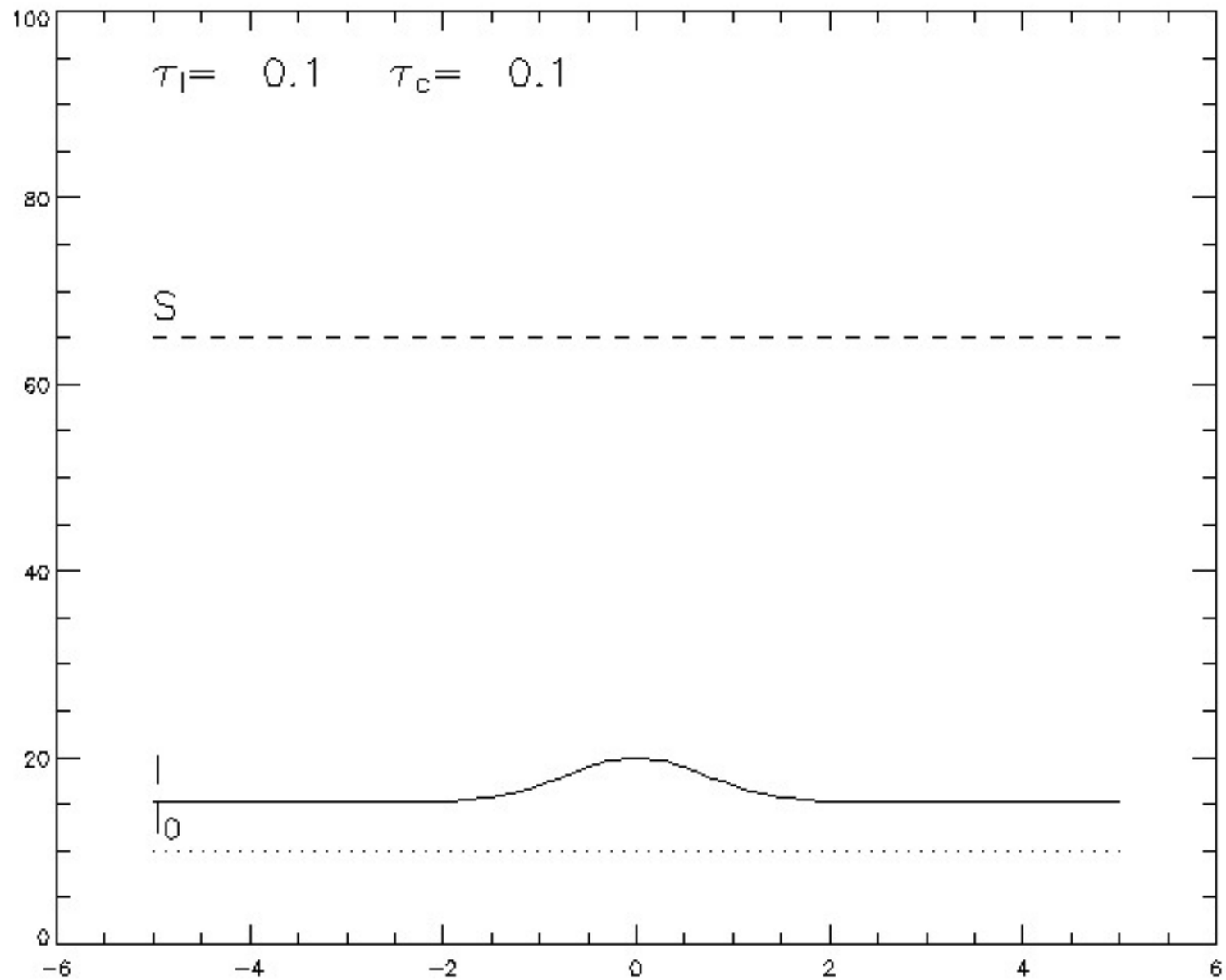

Homogeneous slab

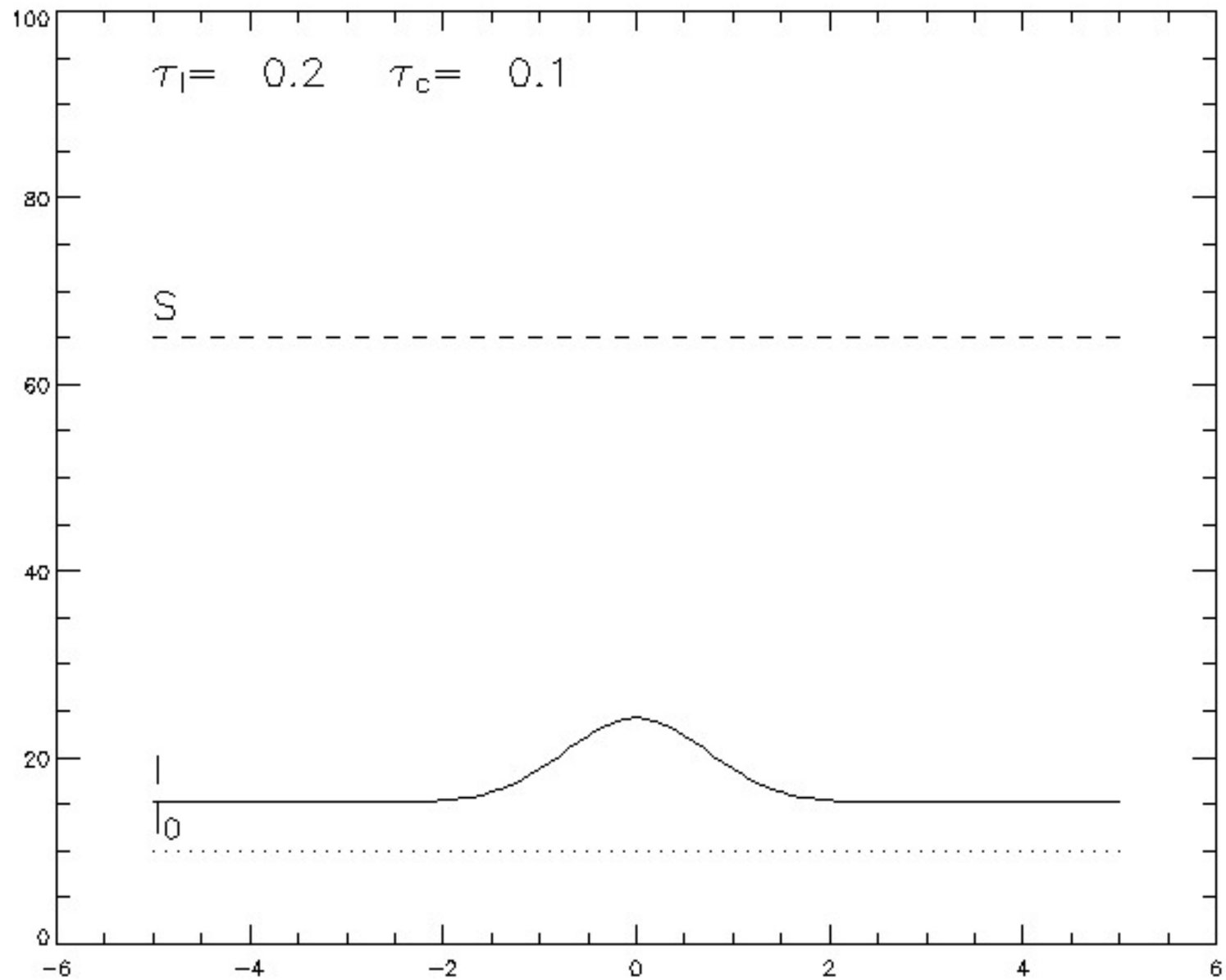

Homogeneous slab

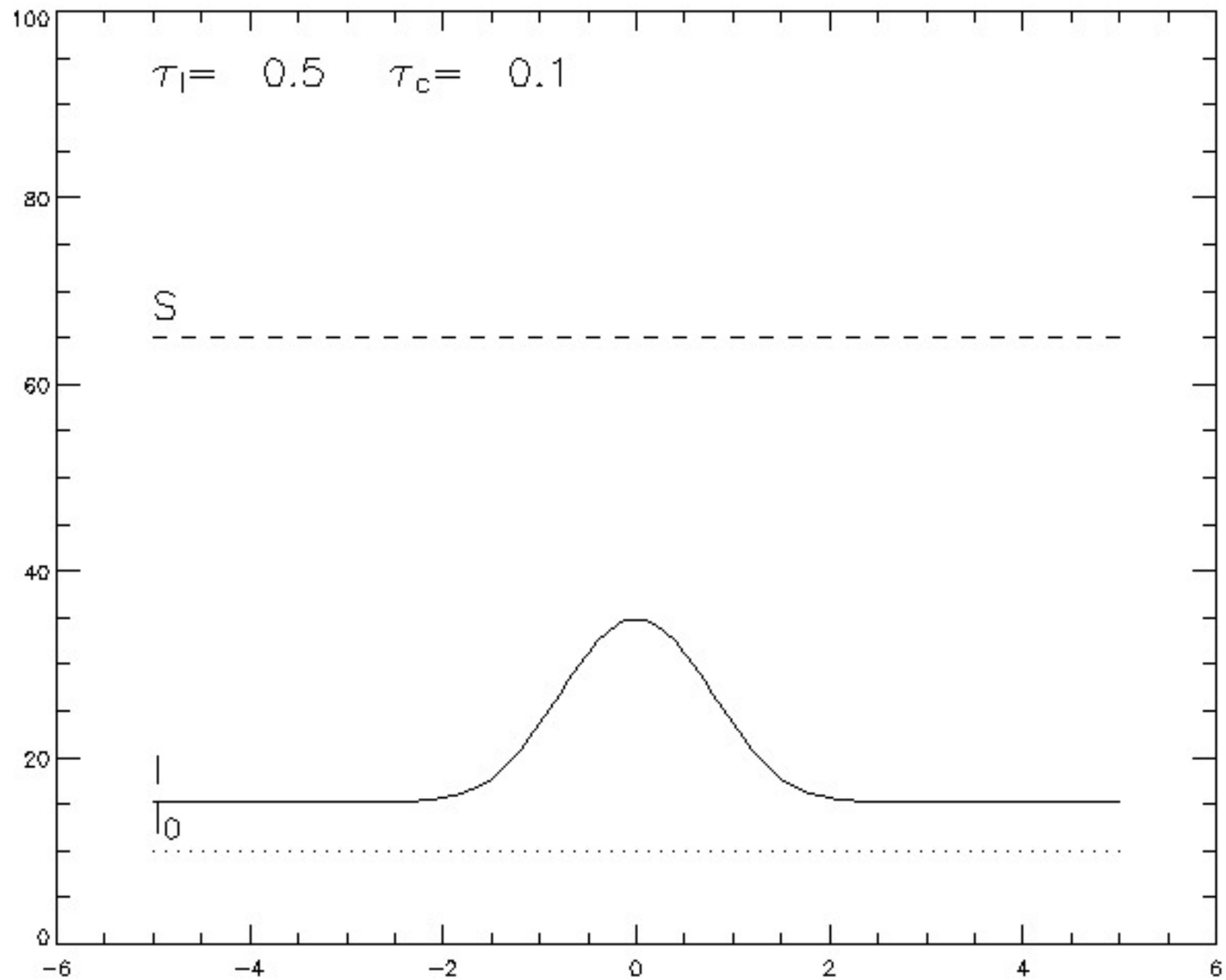

Homogeneous slab

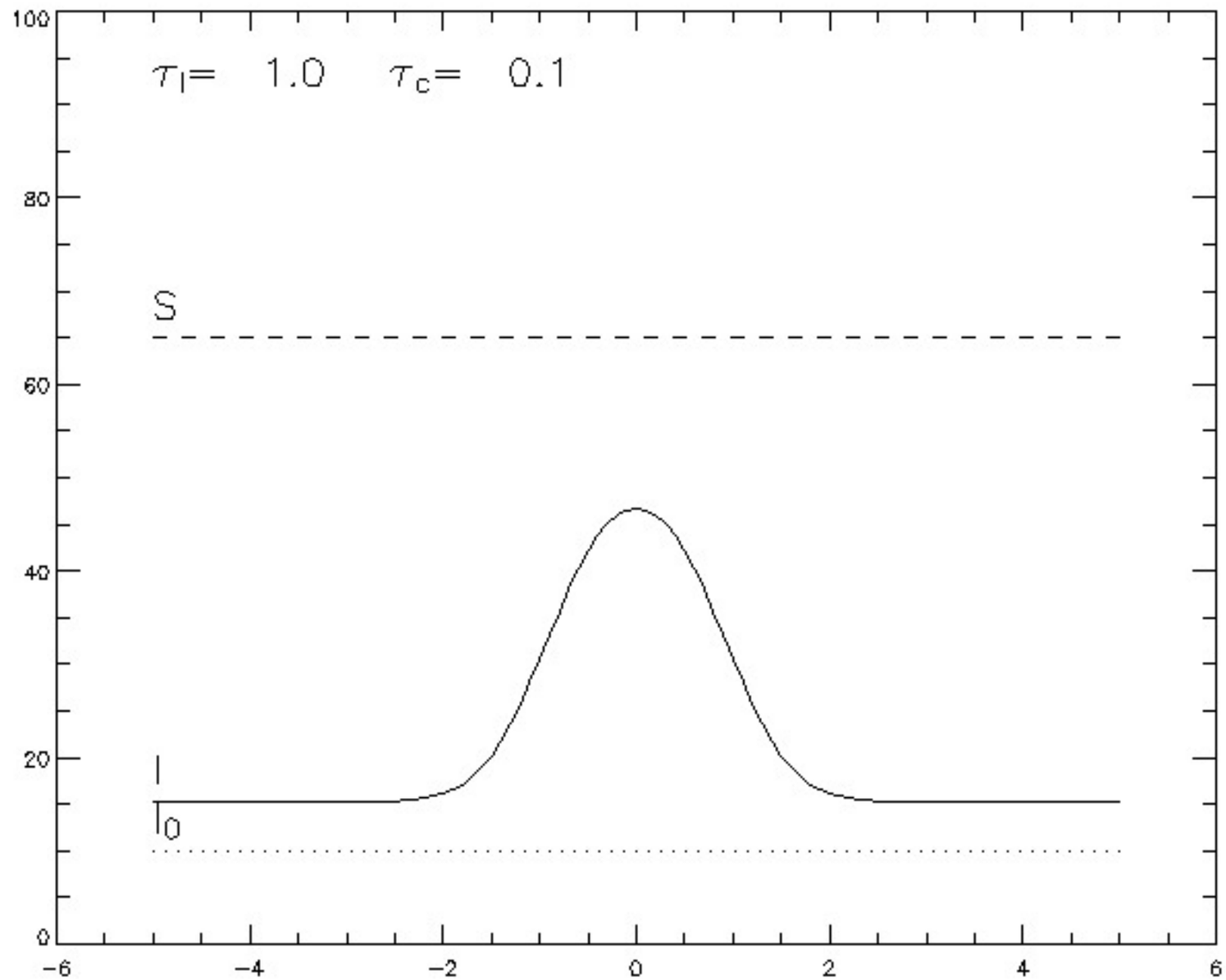

Homogeneous slab

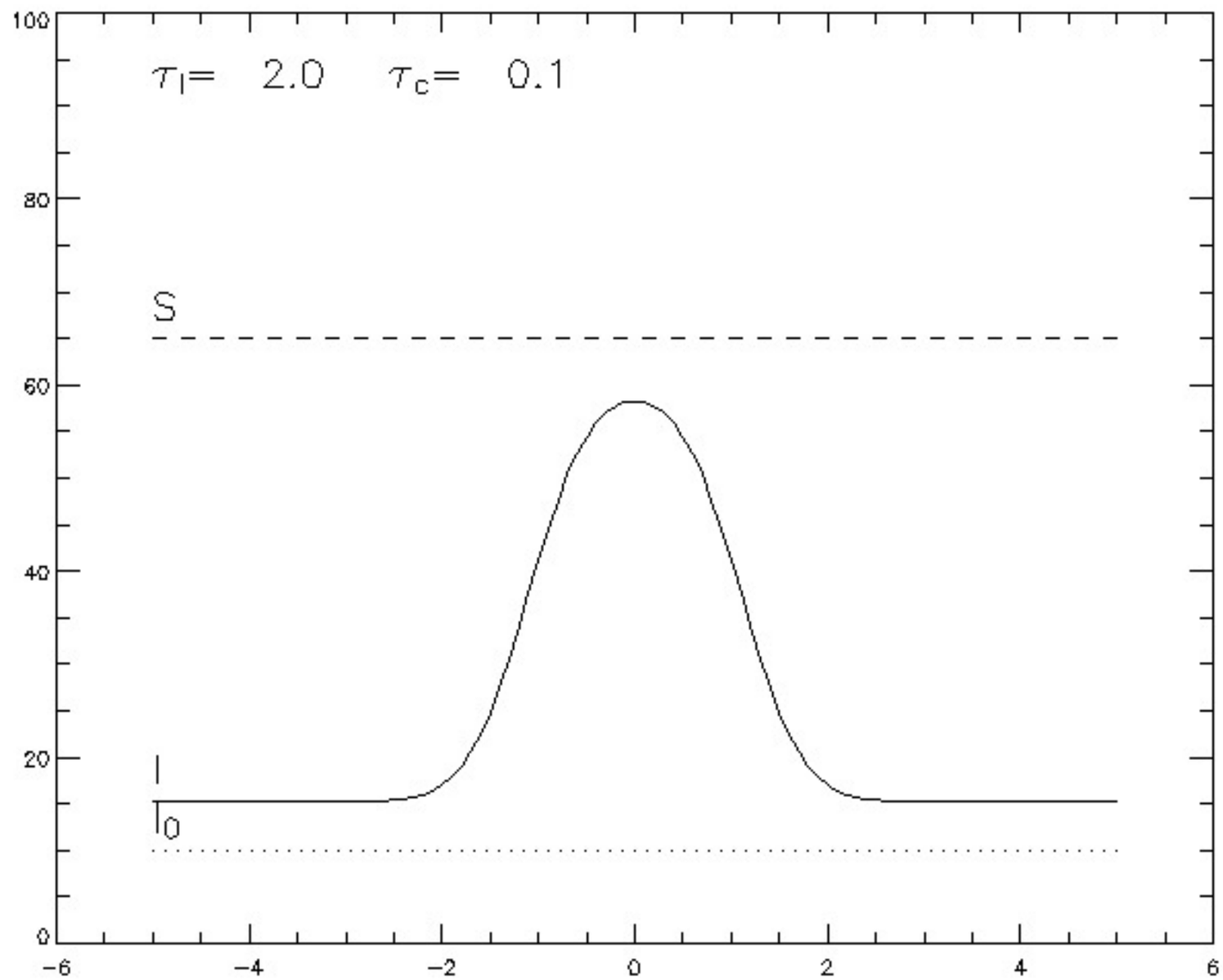

Homogeneous slab

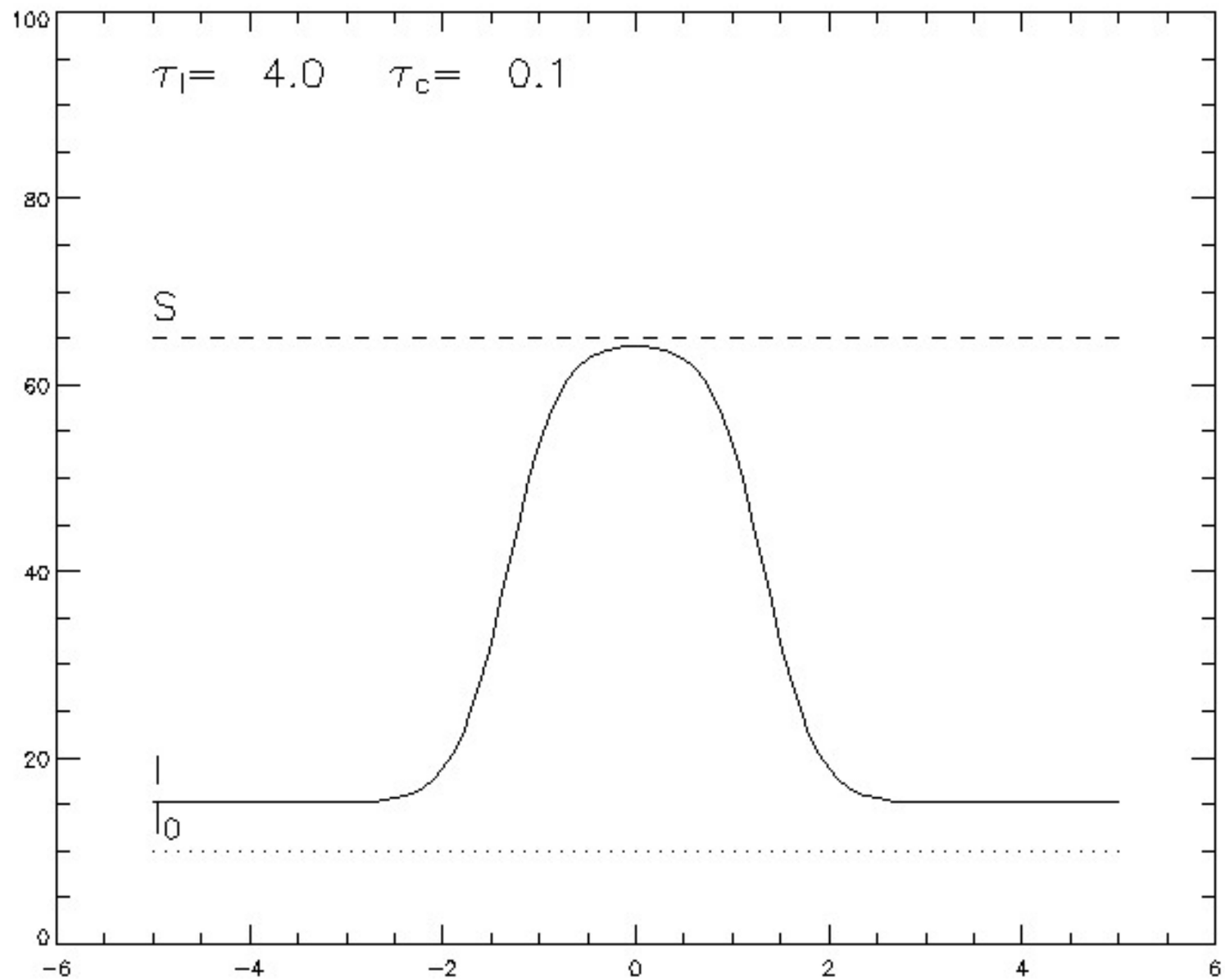

Homogeneous slab

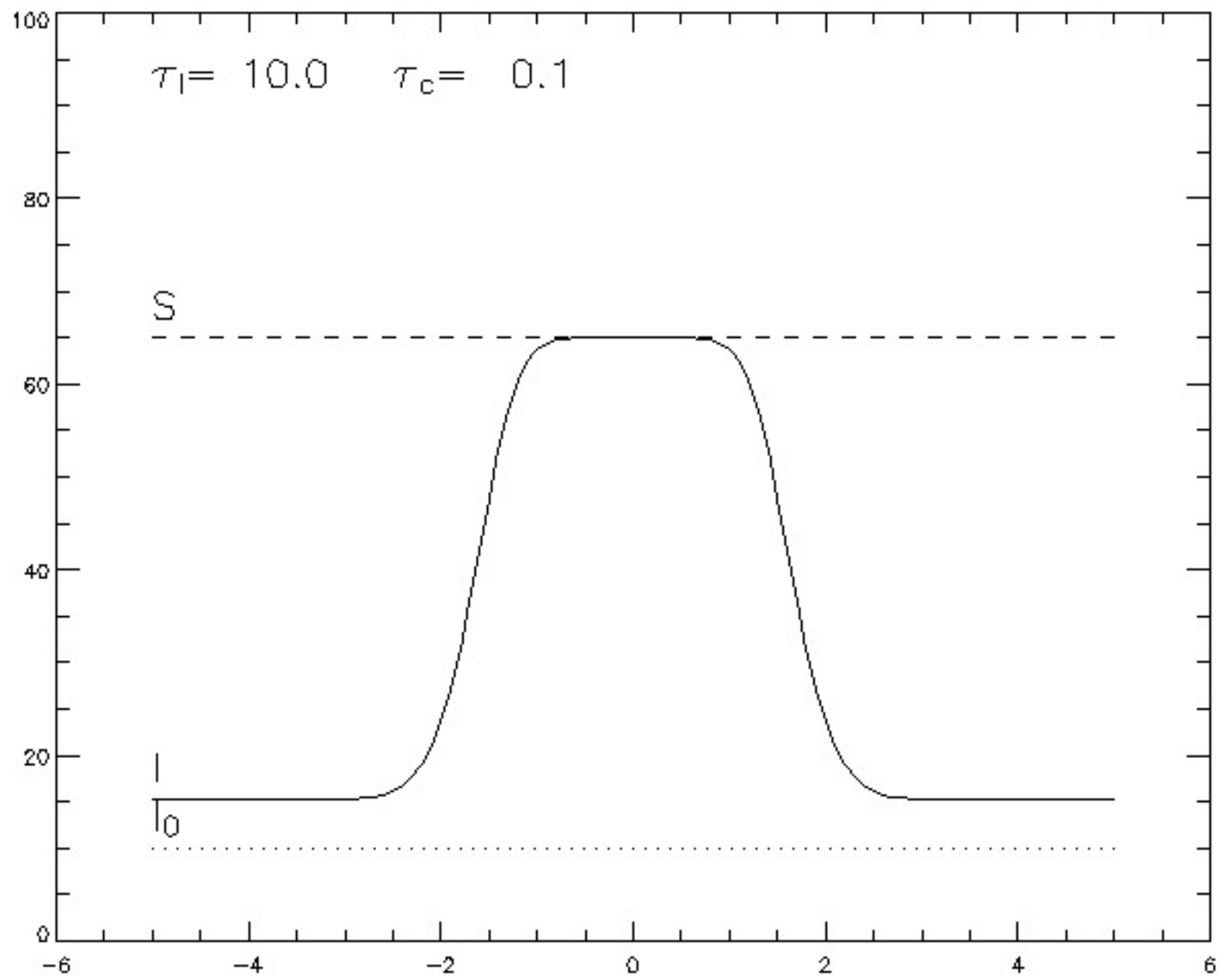

Homogeneous slab

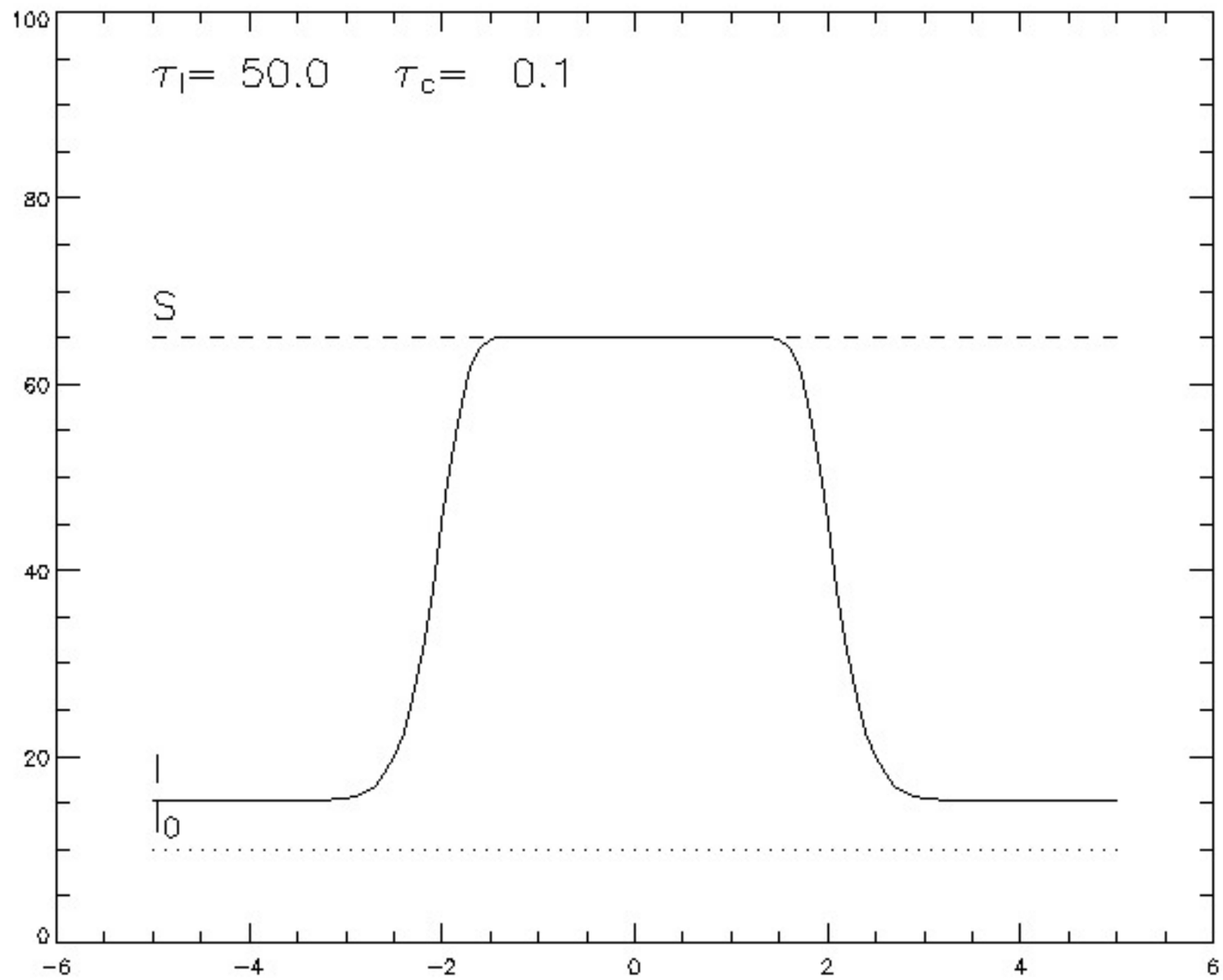

Homogeneous slab

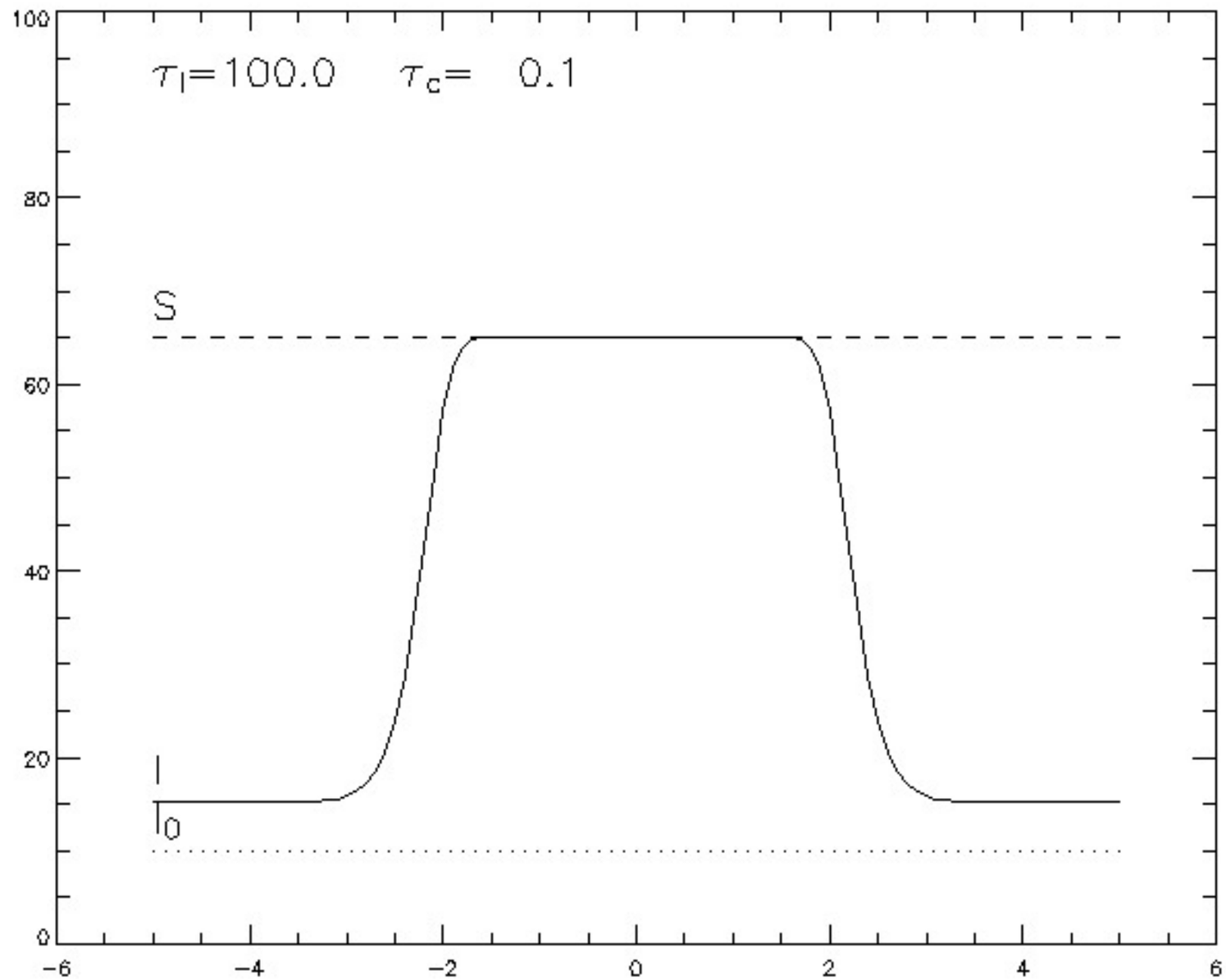

Transfer equation

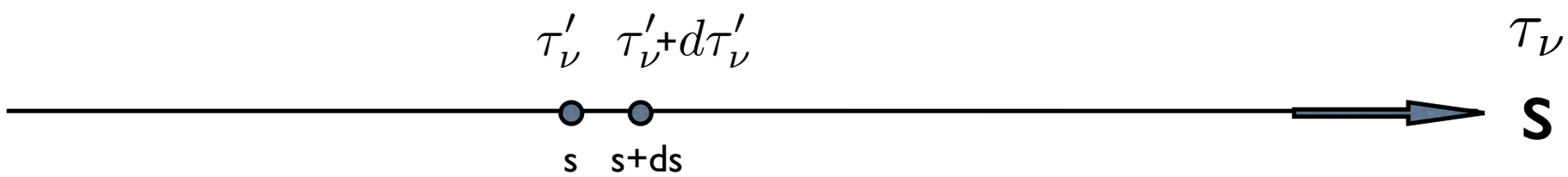

$$I_\nu(\tau_\nu) = I_\nu(0)e^{-\tau_\nu} + \int_0^{\tau_\nu} S_\nu(\tau'_\nu)e^{-(\tau_\nu - \tau'_\nu)}d\tau'_\nu$$

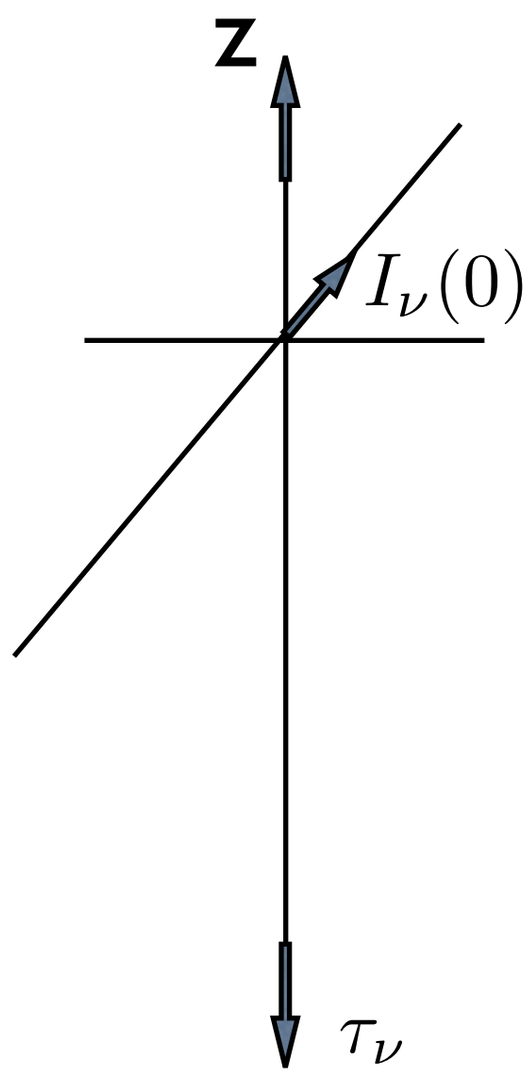

Semi-infinite atmosphere, 1D:

$$I_\nu(0) = \frac{1}{\mu}\int_0^\infty S_\nu(\tau'_\nu)e^{-\tau'_\nu/\mu}d\tau'_\nu$$

where mu is the cosine of the angle between the ray and the normal of the atmosphere

Eddington Barbier relation

Assuming a linear source function:

$$S_\nu(\tau'_\nu) = a + b\tau'_\nu$$

Gives a formal solution:

$$I_\nu(\tau_\nu, \mu) = S_\nu(\tau'_\nu = \tau_\nu + \mu)$$

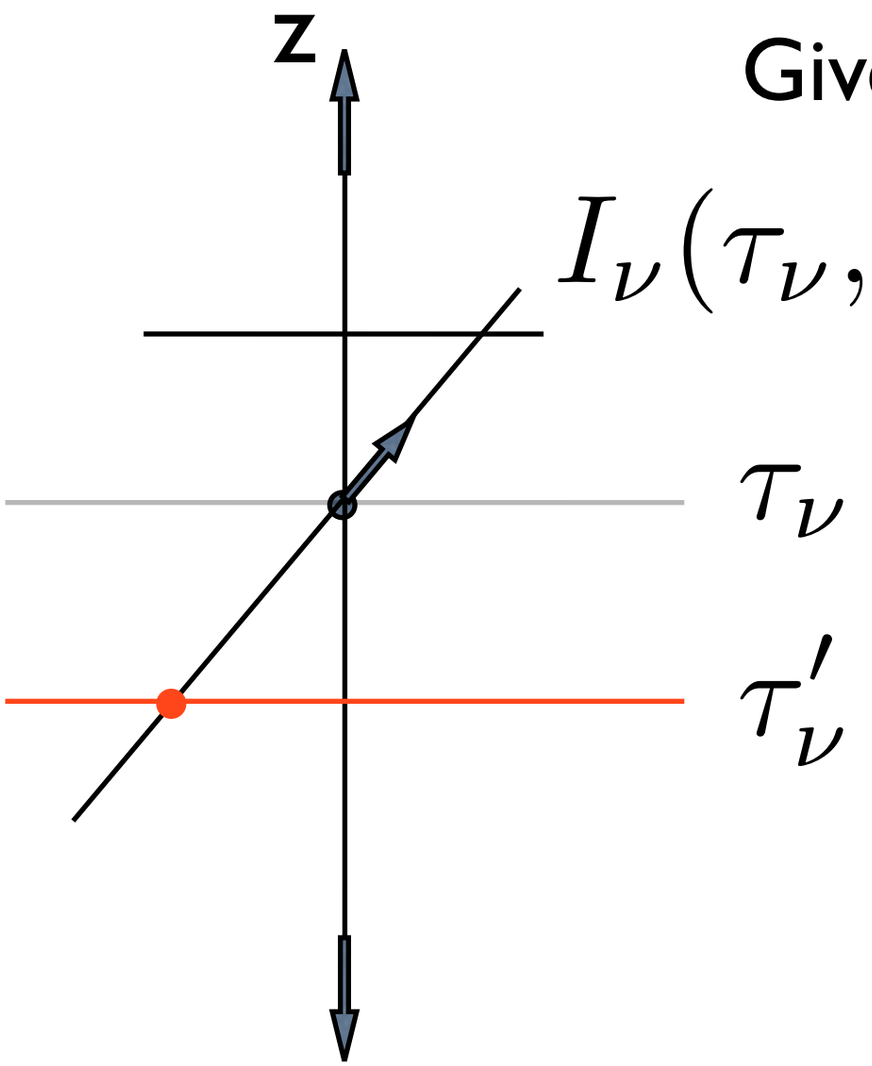

Optically thick line formation I

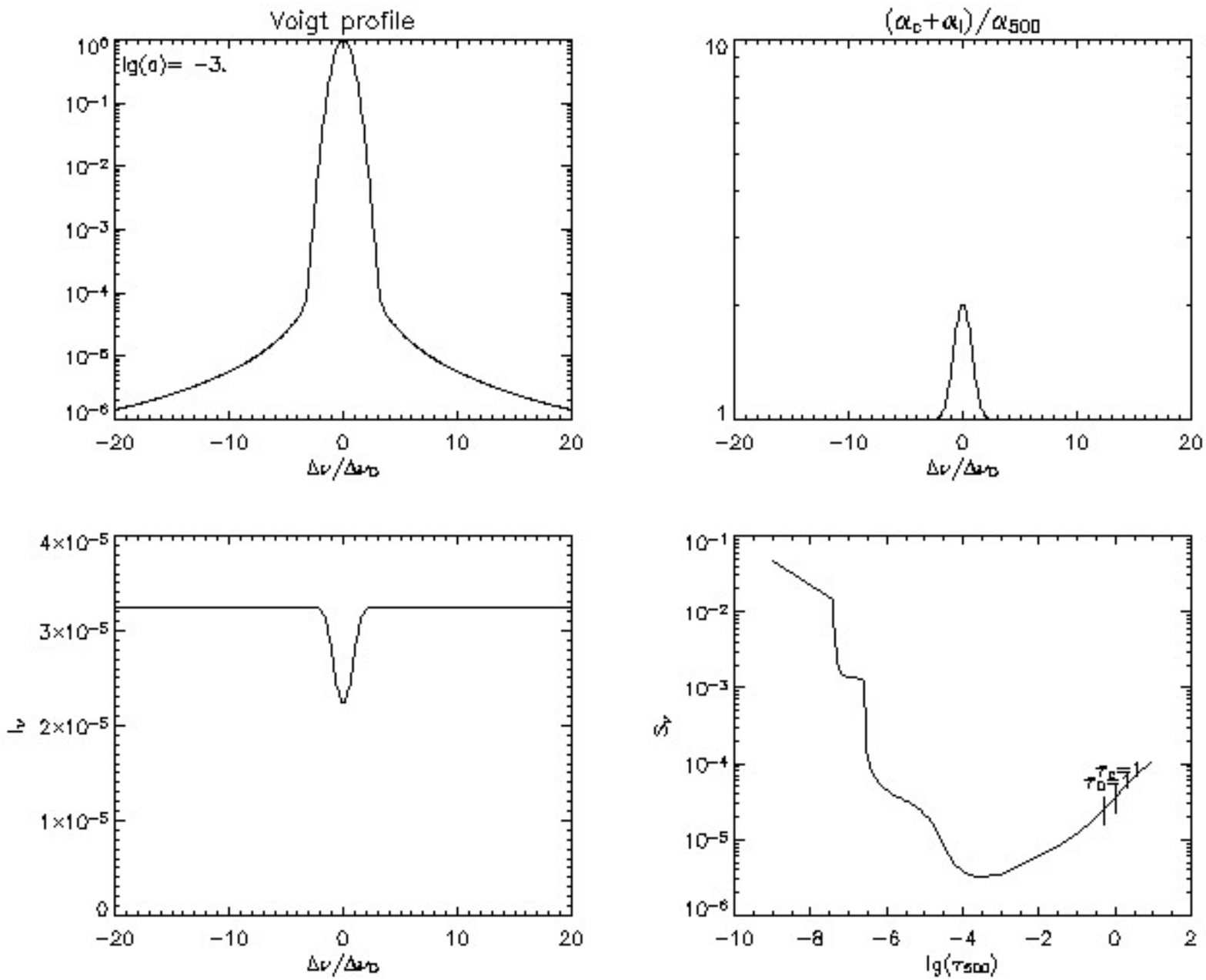

Optically thick line formation

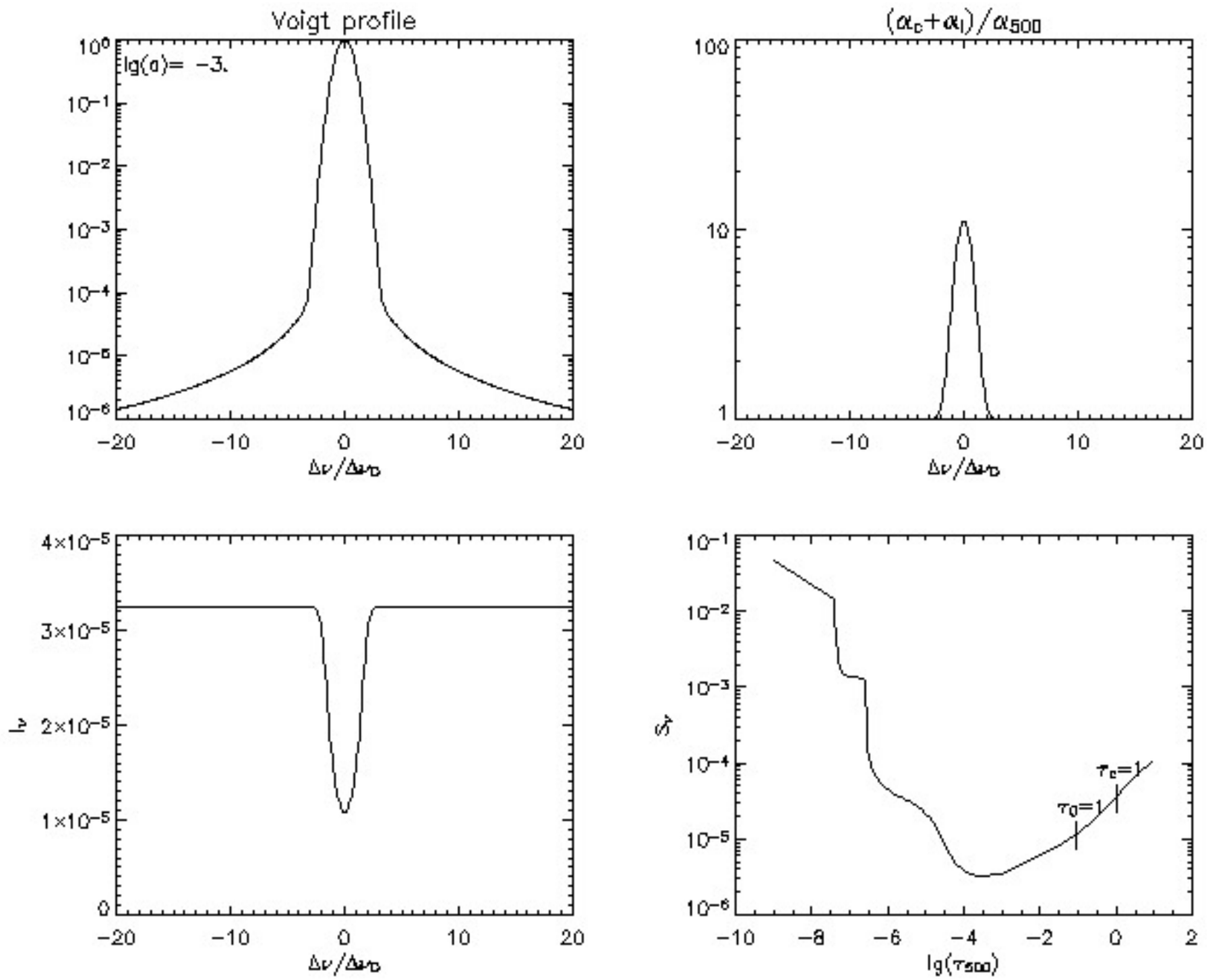

Optically thick line formation

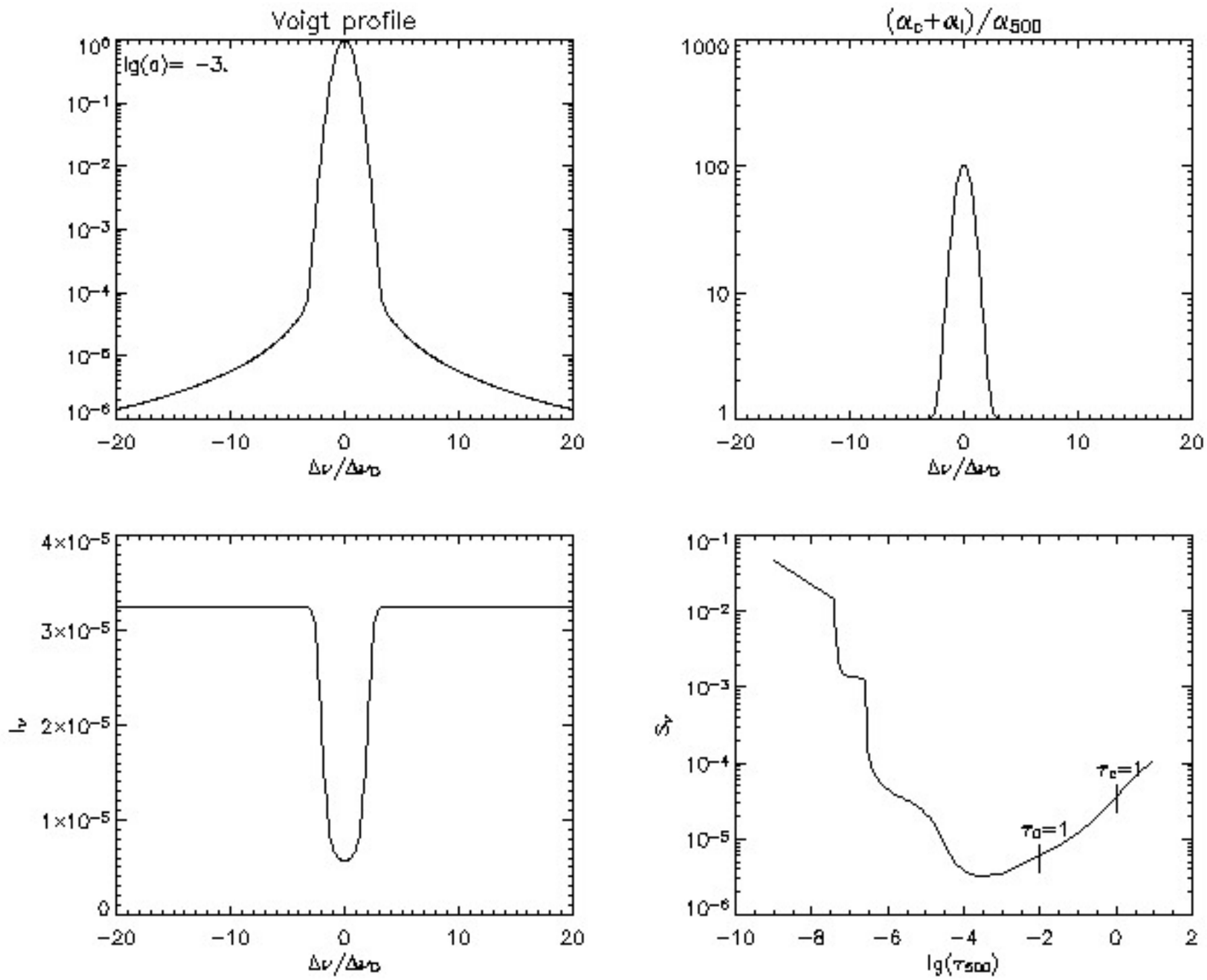

Optically thick line formation

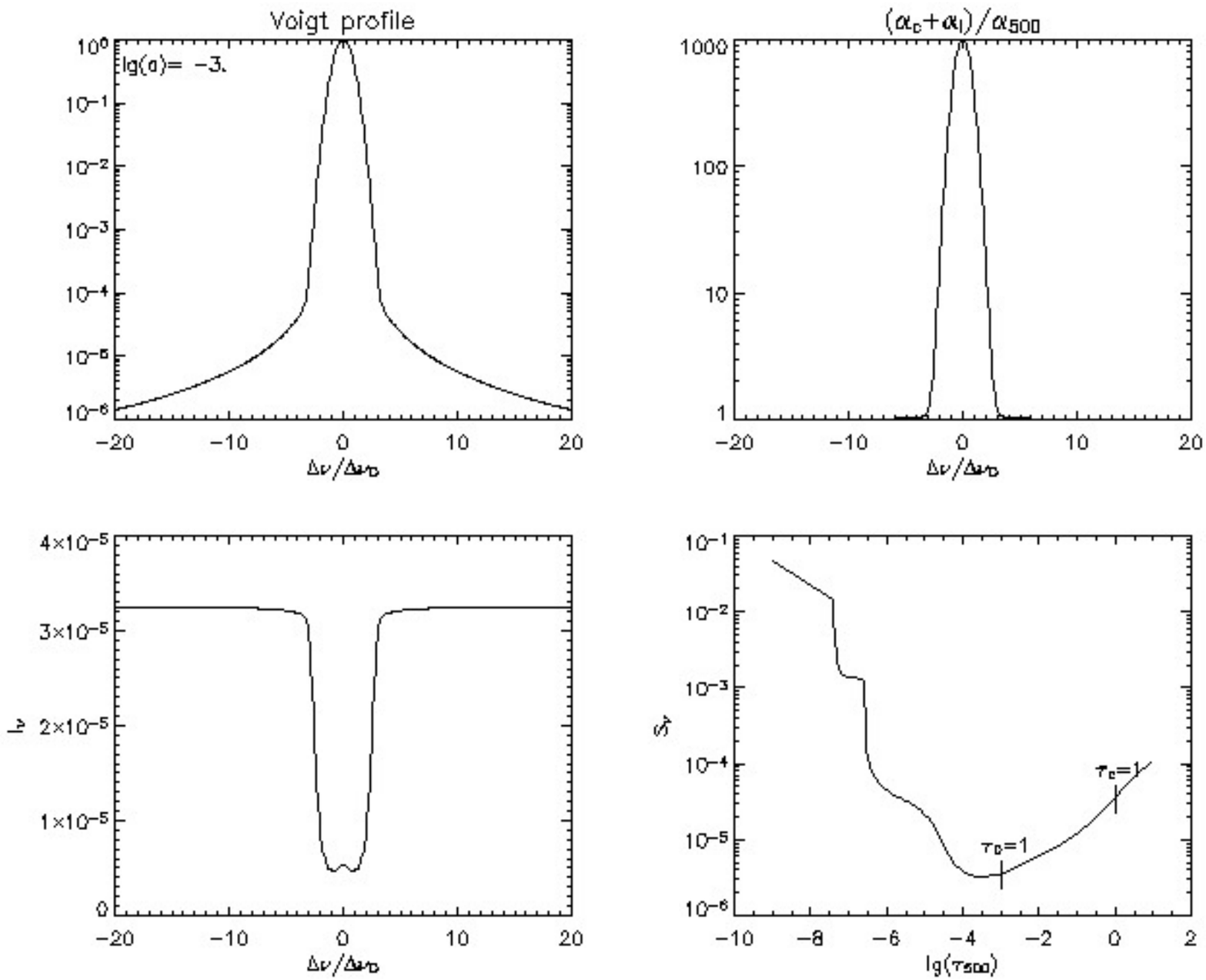

Optically thick line formation

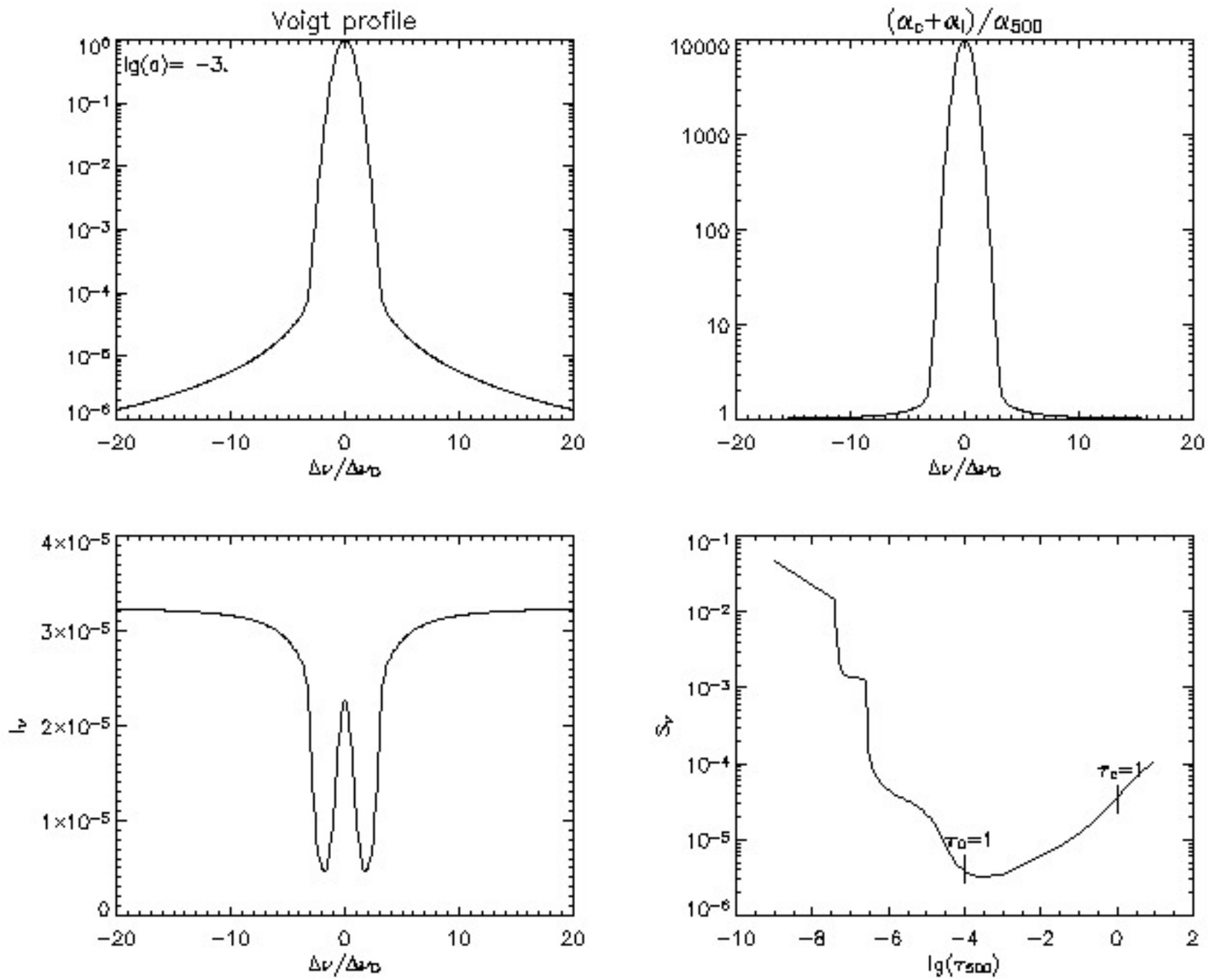

Optically thick line formation

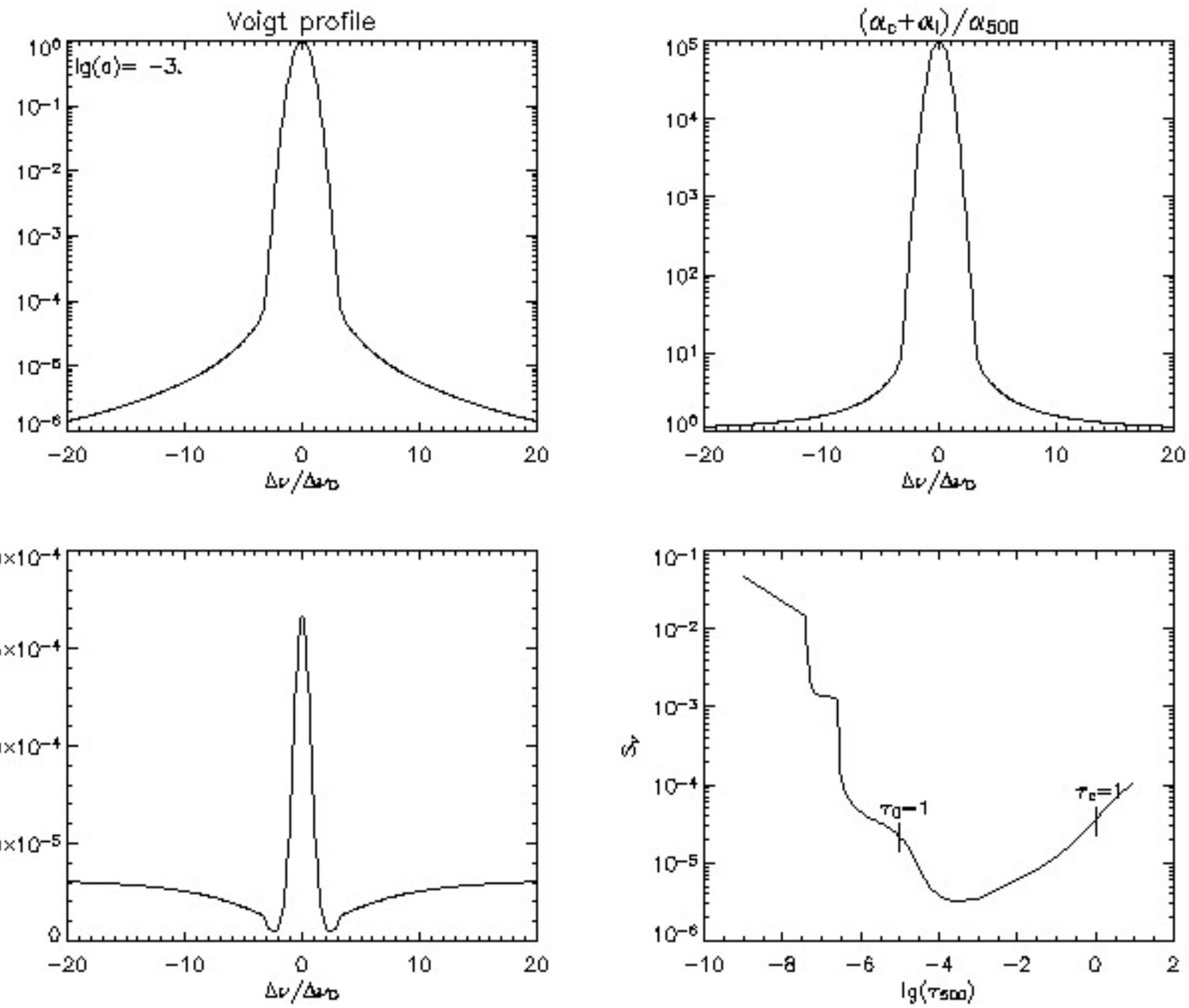

Optically thick line formation

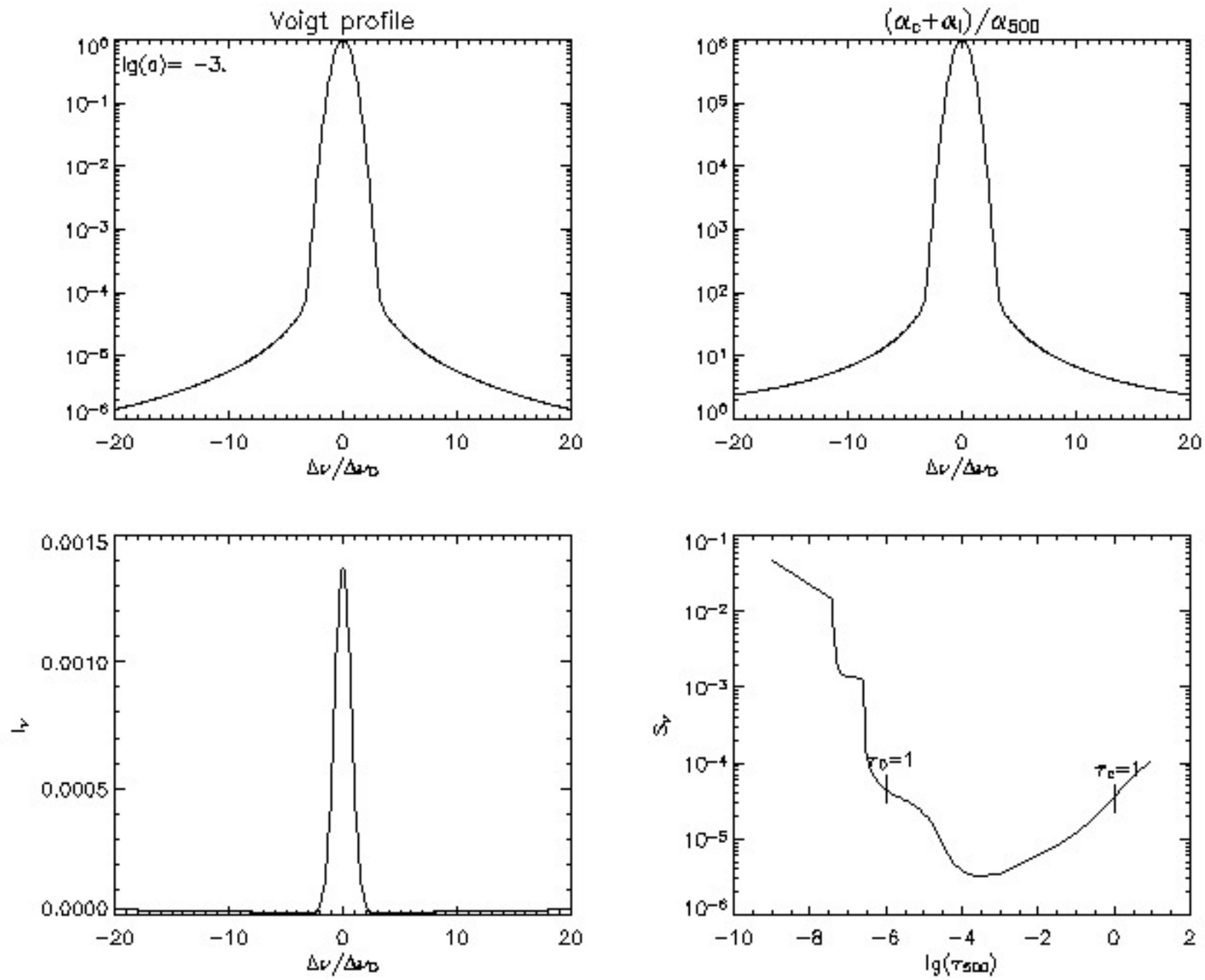

Optically thick line formation 2

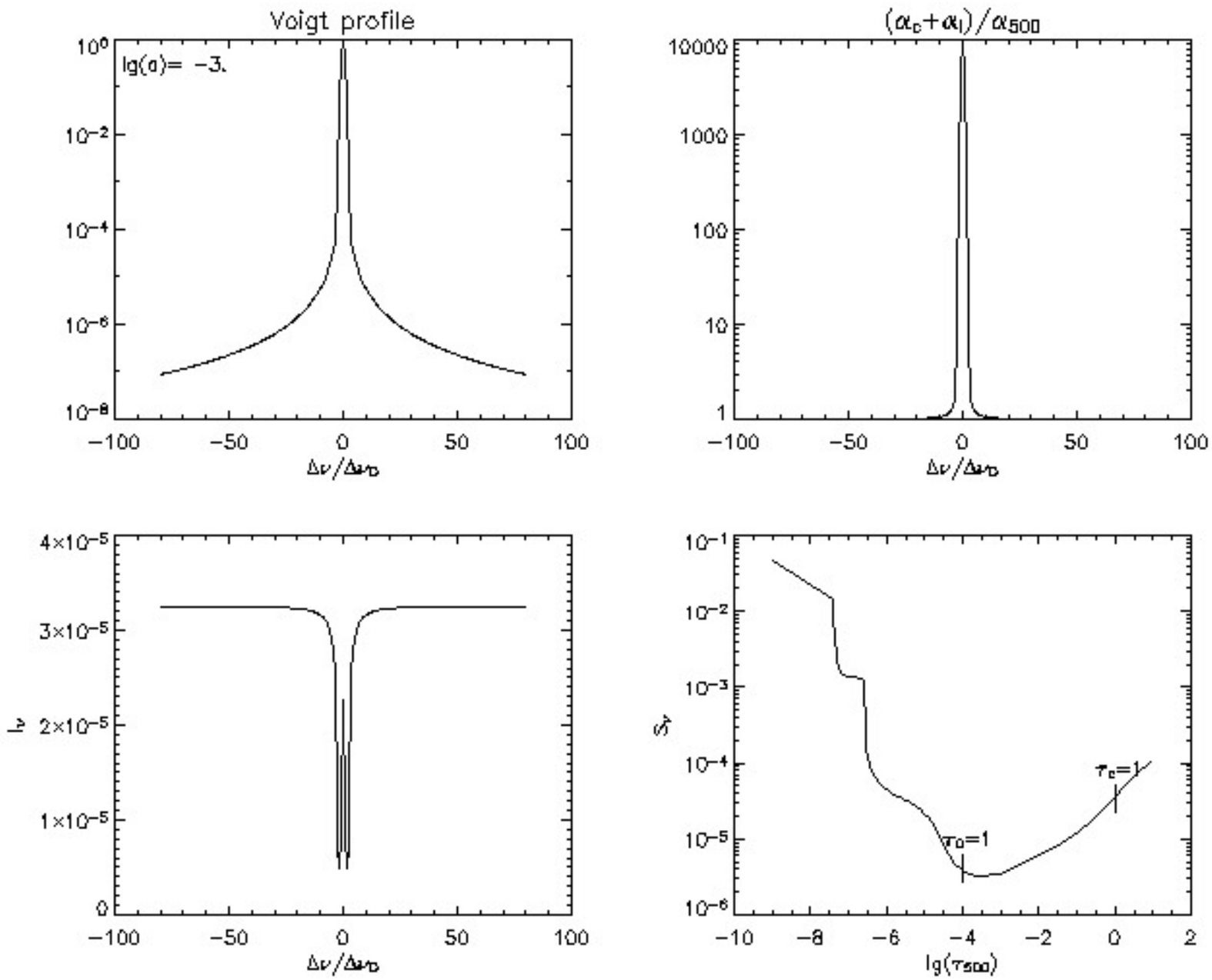

Optically thick line formation

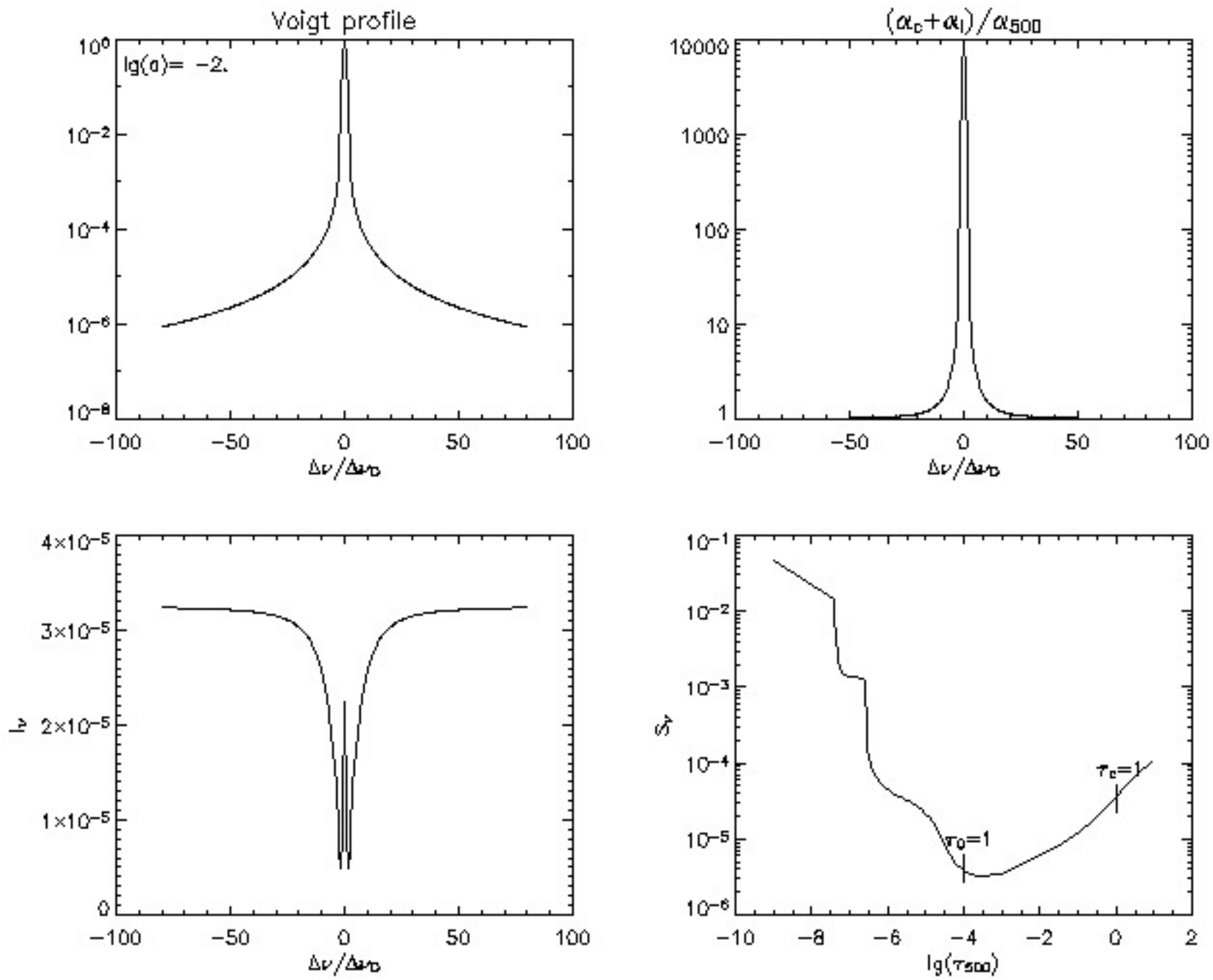

Optically thick line formation

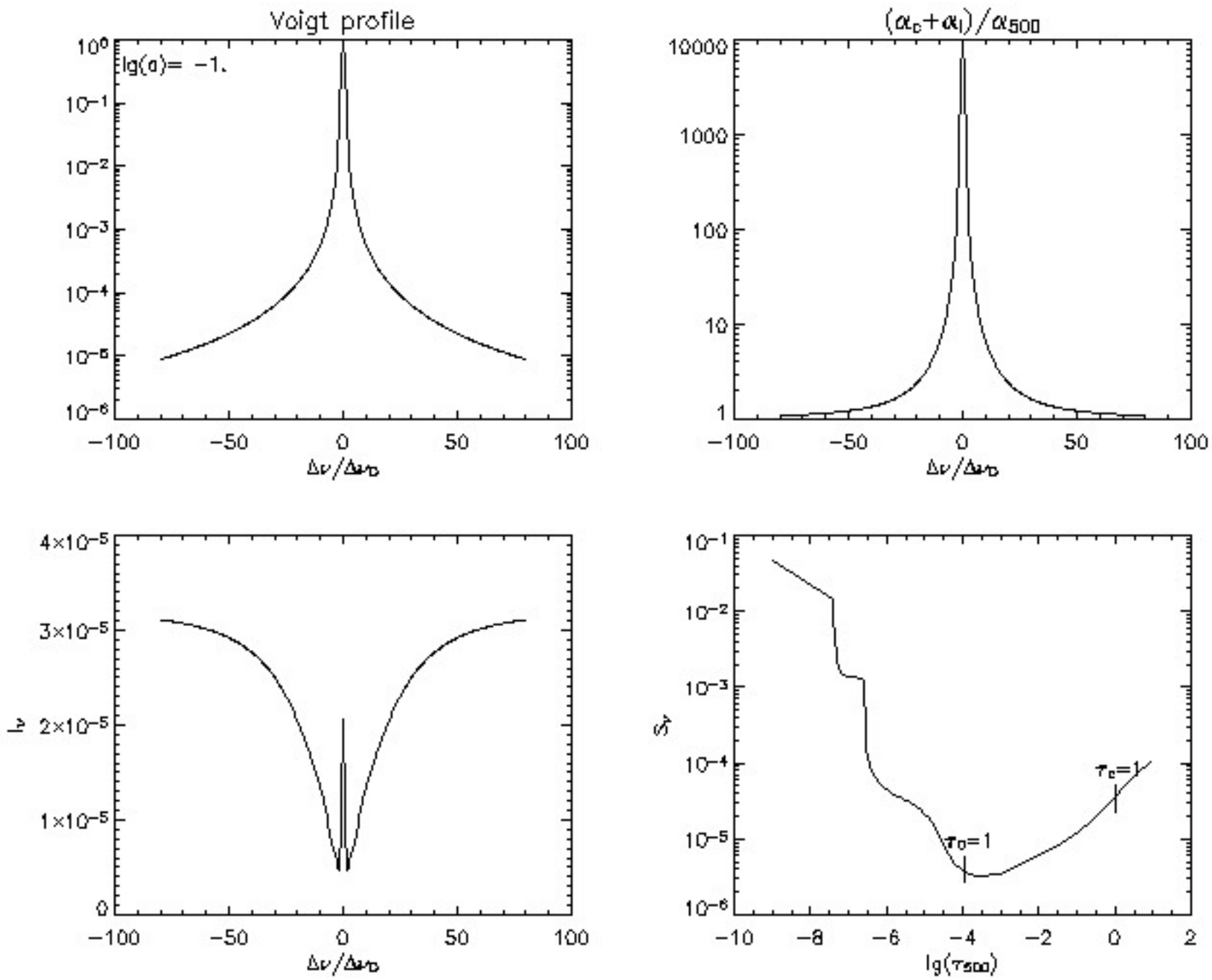

Optically thick line formation 3

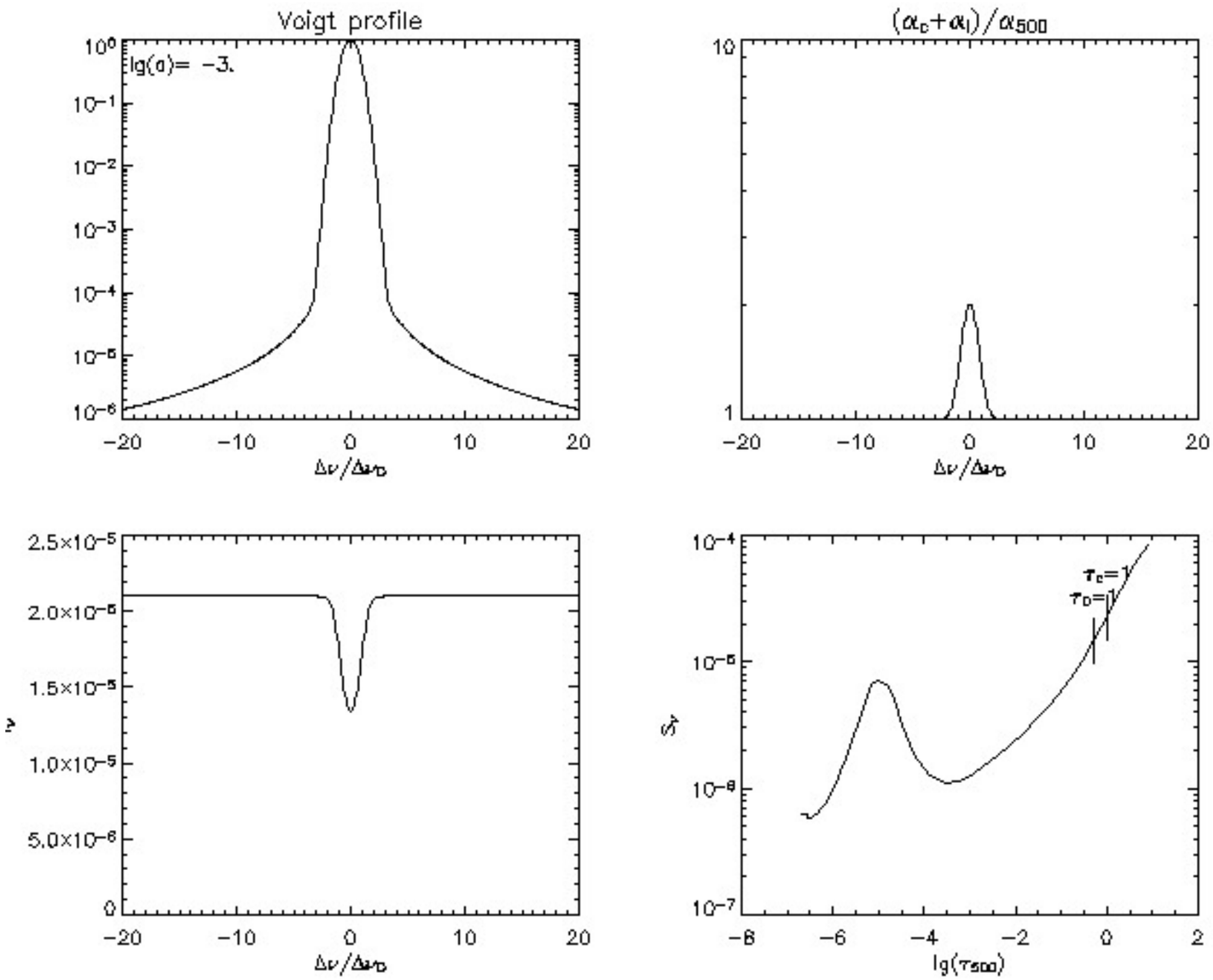

Optically thick line formation

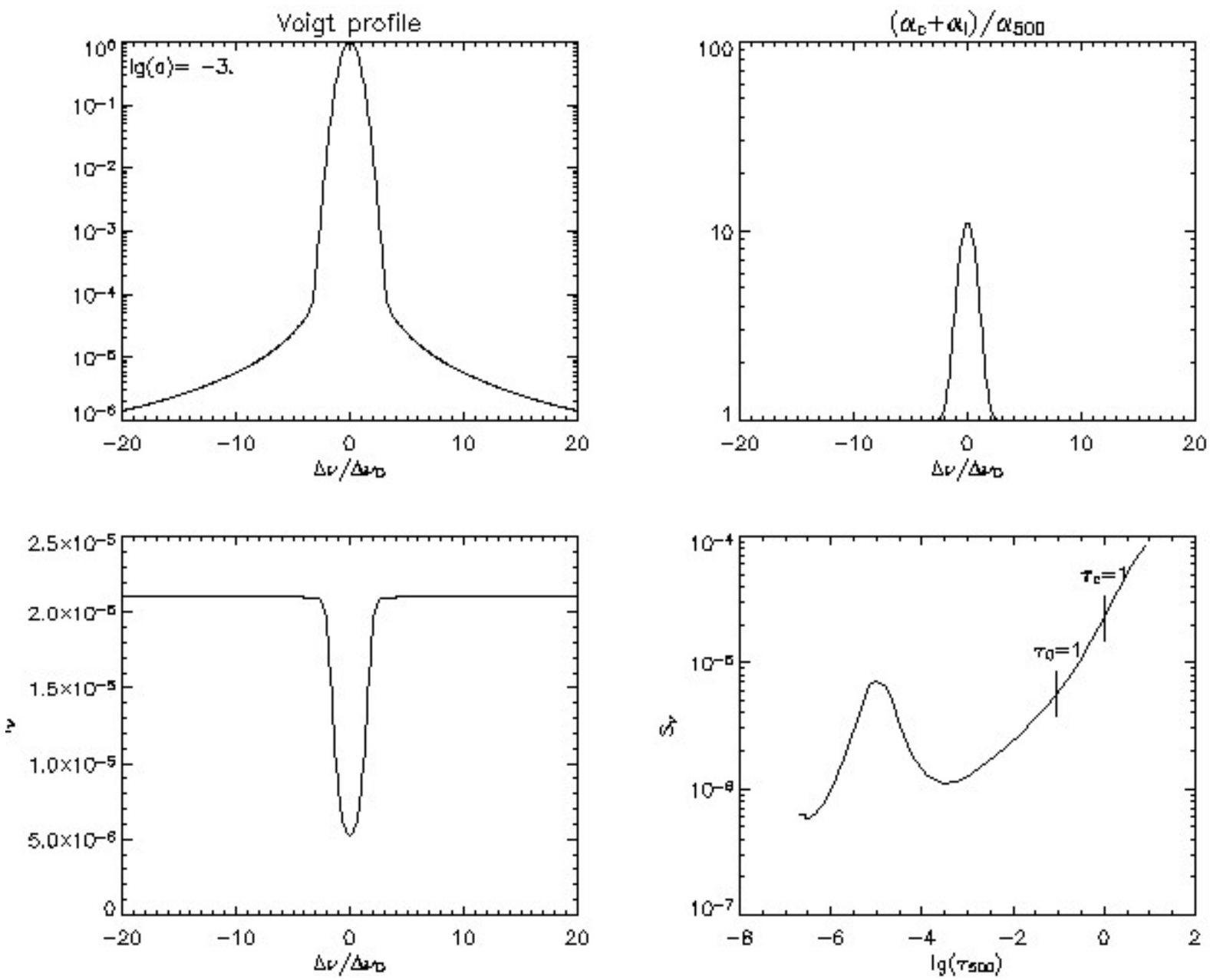

Optically thick line formation

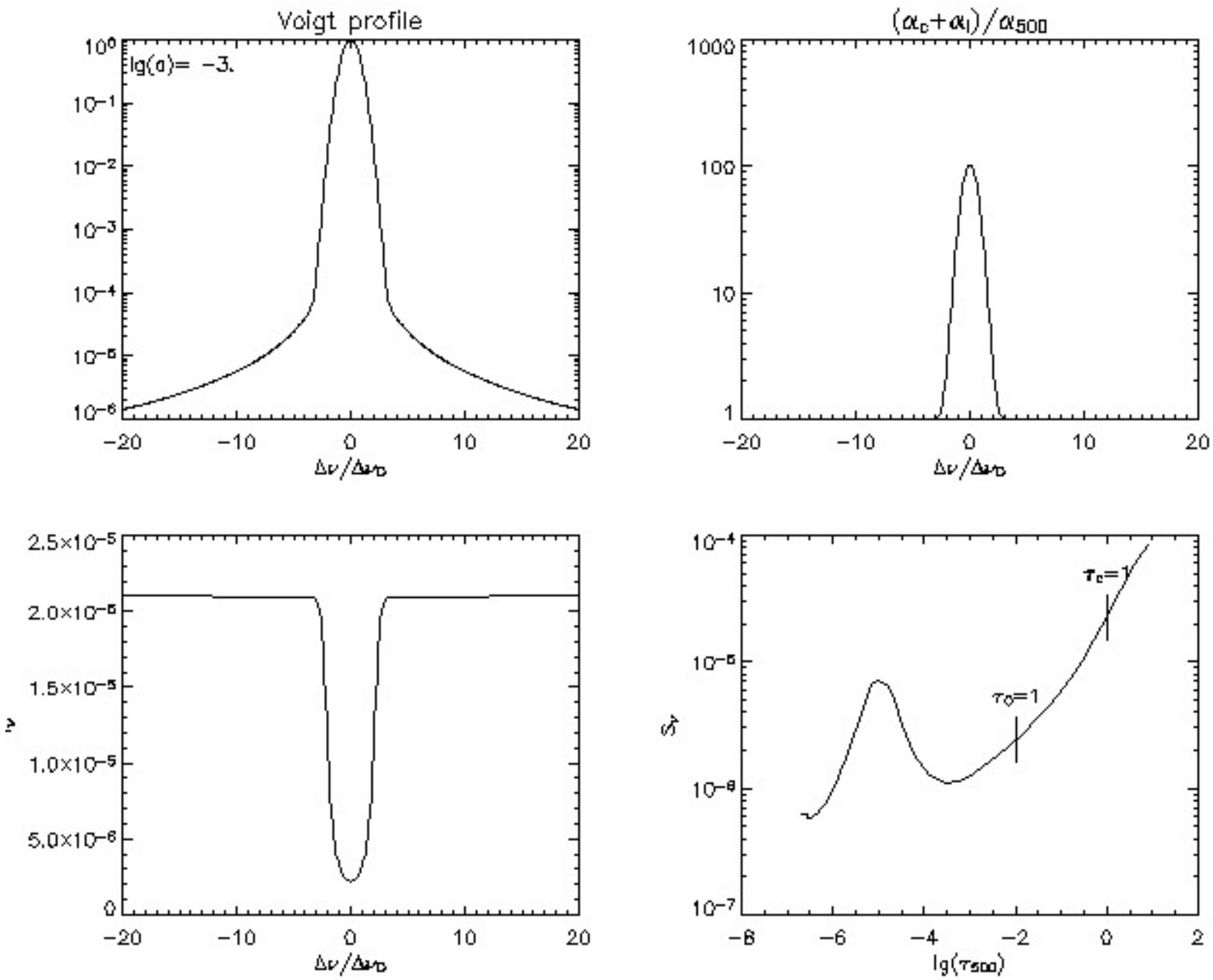

Optically thick line formation

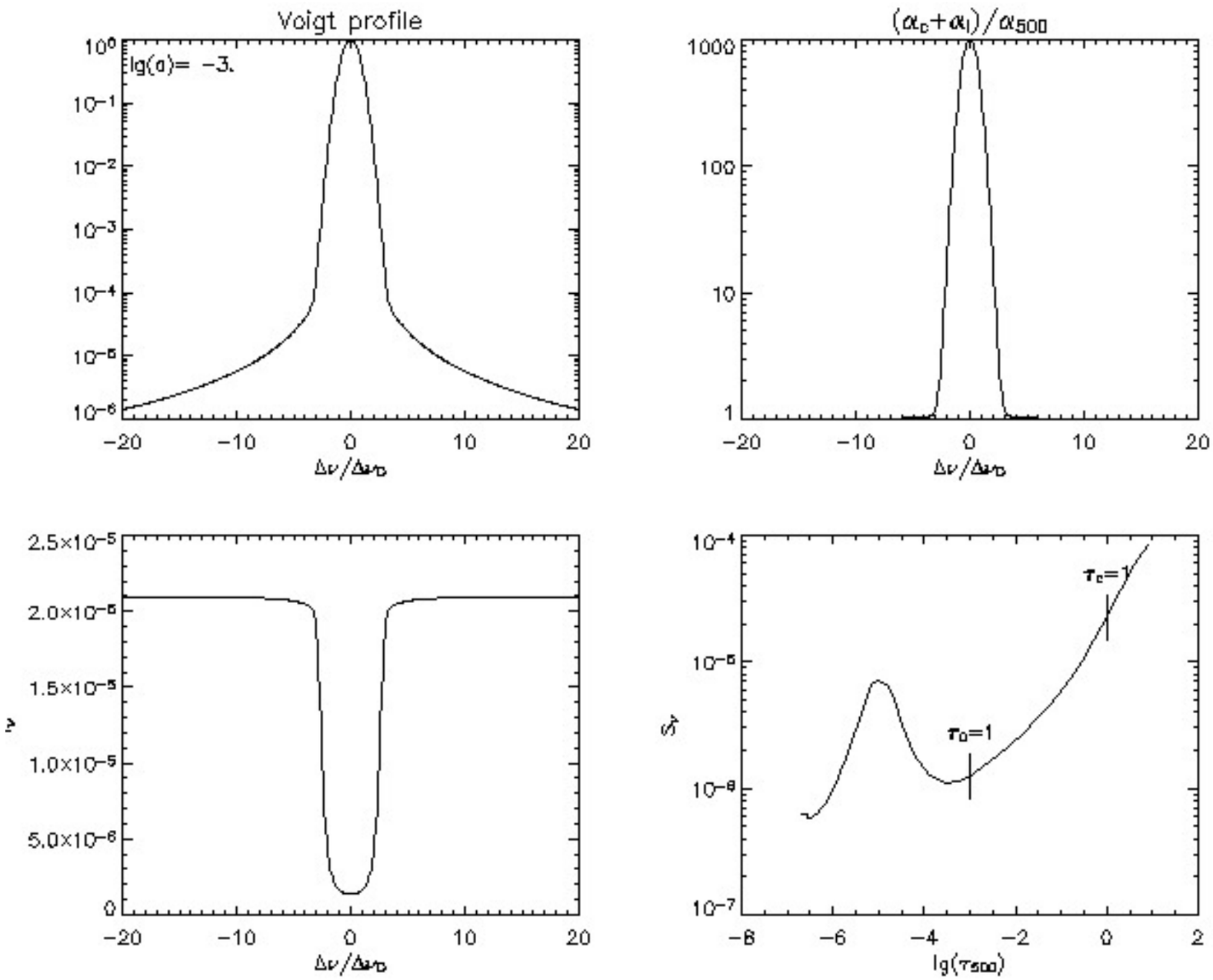

Optically thick line formation

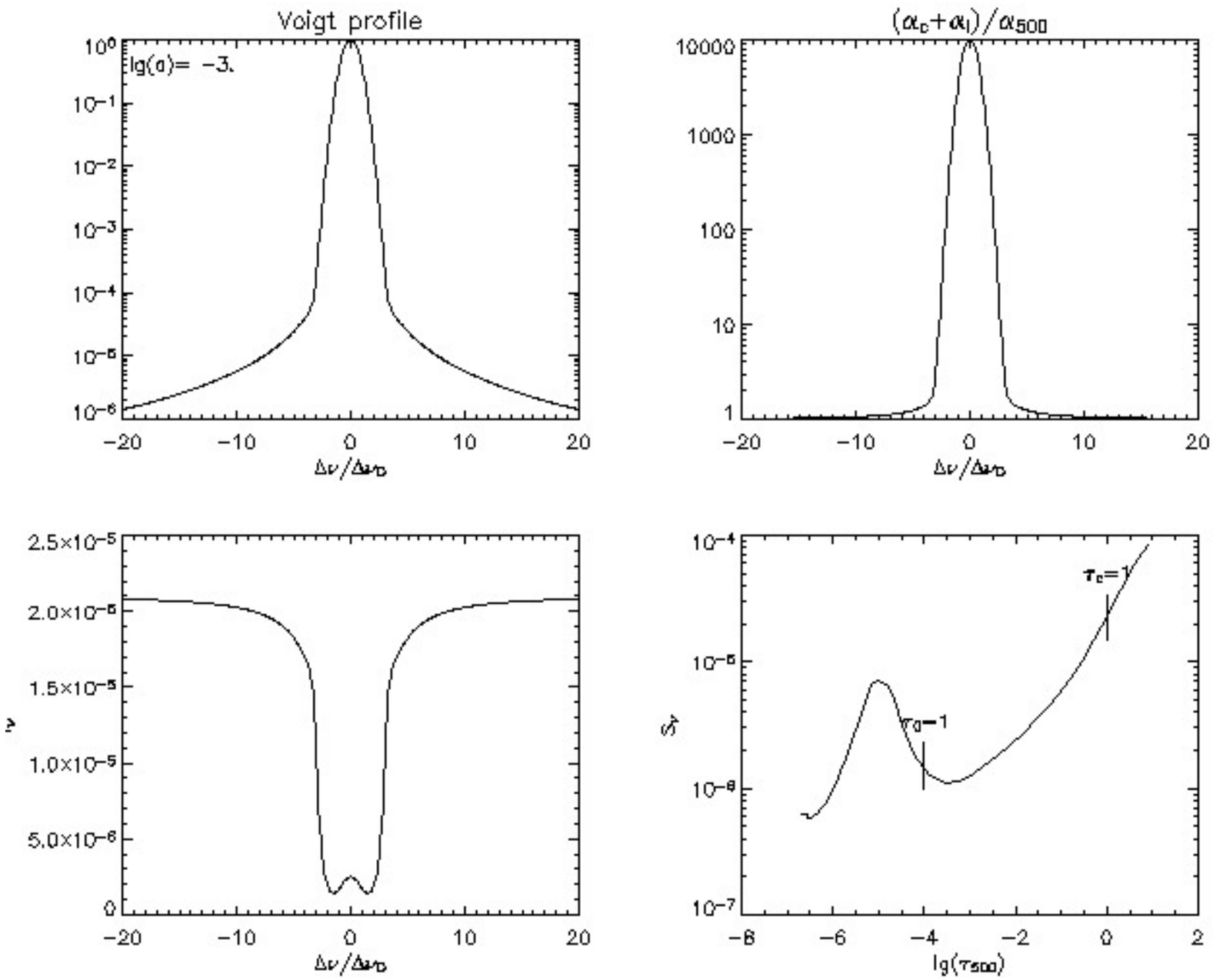

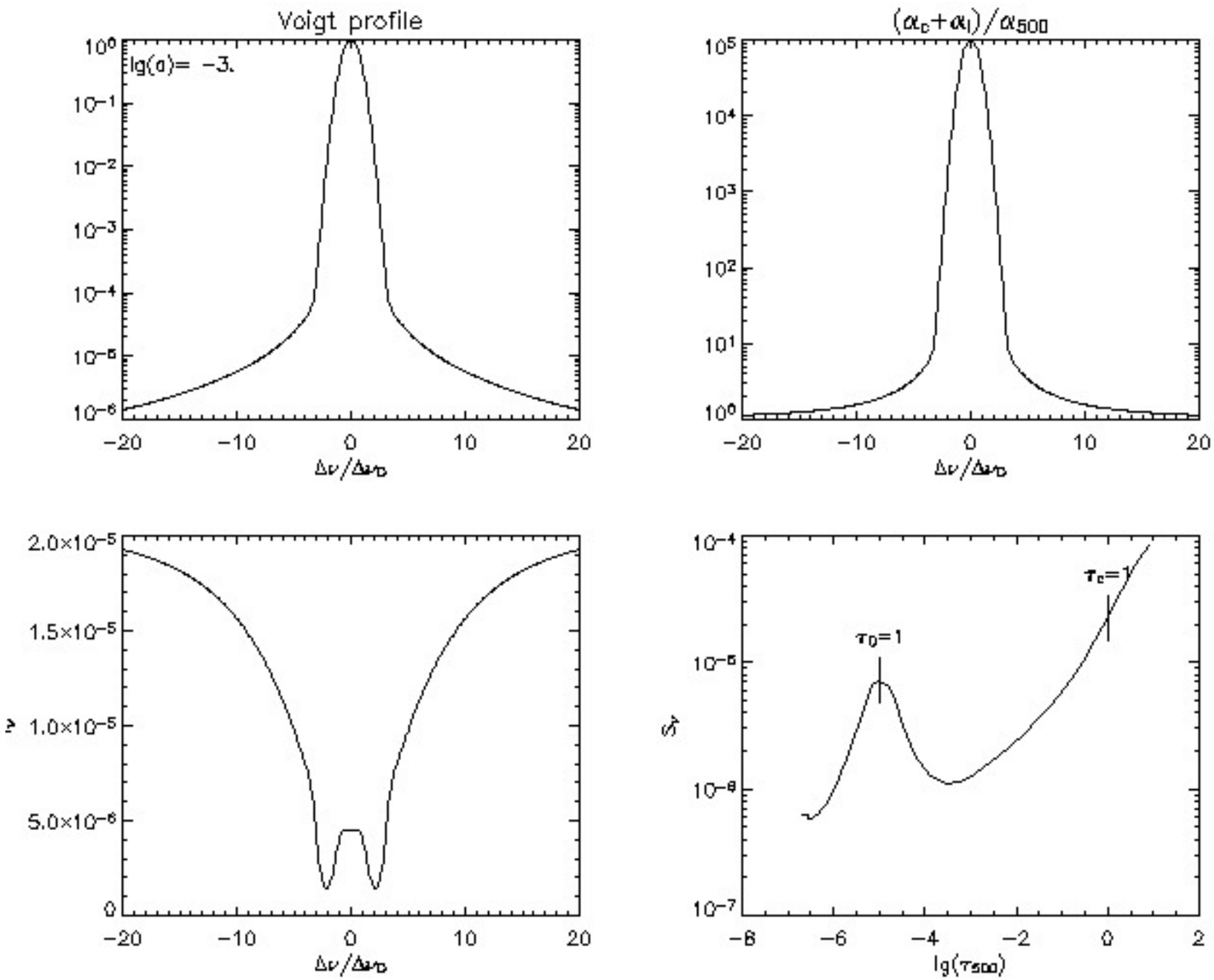
Voigt profile
lg(a)= -3.
$(\alpha_c+\alpha_l)/\alpha_{500}$
$\Delta\nu/\Delta\nu_D$
$\tau_c=1$
$\tau_0=1$
$\lg(\tau_{500})$

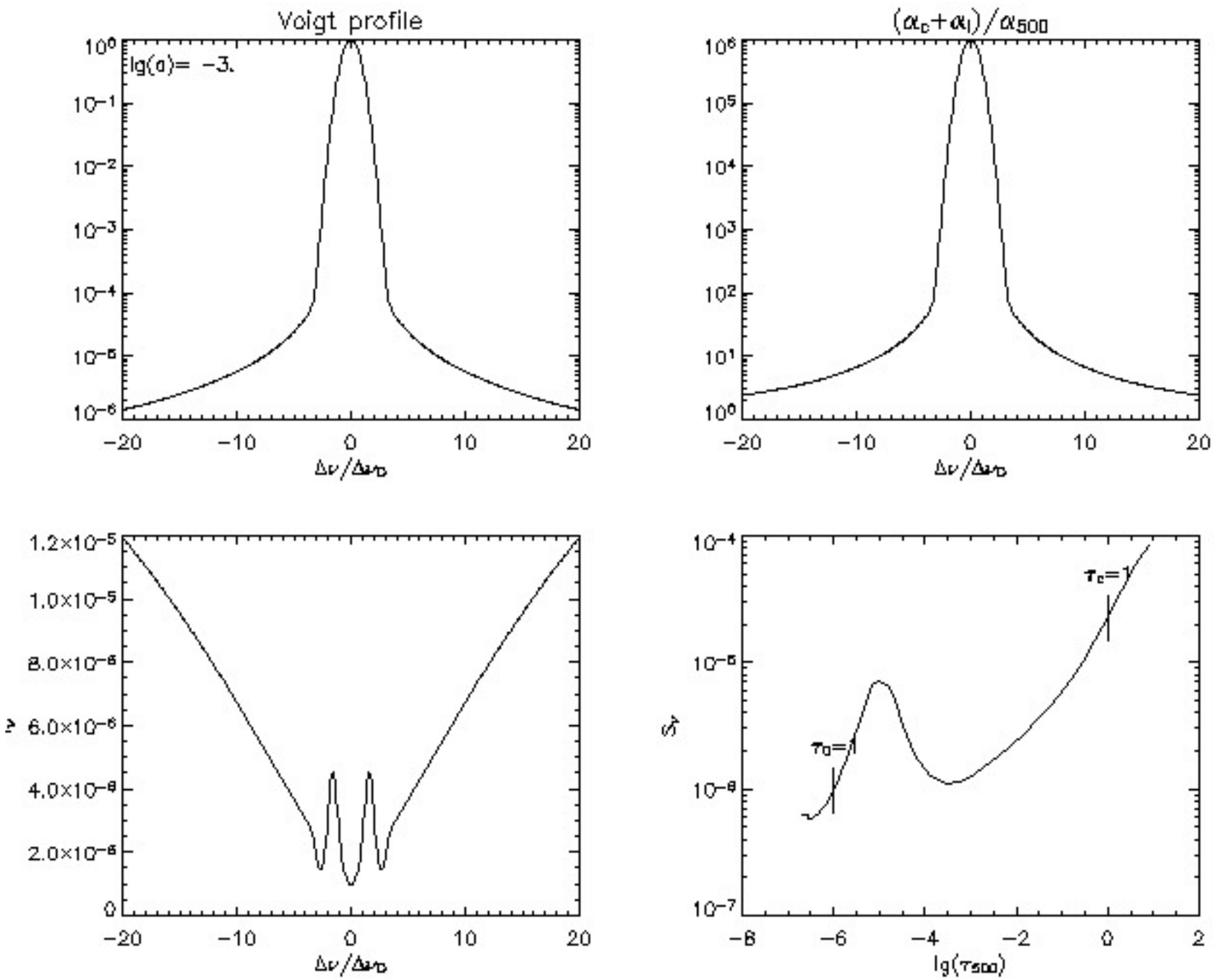
Voigt profile
lg(a)= -3.
$(\alpha_c+\alpha_l)/\alpha_{500}$
$\Delta\nu/\Delta\nu_D$
$\tau_c=1$
$\tau_0=1$
$\lg(\tau_{500})$

Numerical integration

Numerical integration (quadrature)

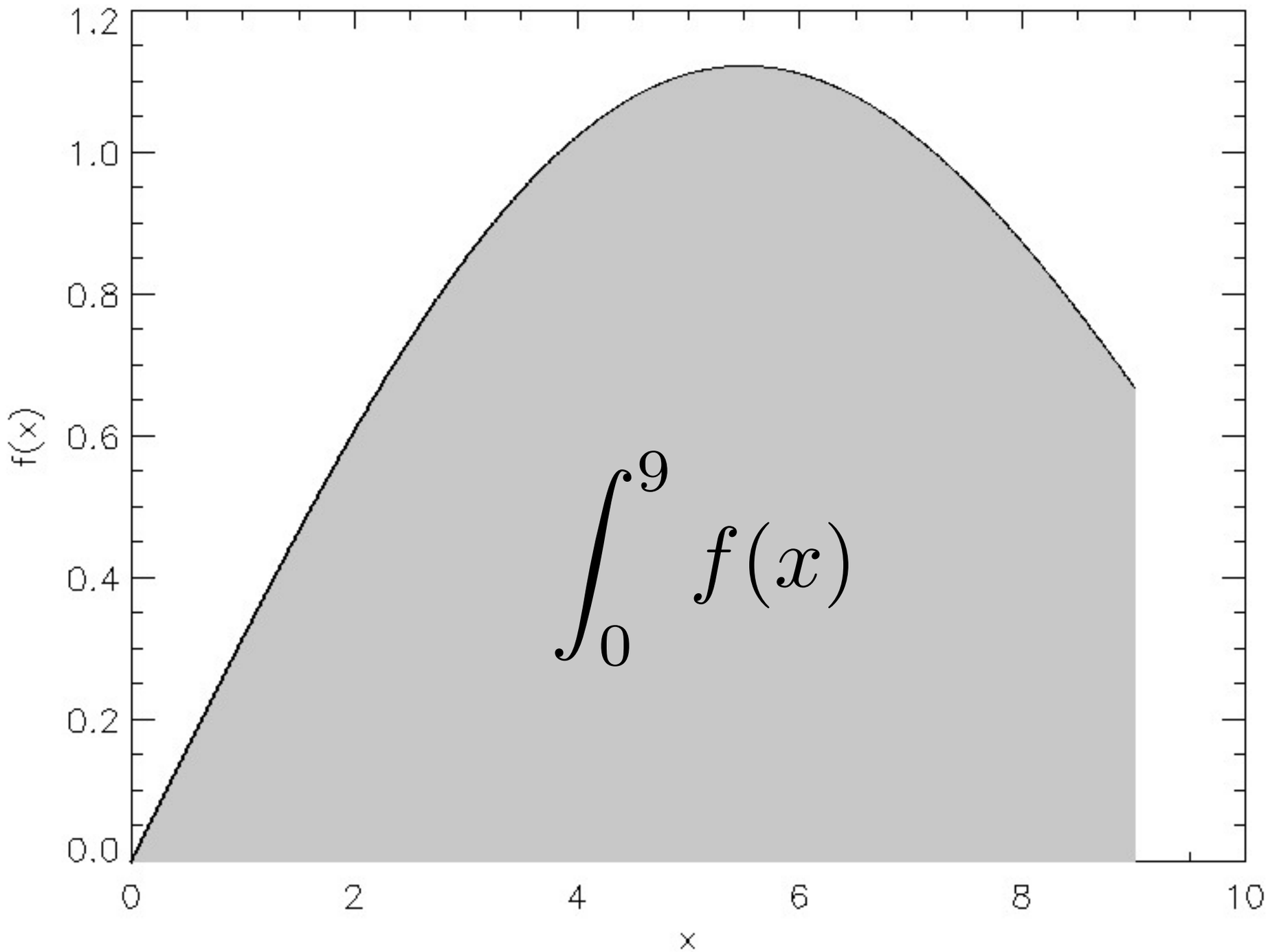

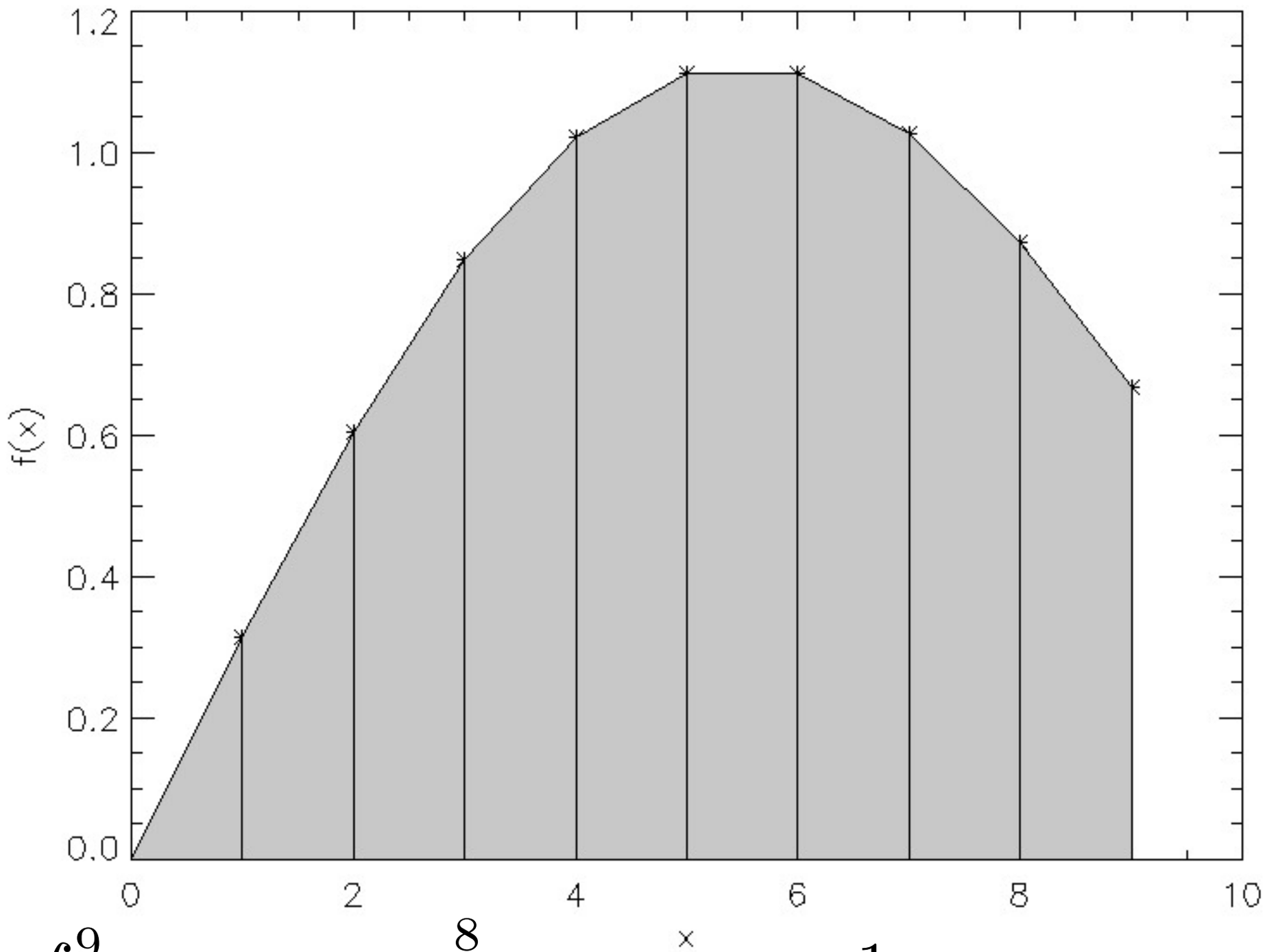

$$\int_0^9 f(x)dx \sim \sum_{i=0}^{8}(x_{i+1} - x_i)\frac{1}{2}(f(x_{i+1} + f(x_i))$$

$$\int_0^9 f(x)dx \sim \sum_{i=0}^{8}(x_{i+1}-x_i)\frac{1}{2}(f(x_{i+1}+f(x_i)) =$$

$$\frac{1}{2}(x_1-x_0)f(x_0)+\sum_{i=1}^{7}\frac{1}{2}(x_{i+1}-x_{i-1})f(x_i)+$$

$$\frac{1}{2}(x_9-x_8)f(x_9)$$

In general:

$$\int_a^b f(x)dx \sim \sum_{i=0}^{N-1} w_i f(x_i)$$

1. Grid points given

Trapezoidal: linear approximation between points

Simpson: parabolic between points

Higher accuracy but risk of overshoot

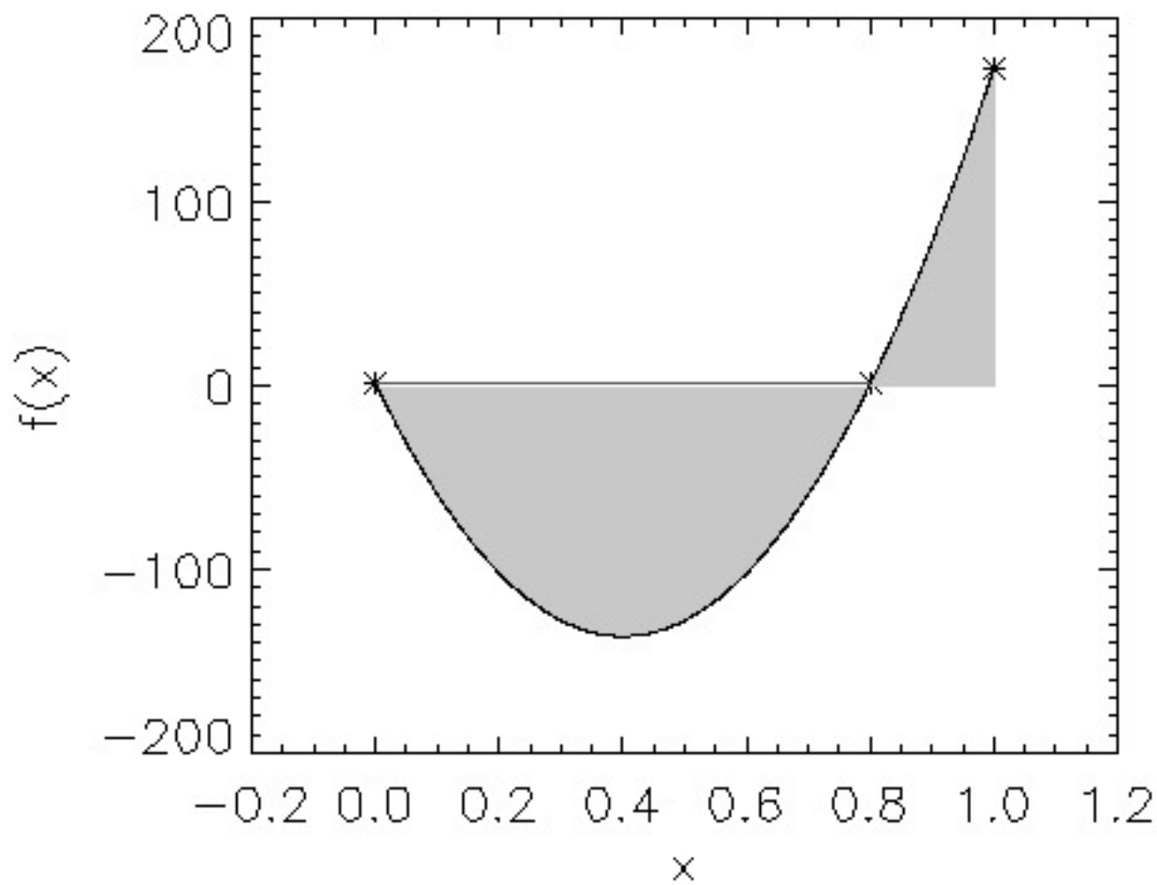

2. Integration method can determine points:

Gaussian quadratures

$$\int_a^b f(x)g(x)dx \sim \sum_{i=0}^{N-1} w_i f(x_i)$$

$g(x) = 1$ Gauss (-Legendre)

$g(x) = e^{-x}; a = 0; b = \infty$ Gauss-Laguerre

Mean intensity: Gaussian quadrature

$$J_\nu(\tau_\nu) = \frac{1}{2}\int_{-1}^{1} I_\nu(\tau_\nu,\mu)d\mu = \int_0^1 \frac{1}{2}(I_\nu^+(\tau_\nu,\mu) + I_\nu^-(\tau_\nu,\mu))d\mu =$$

$$\sum_{i=0}^{N_\mu-1} w_i \frac{1}{2}(I_\nu^+(\tau_\nu,\mu_i) + I_\nu^-(\tau_\nu,\mu_i))$$

$$N_\mu = 3$$

w_i	μ_i
0.277778	0.112702
0.444444	0.500000
0.277778	0.887298

Intensity: Gauss-Laguerre quadrature

$$I_\nu(0) = \frac{1}{\mu}\int_0^\infty S_\nu(\tau_\nu)e^{-\tau_\nu/\mu}d\tau_\nu$$

$$d\tau_{\nu\mu} \equiv \frac{1}{\mu}d\tau_\nu \quad \tau_{\nu\mu} = \frac{1}{\mu}\tau_\nu$$

$$I_\nu(0) = \int_0^\infty S_\nu(\tau_{\nu\mu})e^{-\tau_{\nu\mu}}d\tau_{\nu\mu}$$

	$(\tau_{\nu\mu})_i$	w_i	
$N_{\tau_{\nu\mu}} = 1$	1.0	1.0	=Eddington-Barbier
$N_{\tau_{\nu\mu}} = 2$	0.58579	0.85355	
	3.41421	0.14645	

Source function with scattering

Source function with scattering

$$\eta_\nu = \kappa_\nu B_\nu + \sigma_\nu J_\nu$$
$$\chi_\nu = \kappa_\nu + \sigma_\nu$$

$$S_\nu \equiv \frac{\eta_\nu}{\chi_\nu} = \frac{\kappa_\nu}{\kappa_\nu + \sigma_\nu} B_\nu + \frac{\sigma_\nu}{\kappa_\nu + \sigma_\nu} J_\nu$$

$$S_\nu = B_\nu + \frac{\sigma_\nu}{\kappa_\nu + \sigma_\nu}(J_\nu - B_\nu)$$

$$\rho_\nu \equiv \frac{\sigma_\nu}{\kappa_\nu + \sigma_\nu}$$

$$S_\nu = B_\nu + \rho_\nu(J_\nu - B_\nu)$$

Transfer equation, plane parallel atmosphere

$$\mu \frac{dI_\nu}{d\tau_\nu} = I_\nu - S_\nu$$

Boundary conditions:

$$\lim_{\tau_\nu \to \infty} (I_\nu e^{-\tau_\nu/\mu}) = 0 \qquad I_\nu^-(0) = 0$$

$$I_\nu^+(\tau_\nu) = \frac{1}{\mu} \int_{\tau_\nu}^{\infty} S_\nu(\tau'_\nu) e^{-(\tau'_\nu - \tau_\nu)/\mu} d\tau'_\nu$$

$$I_\nu^-(\tau_\nu) = \frac{1}{\mu} \int_{0}^{\tau_\nu} S_\nu(\tau'_\nu) e^{-(\tau_\nu - \tau'_\nu)/\mu} d\tau'_\nu$$

$$J_\nu(\tau_\nu) = \frac{1}{2} \int_{-1}^{1} I_\nu(\tau_\nu, \mu) d\mu = \int_0^1 \frac{1}{2} (I_\nu^+(\tau_\nu, \mu) + I_\nu^-(\tau_\nu, \mu)) d\mu \equiv \Lambda_\nu[S_\nu]$$

$$J_\nu(\tau_\nu) = \Lambda_\nu[S_\nu] = \Lambda_\nu[B_\nu] + \Lambda_\nu[\rho_\nu(J_\nu - B_\nu)]$$

Λ-iteration:

$$\begin{cases} J_\nu^{(n+1)}(\tau_\nu) & = \Lambda_\nu[B_\nu] + \Lambda_\nu[\rho_\nu(J_\nu^{(n)} - B_\nu)] \\ J^{(0)}(\tau_\nu) & = B_\nu \end{cases}$$

If $\rho_\nu \sim 1$ this scheme won't work

Cases when scattering dominates:
Hot stars, opacity dominated by electron scattering
Cool stars, low [Fe/H]: Rayleigh scattering dominates
Spectral lines: $1 - \rho_\nu \sim 10^{-8}$

Alternative form

$$S_\nu = (1-\epsilon_\nu)J_\nu + \epsilon_\nu B_\nu$$

$$S_\nu = (1-\epsilon_\nu)\Lambda_\nu[S_\nu] + \epsilon_\nu B_\nu$$

Λ-iteration:

$$\begin{cases} S_\nu^{(n+1)} & = (1-\epsilon_\nu)\Lambda_\nu[S_\nu^{(n)}] + \epsilon_\nu B_\nu \\ S_\nu^{(0)} & = B_\nu \end{cases}$$

Lambda-iteration in practice, 100 iterations

$$S_\nu = \epsilon_\nu B_\nu + (1-\epsilon_\nu) J_\nu \quad ; \quad B_\nu = 1$$

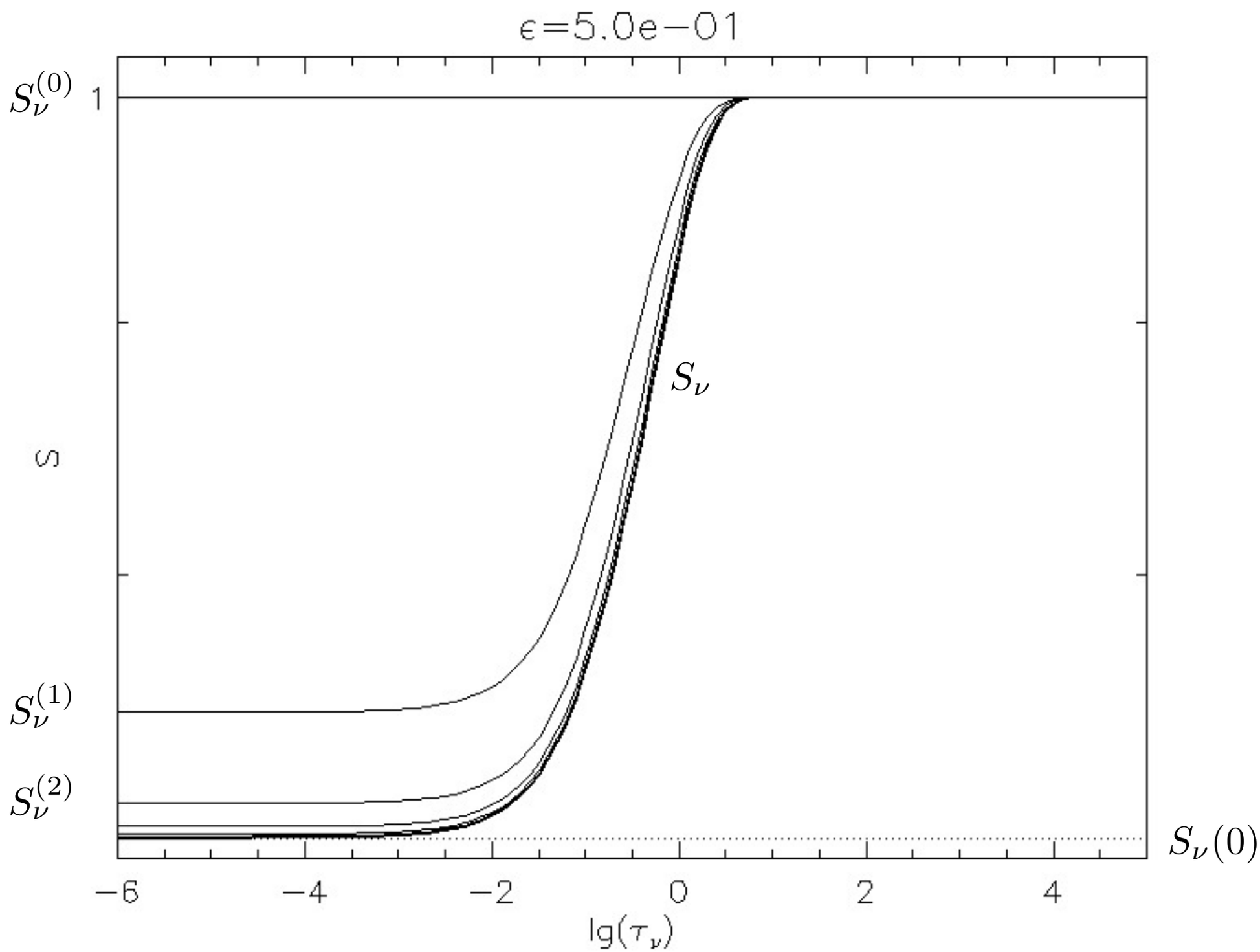

Lambda-iteration in practice, 100 iterations

$$S_\nu = \epsilon_\nu B_\nu + (1-\epsilon_\nu) J_\nu \quad ; \quad B_\nu = 1$$

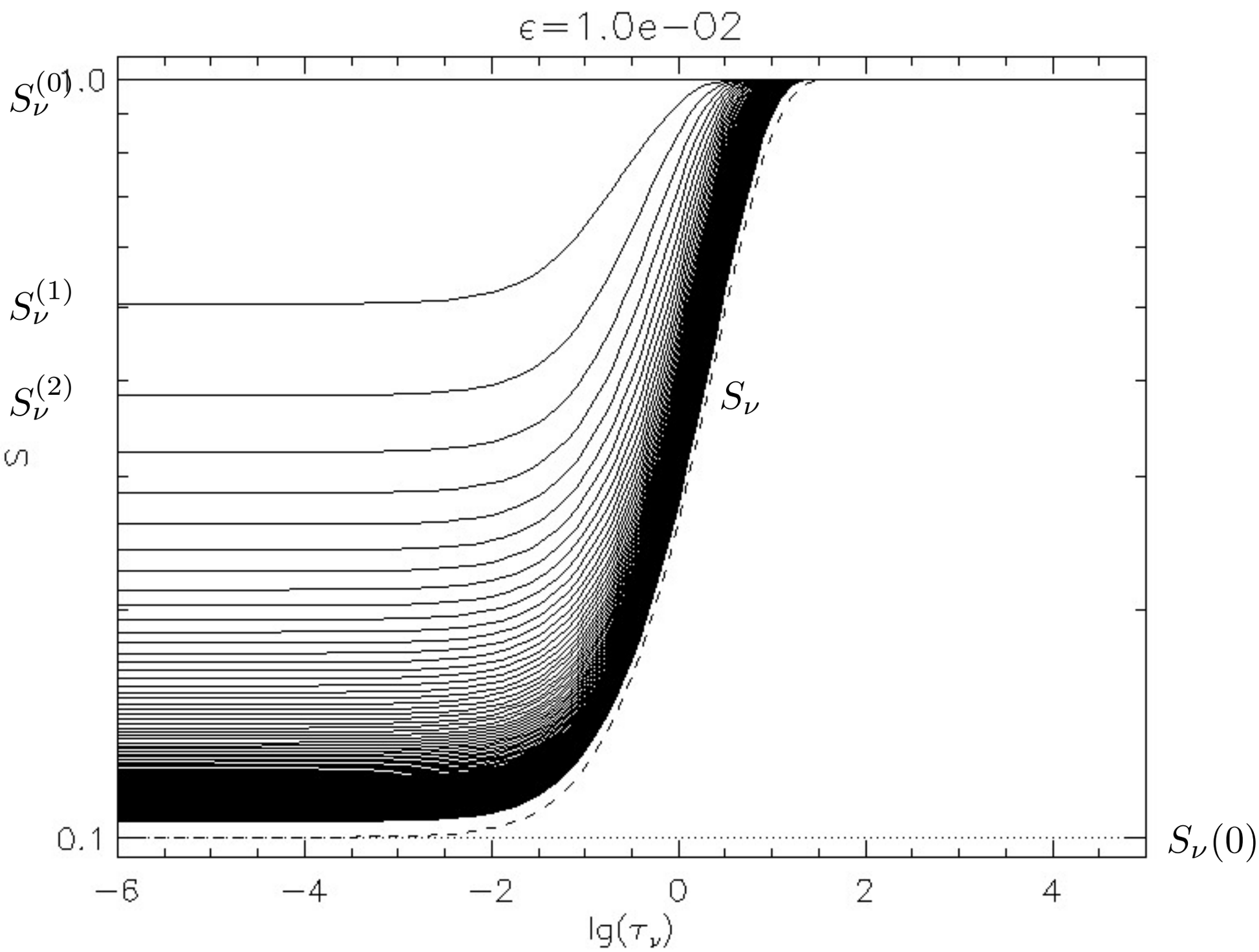

Lambda-iteration in practice, 100 iterations

$$S_\nu = \epsilon_\nu B_\nu + (1-\epsilon_\nu) J_\nu \quad ; \quad B_\nu = 1$$

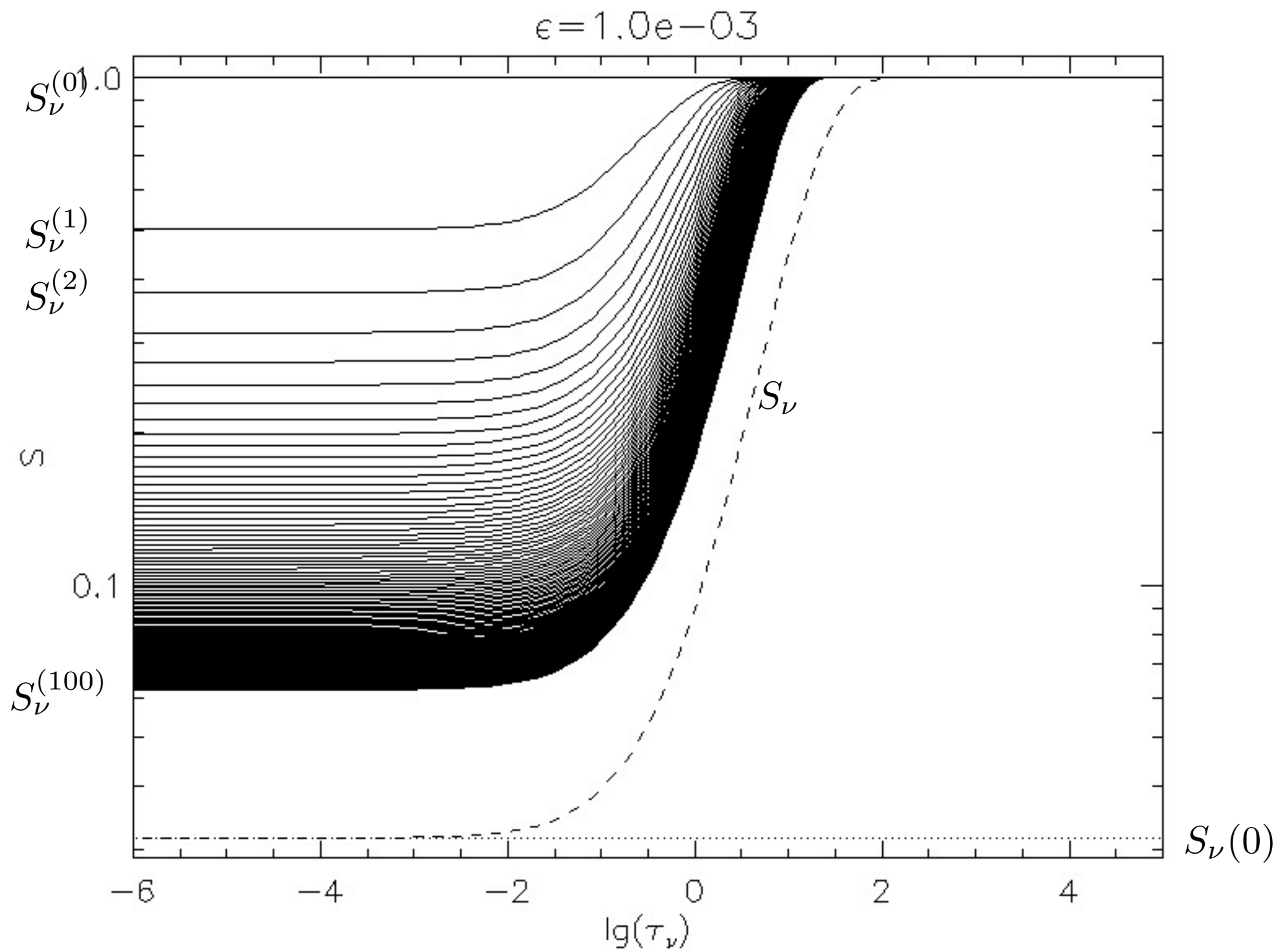

Lambda-iteration in practice, 100 iterations

$$S_\nu = \epsilon_\nu B_\nu + (1-\epsilon_\nu) J_\nu \quad ; \quad B_\nu = 1$$

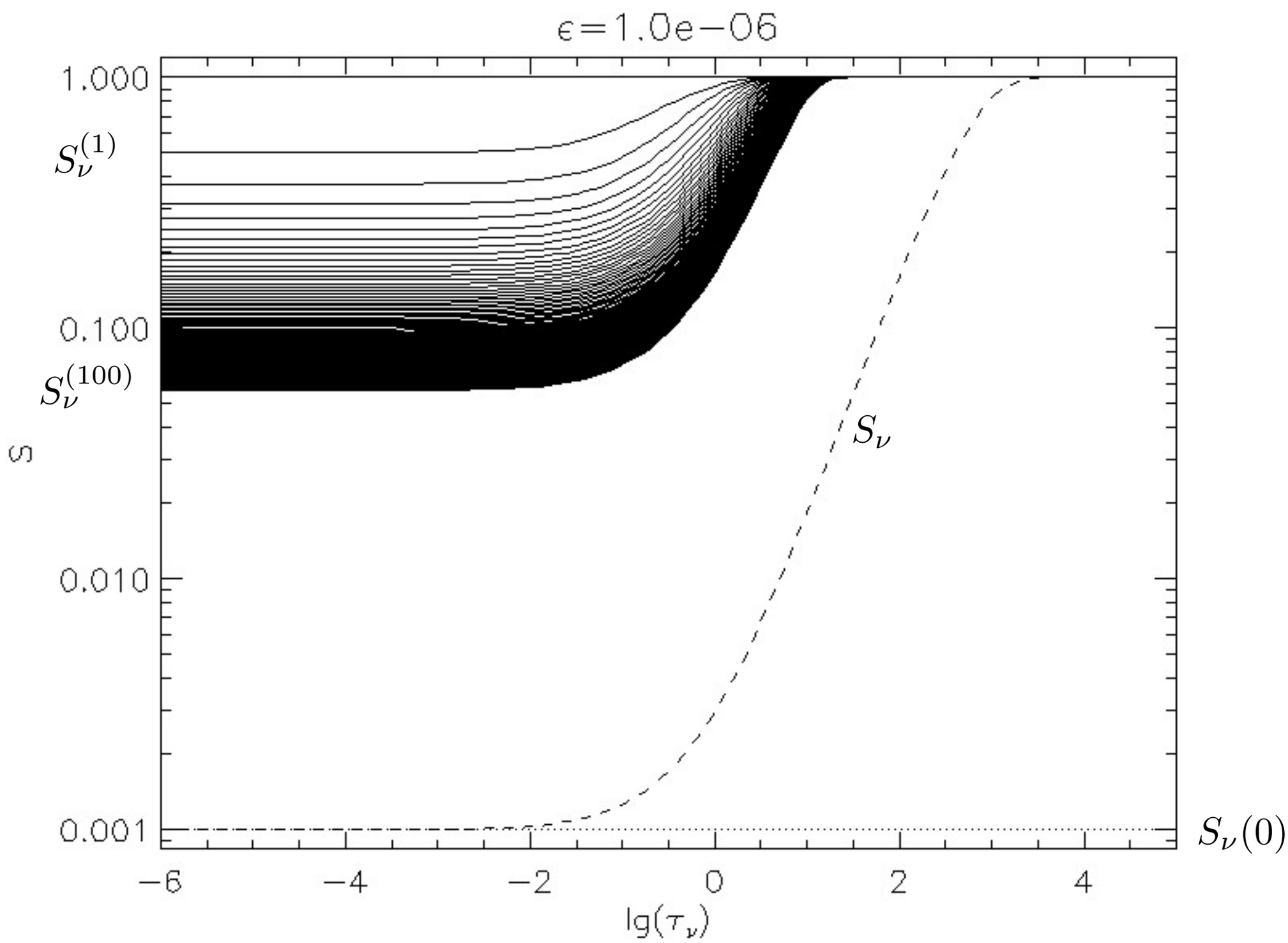

Lambda-iteration in practice

- OK if scattering is small
- Disaster for small epsilon
- Stabilizes instead of converging when epsilon is small (0.5% correction at iteration 100 for $\varepsilon=10^{-6}$ when solution is a factor of 55 from correct solution)

Shooting

Principles

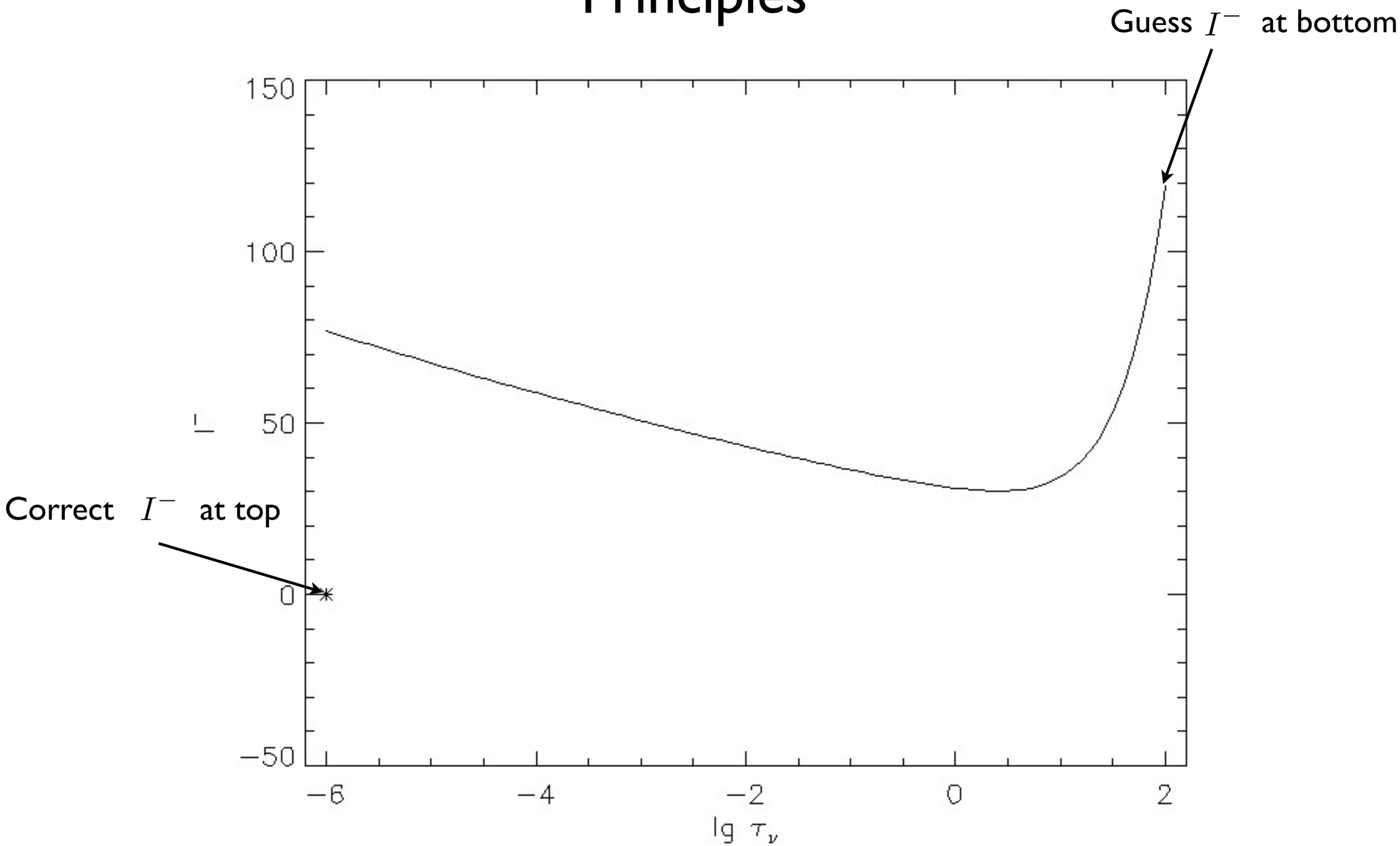

Shooting

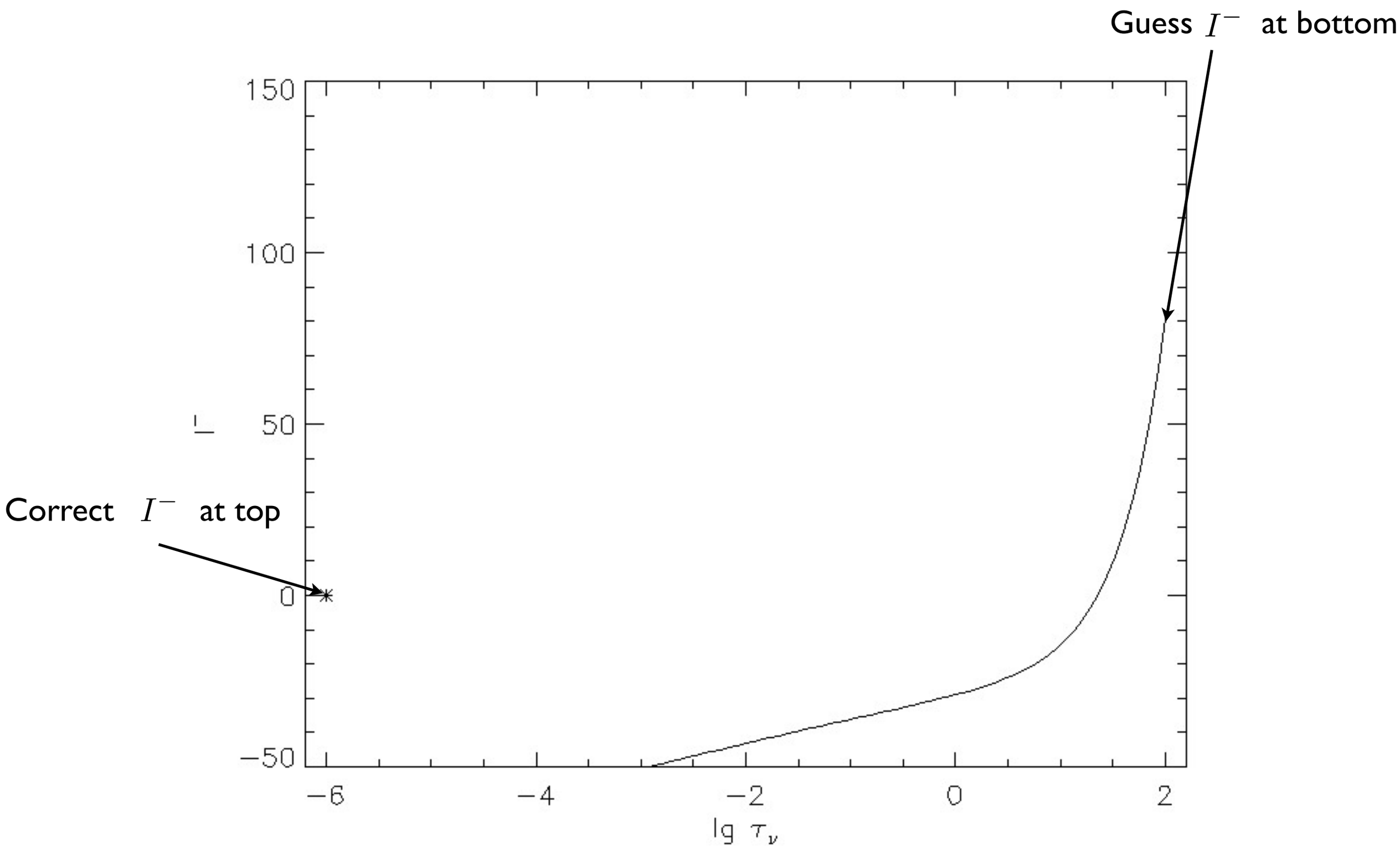
Guess I^- at bottom
Correct I^- at top
150
100
50
0
−50
−6
−4
−2
0
2
lg τ_ν

Shooting

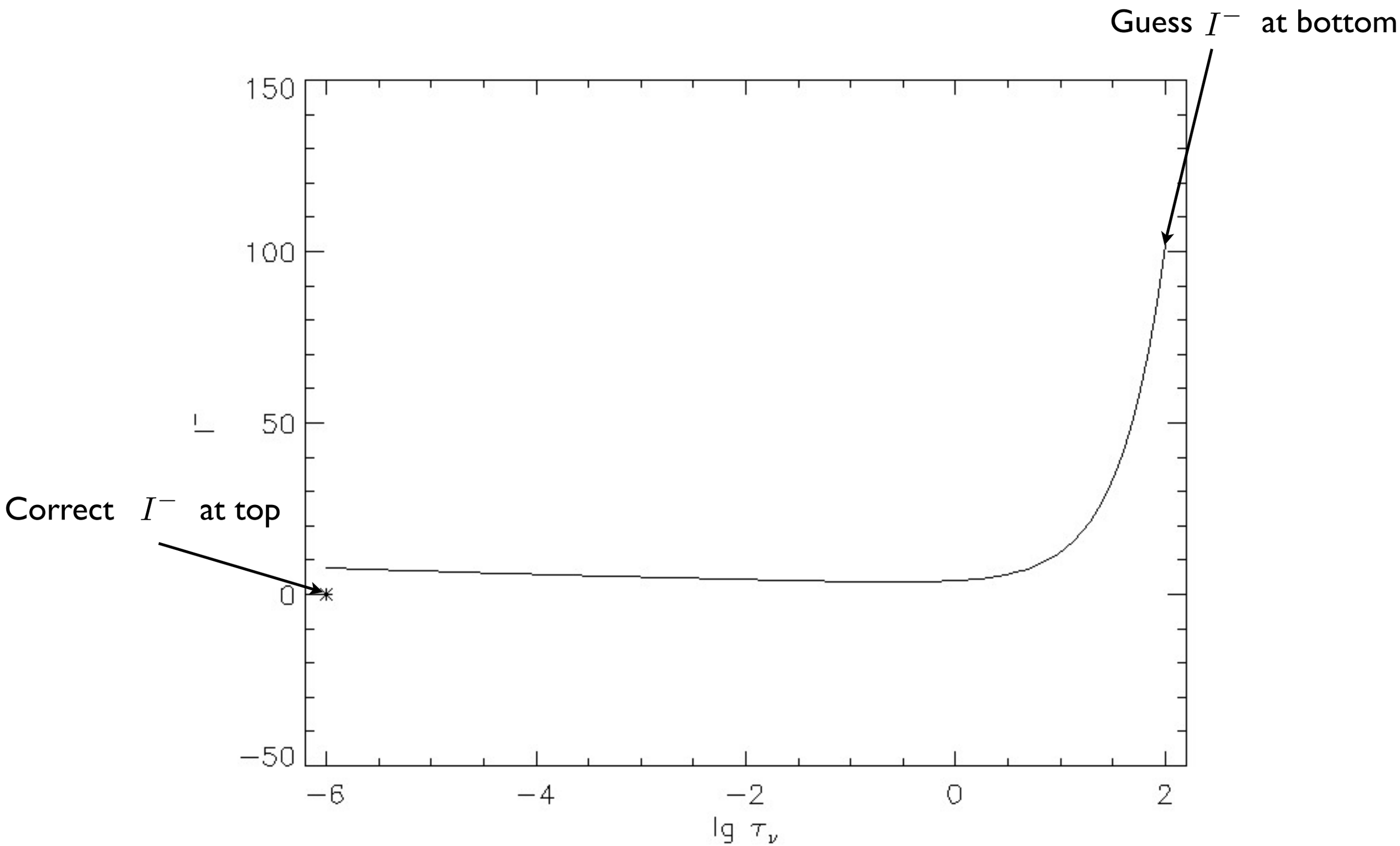
Guess I^- at bottom
Correct I^- at top
150
100
50
0
−50
−6
−4
−2
0
2
lg τ_ν

Shooting

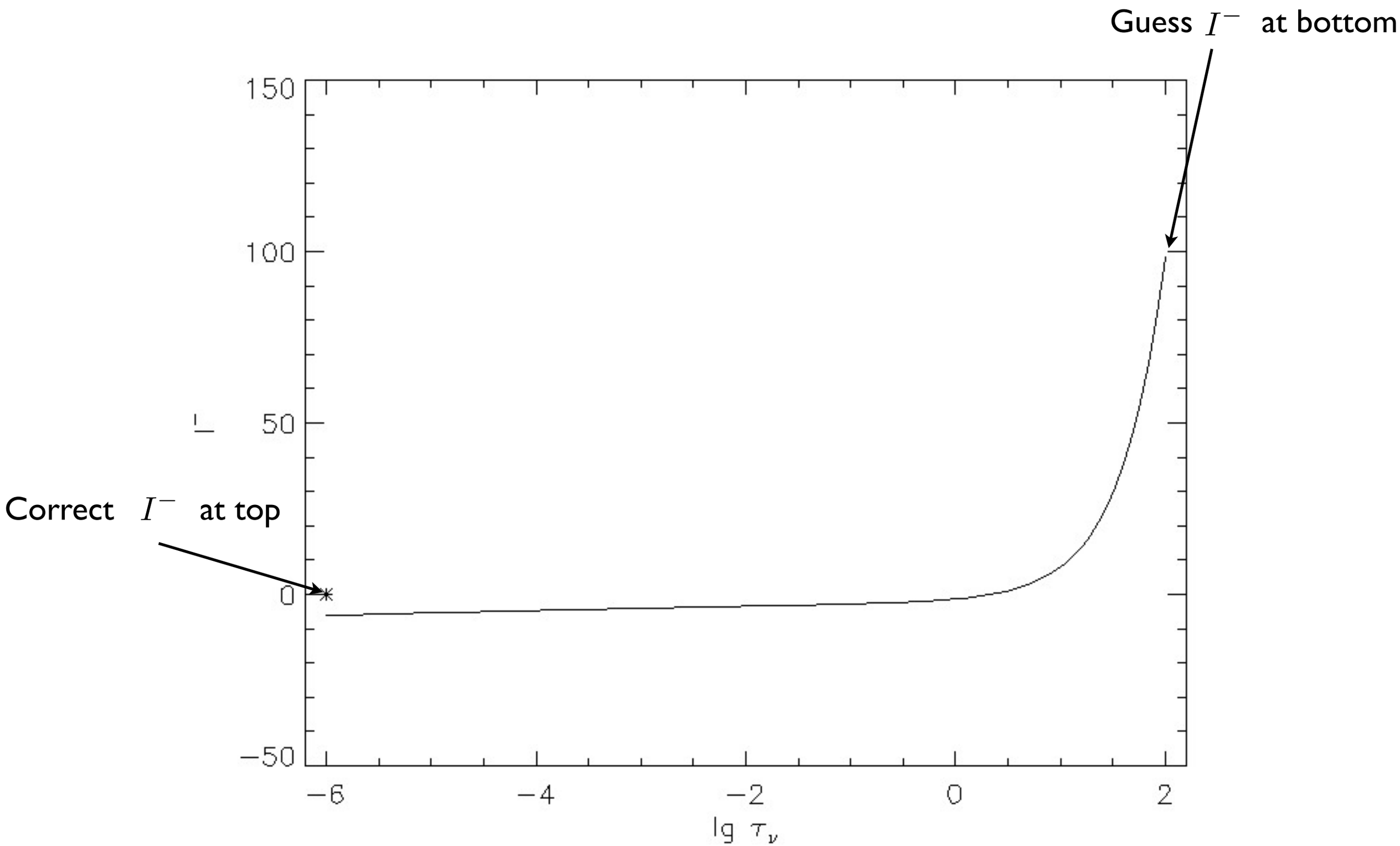
Guess I^- at bottom
Correct I^- at top
150
100
50
0
−50
I^-
−6
−4
−2
0
2
lg τ_ν

Shooting

Now we've found the solution!

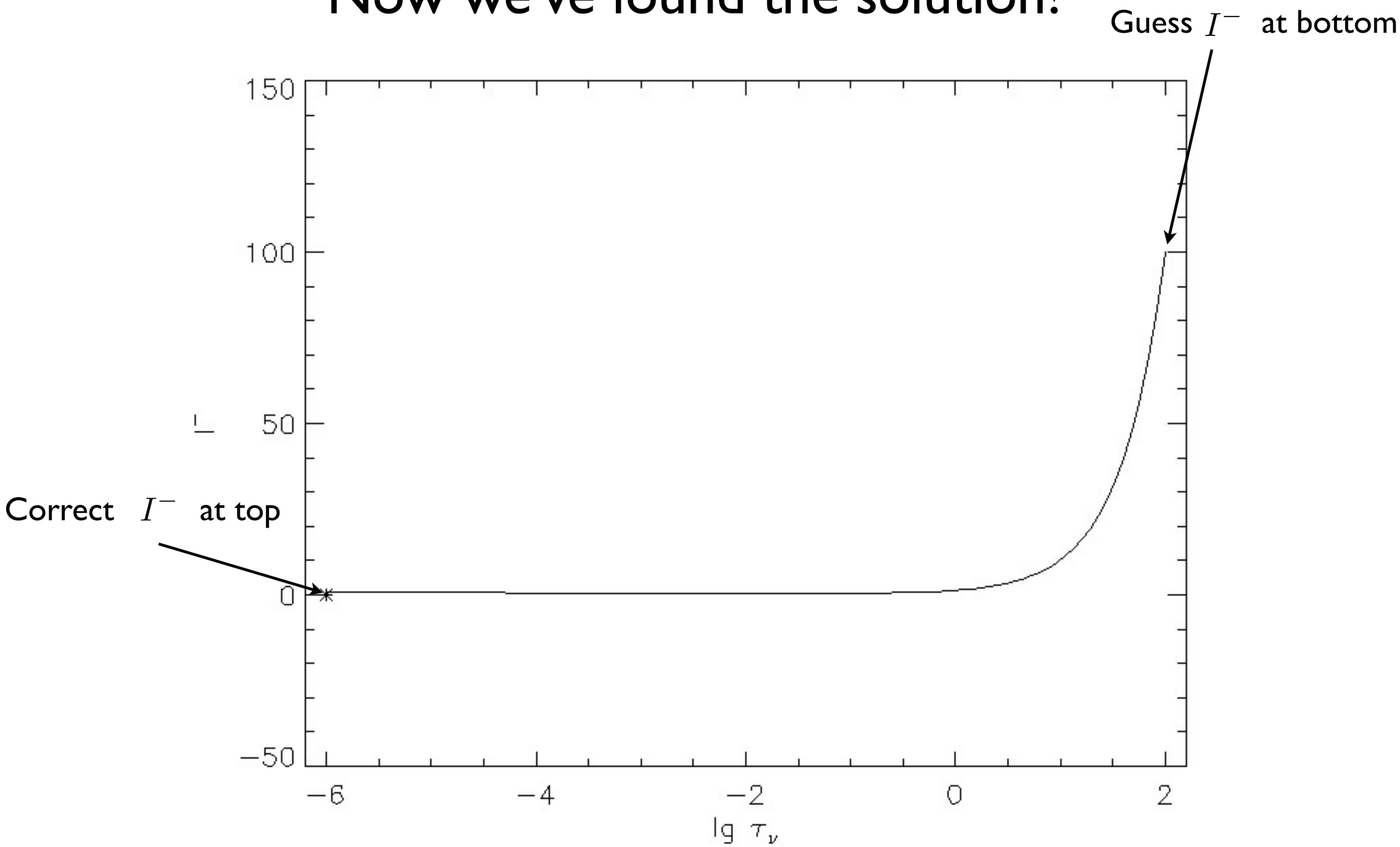

Shooting

Realistic case

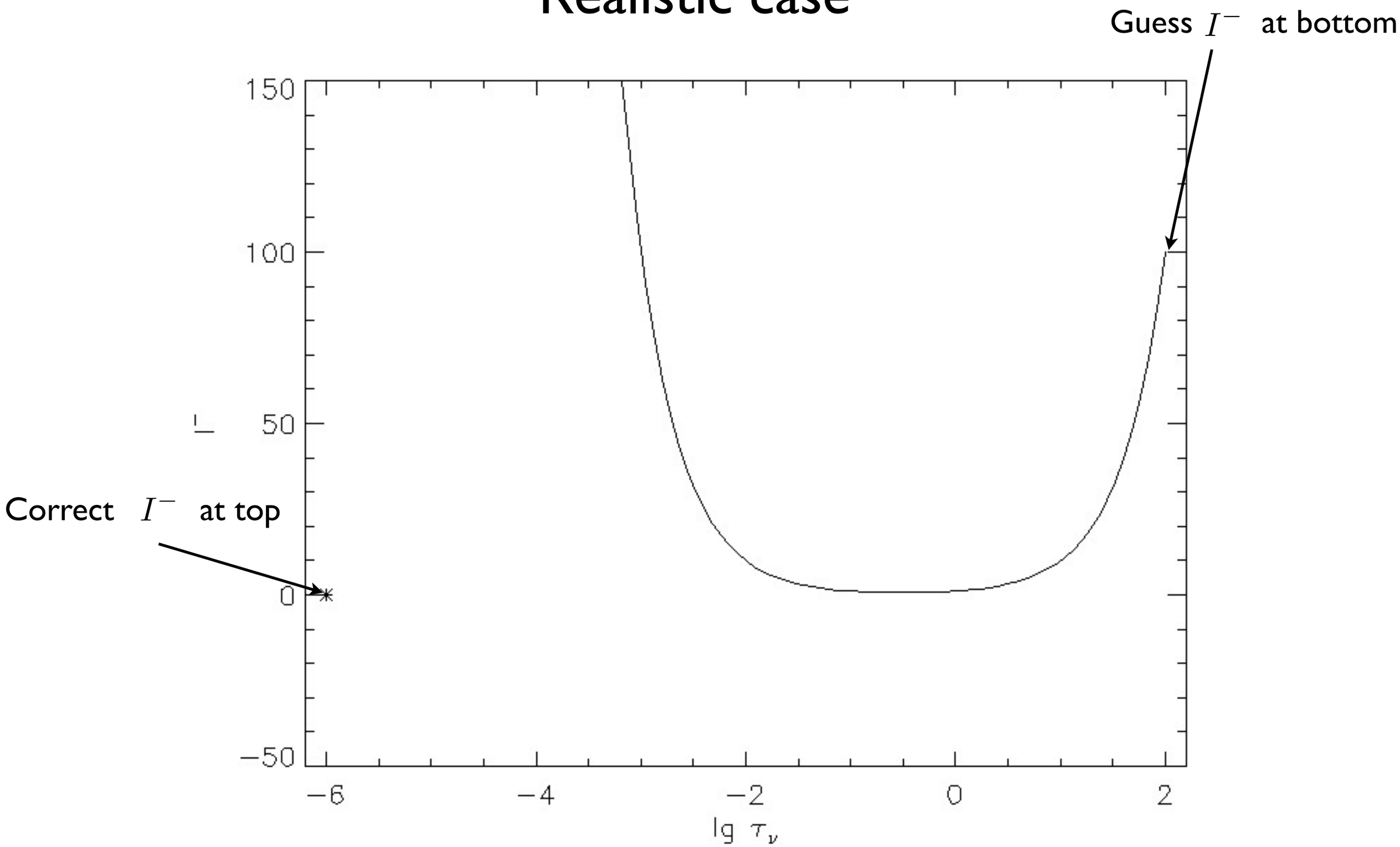

Shooting

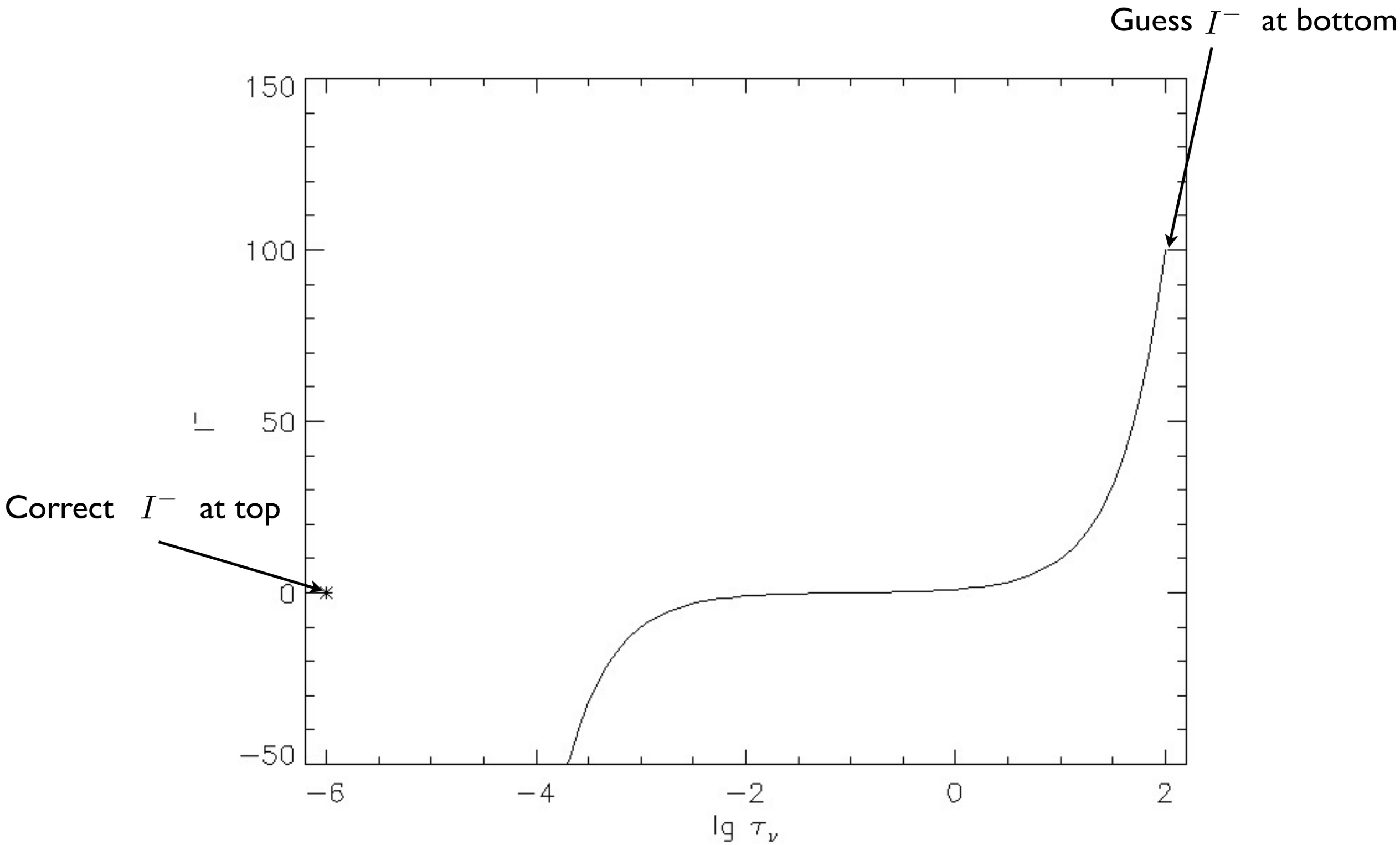
Guess I^- at bottom
Correct I^- at top
150
100
50
0
−50
I^-
−6
−4
−2
0
2
lg τ_ν

Shooting

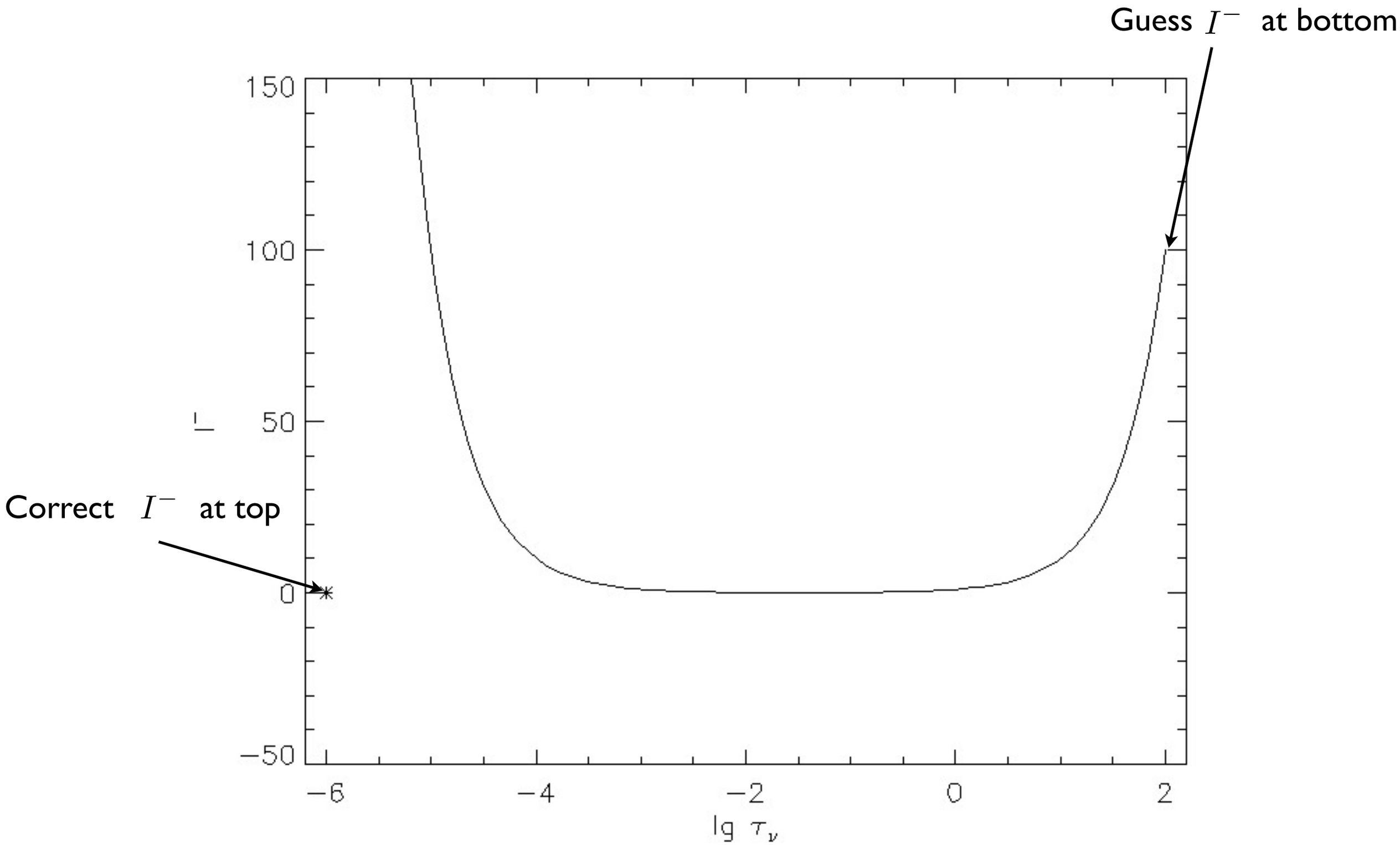
Guess I^- at bottom
Correct I^- at top
150
100
50
0
−50
I^-
−6
−4
−2
0
2
lg τ_ν

Shooting

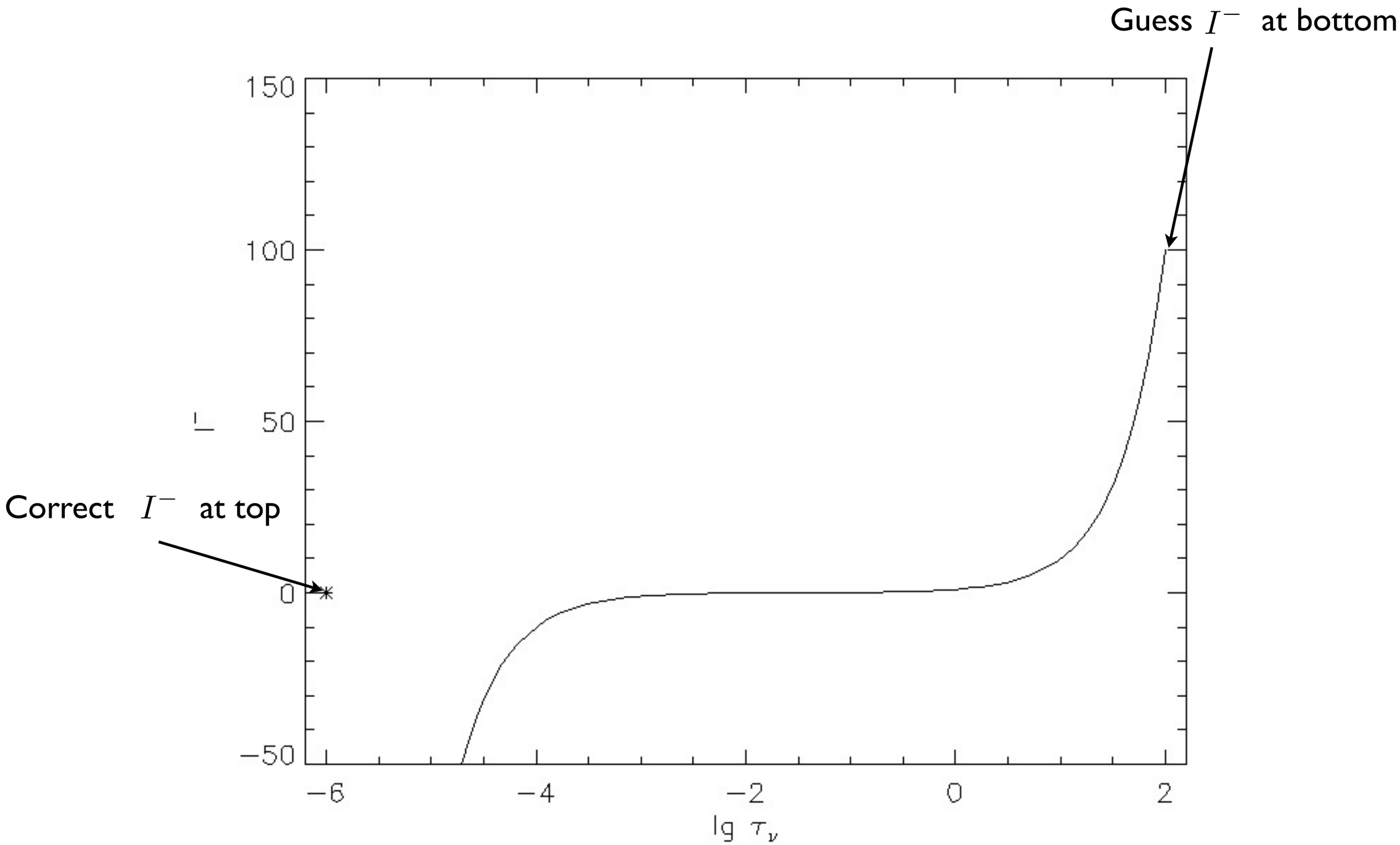
Guess I^- at bottom
Correct I^- at top
150
100
50
0
−50
I^-
−6
−4
−2
0
2
lg τ_ν

Shooting

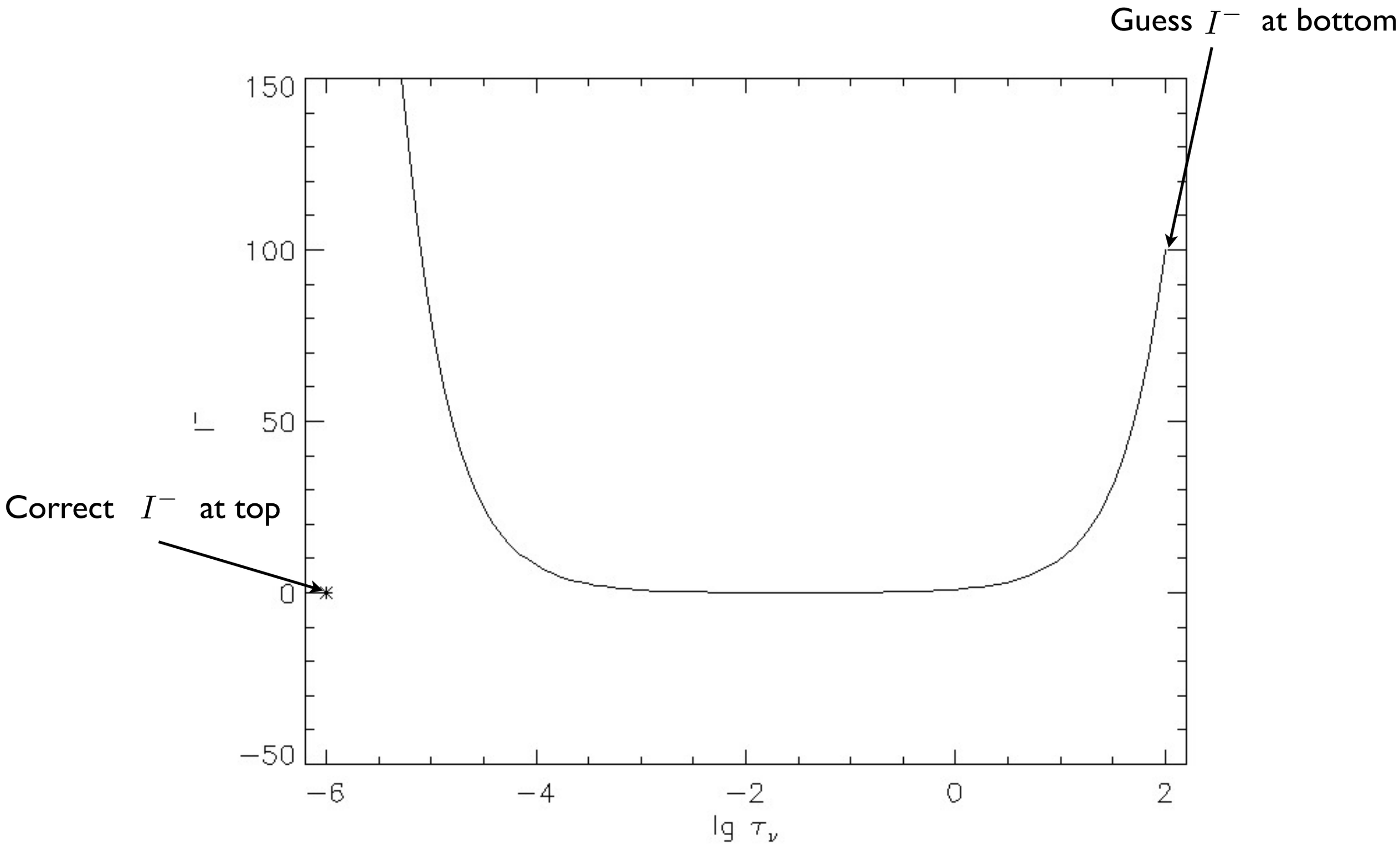
Guess I^- at bottom
Correct I^- at top
150
100
50
0
−50
I^-
−6
−4
−2
0
2
lg τ_ν

Shooting

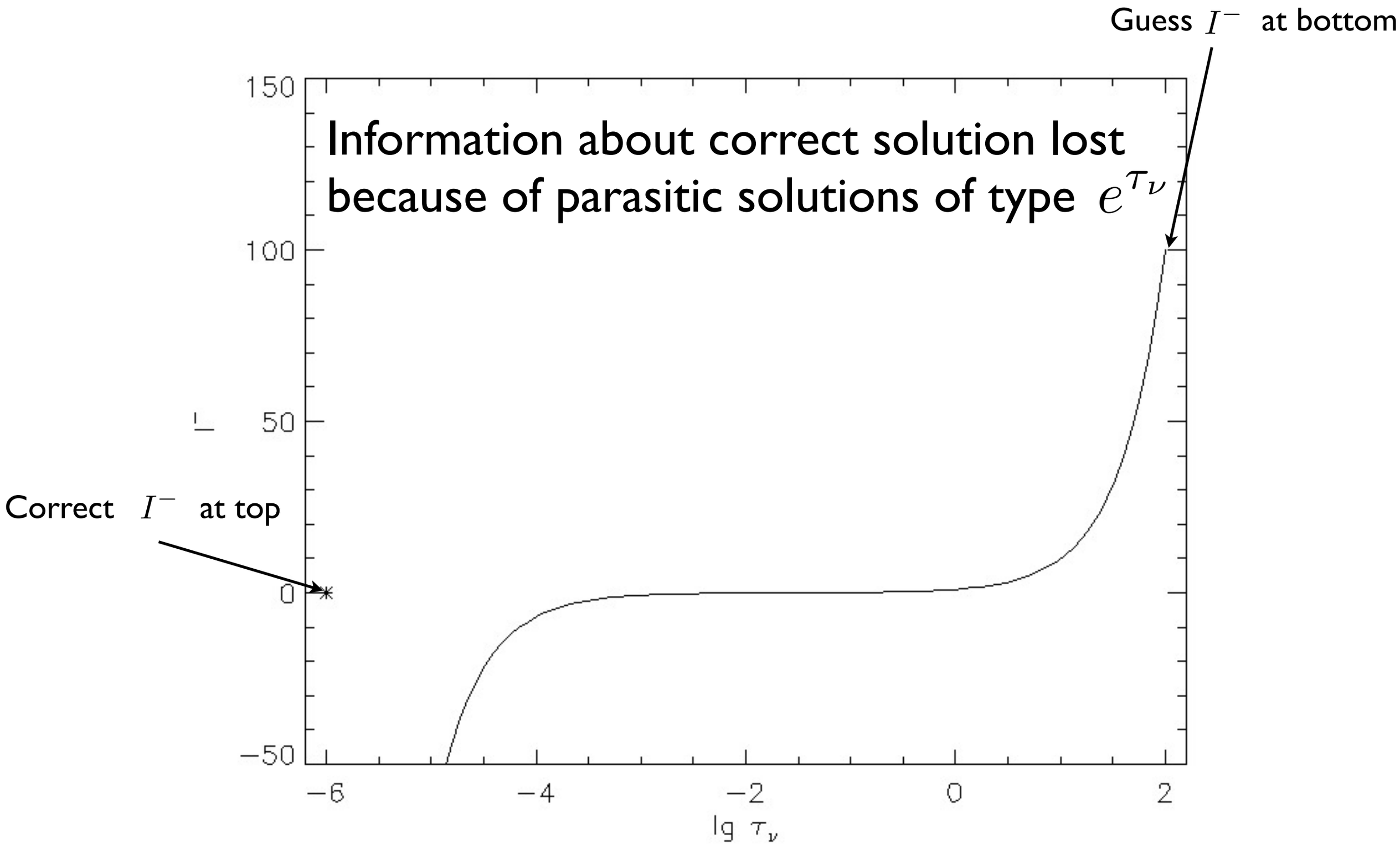
Guess I^- at bottom
Information about correct solution lost because of parasitic solutions of type e^{τ_ν}
Correct I^- at top
150
100
50
0
−50
I^-
−6
−4
−2
0
2
lg τ_ν

Why is there a problem?

- Boundary condition partially given at one boundary, partially at the other
- Need to solve for whole atmosphere and take into account bouth boundaries at the same time

Feautrier's method

Feautrier's method

We drop index ν and location τ_ν :

$$\mu \frac{dI_\mu}{d\tau} = I_\mu - S$$

We write separately for outgoing and incoming rays:

$$\mu \frac{dI_\mu^+}{d\tau} = I_\mu^+ - S^+$$

$$-\mu \frac{dI_\mu^-}{d\tau} = I_\mu^- - S^-$$

Multiplying by $\frac{1}{2}$, assuming $S^+ = S^-$
and adding and subtracting we get

$$\mu \frac{d\frac{1}{2}(I_\mu^+ - I_\mu^-)}{d\tau} = \frac{1}{2}(I_\mu^+ + I_\mu^-) - S^+$$

$$\mu \frac{d\frac{1}{2}(I_\mu^+ + I_\mu^-)}{d\tau} = \frac{1}{2}(I_\mu^+ - I_\mu^-)$$

Using the second equation in the first and introducing

$$P \equiv \frac{1}{2}(I_\mu^+ + I_\mu^-) \qquad R \equiv \frac{1}{2}(I_\mu^+ - I_\mu^-)$$

we get

$$\boxed{\mu^2 \frac{d^2 P}{d\tau^2} = P - S}$$

We discretize: $\tau_\nu \longrightarrow \tau_i \qquad \mu \longrightarrow \mu_j$

Define differences:

$$[\Delta\tau]_{i+1/2} \approx \tau_{i+1} - \tau_i \equiv \Delta\tau_i \tag{5.20}$$

$$[\Delta\tau]_{i-1/2} \approx \tau_i - \tau_{i-1} \equiv \Delta\tau_{i-1} \tag{5.21}$$

Replace derivatives with differences

$$\left[\frac{\mathrm{d}P(\tau,\mu_j)}{\mathrm{d}\tau}\right]_{i+1/2} \equiv \lim_{\Delta\tau\to 0} \frac{[\Delta P(\tau,\mu_j)]_{i+1/2}}{[\Delta\tau]_{i+1/2}}$$

$$\approx \frac{P(\tau_{i+1},\mu_j) - P(\tau_i,\mu_j)}{\tau_{i+1}-\tau_i} = \frac{P_{i+1}-P_i}{\Delta\tau_i},$$

2nd derivative replaced by difference between 1st derivatives:

$$
\begin{aligned}
\left[\frac{\mathrm{d}^2 P(\tau,\mu_j)}{\mathrm{d}\tau^2}\right]_i &\approx \frac{[\Delta P(\tau,\mu_j)/\Delta\tau]_{i+1/2} - [\Delta P(\tau,\mu_j)/\Delta\tau]_{i-1/2}}{[\Delta\tau]_i} \\
&\approx \frac{[\Delta P(\tau,\mu_j)/\Delta\tau]_{i+1/2} - [\Delta P(\tau,\mu_j)/\Delta\tau]_{i-1/2}}{\frac{1}{2}\left([\Delta\tau]_{i+1/2} + [\Delta\tau]_{i-1/2}\right)} \\
&\approx \frac{2}{\Delta\tau_{i-1} + \Delta\tau_i}\left[\frac{P_{i+1}}{\Delta\tau_i} - \frac{P_i}{\Delta\tau_i} - \frac{P_i}{\Delta\tau_{i-1}} + \frac{P_{i-1}}{\Delta\tau_{i-1}}\right] \\
&= \frac{2P_{i-1}}{\Delta\tau_{i-1}\left(\Delta\tau_{i-1} + \Delta\tau_i\right)} - \frac{2P_i}{\Delta\tau_i\,\Delta\tau_{i-1}} + \frac{2P_{i+1}}{\Delta\tau_i\left(\Delta\tau_{i-1} + \Delta\tau_i\right)}.
\end{aligned}
$$

With these (5.17) can be written as:

$$\mu^2 \left[\frac{\mathrm{d}^2 P}{\mathrm{d}\tau^2}\right]_i - P_i = A_i P_{i-1} - B_i P_i + C_i P_{i+1} = -S_i \tag{5.22}$$

with

$$A_i = \frac{2\mu^2}{\Delta\tau_{i-1}\left(\Delta\tau_{i-1} + \Delta\tau_i\right)} \tag{5.23}$$

$$B_i = 1 + \frac{2\mu^2}{\Delta\tau_i\,\Delta\tau_{i-1}} \tag{5.24}$$

$$C_i = \frac{2\mu^2}{\Delta\tau_i\left(\Delta\tau_{i-1} + \Delta\tau_i\right)}. \tag{5.25}$$

Numerically unstable for small $\Delta\tau_i$ (use Stein's trick)

2 level atom with coherent scattering:

$$\mu^2 \frac{\mathrm{d}^2 P(\tau,\mu)}{\mathrm{d}\tau^2} = P(\tau,\mu) - \varepsilon(\tau)B(\tau) - (1-\varepsilon(\tau))\,J(\tau) \tag{5.27}$$

$$= P(\tau,\mu) - \varepsilon(\tau)B(\tau) - (1-\varepsilon(\tau))\sum_{j=1}^{m} a_j P_j(\tau,\mu_j), \tag{5.28}$$

Source function thus introduces all angles for the equation of a given angle

$$\mathbf{TP} = -\varepsilon\mathbf{B}$$

Structure of matrix:

$$
\mathbf{T} = \begin{pmatrix}
x & x & x & x & & & & & & & & & & & & \\
x & x & x & & x & & & & & & & & & & & \\
x & x & x & & & x & & & & & & & & & & \\
x & & & x & x & x & x & & & & & & & & & \\
 & x & & x & x & x & & x & & & & & & & & \\
 & & x & x & x & x & & & x & & & & & & & \\
 & & & x & & & x & x & x & x & & & & & & \\
 & & & & x & & x & x & x & & x & & & & & \\
 & & & & & x & x & x & x & & & x & & & & \\
 & & & & & & \ddots & & & \ddots & & & \ddots & & & \\
 & & & & & & & & & & & & & & & \\
 & & & & & & & & & & & & & x & x & x & x & & \\
 & & & & & & & & & & & & & x & x & x & & x & \\
 & & & & & & & & & & & & & x & x & x & & & x \\
 & & & & & & & & & & & & & x & & & x & x & x \\
 & & & & & & & & & & & & & & x & & x & x & x \\
 & & & & & & & & & & & & & & & x & x & x & x
\end{pmatrix}
$$

Solve for all depths at the same time
Boundaries at both ends taken into account simultaneously

Note that Feautrier's method assumes $\boxed{S^+ = S^-}$
With velocities in the atmosphere this condition is not fulfilled!!
If the absorption profile of a line is symmetric, we can redefine P (and R):

$$P_\mu(\tau, \Delta\nu) \equiv \frac{1}{2}(I_\mu^+(\tau, \Delta\nu) + I_\mu^-(\tau, -\Delta\nu))$$

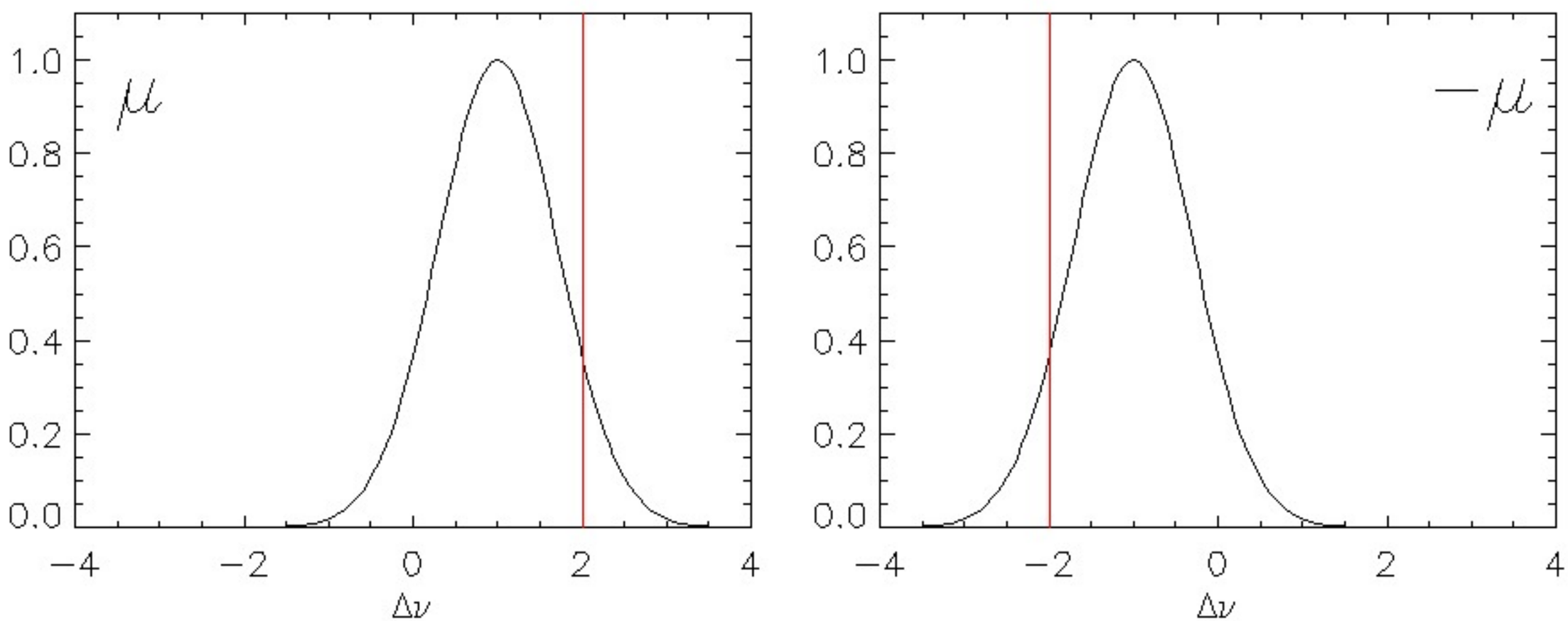

Feautrier's method is fast and accurate (2nd order) and is the method of choice for the formal solution, even when there is no scattering.

There are versions that are 3rd and 4th order accurate (spline and Hermite forms)

Cannot be used if we have both velocity fields and blends!

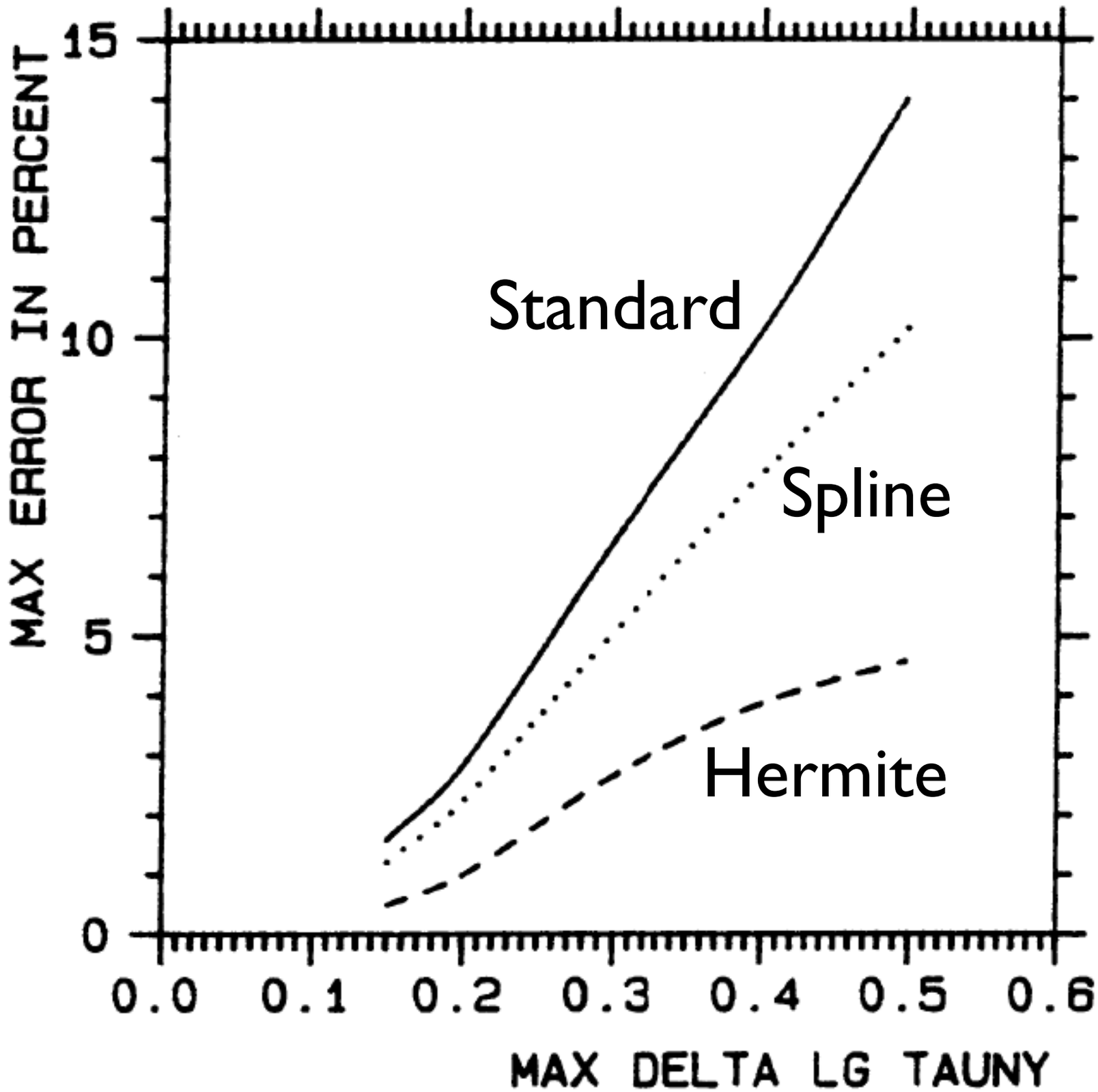
MAX ERROR IN PERCENT
15
10
5
0
0.0
0.1
0.2
0.3
0.4
0.5
0.6
MAX DELTA LG TAUNY
Standard
Spline
Hermite

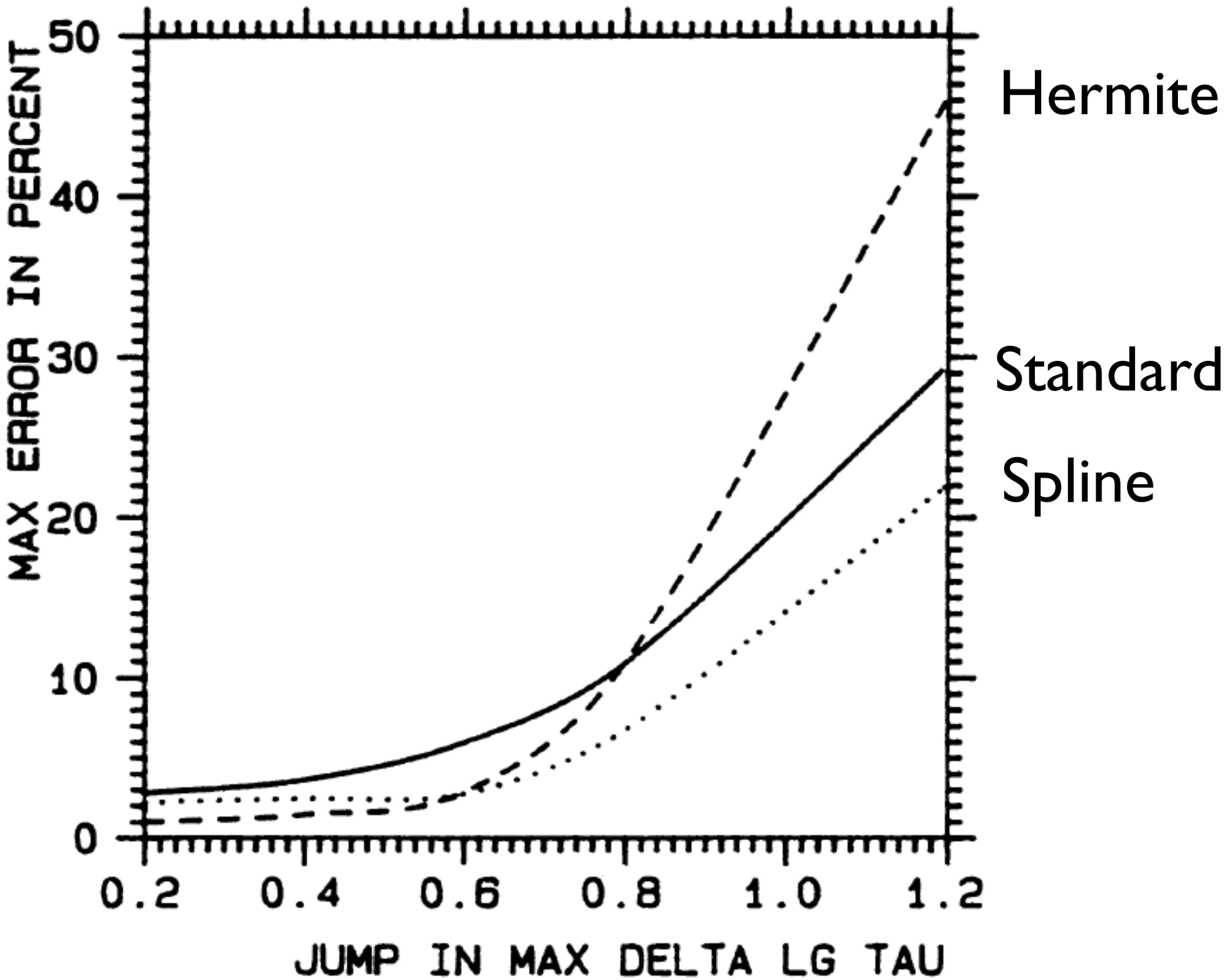
MAX ERROR IN PERCENT
50
40
30
20
10
0
0.2
0.4
0.6
0.8
1.0
1.2
JUMP IN MAX DELTA LG TAU
Hermite
Standard
Spline

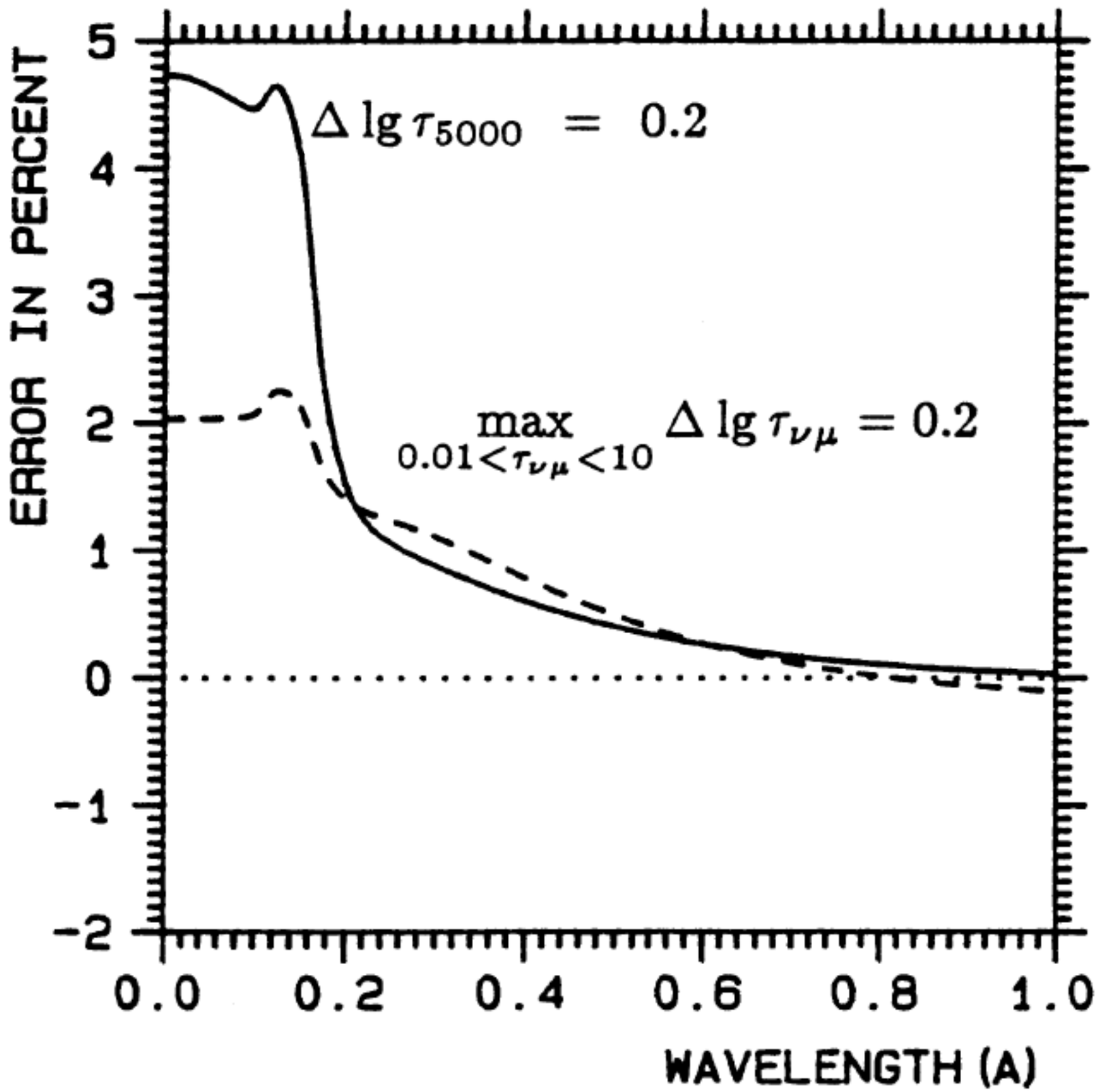
ERROR IN PERCENT
5
4
3
2
1
0
-1
-2
$\Delta \lg \tau_{5000} = 0.2$
$\max_{0.01<\tau_{\nu\mu}<10} \Delta \lg \tau_{\nu\mu} = 0.2$
0.0
0.2
0.4
0.6
0.8
1.0
WAVELENGTH (A)

Velocity fields and blends

Integral methods

- Treat outgoing and incoming rays separately
- Fit source function with a function (e.g. cubic spline)
- Integrate fitting function analytically

ALI

Split the lambda operator into an approximate part and a correction

$$\mathbf{\Lambda}_\nu = \mathbf{\Lambda}^* + (\mathbf{\Lambda}_\nu - \mathbf{\Lambda}^*) \tag{5.39}$$

$$J_\nu = \mathbf{\Lambda}^*_\nu[S] + (\mathbf{\Lambda}_\nu - \mathbf{\Lambda}^*_\nu)[S] \tag{5.40}$$

Classical lambda-iteration: $S^{(n+1)} = (1-\varepsilon)\,\mathbf{\Lambda}[S^{(n)}] + \varepsilon B,$ then becomes (5.33)

NB!

$$S^{(n+1)} = (1-\varepsilon)\,\mathbf{\Lambda}^*[S^{(n+1)}] + (1-\varepsilon)(\mathbf{\Lambda}_\nu - \mathbf{\Lambda}^*)[S^{(n)}] + \varepsilon B \tag{5.41}$$

$$\begin{aligned} S^{(n+1)} - (1-\varepsilon)\,\mathbf{\Lambda}^*[S^{(n+1)}] &= \boxed{(1-\varepsilon)\,\mathbf{\Lambda}_\nu[S^{(n)}] + \varepsilon B} - (1-\varepsilon)\,\mathbf{\Lambda}^*[S^{(n)}] \\ &= \boxed{S^{\mathrm{FS}}} - (1-\varepsilon)\,\mathbf{\Lambda}^*[S^{(n)}], \end{aligned} \tag{5.42}$$

$$S^{(n+1)} = (1-(1-\varepsilon)\,\mathbf{\Lambda}^*)^{-1}\left[S^{\mathrm{FS}} - (1-\varepsilon)\,\mathbf{\Lambda}^*[S^{(n)}]\right]. \tag{5.43}$$

Classical lambda-iteration: $S^{(n+1)} - S^{(n)} = S^{\mathrm{FS}} - S^{(n)},$ (5.44)

Accelerated lambda-iteration:

$$S^{(n+1)} - S^{(n)} = (1-(1-\varepsilon)\,\mathbf{\Lambda}^*)^{-1}\,[S^{\mathrm{FS}} - S^{(n)}]. \tag{5.45}$$

Different choices of approximate lambda operator

Core saturation

Scharmer modified core saturation

Scharmer operator: one point quadrature formula

$$I_\nu(\tau_{\nu\mu},\mu) \equiv I^{\pm}_{\nu\mu} = \mathbf{\Lambda}^*_{\nu\mu}[S_\nu(\tau_{\nu\mu})] \approx W^{\pm}_{\nu\mu}(\tau_{\nu\mu})\, S_\nu\left(f^{\pm}_{\nu\mu}(\tau_{\nu\mu})\right), \tag{5.52}$$

Use a linear test source function to deduce the W and f

$$\mu > 0 \qquad \begin{aligned} W^{+}_{\nu\mu} &= 1 \\ f^{+}_{\nu\mu} &= \tau_{\nu\mu} + 1 \end{aligned} \qquad \text{=EB} \tag{5.60}$$

$$\mu < 0 \qquad \begin{aligned} W^{-}_{\nu\mu} &= 1 - \mathrm{e}^{-\tau_{\nu\mu}} \\ f^{-}_{\nu\mu} &= \frac{\tau_{\nu\mu}}{1 - \mathrm{e}^{-\tau_{\nu\mu}}} - 1 \end{aligned} \tag{5.62}$$

Olson-Auer-Buchler (OAB) operator

The diagonal of the full lambda operator

- Easy to construct (Rybicki-Hummer 1991)
- Easy to “invert” (diagonal matrix)
- Easy to adopt to 3D geometry
- Slow convergence - needs acceleration steps

Convergence acceleration

Ng-acceleration

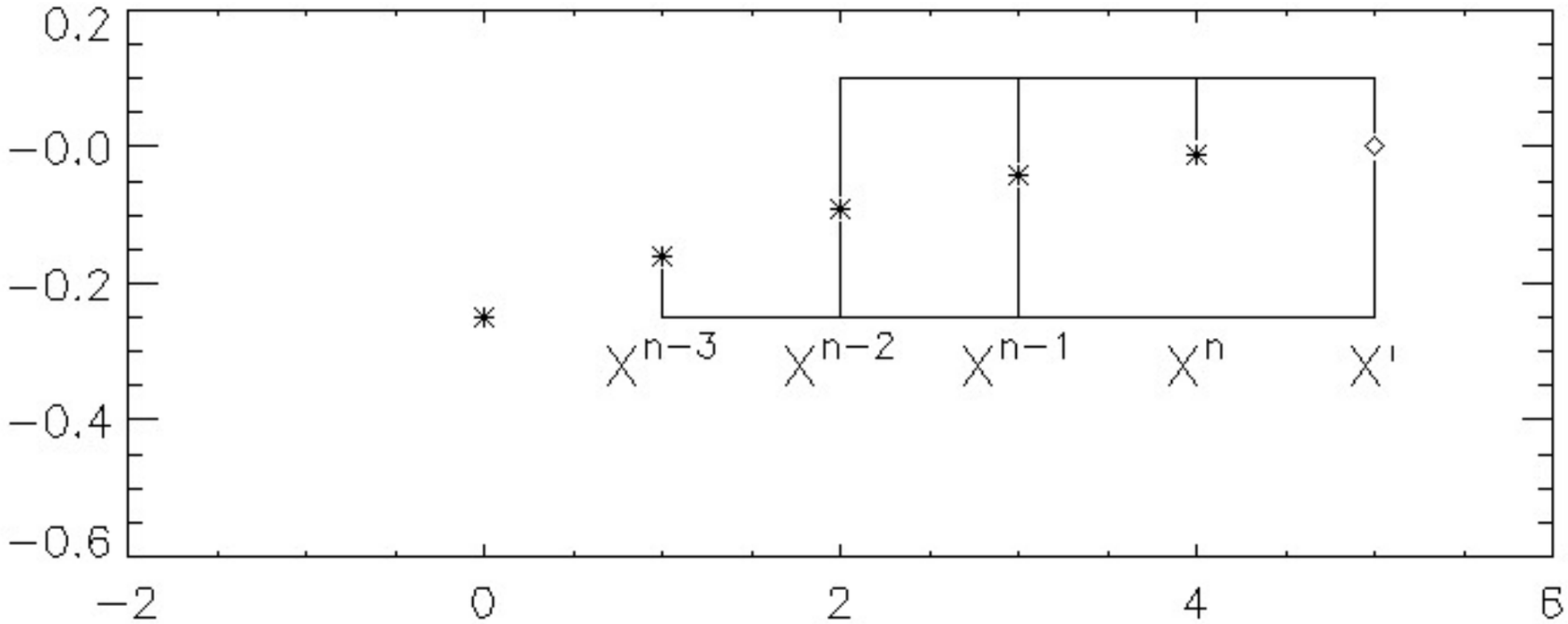

We use M previous iterations to extrapolate $\mathbf{x}$

$$\mathbf{x} = (1 - \sum_{m=1}^{M} \alpha_m)\mathbf{x}^{(n)} + \sum_{m=1}^{M} \alpha_m \mathbf{x}^{(n-m)}$$

$= \alpha_0$ because $\sum_{m=0}^{M} \alpha_m = 1$

Same coefficients applied to one iteration back

$$\mathbf{x}' = (1 - \sum_{m=1}^{M} \alpha_m)\mathbf{x}^{(n-1)} + \sum_{m=1}^{M} \alpha_m \mathbf{x}^{(n-m-1)}$$

α_m determined by minimizing distance between vectors $\mathbf{x}$ and $\mathbf{x}'$ with weights w

$$\text{minimize} \quad r^2 = \sum w_d (x_d - x'_d)^2$$

$$\frac{\partial}{\partial \alpha_i}\left[r^2\right] = 0, \forall i \qquad \text{gives}$$

$$0 = \sum_{d=1}^{N} w_d (x_d - x'_d)\left(\frac{\partial x_d}{\partial \alpha_i} - \frac{\partial x'_d}{\partial \alpha_i}\right), \forall i$$

$$0 = \sum_{d=1}^{N} w_d \left[(1 - \sum_{j=1}^{M} \alpha_j) x_d^{(n)} + \sum_{j=1}^{M} \alpha_j x_d^{(n-j)} - (1 - \sum_{j=1}^{M} \alpha_j) x_d^{(n-1)} - \sum_{j=1}^{M} \alpha_j x_d^{(n-j-1)}\right] \times$$

$$\times \left[-x_d^{(n)} + x_d^{(n-i)} + x_d^{(n-1)} - x_d^{(n-i-1)}\right]$$

introducing

$$\Delta x_d^{(n)} \equiv x_d^{(n)} - x_d^{(n-1)}$$

we get

$$\sum_{d=1}^{N} w_d \sum_{j=1}^{M} \alpha_j (-x_d^{(n)} + x_d^{(n-j)} + x_d^{(n-1)} - x_d^{(n-j-1)})[\Delta x_d^{(n-i)} - \Delta x_d^{(n)}] =$$

$$-\sum_{d=1}^{N} w_d [x_d^{(n)} - x_d^{(n-1)}][\Delta x_d^{(n-i)} - \Delta x_d^{(n)}]$$

we thus get a matrix equation

$$\boldsymbol{A\alpha} = \boldsymbol{b}$$

$$A_{ij} = \sum_{d=1}^{N} w_d (\Delta x_d^{(n)} - \Delta x_d^{(n-j)})(\Delta x_d^{(n)} - \Delta x_d^{(n-i)})$$

$$b_i = \sum_{d=1}^{N} w_d \Delta x_d^{(n)} (\Delta x_d^{(n)} - \Delta x_d^{(n-i)})$$

Linearization

$$x^2 = 2$$

$$(x^{(n)})^2 = 2 + E^{(n)}$$

$$(x^{(n)} + \delta x^{(n)})^2 = 2$$

$$(x^{(n)})^2 + 2x^{(n)}\delta x^{(n)} + \cancel{(\delta x^{(n)})^2} = 2$$

$$\boxed{2x^{(n)}\delta x^{(n)} = -E^{(n)}}$$

$$\delta x^{(n)} = \frac{-E^{(n)}}{2x^{(n)}} = \frac{2 - (x^{(n)})^2}{2x^{(n)}}$$

n	$x^{(n)}$	$lg\lvert x - \sqrt{2}\rvert$
0	1	-0,4
1	1,5	-1,1
2	1,416	-2,6
3	1,414216	-5,7
4	1,414213562	-11,8

Newton-Raphson

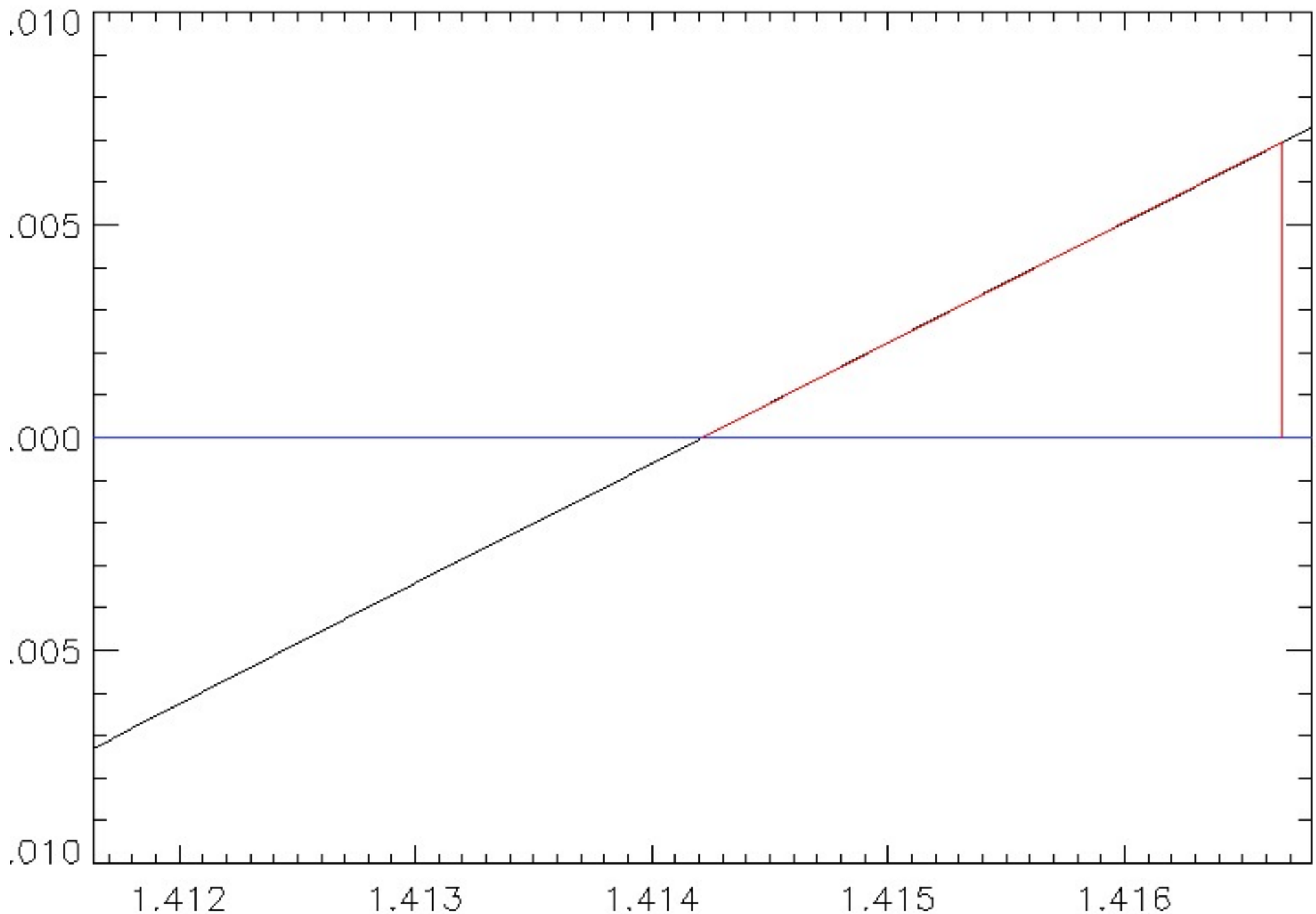

Convergence radius

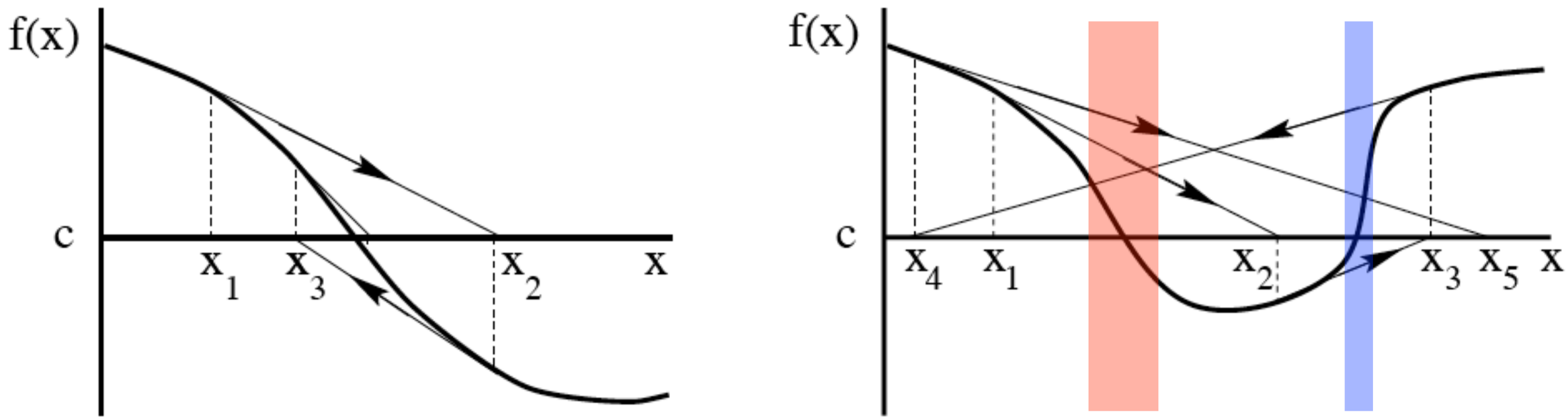

Figure 5.3: Newton-Raphson iteration to find the x for which $f(x) = c$. Find the tangent to $f(x)$ at the first estimate $x = x_1$, find its intersection $x = x_2$ with the constant c, find the tangent to $f(x)$ there, locate its intersection at $x = x_3$, and so on. It works well at left but won't find either solution at right. The convergence region around the solution is small.

Systems of equations

$$\begin{cases} 4x^2 + xy + y^2 - 16 = & 0 \\ 2x + xy^2 - 9 = & 0 \end{cases}$$

$$\begin{pmatrix} 8x^{(n)} + y^{(n)} & x^{(n)} + 2y^{(n)} \\ 2 + (y^{(n)})^2 & 2x^{(n)}y^{(n)} \end{pmatrix} \begin{pmatrix} \delta x^{(n)} \\ \delta y^{(n)} \end{pmatrix} = \begin{pmatrix} -4(x^{(n)})^2 - x^{(n)}y^{(n)} - (y^{(n)})^2 + 16 \\ -2x^{(n)} - x^{(n)}(y^{(n)})^2 + 9 \end{pmatrix}$$

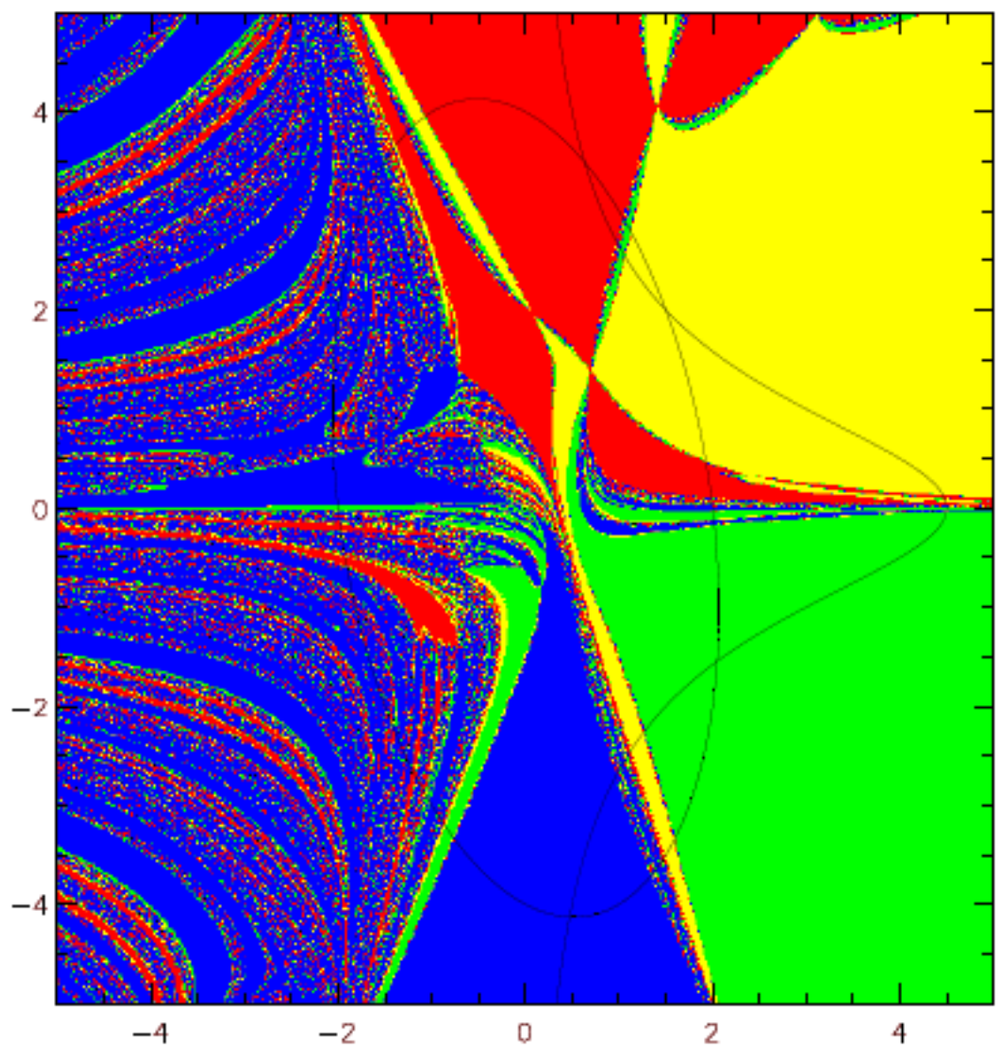

non-LTE

Transfer equation

The intensity depends on the opacity and the source function. The opacity depends on population densities.

Local Thermodynamic Equilibrium (LTE):

- Source function: Planck function
- Population densities: f(T,Ne) (Saha, Boltzmann)

non-LTE:

Source function and population densities depend on the non-local radiation field

non-LTE

$$\frac{dI}{d\tau} = S - I \qquad f(\nu, \mu)$$

$$S_l = \frac{n_j A_{ji} \Psi}{n_i B_{ij} \Phi - n_j B_{ji} \Psi_{se}} \qquad f(\nu, \mu)$$

$$\frac{Dn_i}{Dt} = \sum_{j \neq i}^{N} n_j P_{ji} - n_i \sum_{j \neq i}^{N} P_{ij}$$

P_{ij} is the probability for a transition from level i to level j

non-LTE (CRD)

$$P_{ij} = R_{ij} + C_{ij}$$

$$\begin{aligned} R_{ji} &= A_{ji} + B_{ji}\bar{J}_{ij} \\ R_{ij} &= B_{ij}\bar{J}_{ij} \end{aligned}$$

with A_{ji}, B_{ij} and B_{ji} the Einstein coefficients for spontaneous emission, absorption and stimulated emission, respectively. All these are given by atomic physics. $\bar{J}_{ij}$ is the absorption profile ($\phi_{\nu\mu}$) weighted integrated mean intensity:

$$\bar{J}_{ij} = \frac{1}{2}\int_{-1}^{1}\int_{0}^{\infty} \phi_{\nu\mu} I_{\nu\mu} d\nu d\mu$$

non-LTE

$$\frac{Dn_i}{Dt} = \sum_{j \neq i}^{N} n_j P_{ji} - n_i \sum_{j \neq i}^{N} P_{ij}$$

P_{ij} contains the intensities and thus an integral of the source function over the whole atmosphere. The source function depends on the population densities. We thus have a non-local, non-linear problem to solve.

Statistical equilibrium, particle conservation and radiative transfer equations are to be solved together through linearization

(Equation numbers from Uppsala Report 33)

$$n_i \sum_{j \neq i}^{n_l} P_{ij} - \sum_{j \neq i}^{n_l} n_j P_{ji} = 0 \qquad (2.1)$$

$$\sum_{j=1}^{n_l} n_j = n_{tot} \qquad (2.2)$$

$$\mu \frac{dI_{\nu\mu}}{dz} = -\kappa_{\nu\mu} I_{\nu\mu} + j_{\nu\mu} \qquad (2.3)$$

Rates are the sum of radiative and collisional rates

$$P_{ij} = R_{ij} + C_{ij} \tag{2.4}$$

Radiative (bb) and (bf) rates can be written in general form

$$R_{ij} = \begin{cases} \frac{1}{2}\int_{-1}^{1}\int_{0}^{\infty} \frac{4\pi}{h\nu}\alpha_{ji}G_{ji}(I_{\nu\mu} + \frac{2h\nu^3}{c^2})d\nu d\mu & \text{if } i > j \\ \frac{1}{2}\int_{-1}^{1}\int_{0}^{\infty} \frac{4\pi}{h\nu}\alpha_{ij}I_{\nu\mu}d\nu d\mu & \text{if } i < j \end{cases} \tag{2.5}$$

$$\alpha_{ij} = \begin{cases} B_{ij}\frac{h\nu_{ij}}{4\pi}\phi_{\nu\mu} & \text{(b-b);} \\ \alpha_c(\nu) & \text{(b-f).} \end{cases} \tag{2.6}$$

$$G_{ij} = \begin{cases} g_i/g_j & \text{(b-b);} \\ \frac{n_i^\star}{n_j^\star}e^{\frac{-h\nu}{kT}} & \text{(b-f).} \end{cases} \tag{2.7}$$

For bb transitions this simplifies to the familiar form:

$$R_{ij} = \begin{cases} A_{ij} + B_{ij}\bar{J}_{ij}, & \text{if } i > j; \\ B_{ij}\bar{J}_{ij}, & \text{if } i < j. \end{cases} \tag{2.8}$$

$$\bar{J}_{ij} = \frac{1}{2}\int_{-1}^{1}\int_{0}^{\infty} \phi_{\nu\mu} I_{\nu\mu} d\nu d\mu \tag{2.9}$$

$$\frac{1}{2}\int_{-1}^{1}\int_{0}^{\infty} \phi_{\nu\mu} d\nu d\mu = 1$$

Opacity and emissivity in general form:

Background (continuum) contribution

$$\kappa_{\nu\mu} = \kappa_{\nu c} + \alpha_{ij}(\nu, \mu)(n_i - G_{ij} n_j) \tag{2.10}$$

$$j_{\nu\mu} = j_{\nu c} + \frac{2h\nu^3}{c^2} G_{ij} \alpha_{ij}(\nu, \mu) n_j \tag{2.11}$$

$$S_{\nu\mu} = j_{\nu\mu} / \kappa_{\nu\mu} \tag{2.12}$$

(Equation numbers from Scharmer & Carlsson 1981)

$$n_i^{(n)} \sum_{j \neq i}^{n_l} P_{ij}^{(n)} - \sum_{j \neq i}^{n_l} n_j^{(n)} P_{ji}^{(n)} = E_i^{(n)} \tag{3.1}$$

$$n_i^{(n+1)} = n_i^{(n)} + \delta n_i^{(n)} \tag{3.2}$$

$$P_{ij}^{(n+1)} = P_{ij}^{(n)} + \delta P_{ij}^{(n)} \tag{3.3}$$

$$n_i^{(n+1)} \sum_{j \neq i}^{n_l} P_{ij}^{(n+1)} - \sum_{j \neq i}^{n_l} n_j^{(n+1)} P_{ji}^{(n+1)} = 0 \tag{3.4}$$

We insert 3.2 and 3.3 in 3.4, subtract 3.1 and neglect non-linear terms

$$\delta n_i^{(n)} \sum_{j\neq i}^{n_l} P_{ij}^{(n)} + n_i^{(n)} \sum_{j\neq i}^{n_l} \delta P_{ij}^{(n)} - \sum_{j\neq i}^{n_l} \delta n_j^{(n)} P_{ji}^{(n)} \quad (3.5)$$

$$- \sum_{j\neq i}^{n_l} n_j^{(n)} \delta P_{ji}^{(n)} = -E_i^{(n)}$$

$$\delta P_{ij}^{(n)} = B_{ij} \delta \bar{J}_{ij}^{(n)} = B_{ij} \frac{1}{2} \int_{-1}^{1} \int_{0}^{\infty} \phi_{\nu\mu} \delta I_{\nu\mu}^{(n)} d\nu d\mu \quad (3.6)$$

We need to express $\delta I_{\nu\mu}^{(n)}$ in terms of $\delta n_i^{(n)}$ and $\delta n_j^{(n)}$

We use the transfer equation:

$$\mu \frac{dI_{\nu\mu}^{(n)}}{dz} = -\kappa_{\nu\mu}^{(n)} I_{\nu\mu}^{(n)} + j_{\nu\mu}^{(n)} \tag{3.7}$$

$$\mu \frac{d}{dz} \delta I_{\nu\mu}^{(n)} = -\kappa_{\nu\mu}^{(n)} \delta I_{\nu\mu}^{(n)} - I_{\nu\mu}^{(n)} \delta\kappa_{\nu\mu}^{(n)} + \delta j_{\nu\mu}^{(n)} \tag{3.8}$$

Usual definition of optical depth along a ray

$$d\tau_{\nu\mu}^{(n)} = -\kappa_{\nu\mu}^{(n)} dz/\mu \tag{3.9}$$

We *define* an equivalent source function perturbation:

$$\delta S_{\nu\mu}^{(n)} = \delta j_{\nu\mu}^{(n)} / \kappa_{\nu\mu}^{(n)} - I_{\nu\mu}^{(n)} \delta\kappa_{\nu\mu}^{(n)} / \kappa_{\nu\mu}^{(n)} \tag{3.10}$$

This gives the usual transfer equation, now for the perturbations

$$\frac{d}{d\tau_{\nu\mu}^{(n)}} \delta I_{\nu\mu}^{(n)} = \delta I_{\nu\mu}^{(n)} - \delta S_{\nu\mu}^{(n)} \tag{3.11}$$

$$\kappa_{\nu\mu} = \kappa_{\nu c} + \alpha_{ij}(\nu,\mu)(n_i - G_{ij}n_j) \tag{2.10}$$

$$j_{\nu\mu} = j_{\nu c} + \frac{2h\nu^3}{c^2} G_{ij}\alpha_{ij}(\nu,\mu)n_j \tag{2.11}$$

$$\delta S^{(n)}_{\nu\mu} = \delta j^{(n)}_{\nu\mu}/\kappa^{(n)}_{\nu\mu} - I^{(n)}_{\nu\mu}\delta\kappa^{(n)}_{\nu\mu}/\kappa^{(n)}_{\nu\mu} \tag{3.10}$$

Gives

$$\delta S^{(n)}_{\nu\mu} = c^{(n)}_l \delta n^{(n)}_i + c^{(n)}_u \delta n^{(n)}_j \tag{3.13}$$

$$c^{(n)}_l = -\alpha_{ij}(\nu,\mu) I^{(n)}_{\nu\mu}/\kappa^{(n)}_{\nu\mu} \tag{3.14}$$

$$c^{(n)}_u = G_{ij}\alpha_{ij}(\nu,\mu)\left(\frac{2h\nu^3}{c^2} + I^{(n)}_{\nu\mu}\right)/\kappa^{(n)}_{\nu\mu} \tag{3.15}$$

We have thus expressed $\delta S^{(n)}_{\nu\mu}$ in $\delta n^{(n)}_i$ and $\delta n^{(n)}_j$

$$\delta I_{\nu\mu}^{(n)} = \Lambda_{\nu\mu}^{(n)}[\delta S_{\nu\mu}^{(n)}] \qquad (3.12)$$

completes the task of expressing

$\delta I_{\nu\mu}^{(n)}$ in terms of $\delta n_i^{(n)}$ and $\delta n_j^{(n)}$

We now have a non-local but linear system of equations for the unknowns $\delta \mathbf{n}$

For $\Lambda_{\nu\mu}^{(n)}$ we may choose

Exact operator: slow to construct, slow to invert
Scharmer's operator: faster and global
Local operator (OAB): fast to construct, invert, but slow convergence.

Coefficient matrix for Scharmer operator

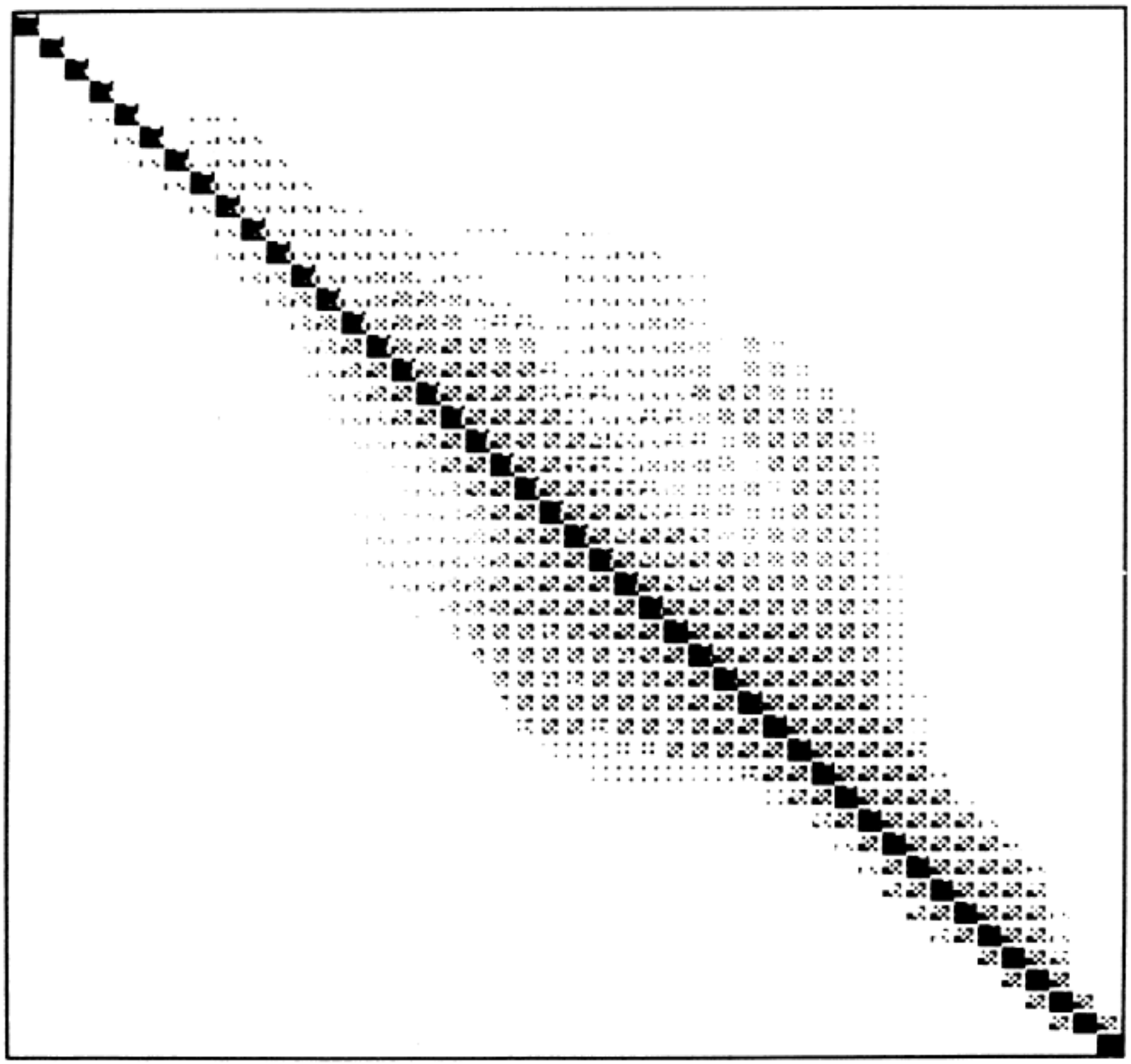

Convergence properties

Lambda iteration

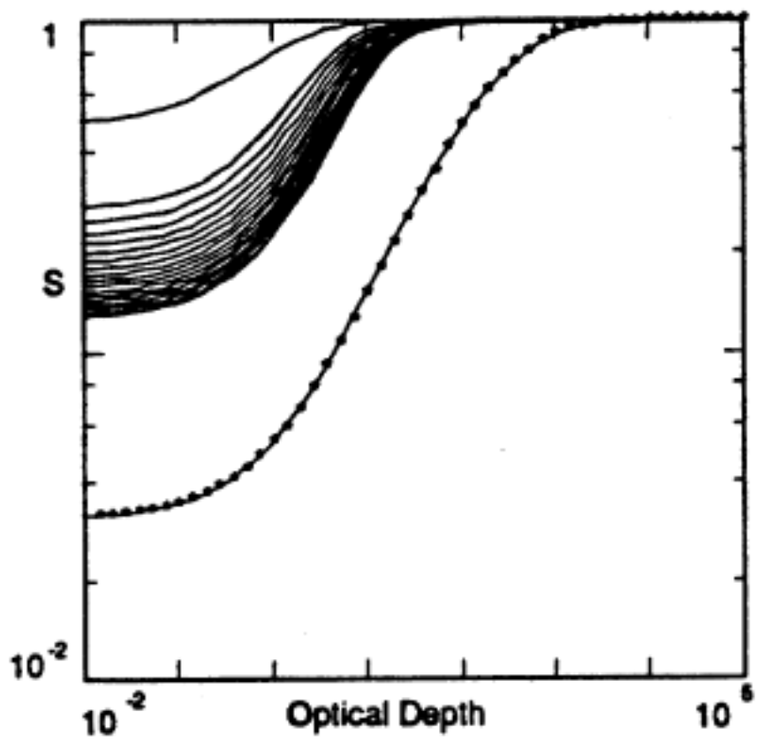

Scharmer operator

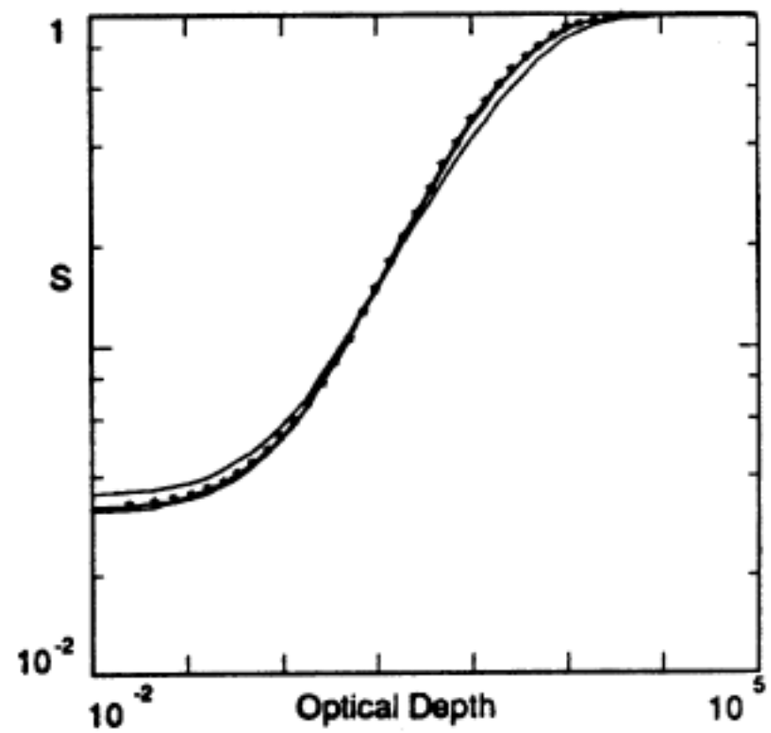

Local operator

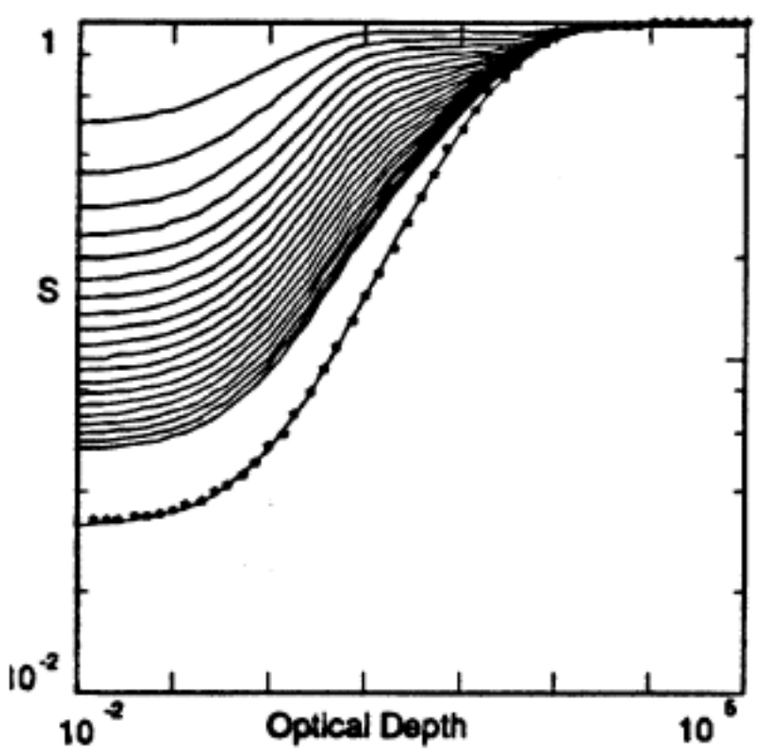

Local + acceleration

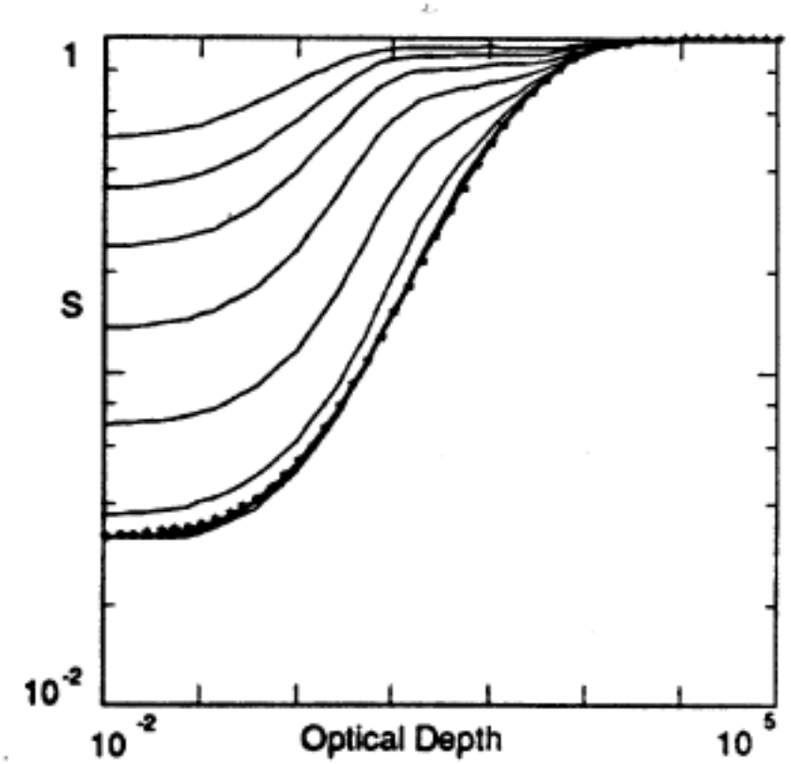

CRSW

Collisional-Radiative Switching

Multiply collisional rates with a factor that is changed from iteration to iteration

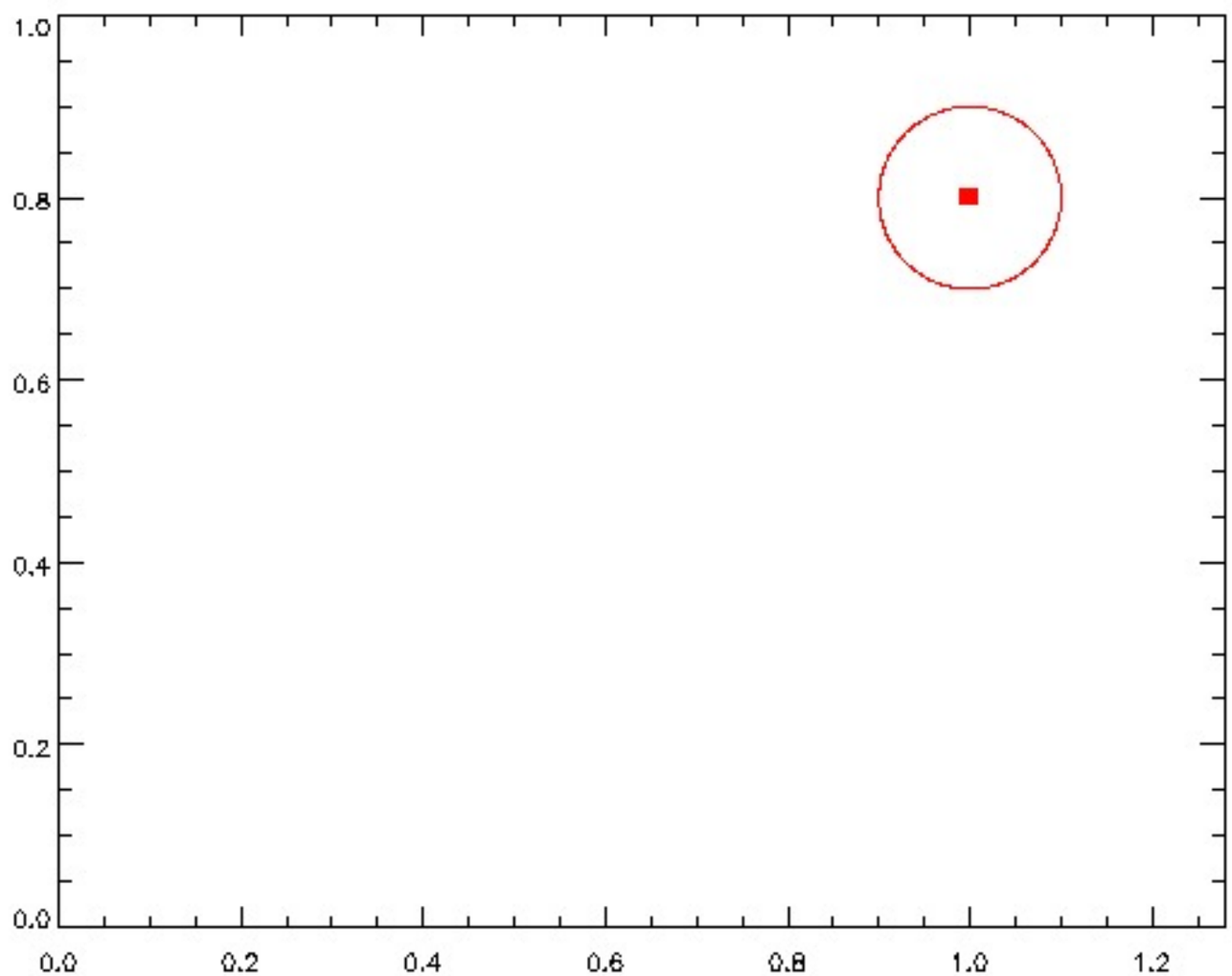

2D-3D

In 1D all rays pass through all grid "points" (planes).

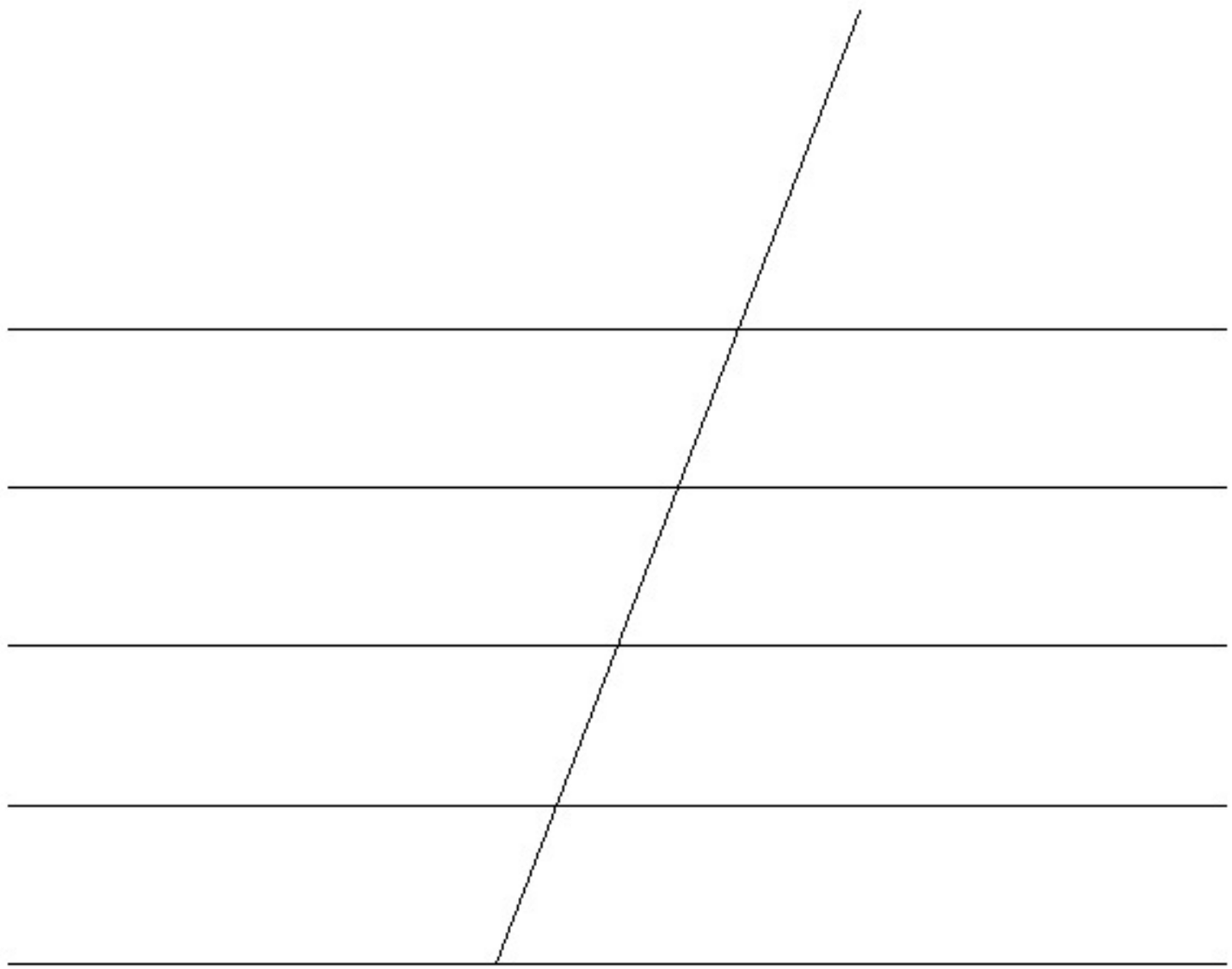

Long characteristics through all grid-points

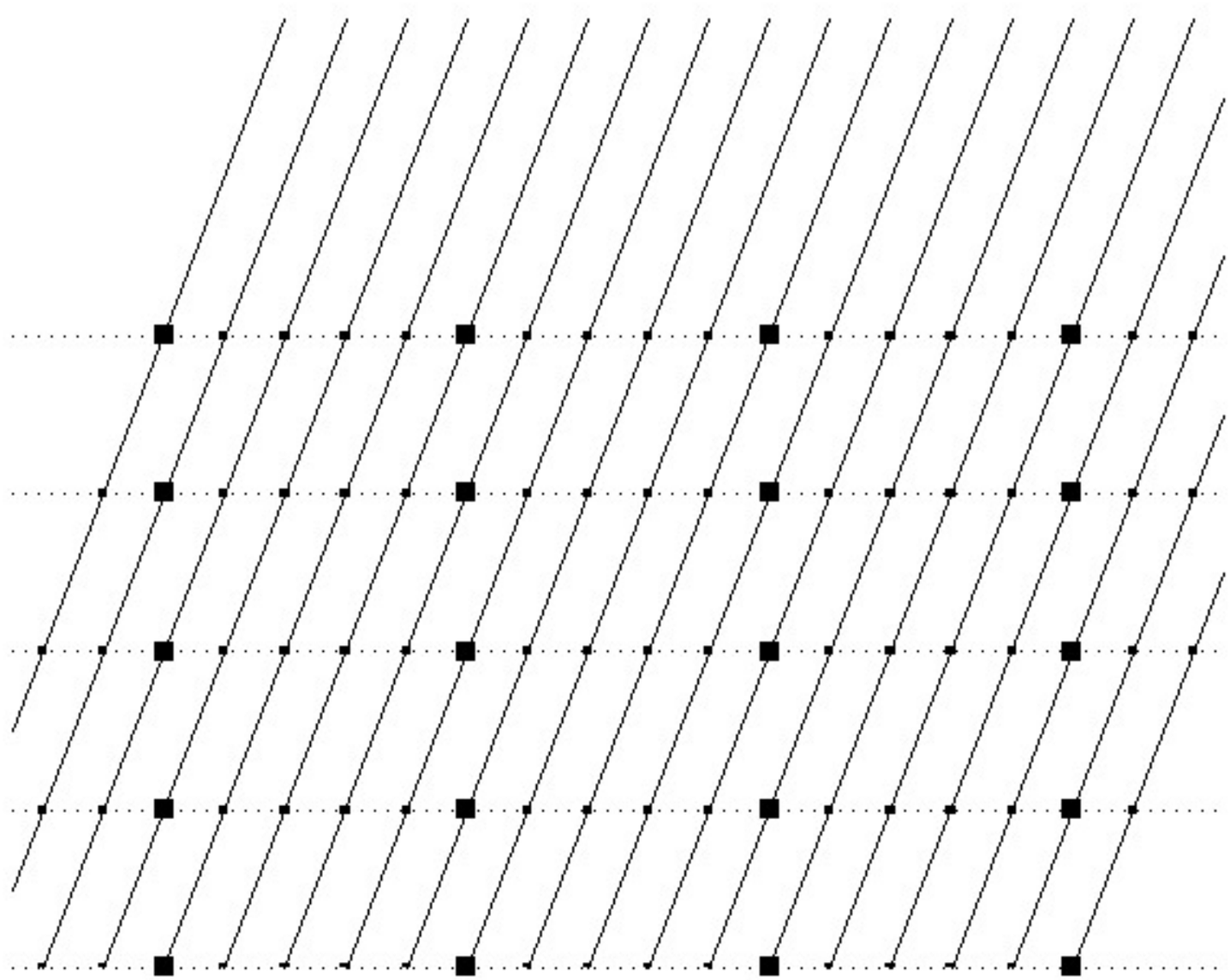

Many rays: slow

Long characteristics through one plane

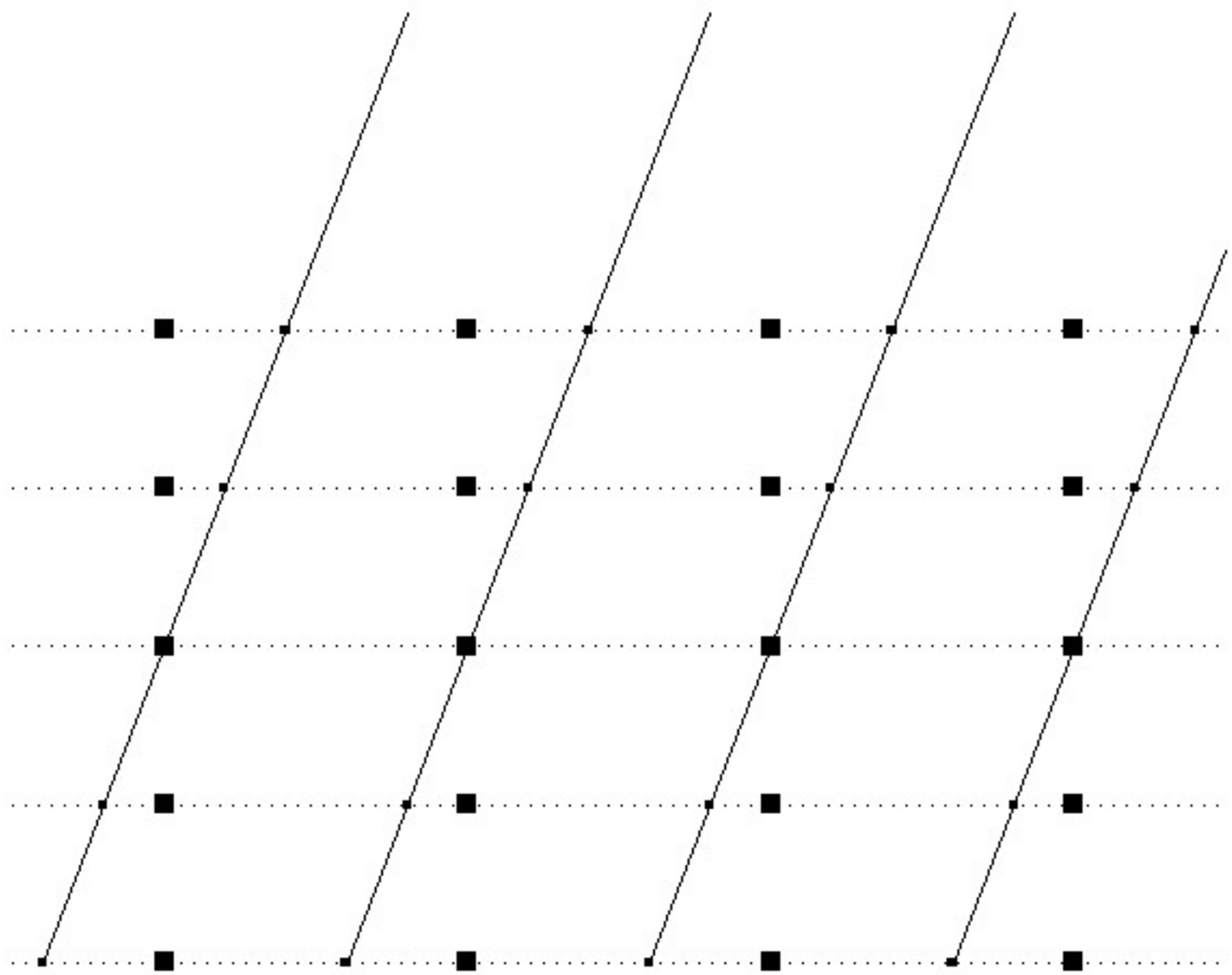

Fast but may miss localized sources

Short characteristics

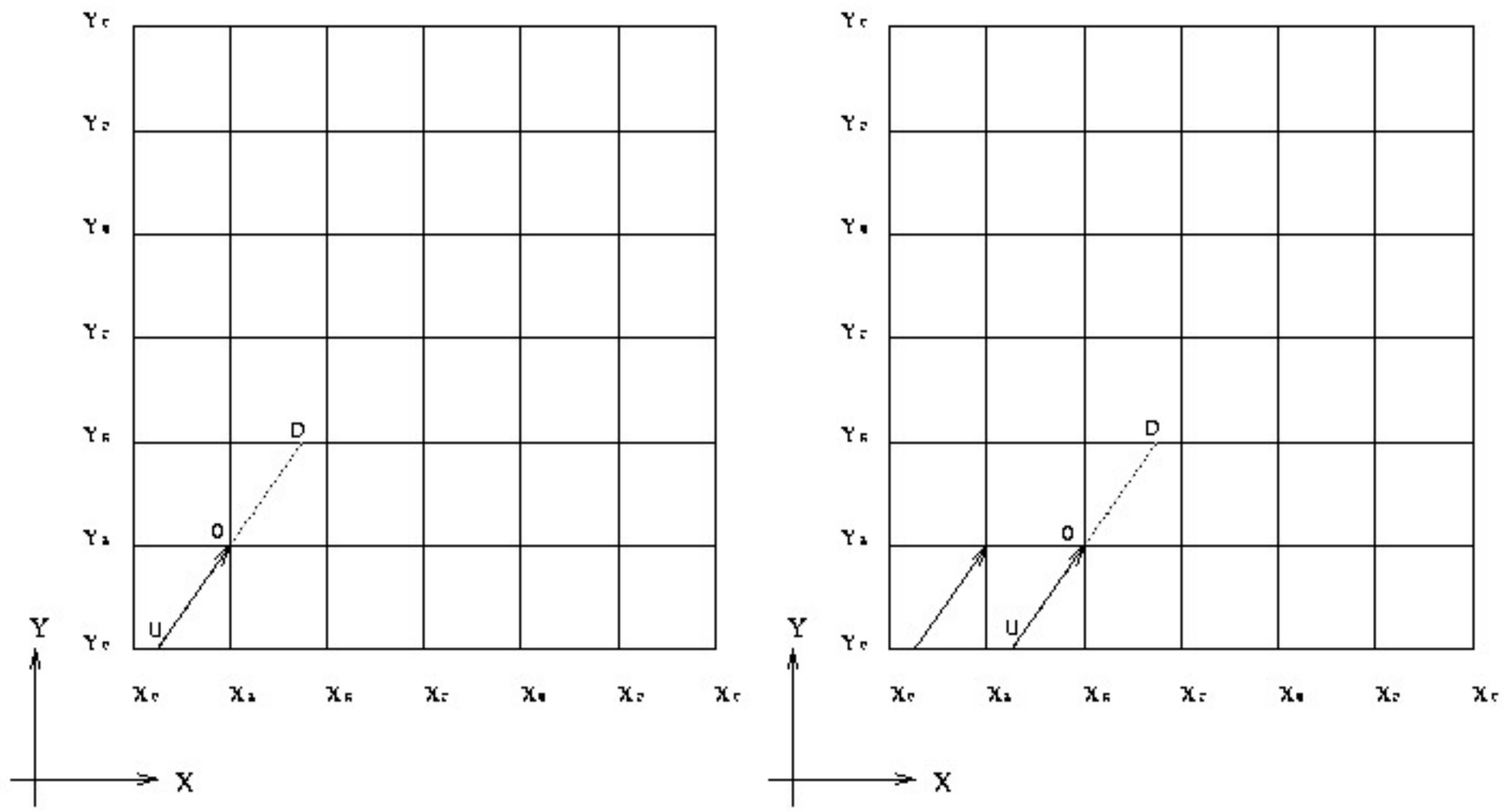

Approximate S through 3 points (U, O, D), integrate analytically

Diffusive

Short characteristics in 3D

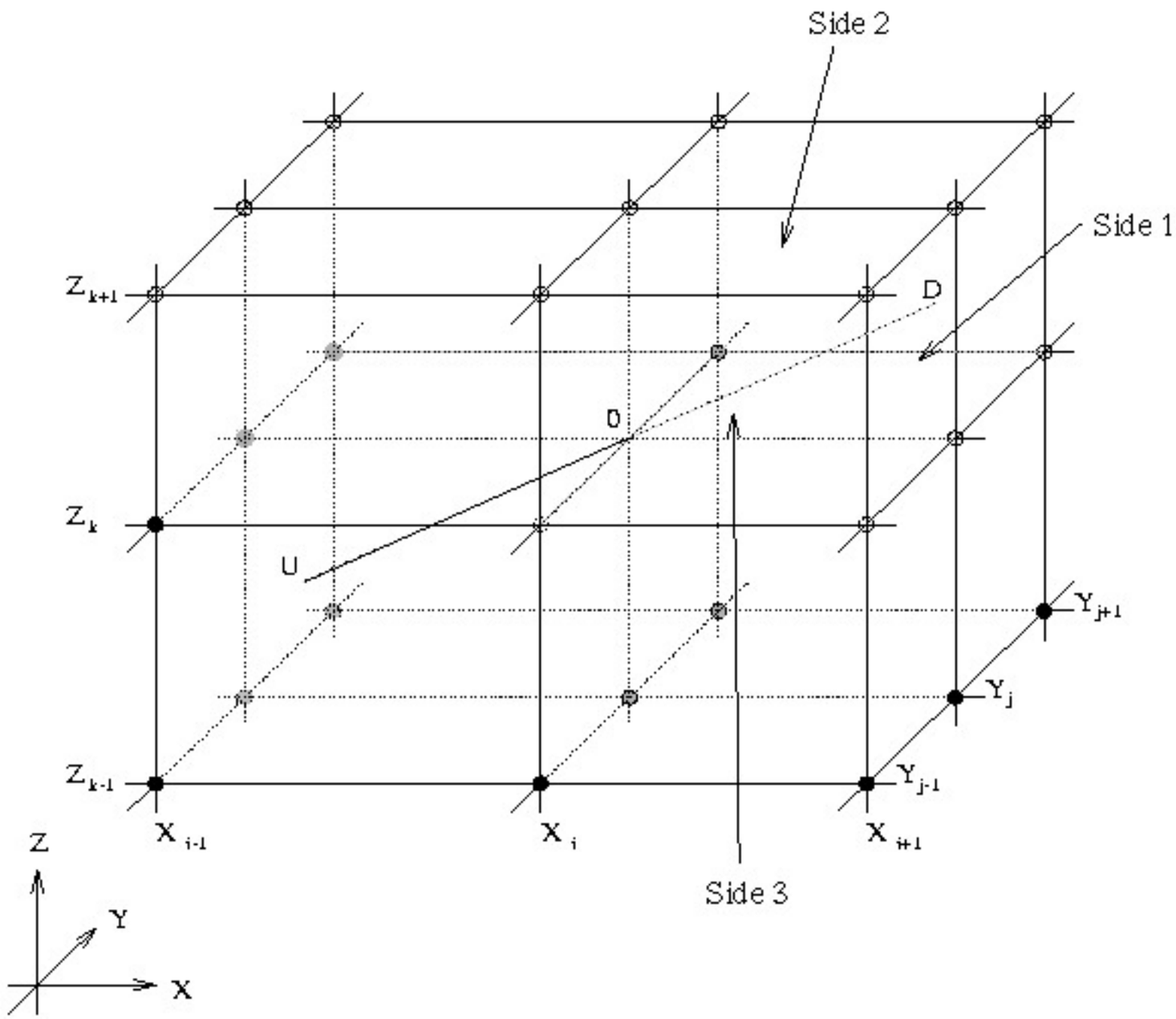

Parallelization strategies

over rays: SMP OK

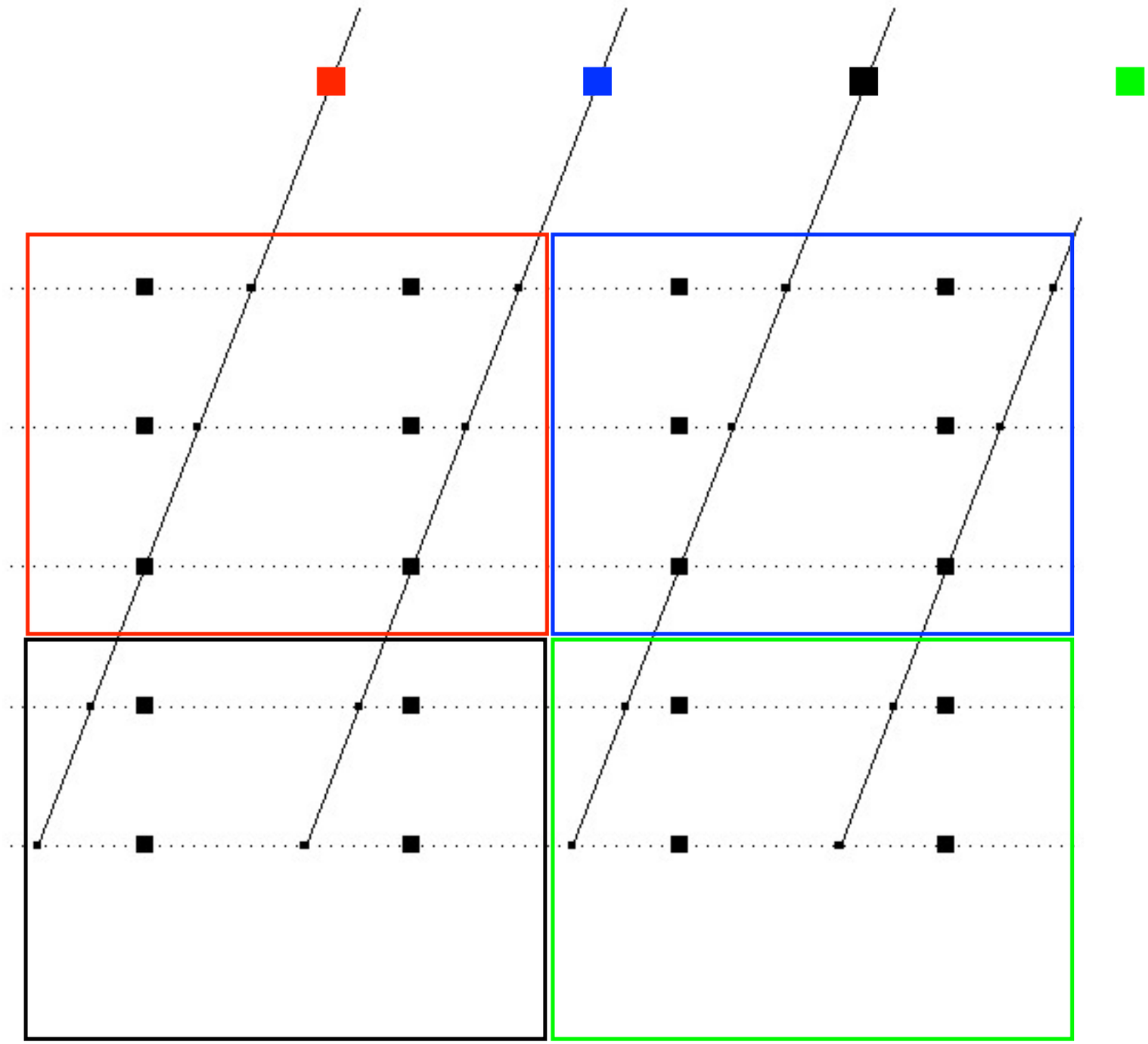

MPI: massive communication

Parallelization strategies

Local rays

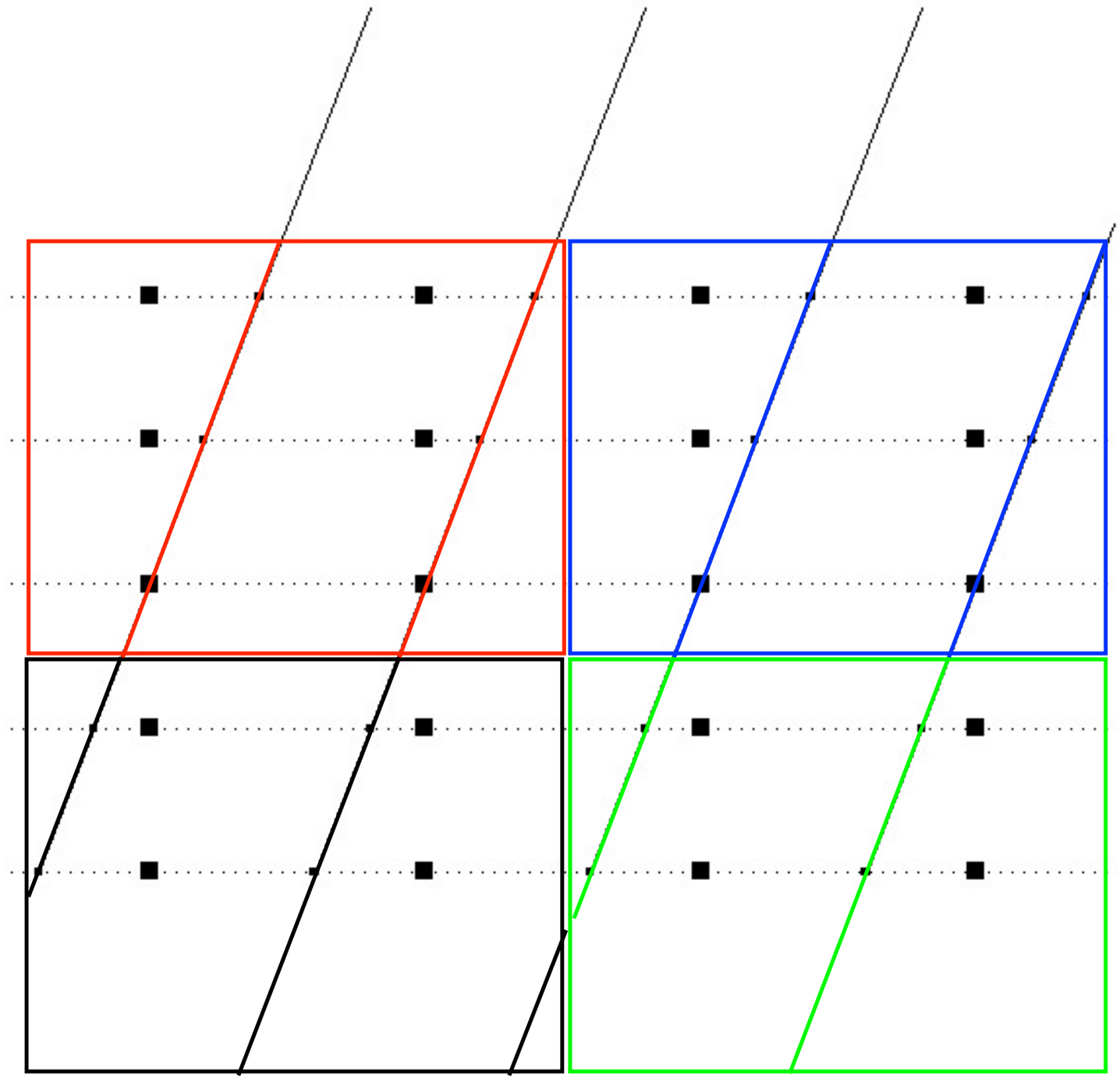

MPI: simple communication, complicated admin

Short characteristics

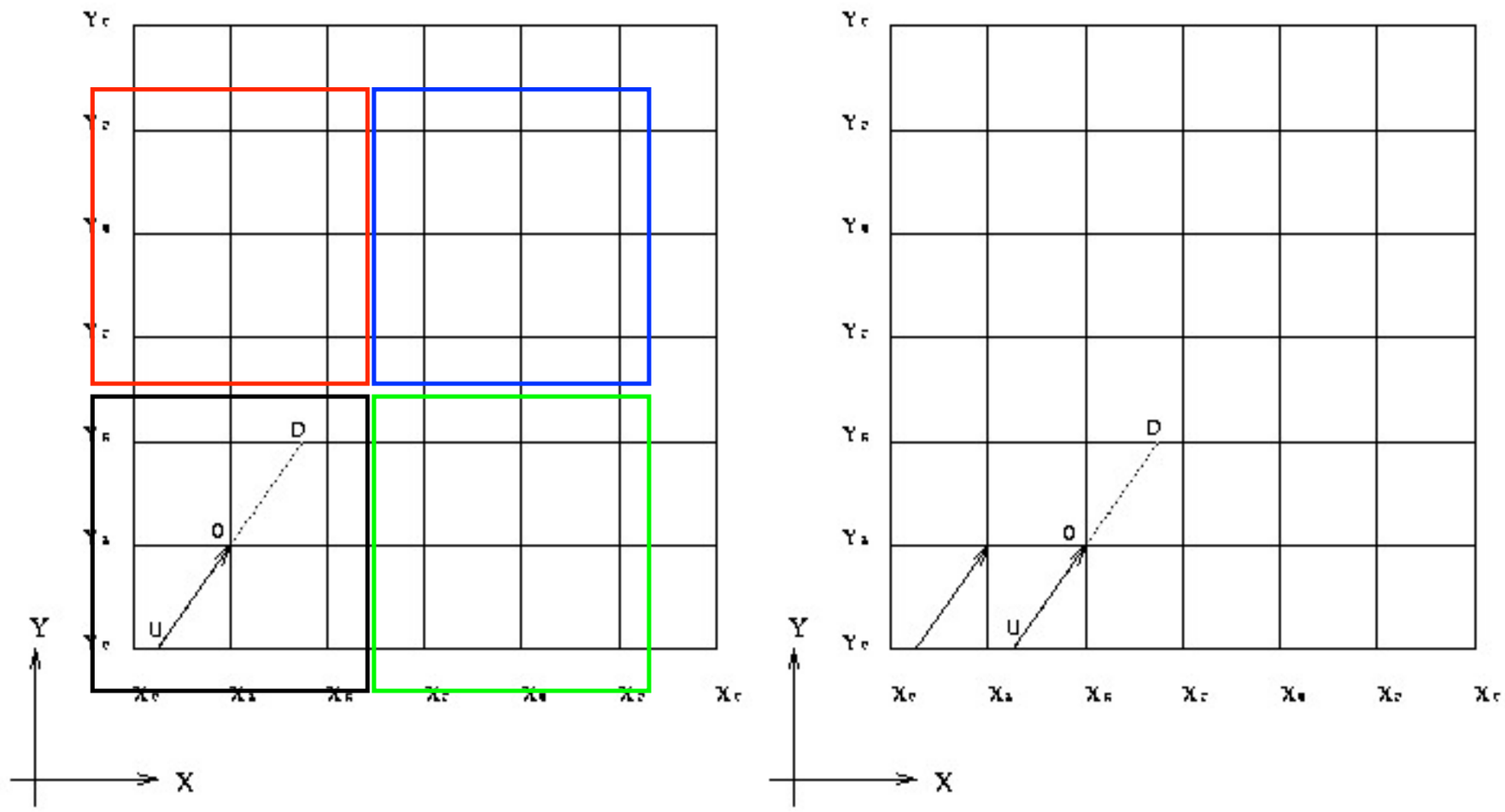

Order: passive processors
multiple sweeps

Energy equation

Radiative equilibrium

$$F_{\mathrm{rad}} = \sigma T_{\mathrm{eff}}^4$$

$$\nabla F = 0$$

$$\mu \frac{dI_\nu}{dz} = \chi_\nu (S_\nu - I_\nu)$$

integrate over angle

$$\frac{dF_\nu}{dz} = 2\pi \int_{-1}^{1} \chi_\nu (S_\nu - I_\nu) d\mu$$

integrate over frequency

$$\frac{dF}{dz} = 2\pi \int_{-1}^{1} \int_{0}^{\infty} \chi_\nu (S_\nu - I_\nu) d\nu d\mu = 0$$

isotropic χ_ν, S_ν gives

$$\int_{0}^{\infty} \chi_\nu (S_\nu - J_\nu) d\nu = 0$$

NB! flux not specified, only its constancy

We thus need to solve the transfer equation at many frequencies throughout the spectrum

OS: Opacity sampling. Sample throughout the spectrum, enough points to get a statistically good representation of the integral $\sim$10000 points.

ODF: Opacity distribution function. Reorder frequency points to get smoother function. Fewer points needed $\sim$1000 points. Assumes that high opacity line up.

Multi group opacities. As ODF but average also the source function. $\sim$4 points.

ODF

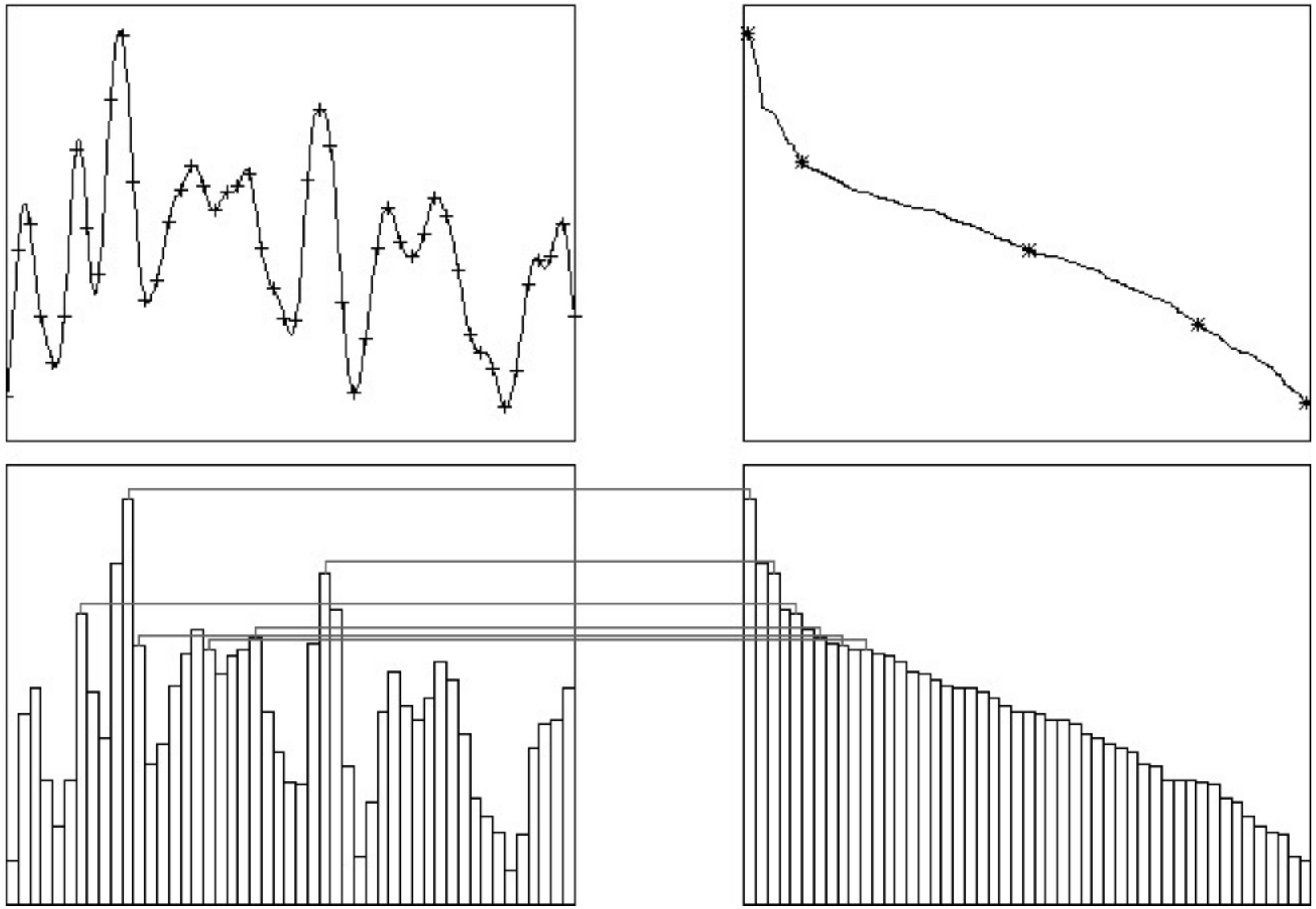

Multi-group opacities

$$\int Y_\lambda d\lambda = \sum_\lambda Y_{\lambda ij} w_{ij} = \sum_i \sum_j Y_{\lambda ij} w_{ij}$$

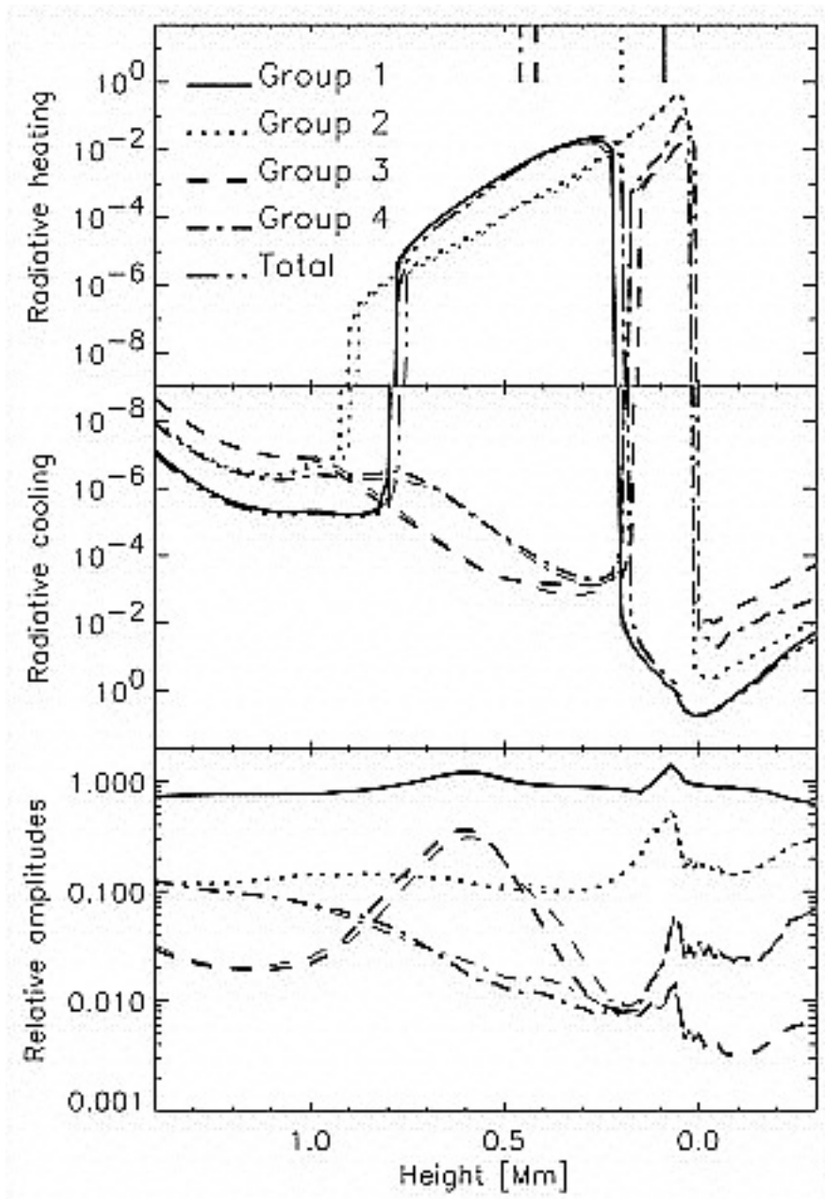

Linearization

We used to have:

$$\delta j_{\nu\mu} = \frac{\partial j_{\nu\mu}}{\partial n_i}\delta n_i + \frac{\partial j_{\nu\mu}}{\partial n_j}\delta n_j$$

If the atmosphere is not given we get extra variables to solve for:

$$\delta\rho, \delta T, \delta n_e$$

and extra derivatives with respect to these variables

$$\delta j_{\nu\mu} = \frac{\partial j_{\nu\mu}}{\partial \rho}\delta\rho + \frac{\partial j_{\nu\mu}}{\partial T}\delta T + \frac{\partial j_{\nu\mu}}{\partial n_e}\delta n_e + \sum_{i=1}^{N_L}\frac{\partial j_{\nu\mu}}{\partial n_i}\delta n_i$$

$$\frac{\partial j_{\nu c}}{\partial x}, \frac{\partial \kappa_{\nu c}}{\partial x}, \frac{\partial \alpha_{ij}}{\partial x}, \frac{\partial G_{ij}}{\partial x}, \frac{\partial C_{ij}}{\partial x}$$

are no longer zero

Extra equations: Hydrostatic equilibrium
Energy equation, charge conservation

Examples, non-LTE

- non-local, non-linear
- 1D: Accelerated Lambda Iteration (ALI)
  - 500-1000 atomic levels possible
  - codes available (MULTI, RH (Uitenbroek),...)
- 3D: ALI + long or short characteristics
  - 20-30 levels possible
  - not as easy to use as black-box (convergence problems, discretization issues etc) (RH (Uitenbroek), MULTI3D)

Examples

- Contribution & response functions
- non-Statistical equilibrium
- 3D simulations from convection zone to corona
- 3D radiative transfer
- IRIS
- Mg II diagnostics

Contribution functions

$$I_{\nu\mu}(0) = \int C_I(x)dx$$

$$C_I(\tau_\nu) = \frac{1}{\mu} S_\nu(\tau_\nu) e^{-\tau_\nu/\mu}$$

$$C_I(z) = \frac{1}{\mu} S_\nu(\tau_\nu) e^{-\tau_\nu/\mu} \chi_\nu$$

Contribution functions give the contributions from different layers of the atmosphere to a given quantity.

Rewrite of contribution function

$$C_I(z) = \frac{1}{\mu} S_\nu(\tau_\nu) e^{-\tau_\nu/\mu} \chi_\nu$$

$$C_I(z) = S_\nu(\tau_\nu) \frac{1}{\mu} \tau_\nu e^{-\tau_\nu/\mu} \frac{\chi_\nu}{\tau_\nu}$$

Source term

Maximum for $\tau_\nu = \mu$

Dynamic term

G-band vs Ca H filtergram

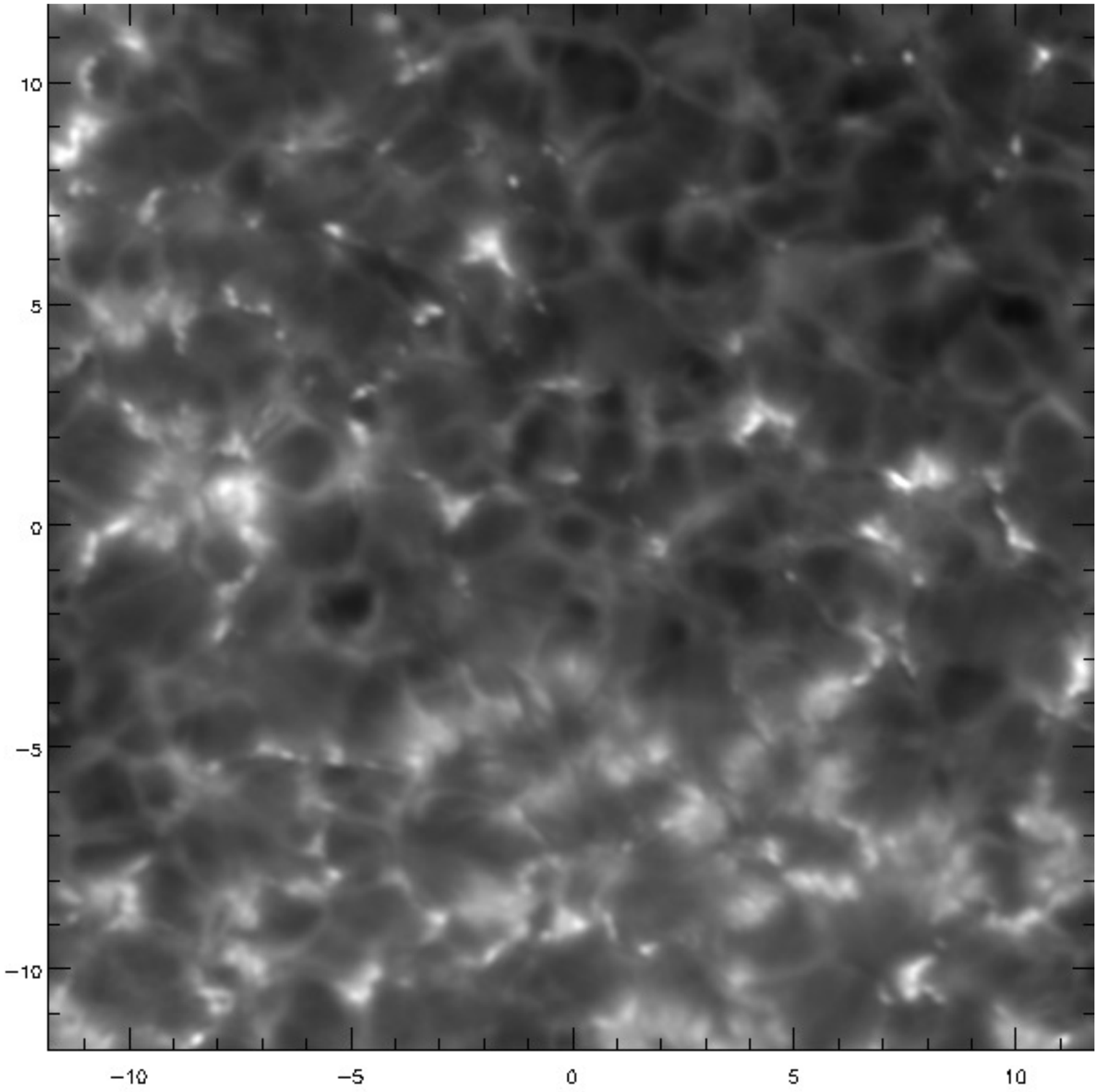

Synthetic spectrum

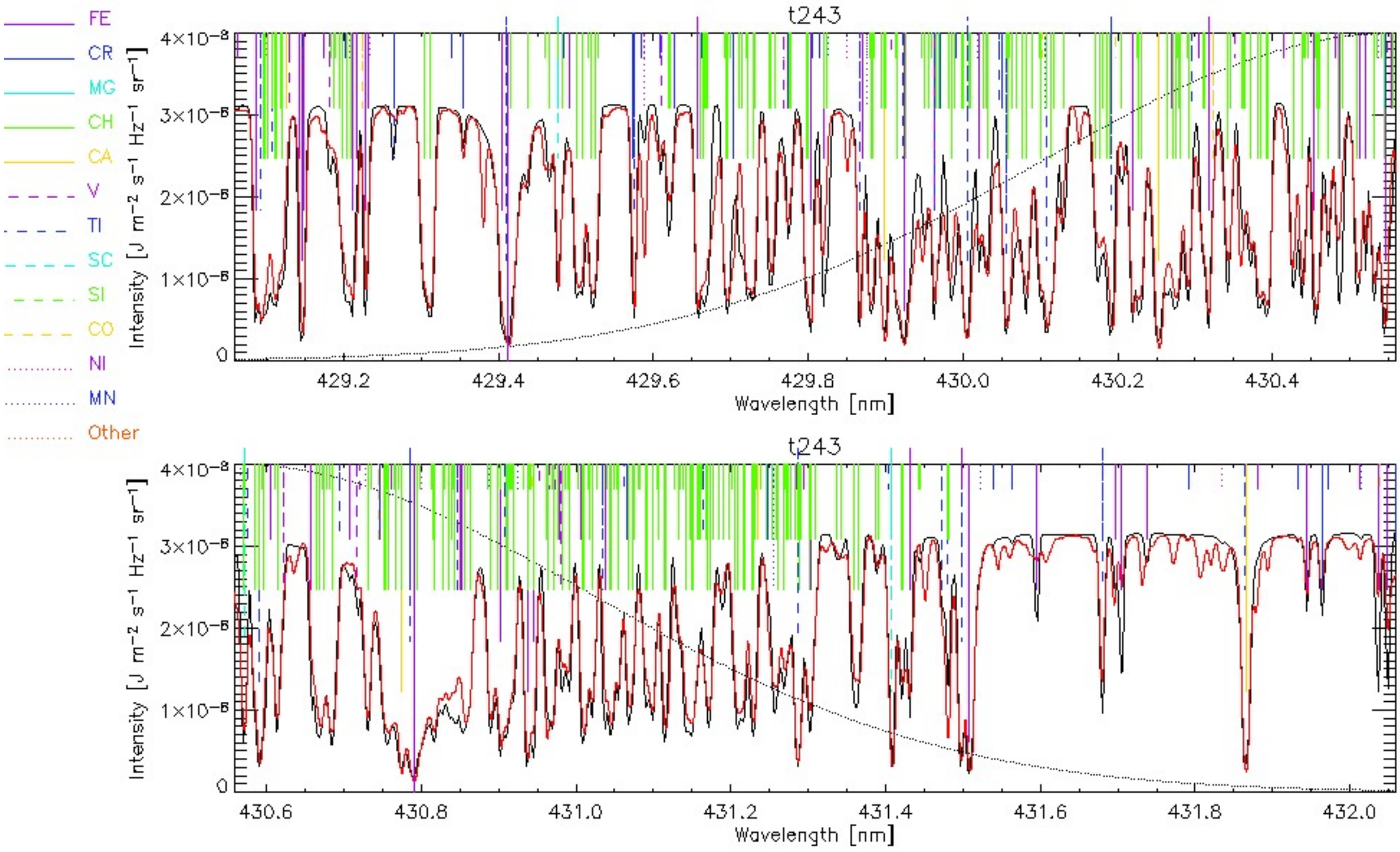

LaPalma Ca H filters

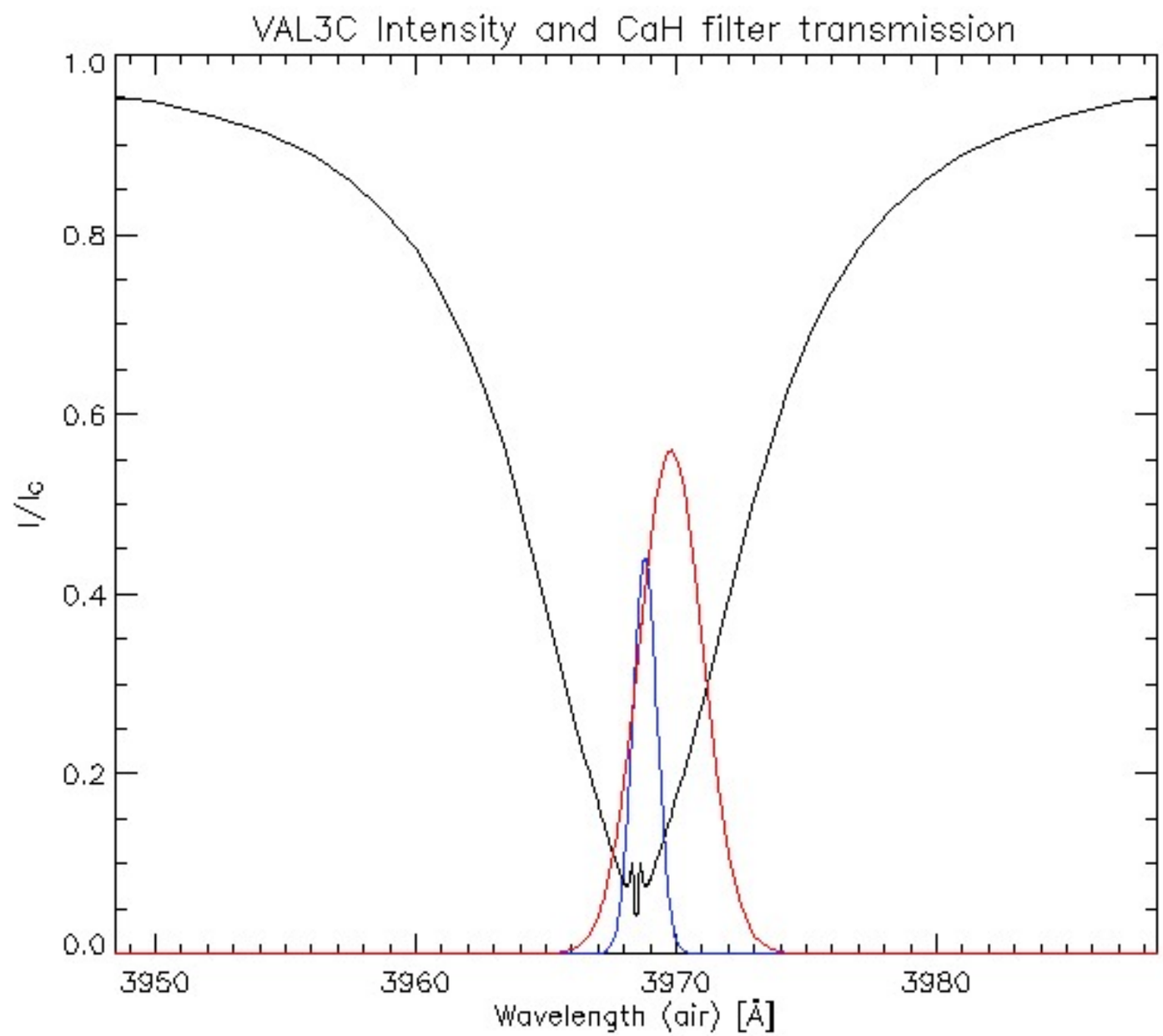

Contribution to Ca-H filter intensity

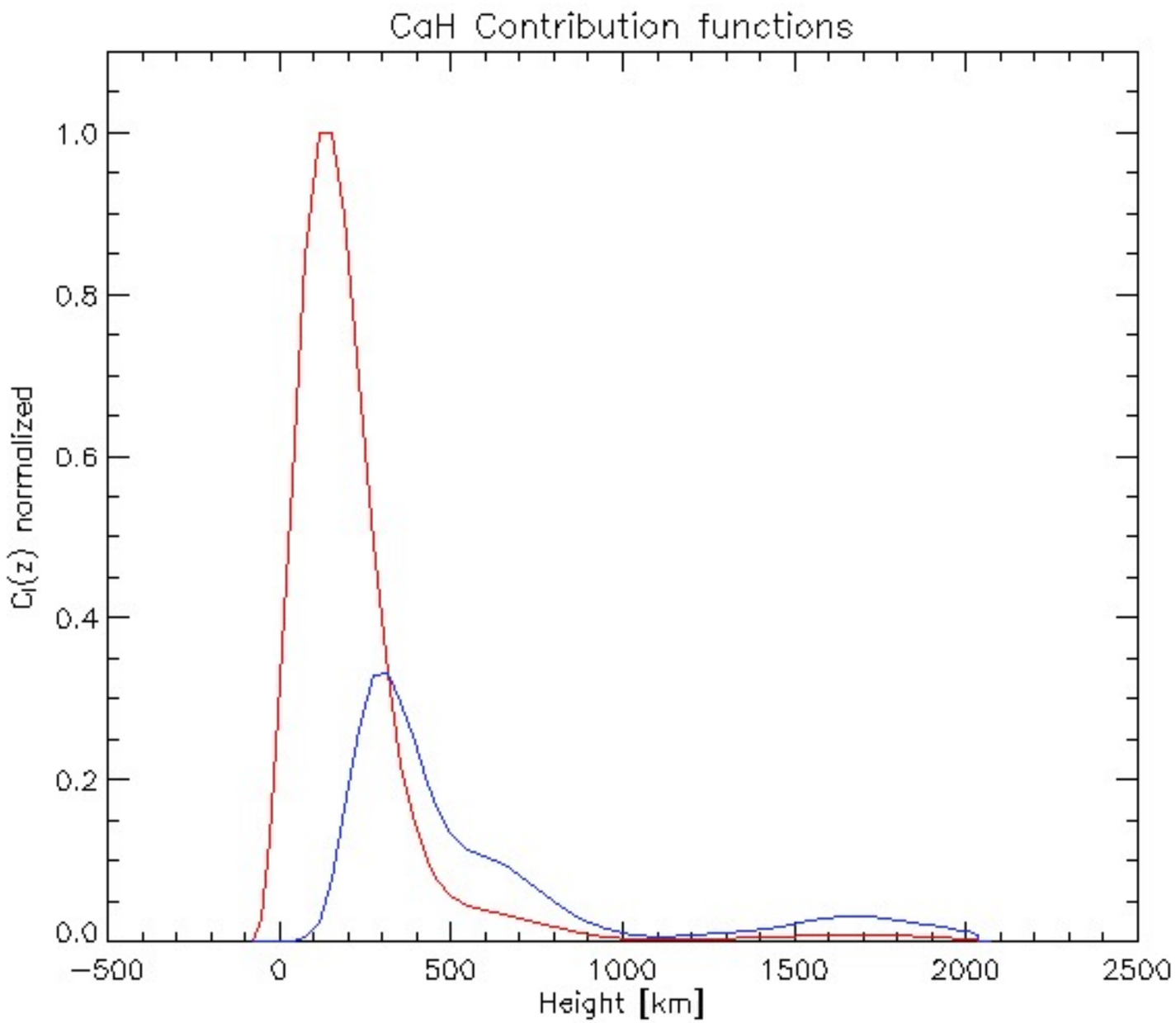

Response functions

$$\frac{\Delta I}{I} = \int_{-\infty}^{\infty} R(z) \frac{\Delta T}{T}(z) dz$$

Numerical calculation of a response function

$$\frac{\Delta T}{T}(z) = C, z \leq z'$$
$$= 0 \quad z > z'$$

$$\frac{\Delta I}{I}(z') = C \int_{-\infty}^{z'} R(z) dz$$

$$R(z') = \frac{1}{C} \frac{d}{dz'} \frac{\Delta I}{I}(z')$$

Response functions of Hinode wide band filters

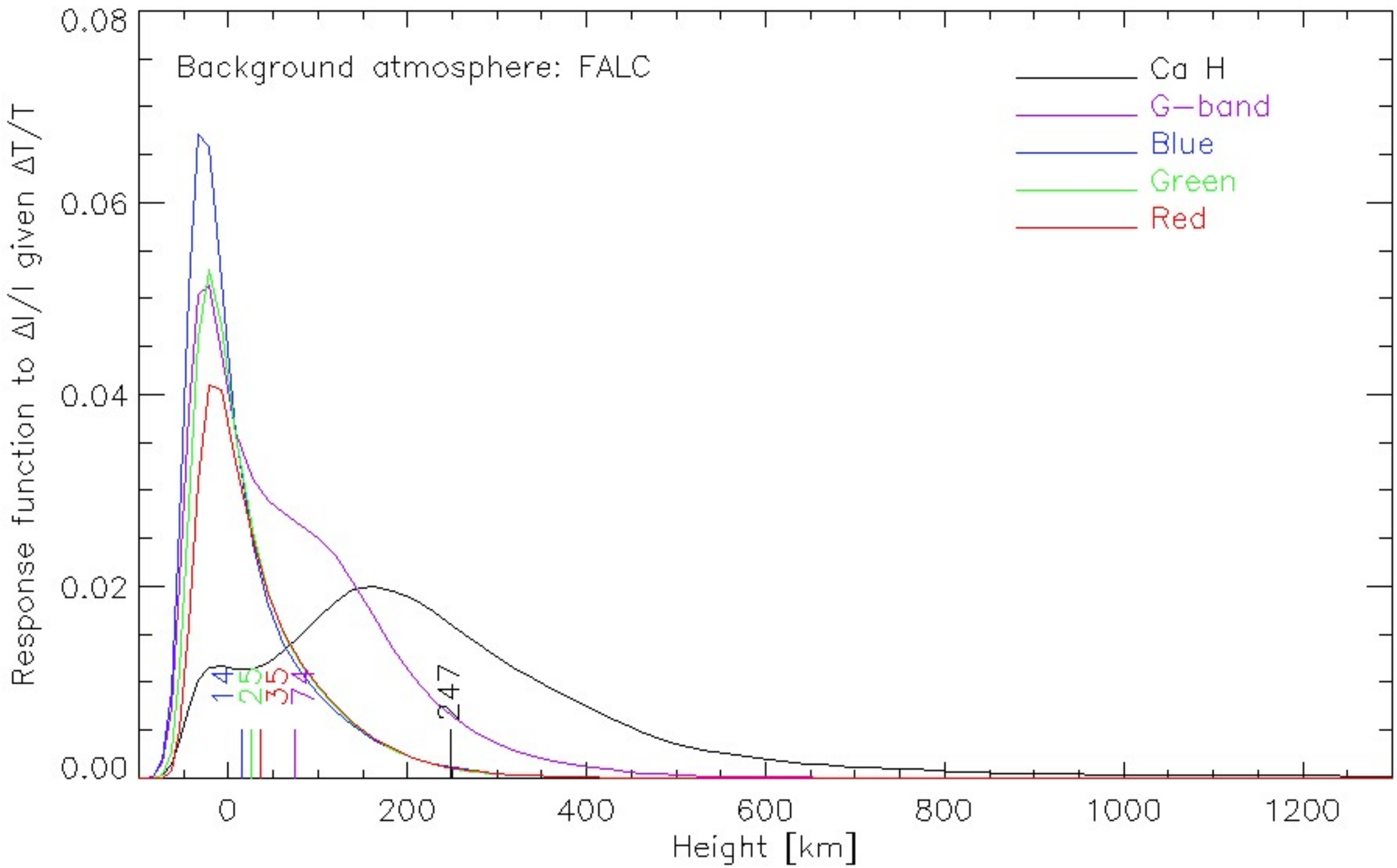

non-Statistical equilibrium

- 2-level case
- linear rate matrix
- hydrogen ionization

non-Statistical equilibrium

$$\frac{Dn_i}{Dt} = \sum_{j \neq i}^{N} n_j P_{ji} - n_i \sum_{j \neq i}^{N} P_{ij}$$

2-level case:

$$n_1(t) = n_1(\infty) + (n_1(0) - n_1(\infty))e^{-(P_{12}+P_{21})t}$$

Timescale depends on both upward and downward rate
There is only one timescale involved

non-Statistical equilibrium

$$\frac{Dn_i}{Dt} = \sum_{j \neq i}^{N} n_j P_{ji} - n_i \sum_{j \neq i}^{N} P_{ij}$$

$$\frac{D\mathbf{n}}{Dt} = \mathbf{W}\mathbf{n}$$

linear rate matrix:

Populations can be written as linear combination of eigenvectors of W with time-evolution given by eigenvalues of W (Judge 2005, JQSRT, 92, 479)

Hydrogen ionization

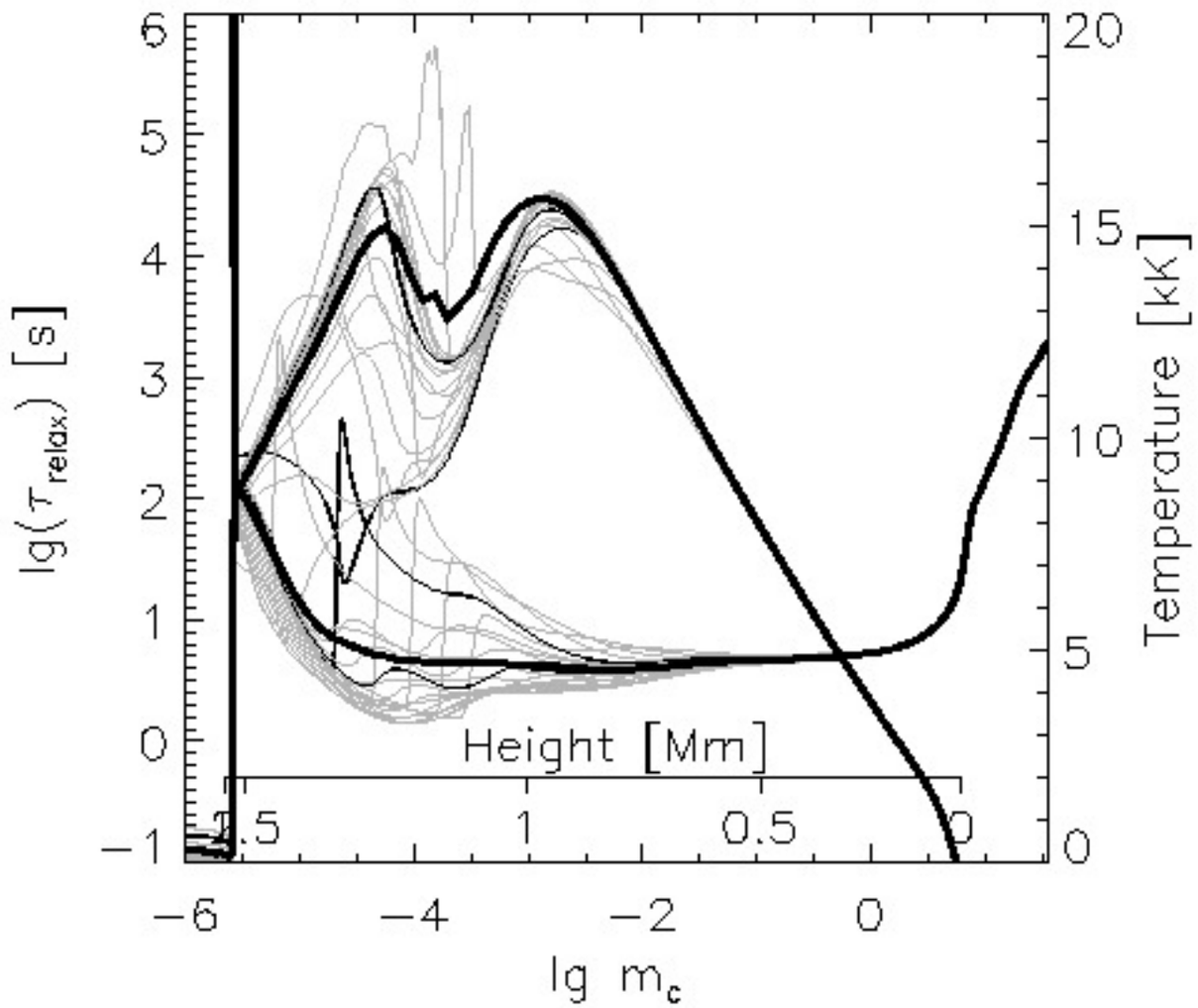

Time scale for hydrogen ionization/recombination is highly time-varying. Fast rates when temperature is high (ionizing phase), slow rates when temperature is low (recombining phase).

Hydrogen ionization

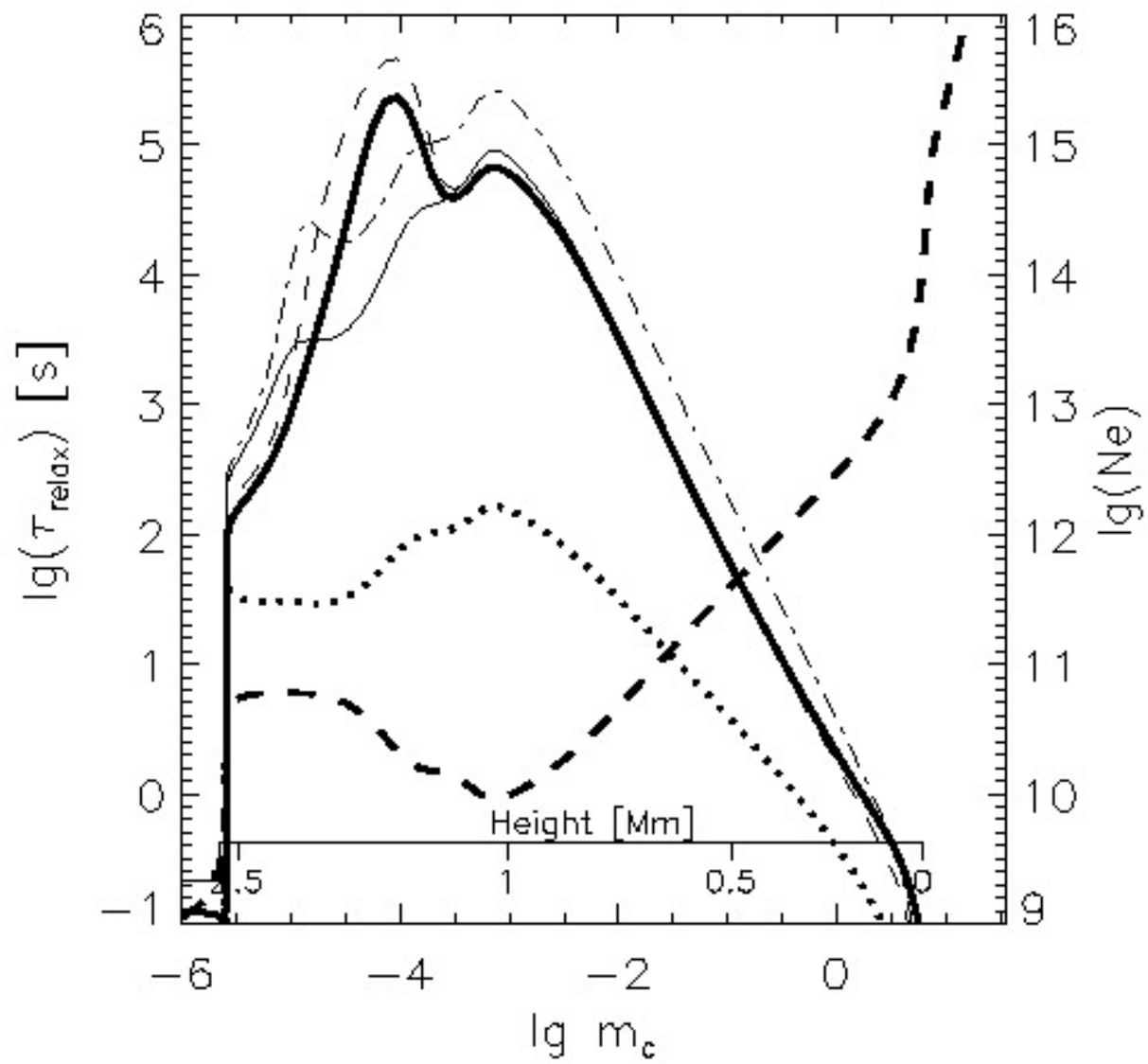

Electron density (thick dashed)
Eigenvalue timescales (thick dotted)
only collisions (dot-dashed)
Lyman lines in detailed balance (thin solid)
Lyman-alpha in escape probability (dashed)
Numerical result (thick solid)

Eigenvalues of rate-matrix give erroneous timescales for non-linear rate-matrix. Exclusion of large, canceling rates (Lyman transitions) give much better results.

(Carlsson & Stein, 2002, ApJ 572,626)

Hydrogen ionization

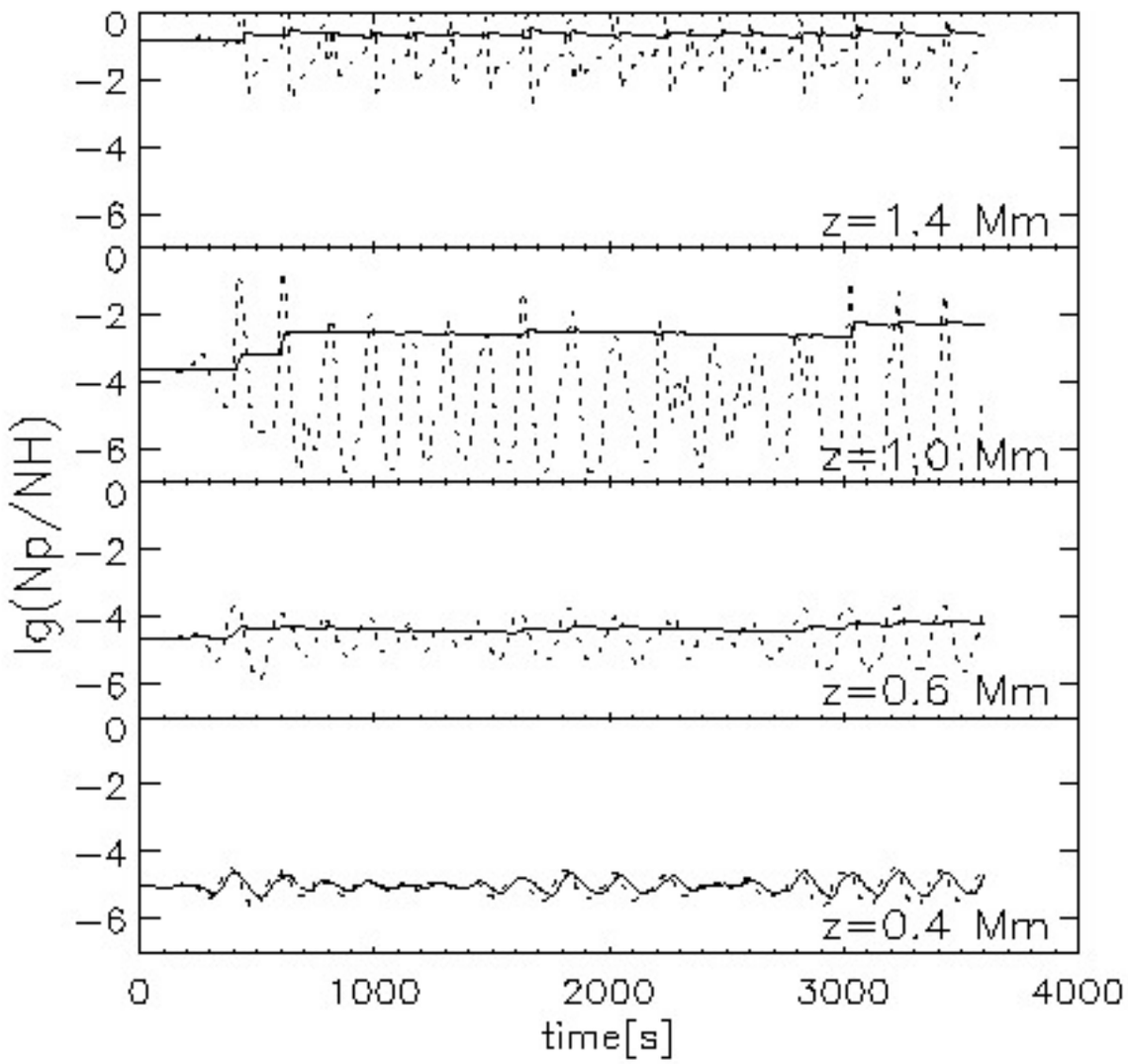

Time dependent ionization (solid)
Equilibrium ionization (dashed)

Slow rates when recombining results in ionization higher than equilibrium values.

3D RMHD models

BIFROST

Hansteen 2004, Hansteen, Carlsson, Gudiksen 2007, Sykora, Hansteen, Carlsson 2008,
Gudiksen et al 2011

- 6th order scheme, with "artificial viscosity/diffusion"
- Open vertical boundaries, horizontally periodic
- Possible to introduce field through bottom boundary

- "Realistic" EOS
- Detailed radiative transfer along 48 rays
  - Multi group opacities (4 bins) with scattering
- NLTE losses in the chromosphere, optically thin in corona

- Conduction along field lines
  - Operator split and solved by using multi grid method

- Time dependent Hydrogen ionization
- Generalized Ohm's Law

“enhanced network” simulation

http://sdc.uio.no/search/simulations

IRIS Technical Note 33; Carlsson et al 2014

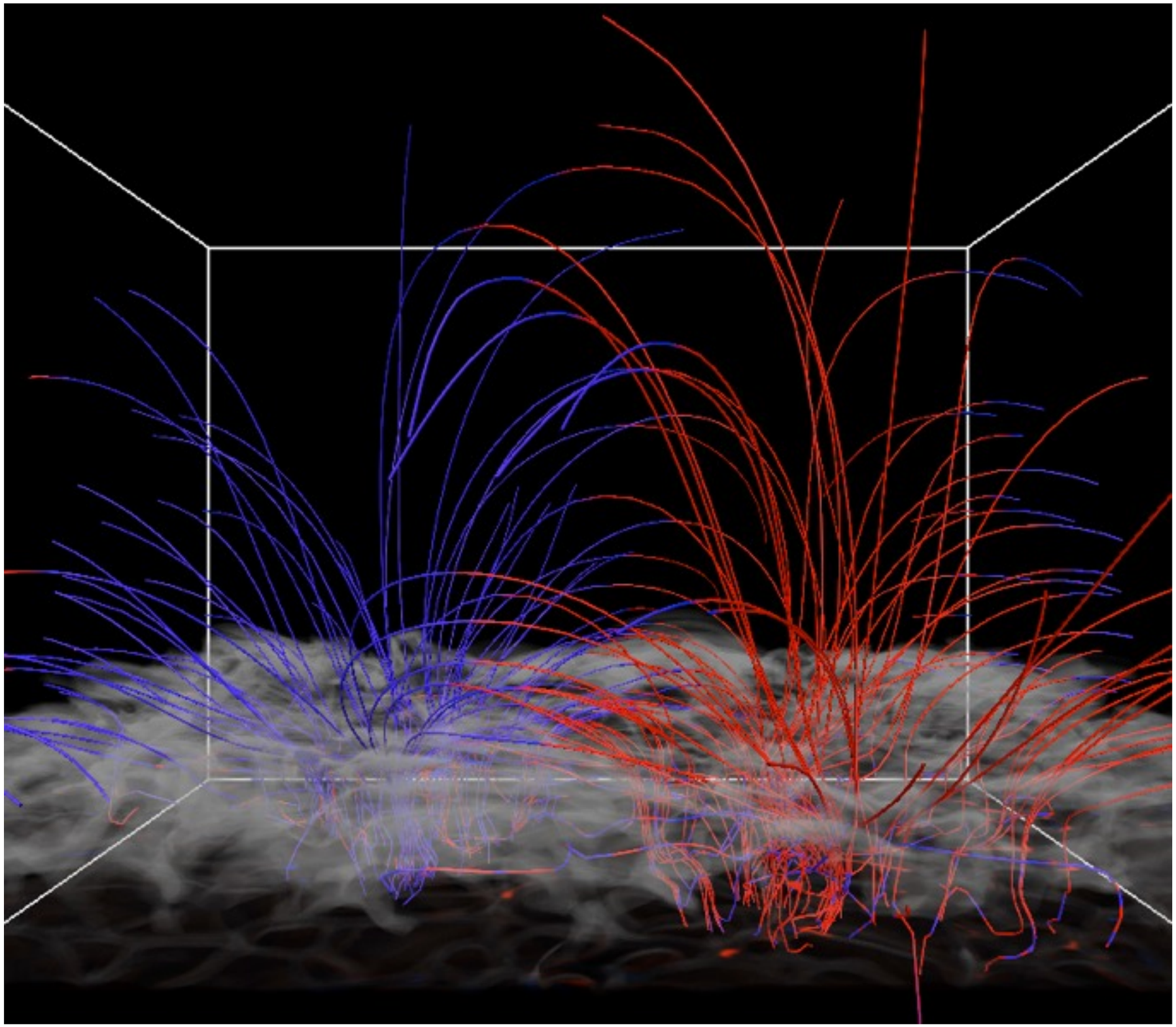

Corona

Transition region

Chromosphere

Photosphere

Convection zone

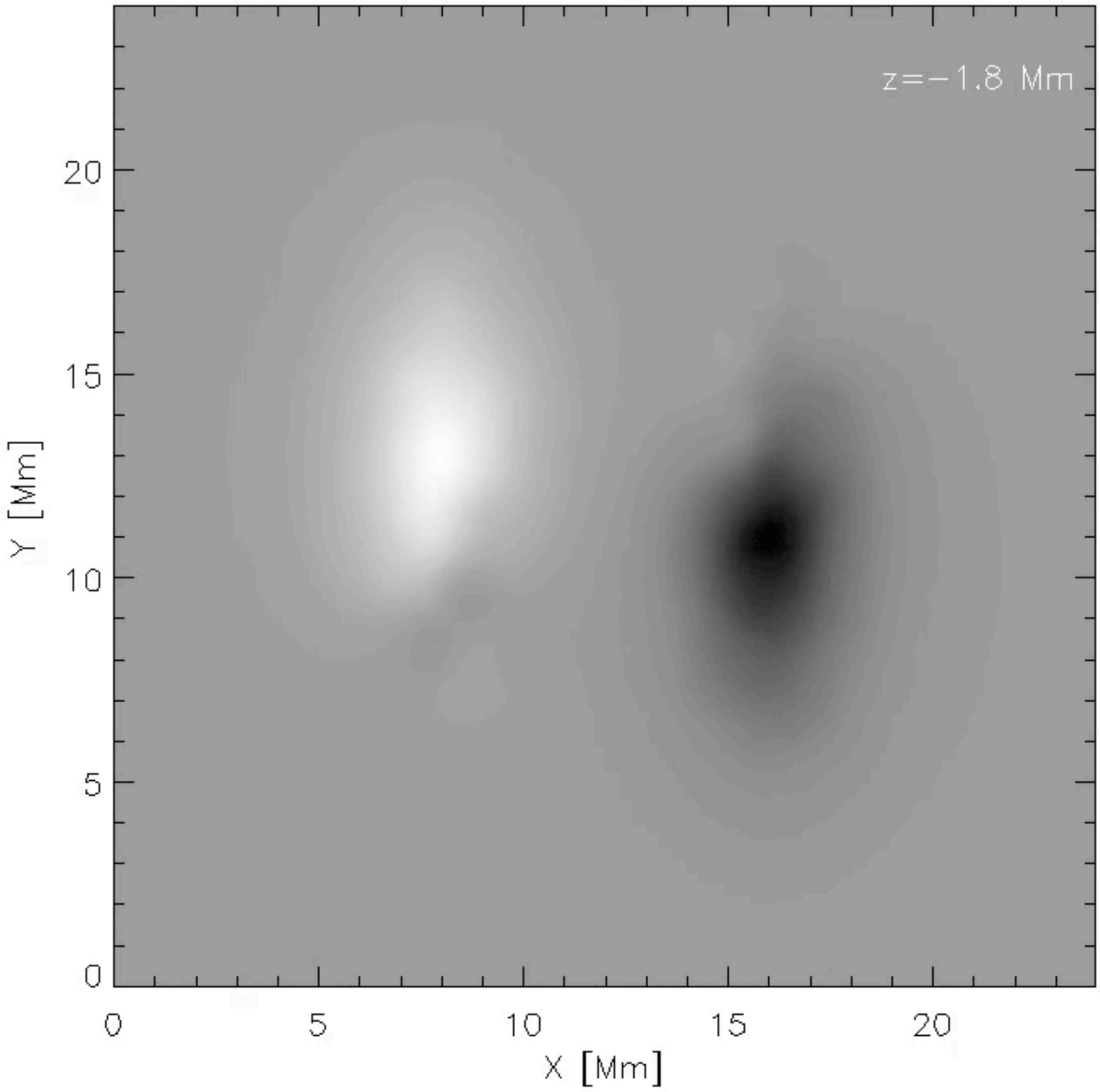
z=−1.8 Mm
Y [Mm]
X [Mm]
0
5
10
15
20
0
5
10
15
20

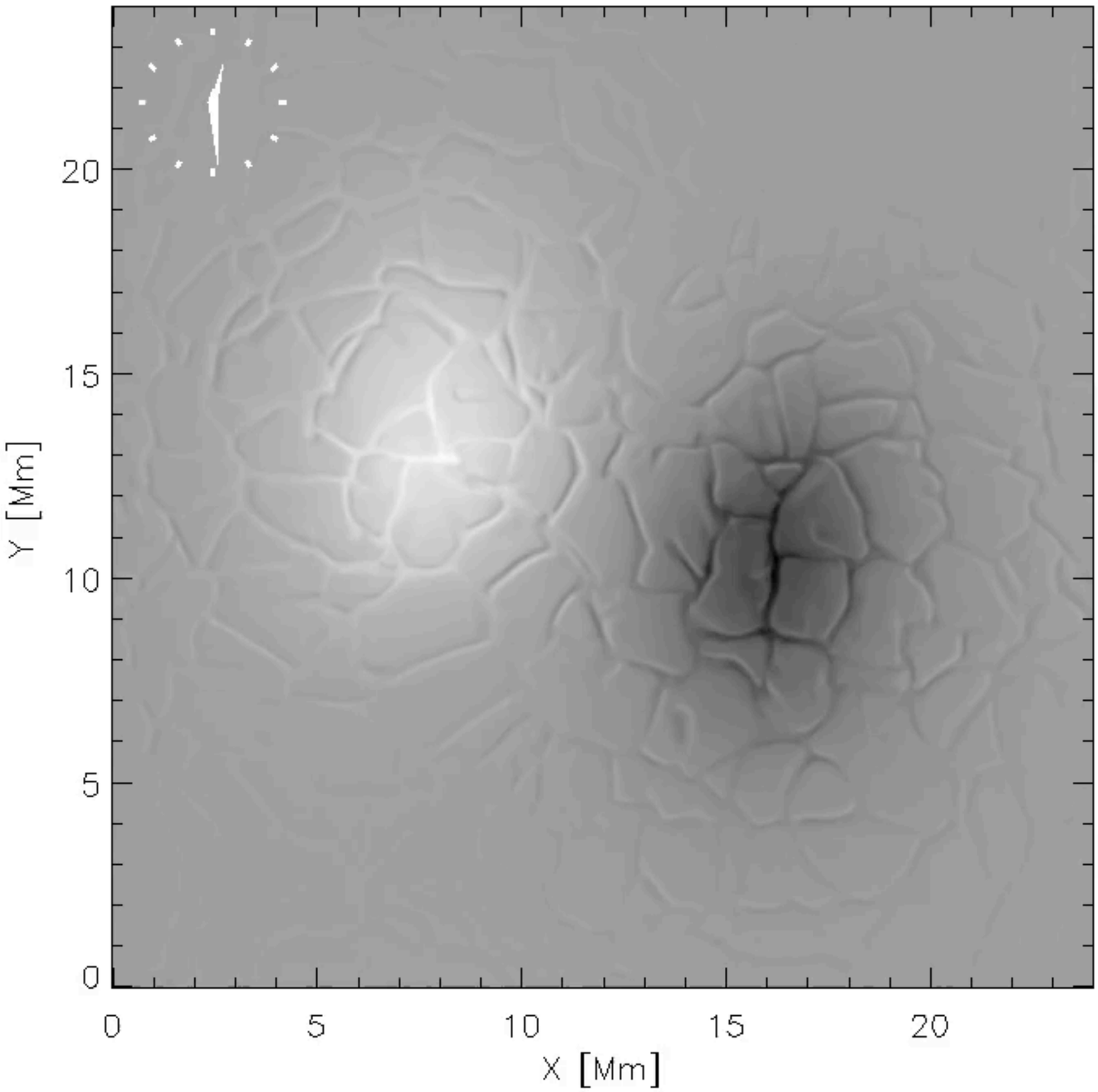
20
15
10
5
0
Y [Mm]
0
5
10
15
20
X [Mm]

Transition region corrugated

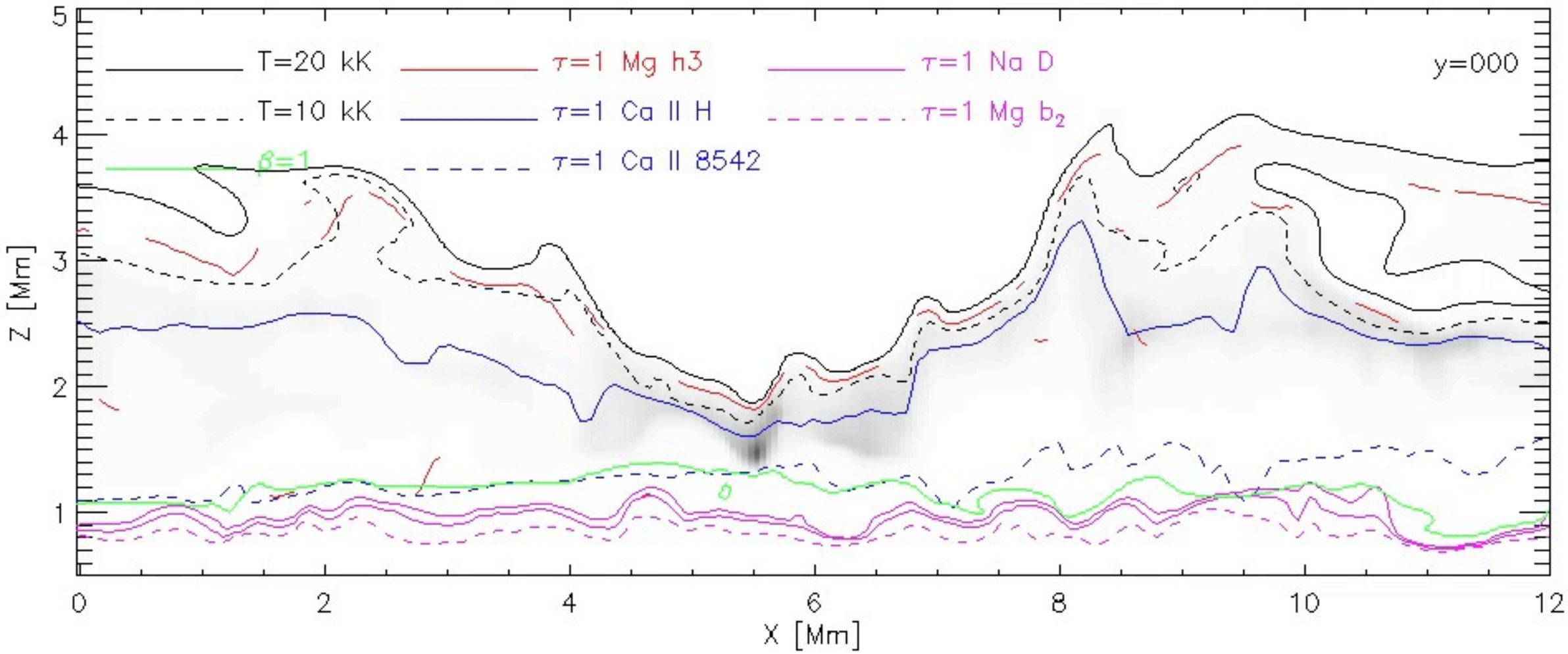

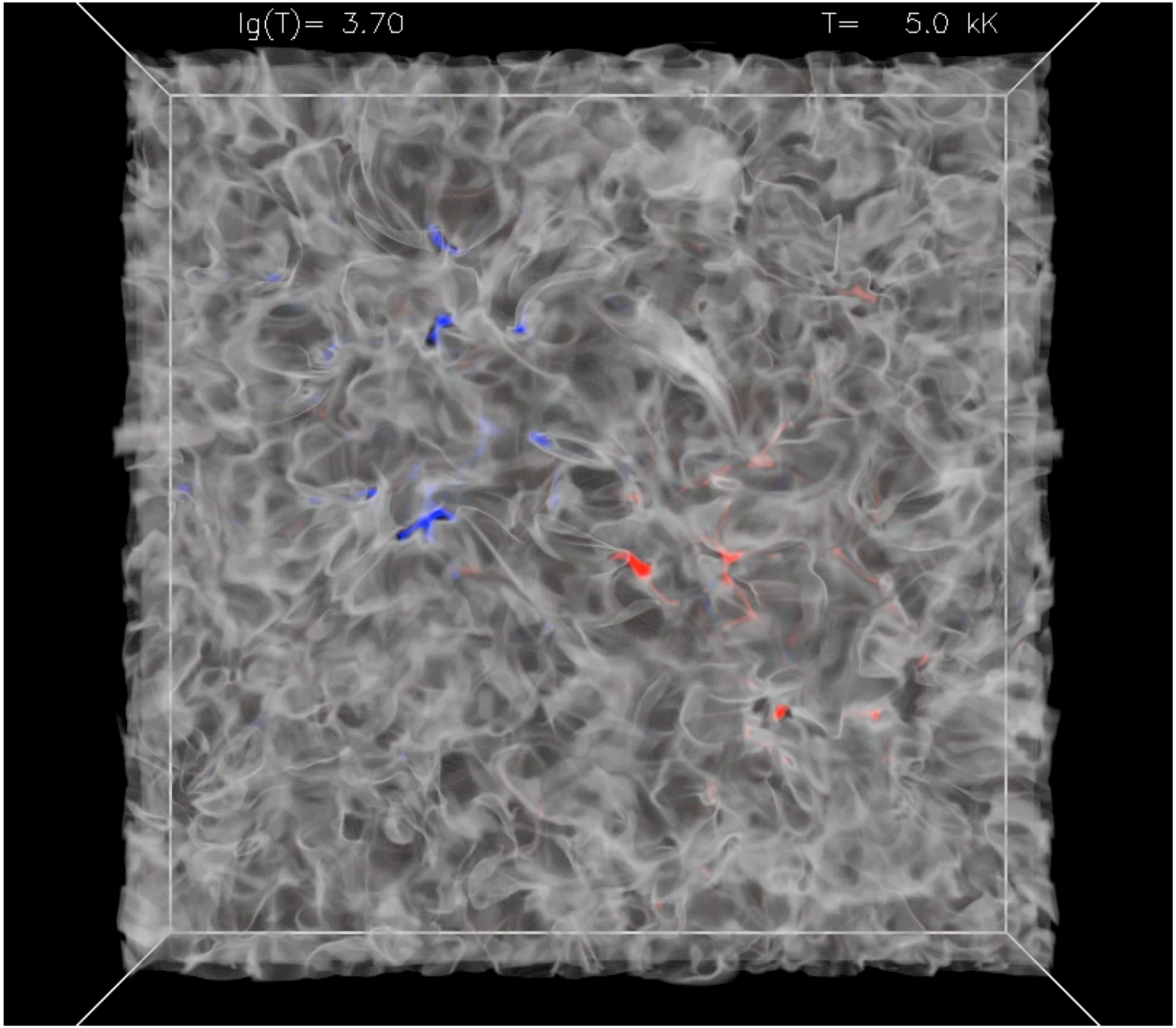
lg(T)= 3.70
T= 5.0 kK

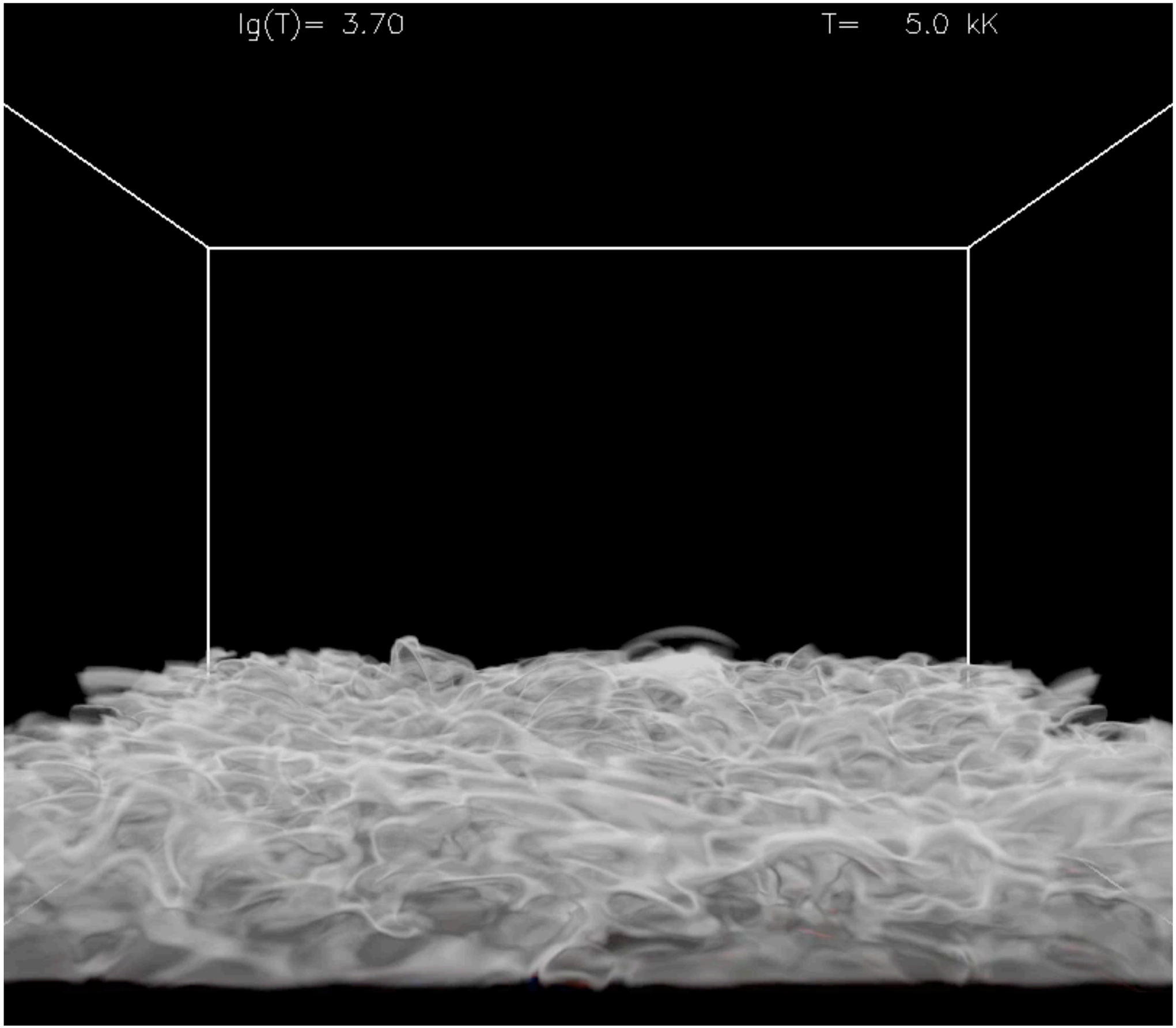
lg(T)= 3.70
T= 5.0 kK

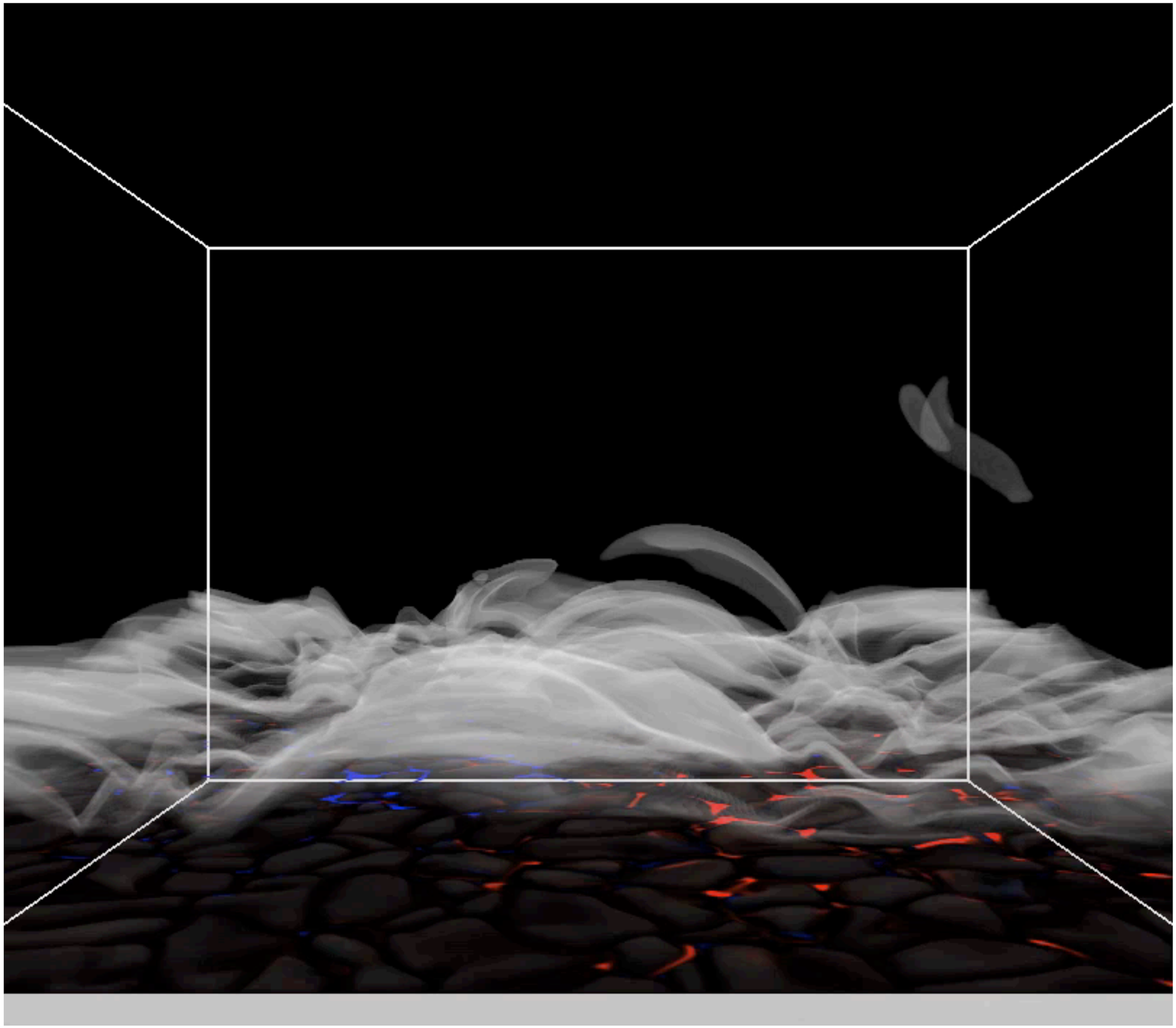

3D radiative transfer

Mg II h & k lines

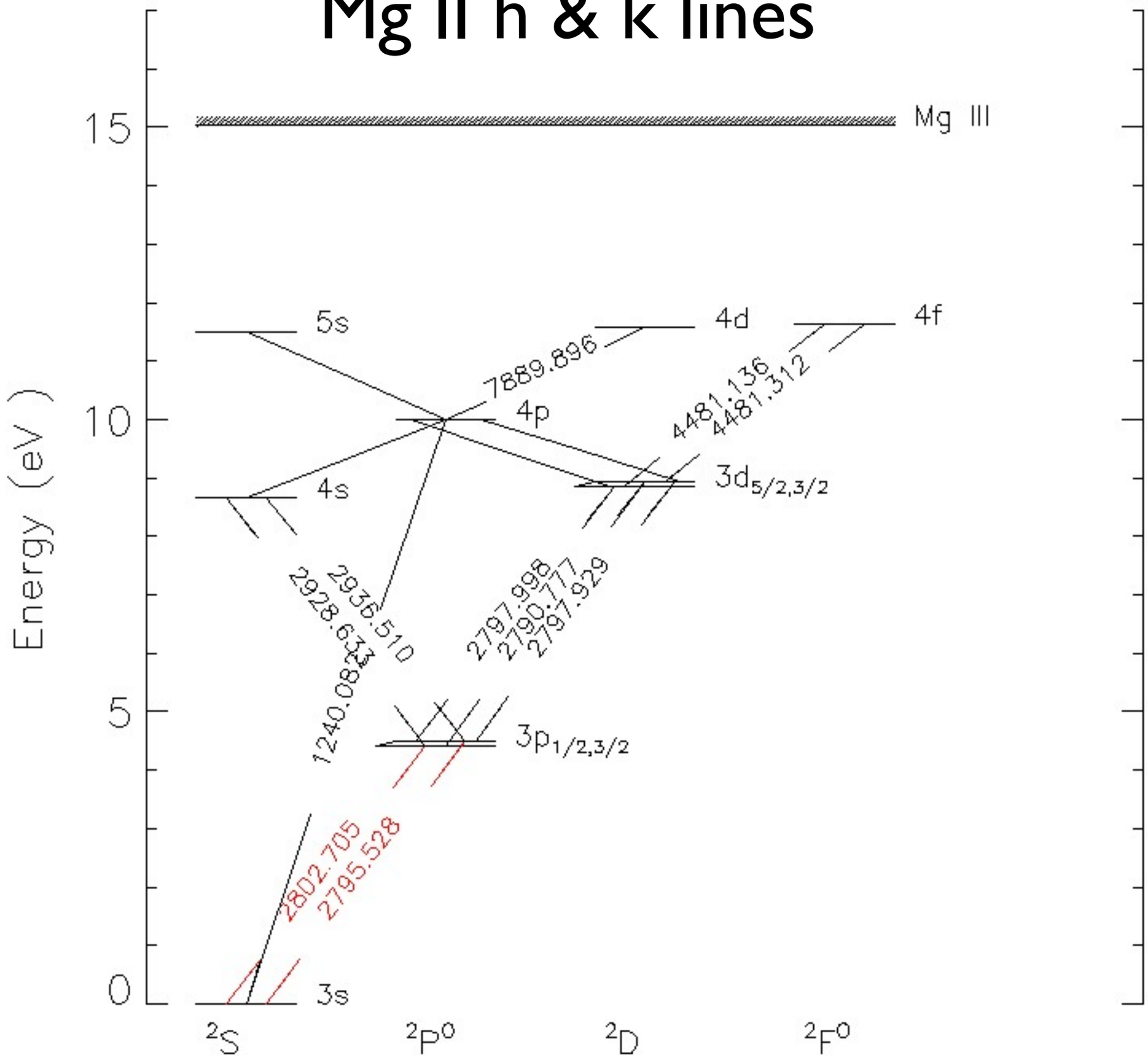

Mg II h & k lines

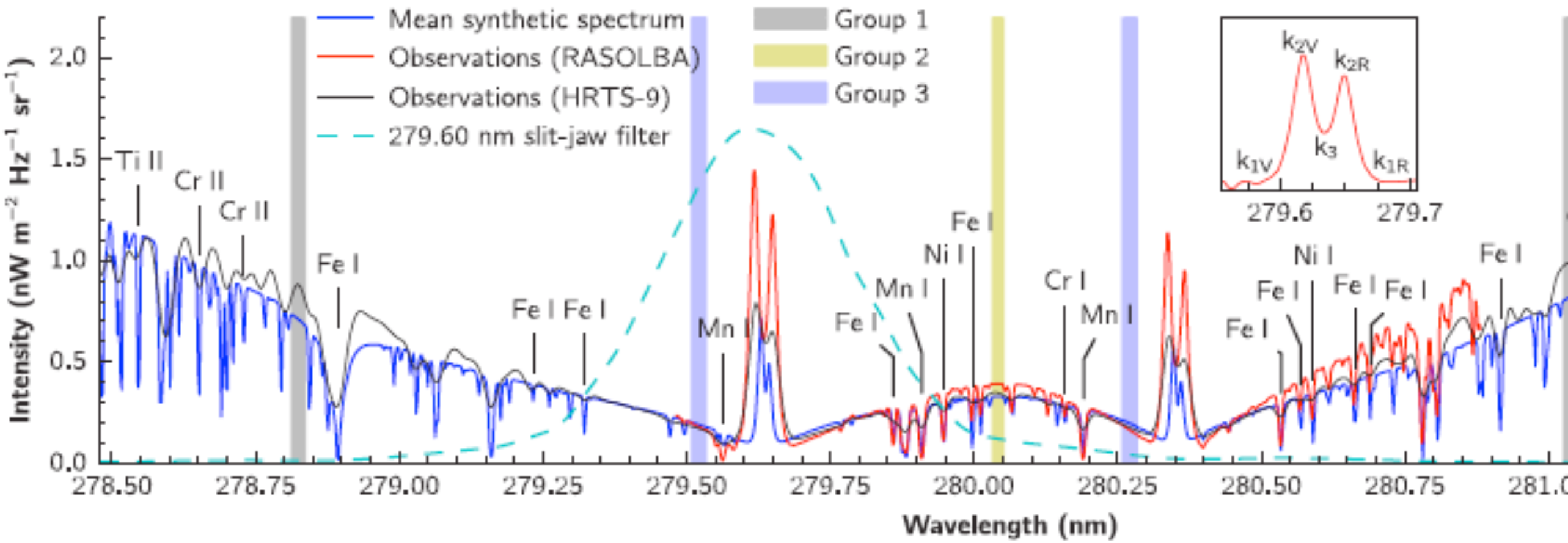

Pereira, Leenaarts, De Pontieu, Carlsson, Uitenbroek, 2013, ApJ 778,143

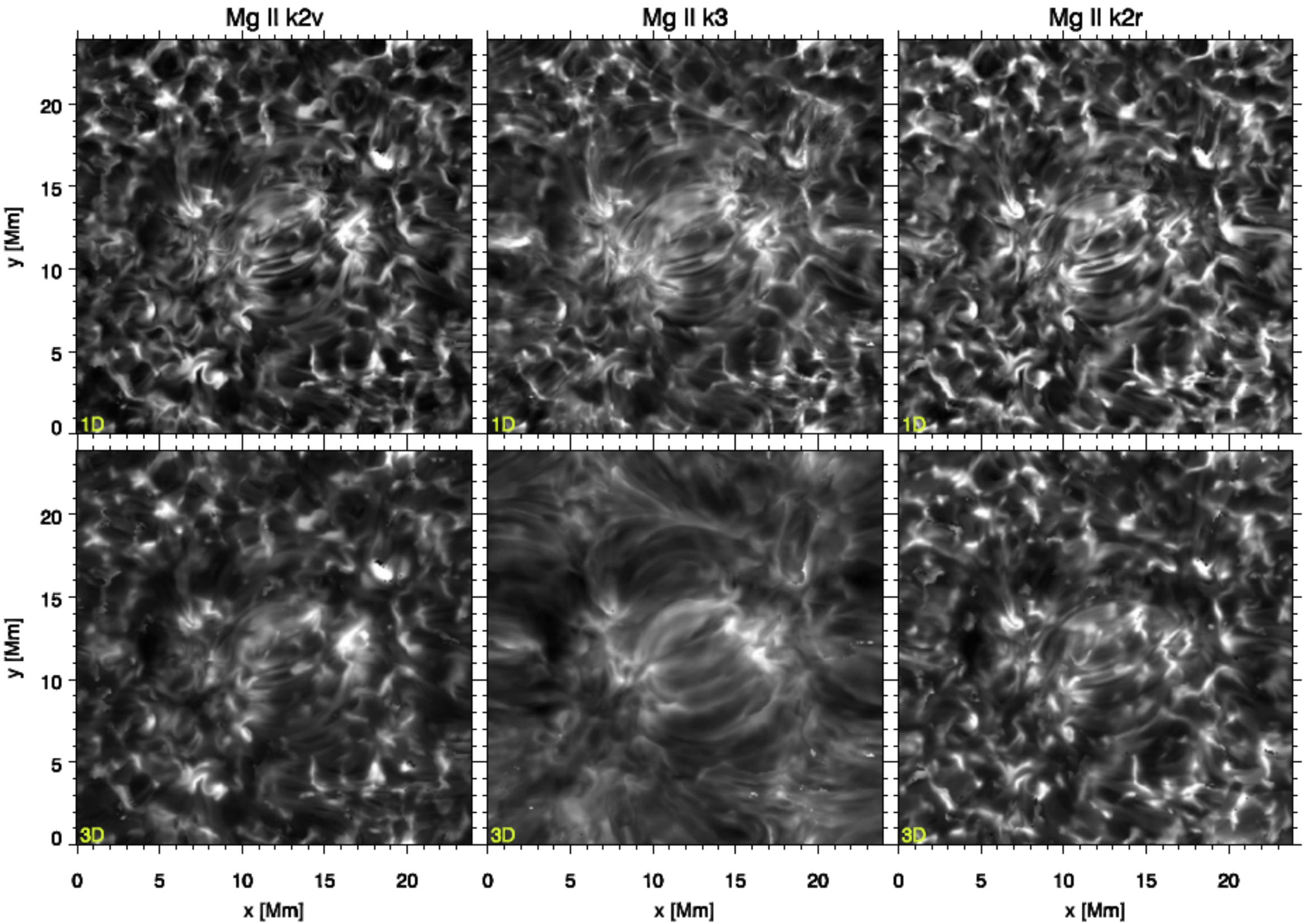

Leenaarts, Pereira, Carlsson, Uitenbroek, De Pontieu, 2013, ApJ 772,89

H-α

Leenaarts, Carlsson, Rouppe van der Voort (2012, ApJ 749,L136)

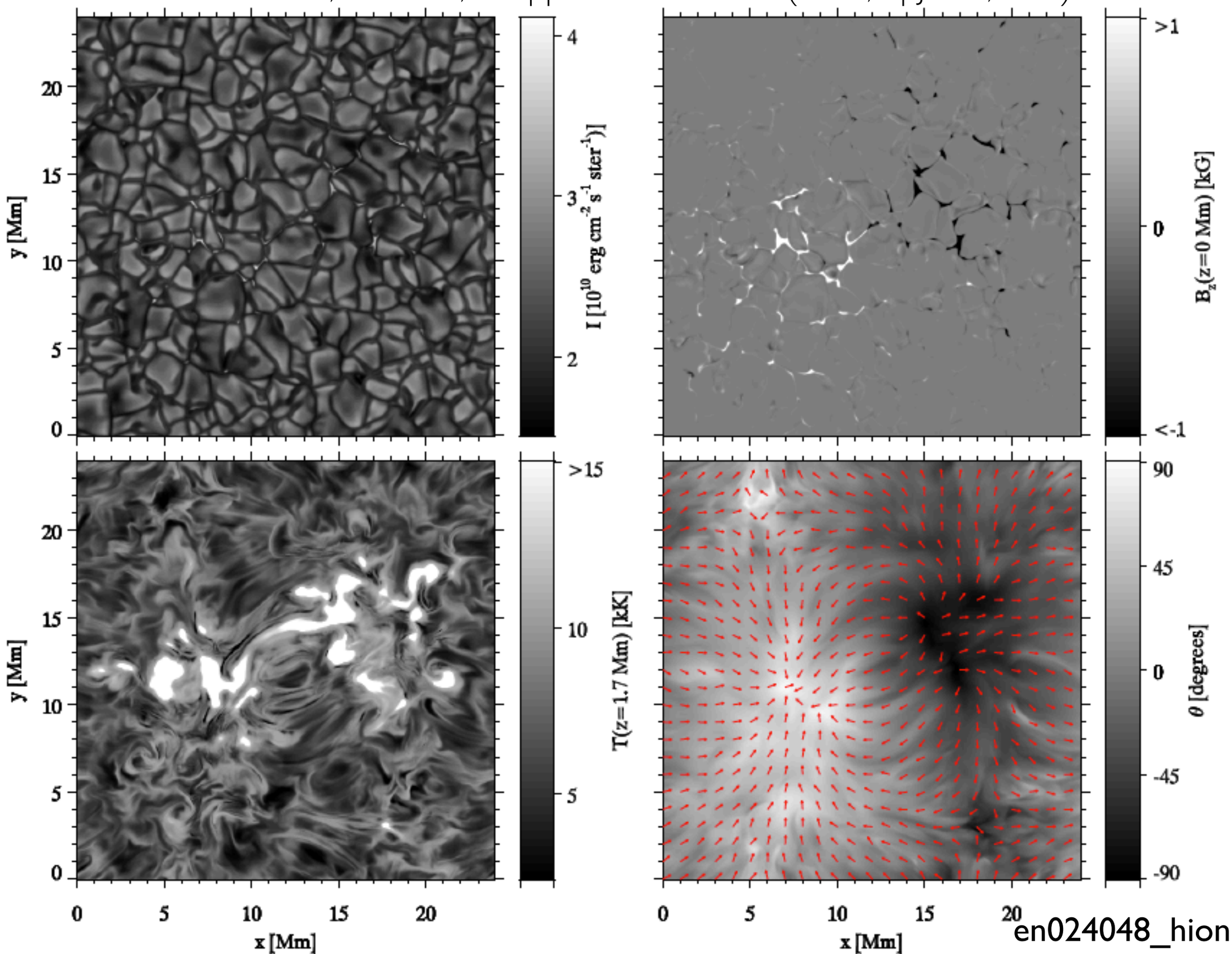

1D

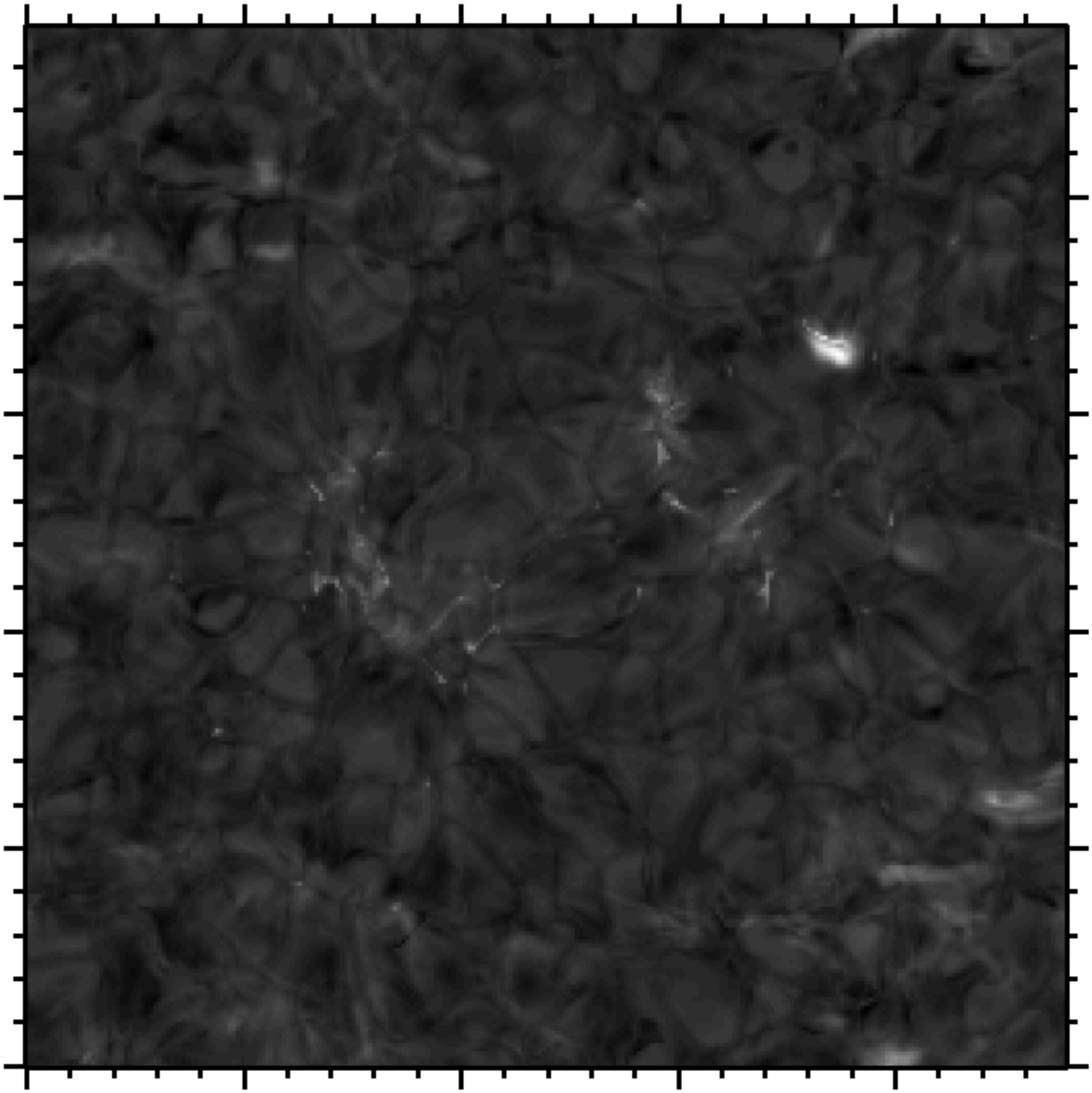

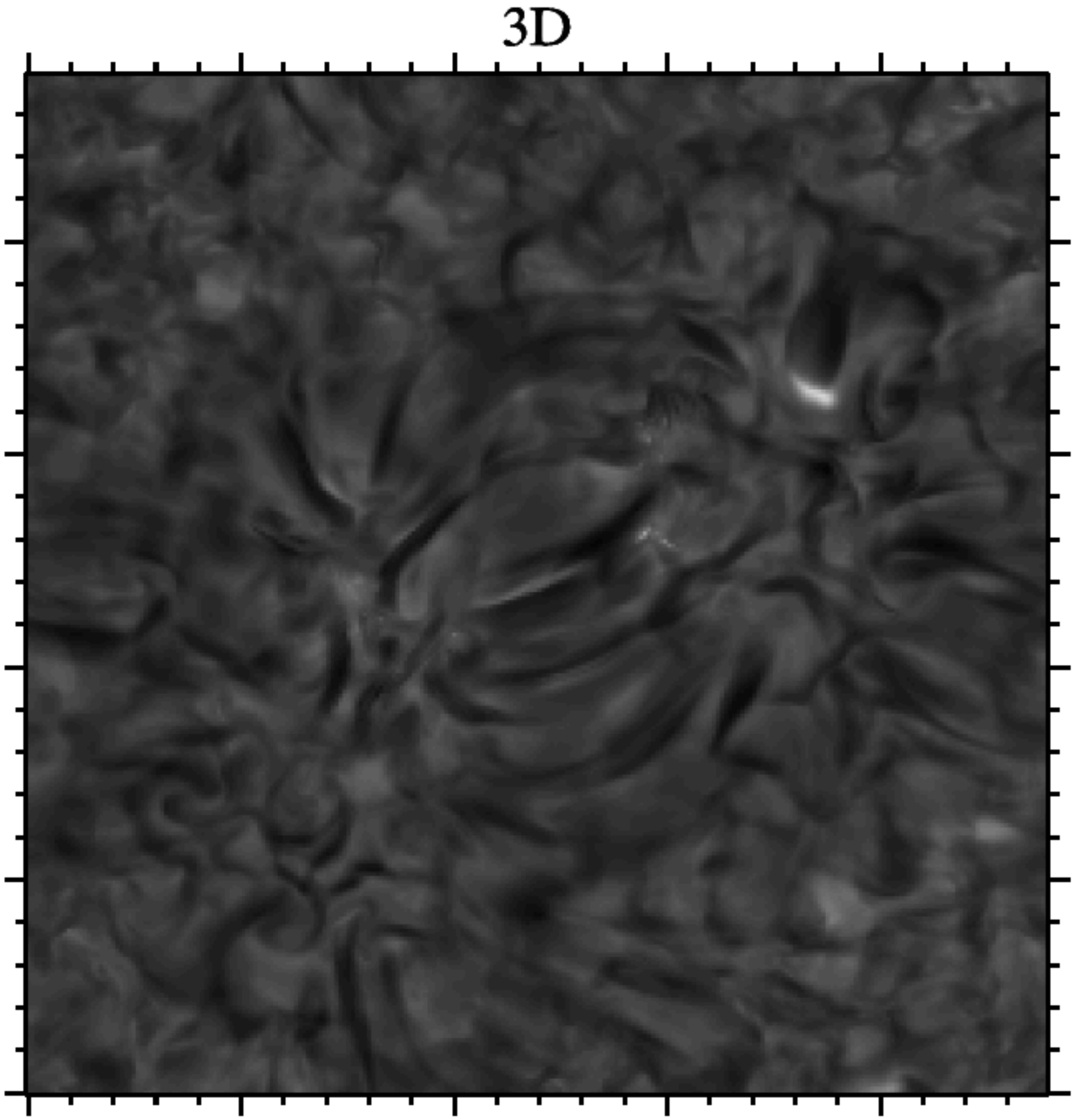
3D

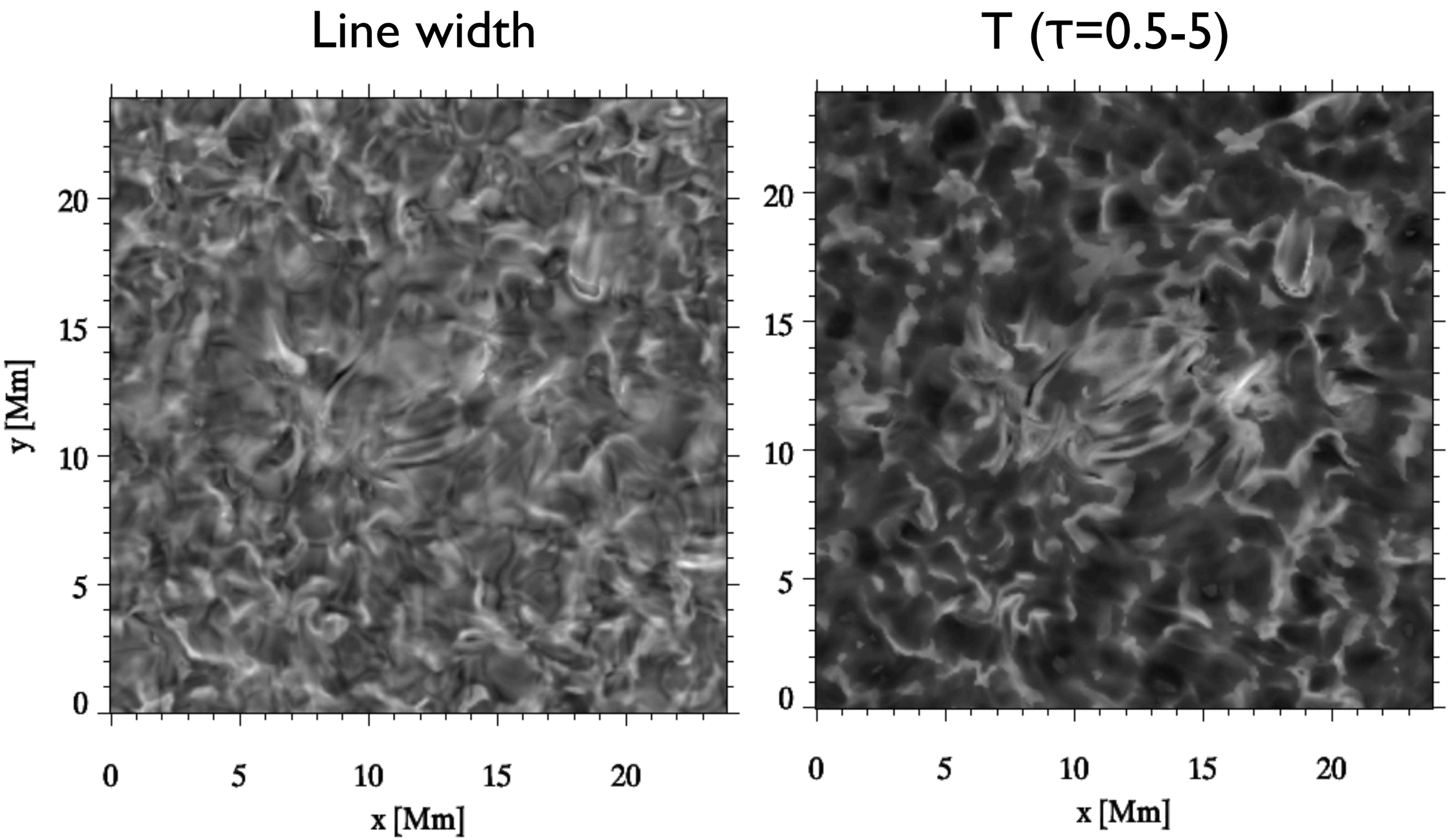
Line width
T (τ=0.5-5)
y [Mm]
x [Mm]
x [Mm]
0
5
10
15
20


INTERFACE REGION IMAGING SPECTROGRAPH
IRIS
NASA LMSAL LMS&ES ARC SAO UiO MSU LSJU

IRIS milestones and schedule

SMEX Announcement of Opportunity	Sep 2007
IRIS downselect, phase A	Jun 2008
IRIS concept study report (CSR) submittal	Dec 2008
IRIS site visit	Mar 2009
IRIS award	Jun 2009
IRIS bridge phase start (abbreviated	Aug 2009
Phase B start	Oct 2009
System Requirements Review (SRR)	Jan 2010
Preliminary Design Review (PDR)	May 2010
Critical Design Review (CDR)	Dec 2010
Mission Operations Review (MOR)	Dec 2011
Systems Integrations Review (SIR)	Jun 2012
Flight Operations Review (FOR)	Nov 2012
Launch	June 27 2013

IRIS

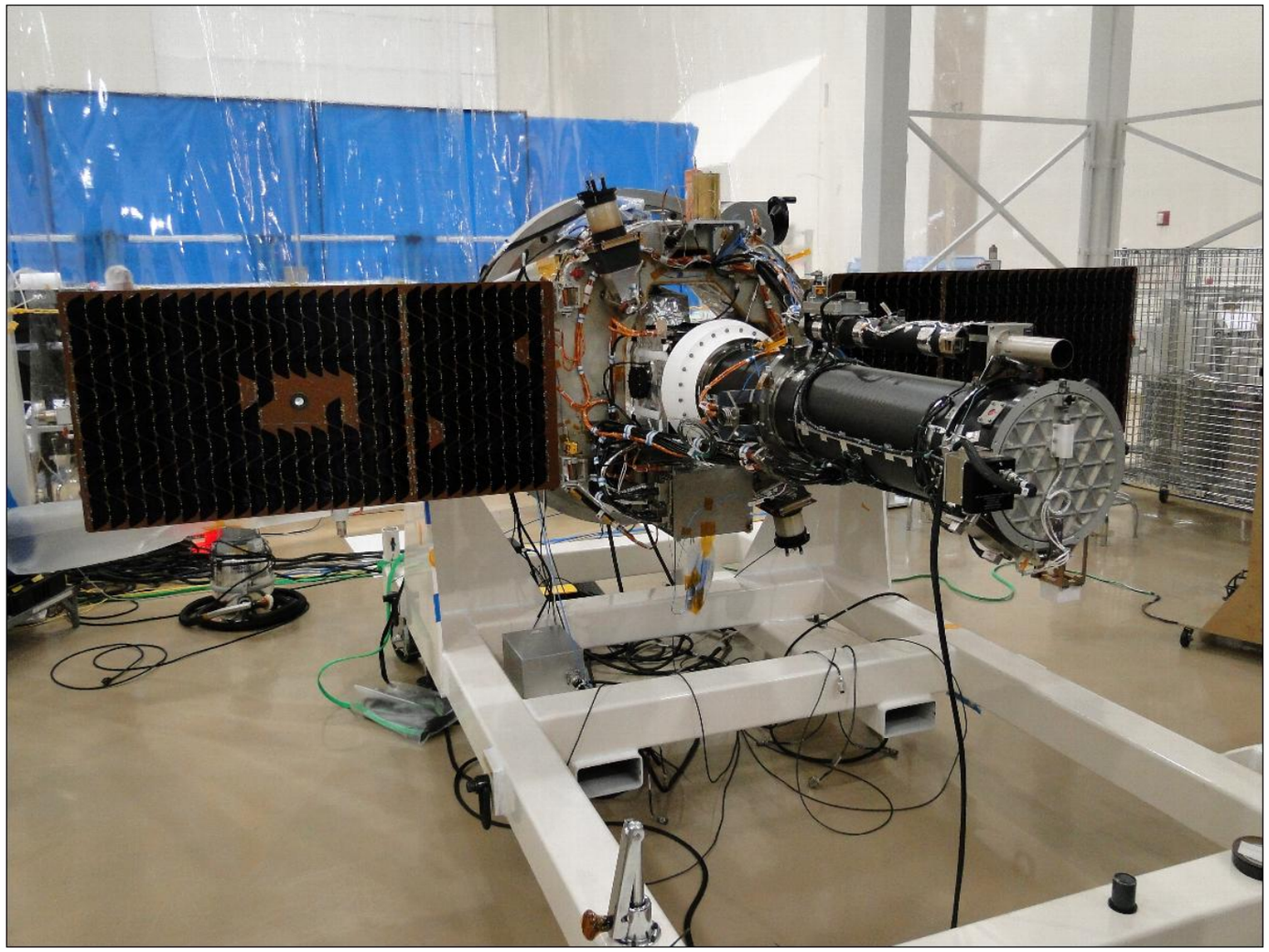

- NASA SMEX mission. Selected June 2009
- developed at LMSAL under the direction of PI Alan Title with major contributions from SAO, MSU, UiO, LSJU, NASA Ames and LMSES (spacecraft)
- 26 June 2013: Pegasus launch into Sun-synchronous polar orbit (620-670 km)

Basic Science Goals

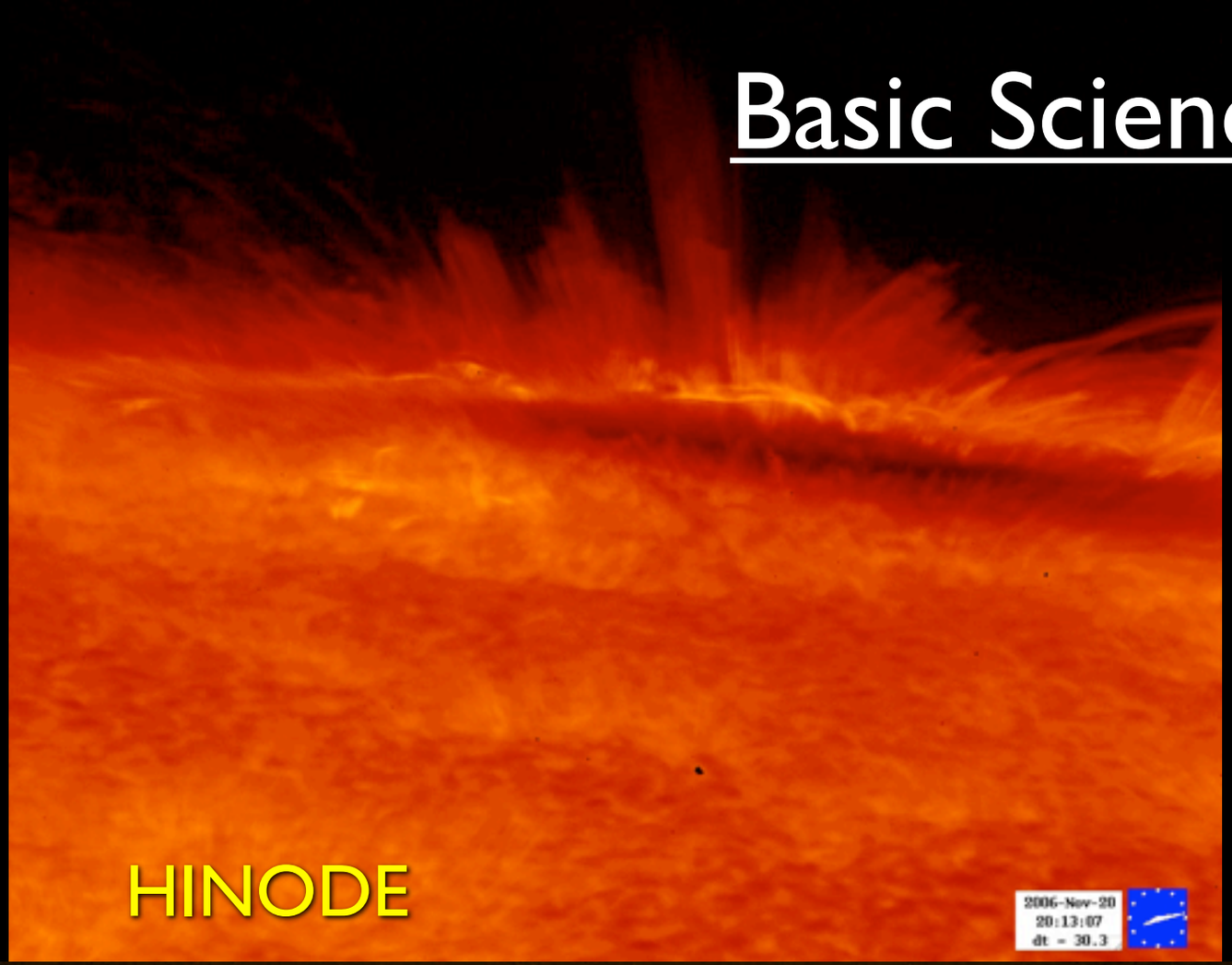

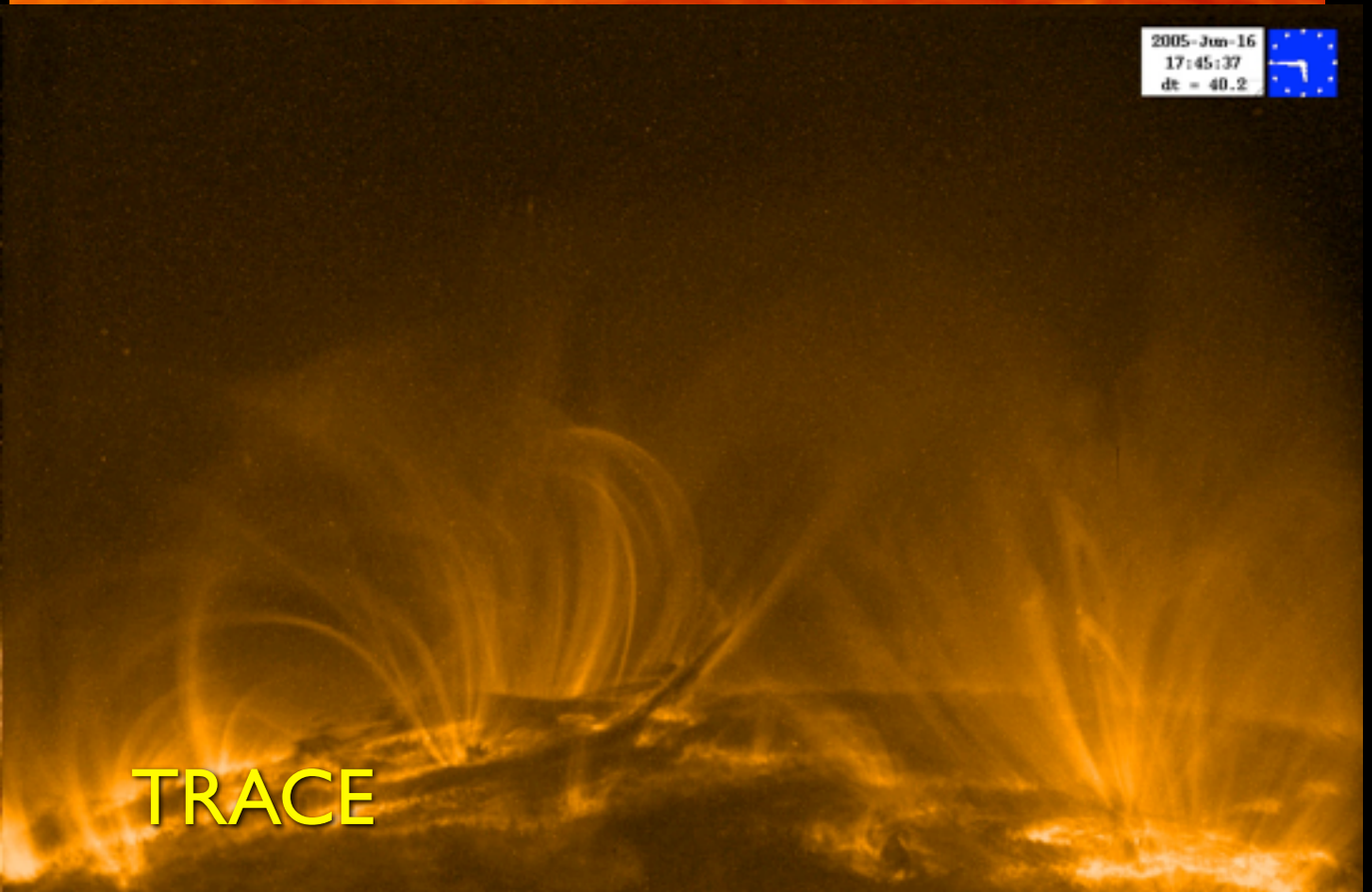

A. The types of non-thermal energy that dominate in the chromosphere and beyond.

B. How the chromosphere regulates the mass and energy supplied to the corona and heliosphere.

C. The ways that magnetic flux and matter rise through the lower atmosphere, and role of flux emergence in powering flares and mass ejections.

IRIS observables

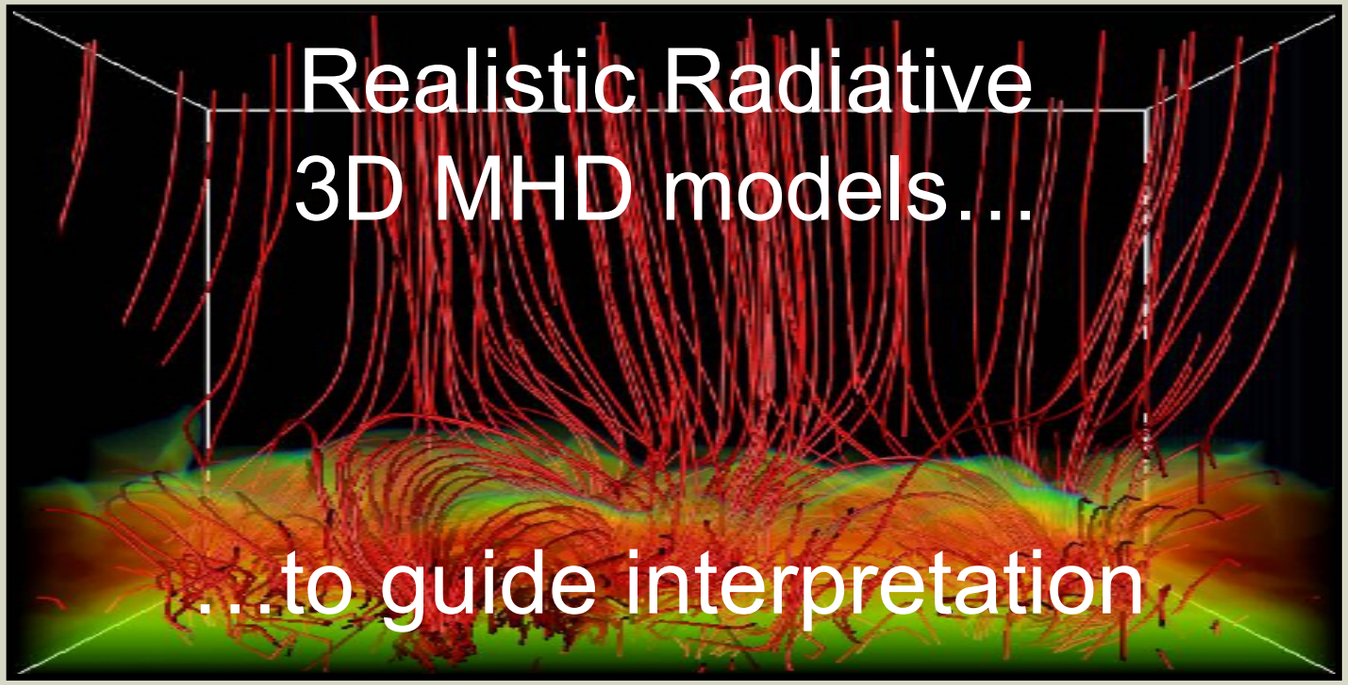

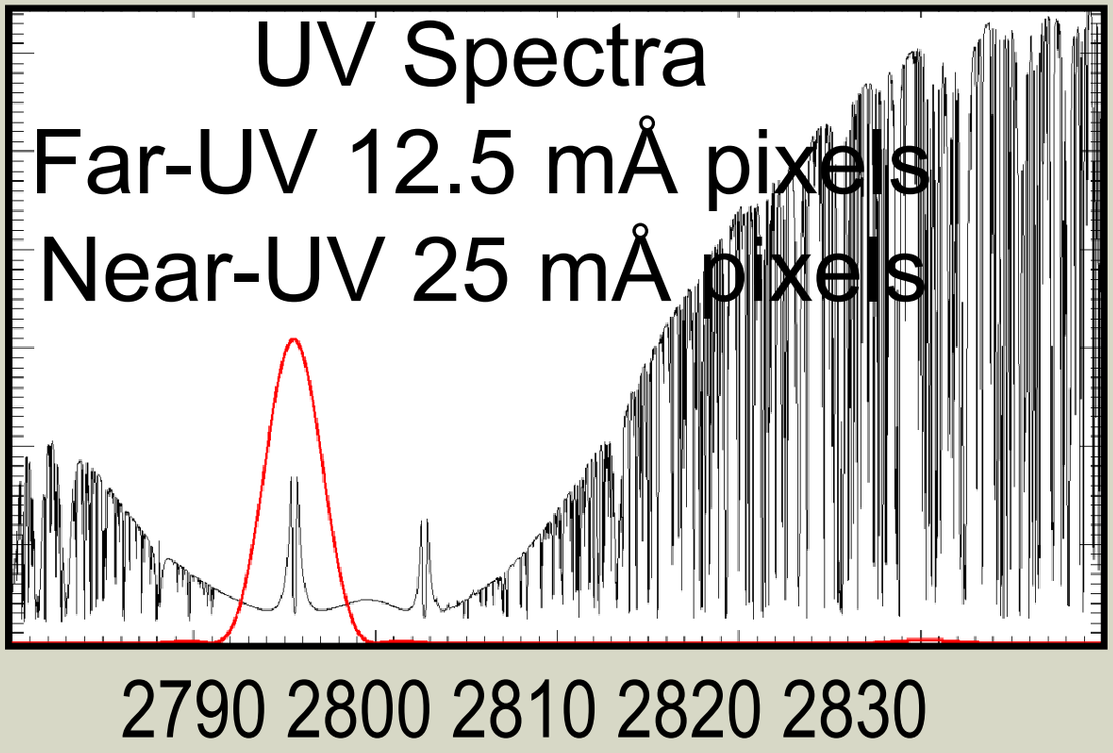

20 cm UV telescope:

1/6 arcsec pixels

Observable	Wavelength range (Å)	Spectral Dispersion (mÅ)	Spectral Resolution	Spatial range (arcsec)	Spatial pixel size (arcsec)	Spatial Resolution (arcsec)	Effective Area (cm^2)
Spectrograph FUV 1	1331.6-1358.4	12,98	28-33mÅ	0.33x175	0,16	0,33	2,1
Spectrograph FUV 2	1380.6-1406.8	12,72	28-33mÅ	0.33x175	0,16	0,33	2,5
Spectrograph NUV	2782.6-2833.9	25,46	55-80mÅ	0.33x175	0,16	0,4	0,27
Slitjaw C II	1335		40Å	175 x 175	0,16	0,33	0,6
Slitjaw Si IV	1400		40Å	175 x 175	0,16	0,33	0,6
Slitjaw Mg II h/k	2796		4Å	175 x 175	0,16	0,4	0,007
Slitjaw Mg II wing	2830		4Å	175 x 175	0,16	0,4	0,006


HUSKY
VAB 1555

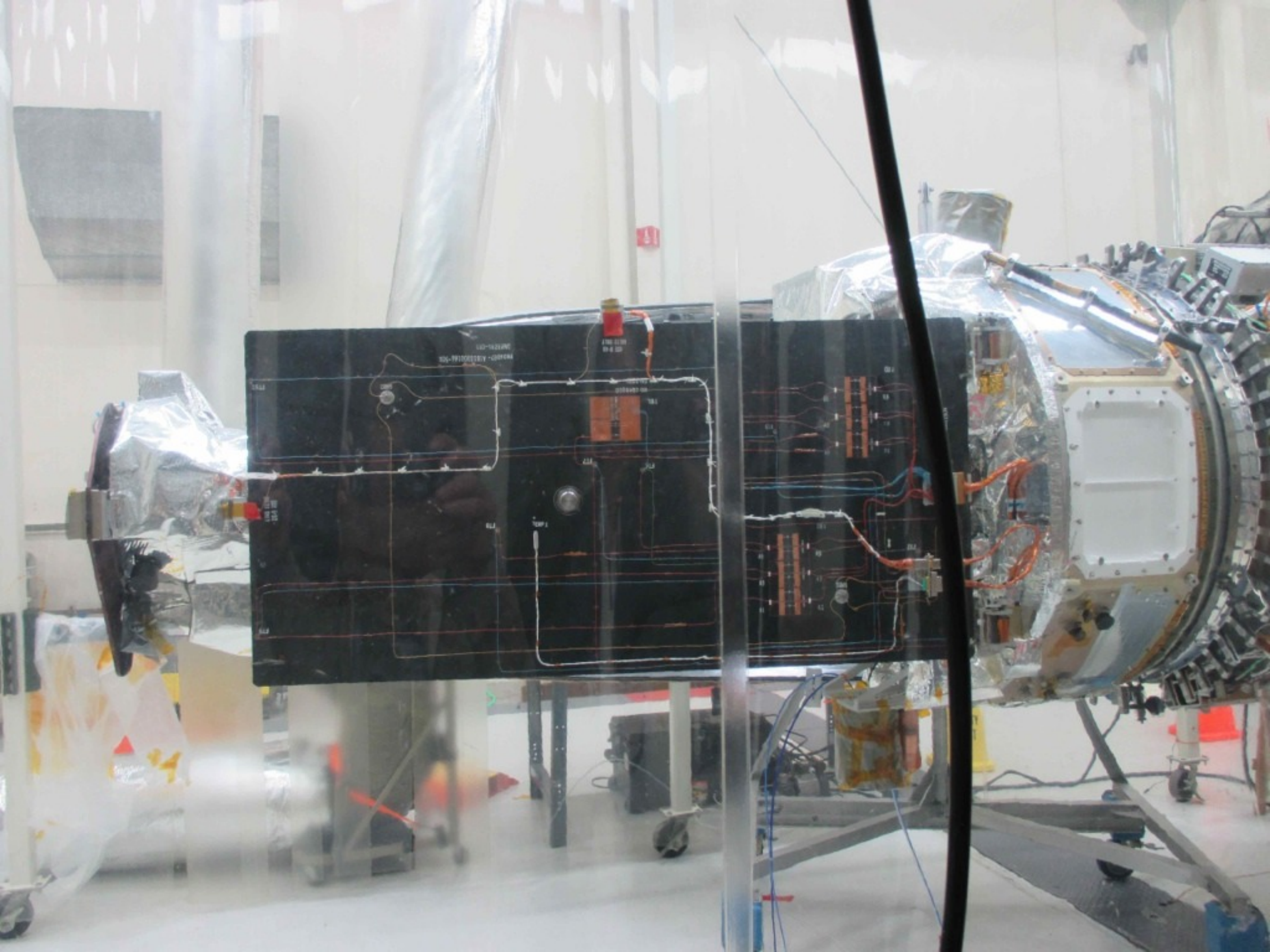


ESD AREA

Pegasus/WIRE Mission
March 4, 1999

Presented To
VAFB Operations

For Your Dedication to Total Mission Success

IRIS spectra and slit-jaw imaging cover the photosphere, chromosphere, transition region and corona - 4,500 to 10,000,000 K

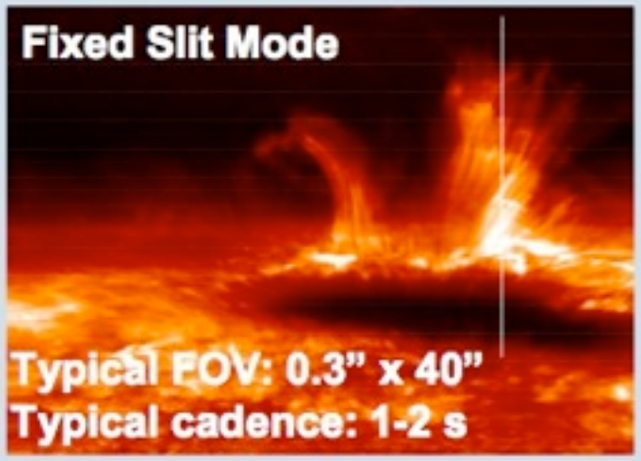

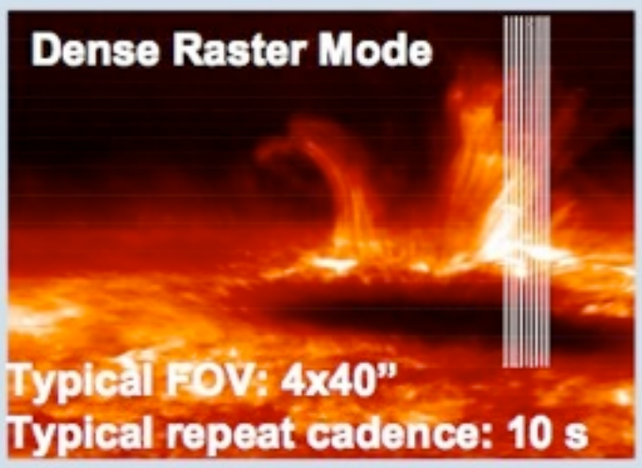

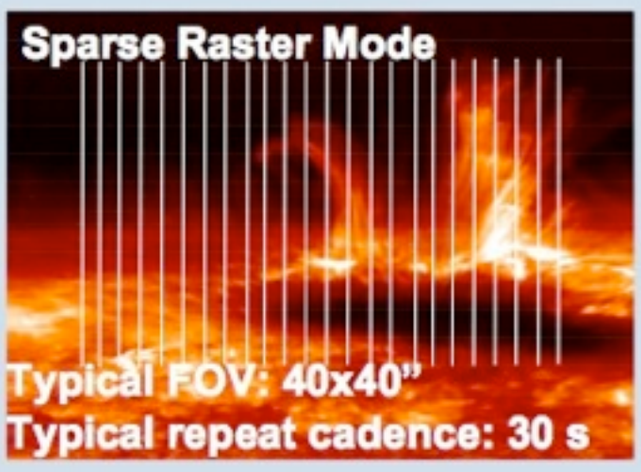

Ion Spectrum	λ	Δλ	Log T	Estimated Count Rate (e^-/s/line/spatial pixel)			Detector
	Å	mÅ	K	Quiet Sun	Active Region	Flare	
UV Spectra (effective area 2.1-2.4 cm^2 for FUV, 0.27 cm^2 for Mg passband, continuum is 1 Å)							
†: Count rates for Mg II wing, h and k are in e^-/s/spectral pixel/spatial pixel							
Mg II wing	2820	25	3.7-3.9	3800†	13500†	13500†	3
O I	1356	12.5	3.8	70	190	480	1
Mg II h	2803	25	4.0	1500†	5800†	22000†	3
Mg II k	2796	25	4.0	1900†	7800†	16000†	3
C II	1335	12.5	4.3	780	5000	52000	1
C II	1336	12.5	4.3	1070	6600	64000	1
Si IV	1403	12.5	4.8	220	4000	4e6	2
Si IV	1394	12.5	4.8	490	8000	1e7	2
O IV	1401	12.5	5.2	60	300	5e5	2
O IV	1400	12.5	5.2	15	90	1e5	2
Fe XII	1349	12.5	6.2	23	60	580	1
Fe XXI	1354	12.5	7.0	10	45	5e4	1
UV Slit-Jaw Images				**Estimated Count Rate (e^-/s/pixel)**			
Effective area 0.006 cm^2 with 4 Å FWHM filter for Mg II; 0.6 cm^2 with 40 Å FWHM for far-UV.							
Mg II wing	2831		3.7-3.9	3600	8200	8200	4
Mg II k	2796		4.0	900	4200	10000	4
C II	1335		4.3	650	2100	21000	4
Si IV	1400		4.8	500	2000	4e5	4

IRIS data

- Public data policy (see TRACE/SDO): IRIS observations are available within a day of observing
- IRIS data are available from SDO/JSOC and included in the Hinode data center in Oslo
- Quicklook software tailored for IRIS data are available in solarsoft
- IRIS data center:
  - includes IRIS data at level2
  - makes available several numerical simulations (physical variables) and synthetic IRIS observables (both optically thick and thin) for various magnetic field configurations
  - will include whatever high-quality, co-aligned ground-based datasets that are obtained during IRIS-led coordinated campaigns

Model of IRIS "printed" from CAD drawings.

IRIS operations

- Sun-synchronous, polar orbit for continuous observations.
- Baseline: 10s cadence for UV slit jaw images, 2s for 6 spectral windows, rastering to map solar regions; 2 year mission life.
- Average data rate 0.7 Mbits/s (much less than SDO!), ~10-13 X-band passes/day, with most provided by Norwegian Space Center
- TRACE/Hinode-SOT like operations with daily upload of observing programs, also based on community requests/input
- Focus on coordination with ground-based observatories and Hinode, SDO, STEREO, with community input

Model of IRIS "printed" from CAD drawings.

IRIS will rarely read out full FUV spectra: typically 4-6 3-4Å wide windows focused on bright lines

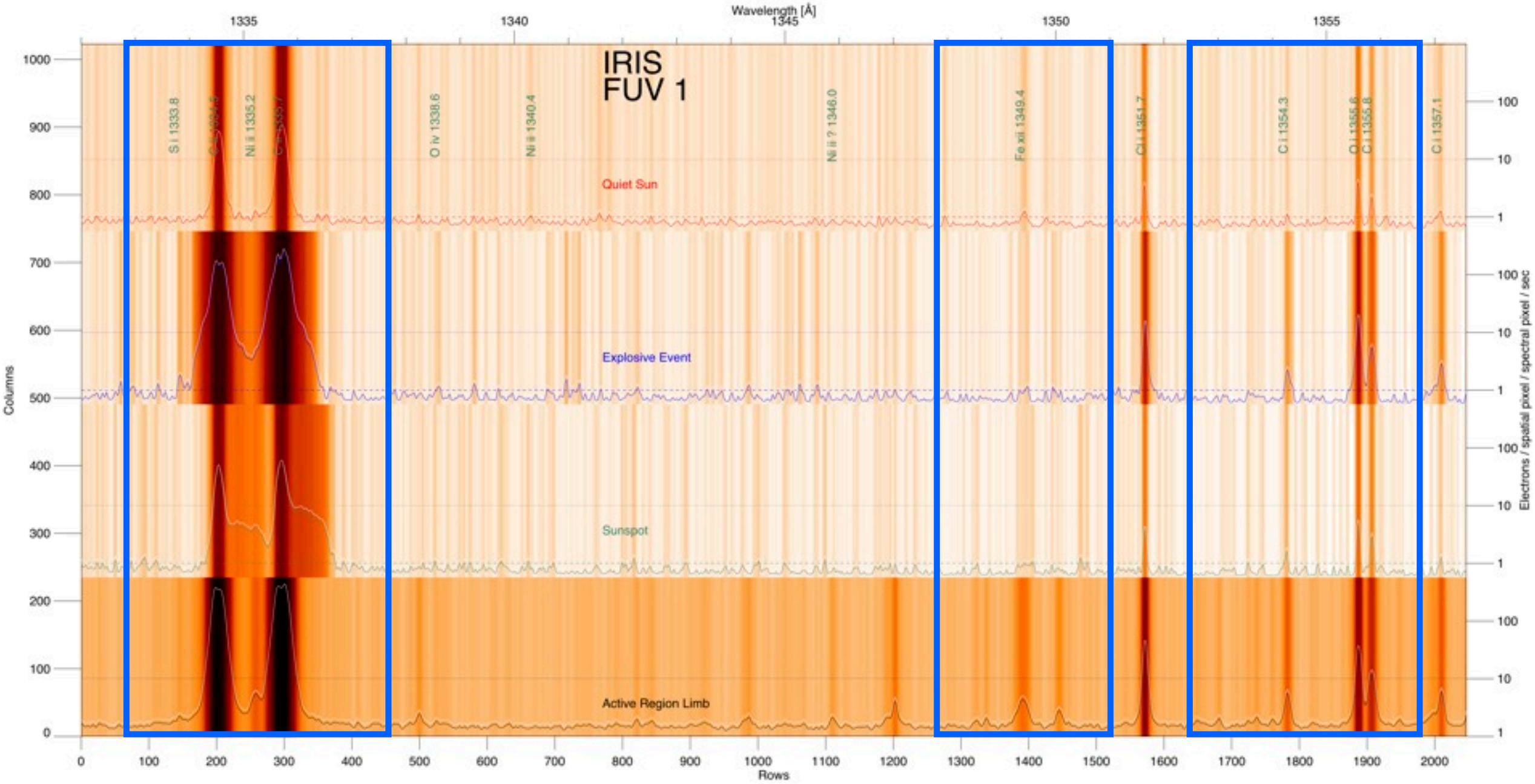

IRIS will rarely read out full FUV spectra: typically 4-6 3-4Å wide windows focused on bright lines

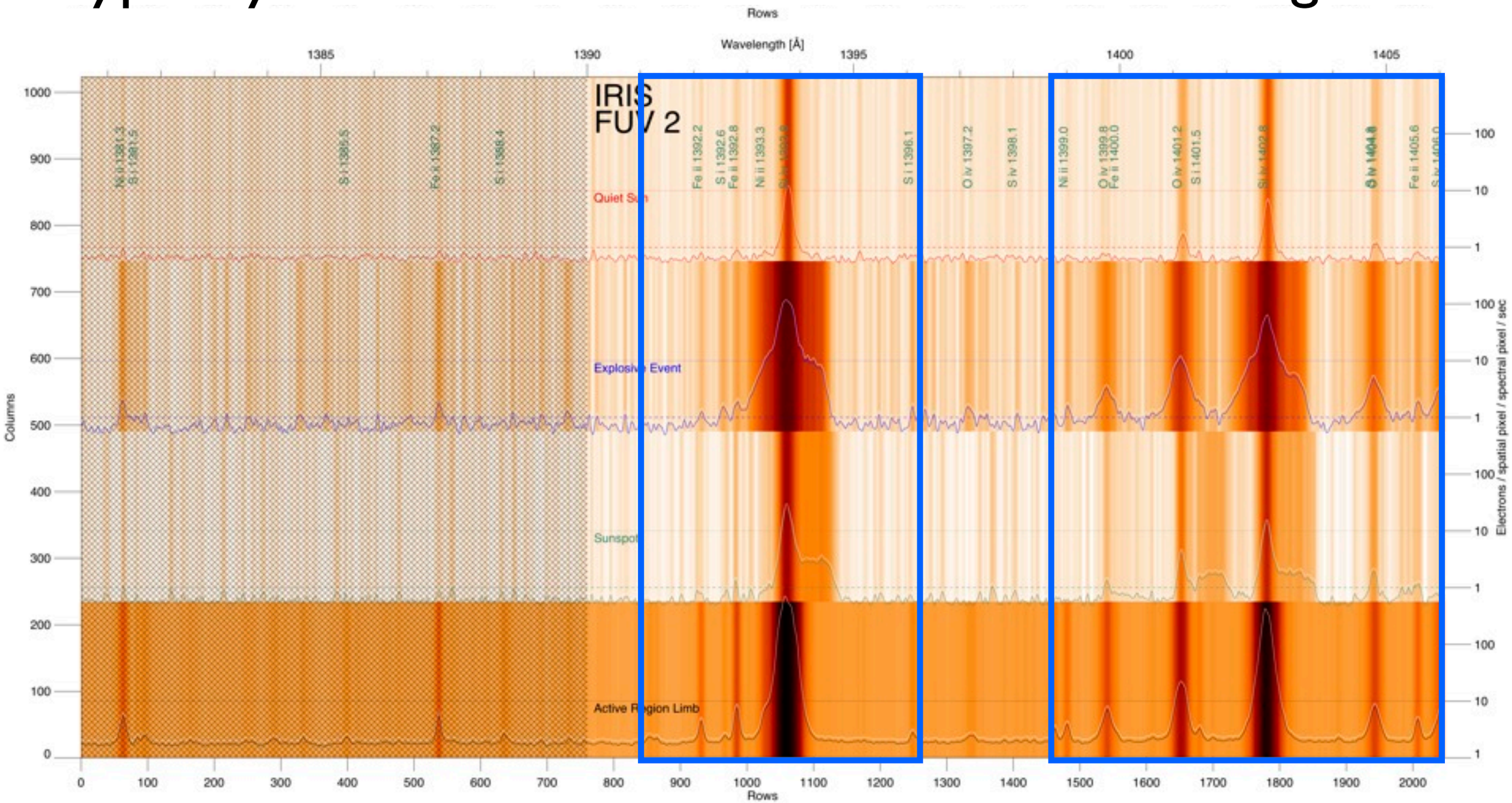

IRIS will rarely read out full NUV spectra: typically 2-3 2-13Å wide windows focused on regions of interest

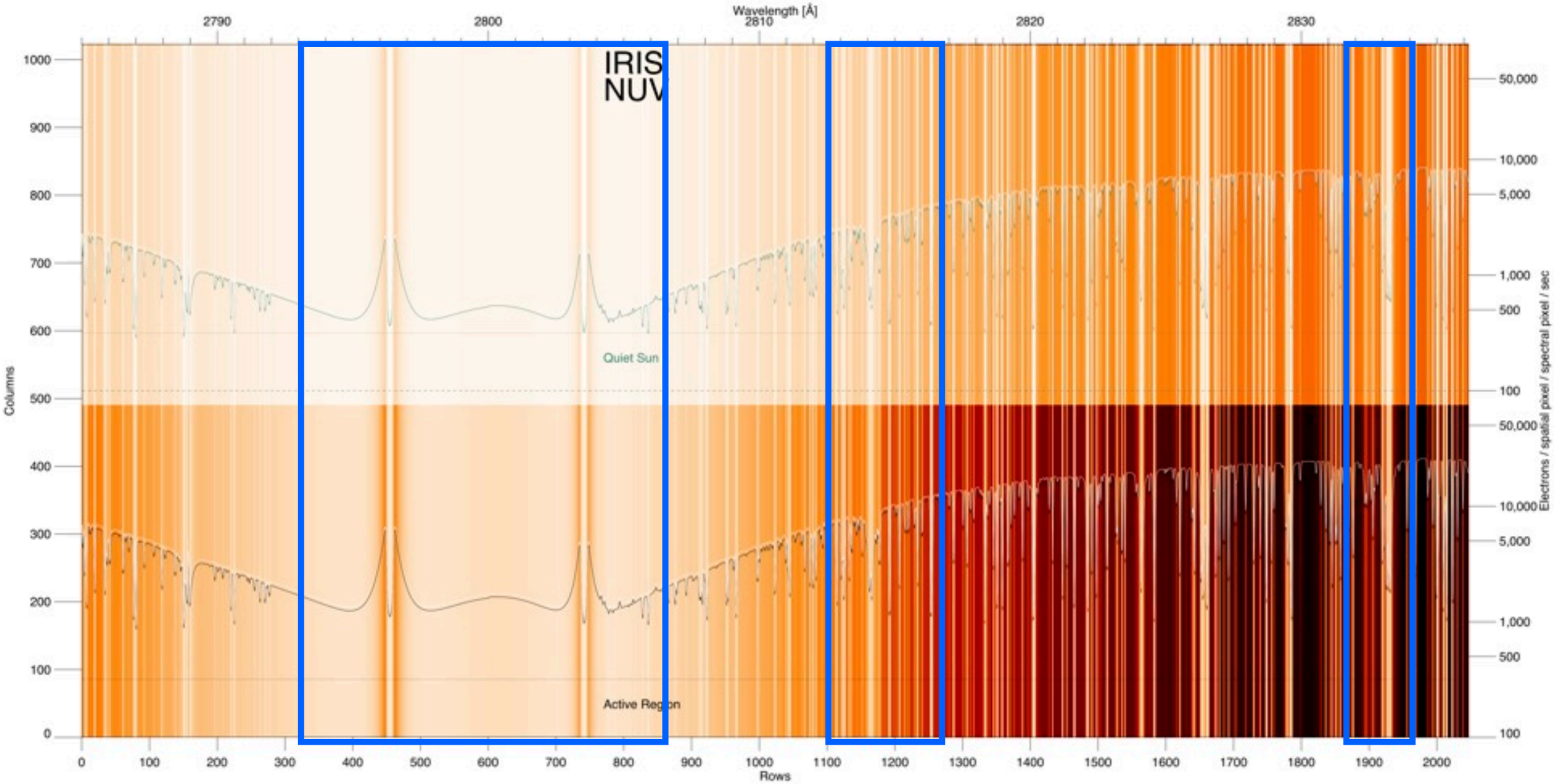

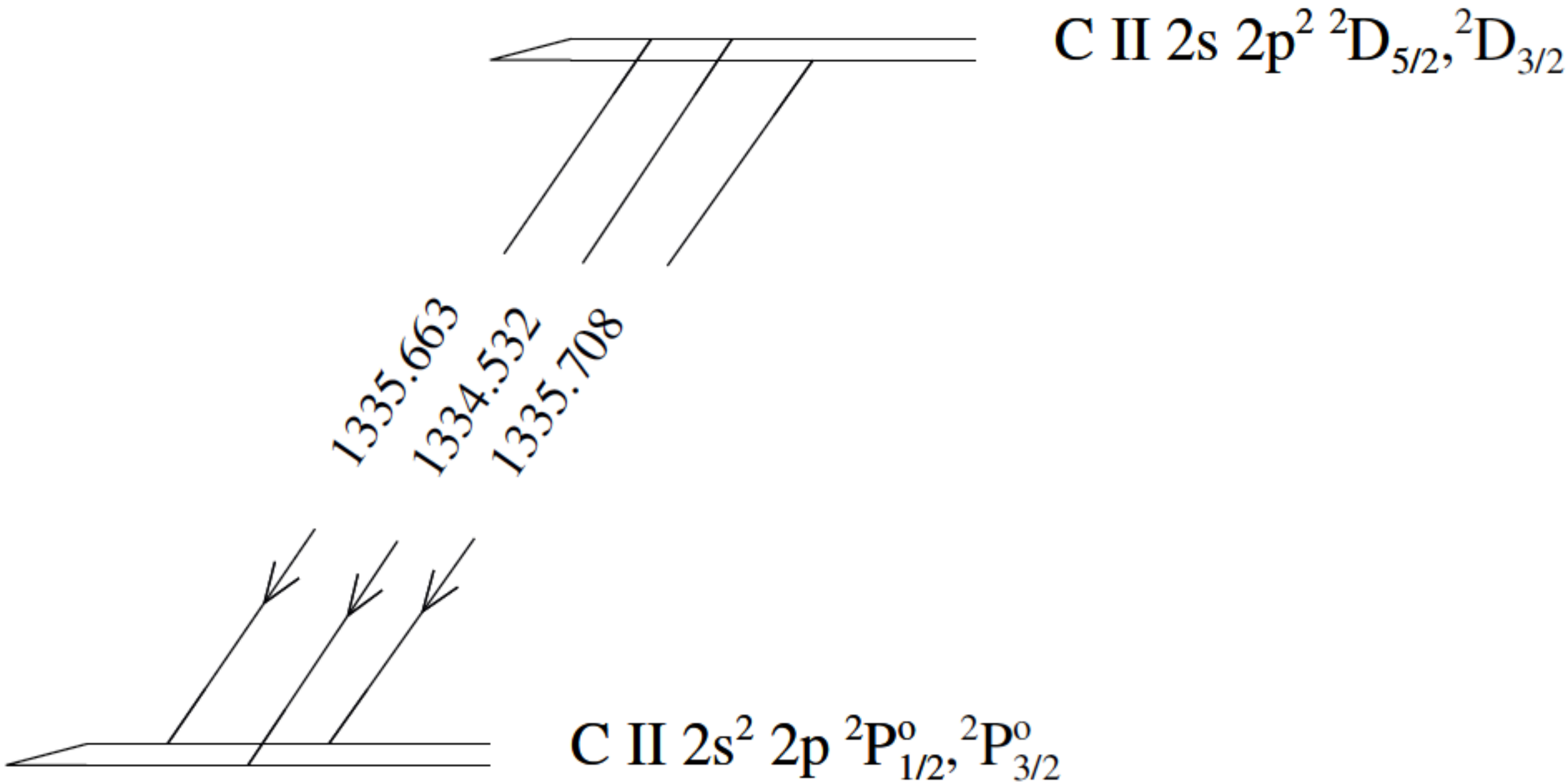
C II 2s 2p^2 $^2D_{5/2}$,$^2D_{3/2}$
1335.663
1334.532
1335.708
C II 2s^2 2p $^2P^o_{1/2}$,$^2P^o_{3/2}$

C II 1335 multiplet

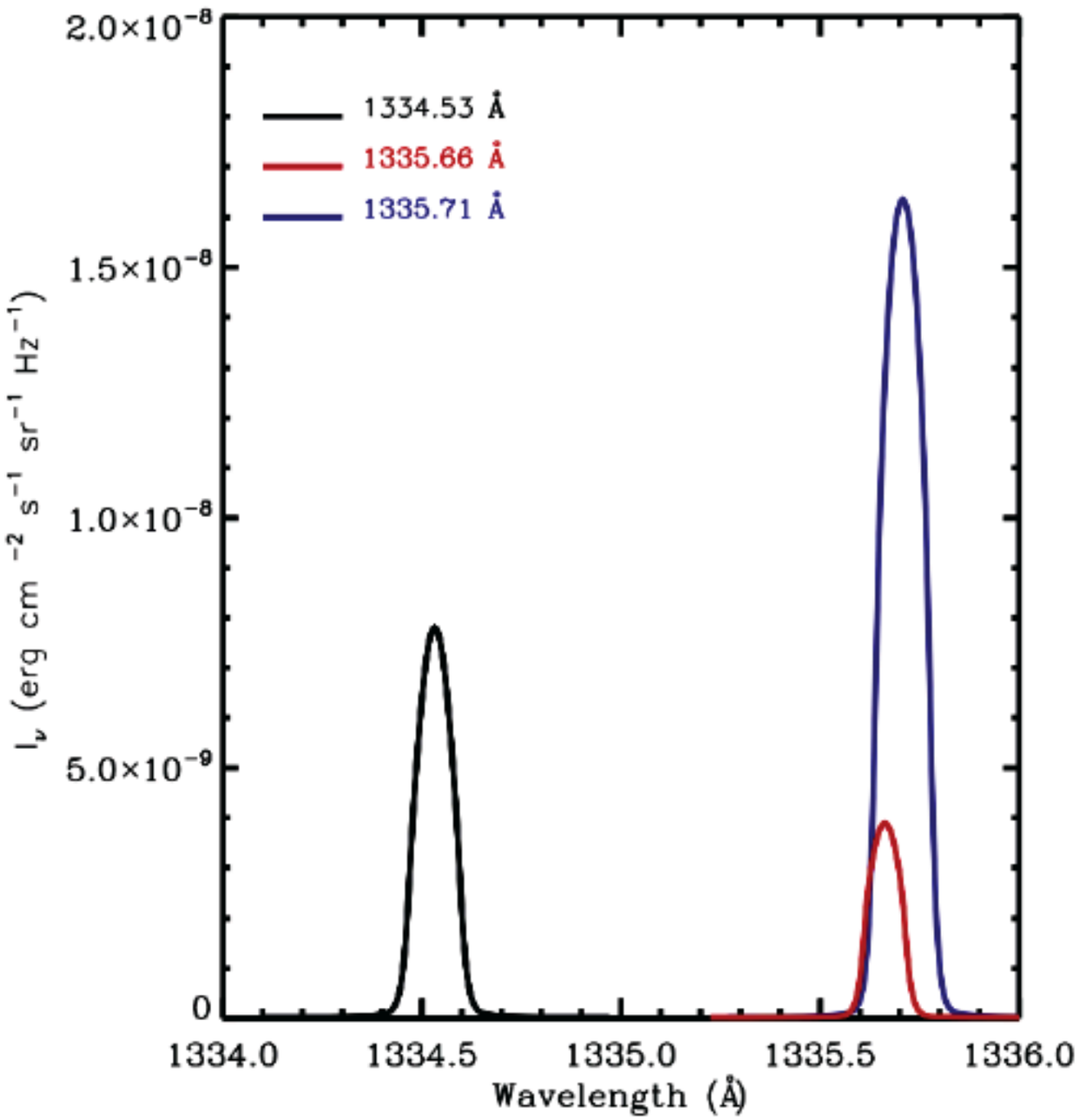

Wavelength (Å)	J_u	J_l	gf
1334.5323	3/2	1/2	0.257
1335.6625	3/2	3/2	0.0512
1335.7077	5/2	3/2	0.464

Rathore & Carlsson, in prep

IRIS observations

30s exposures, 400 step raster

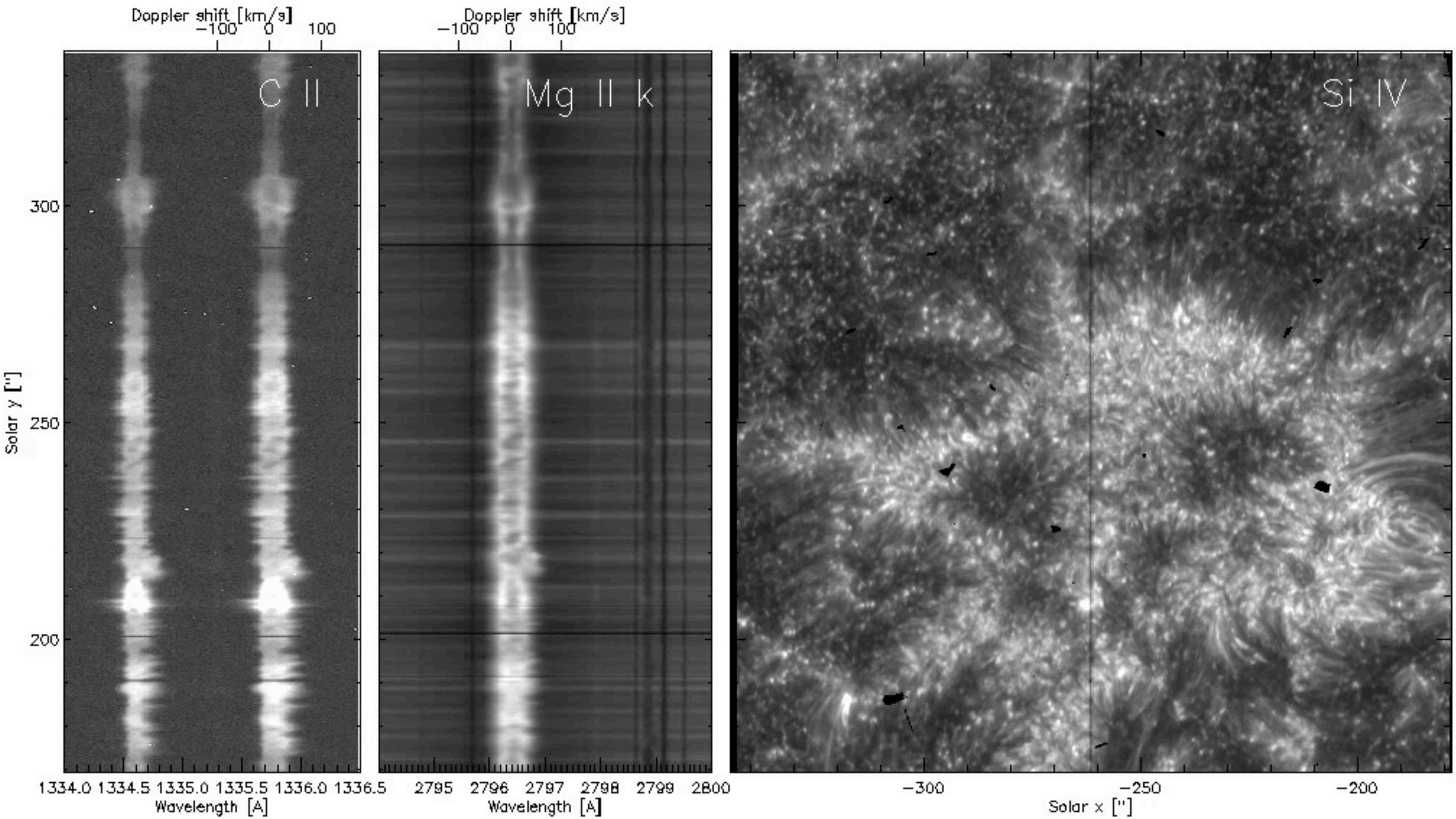

20131018_195030_3820013446

Temporal behaviour

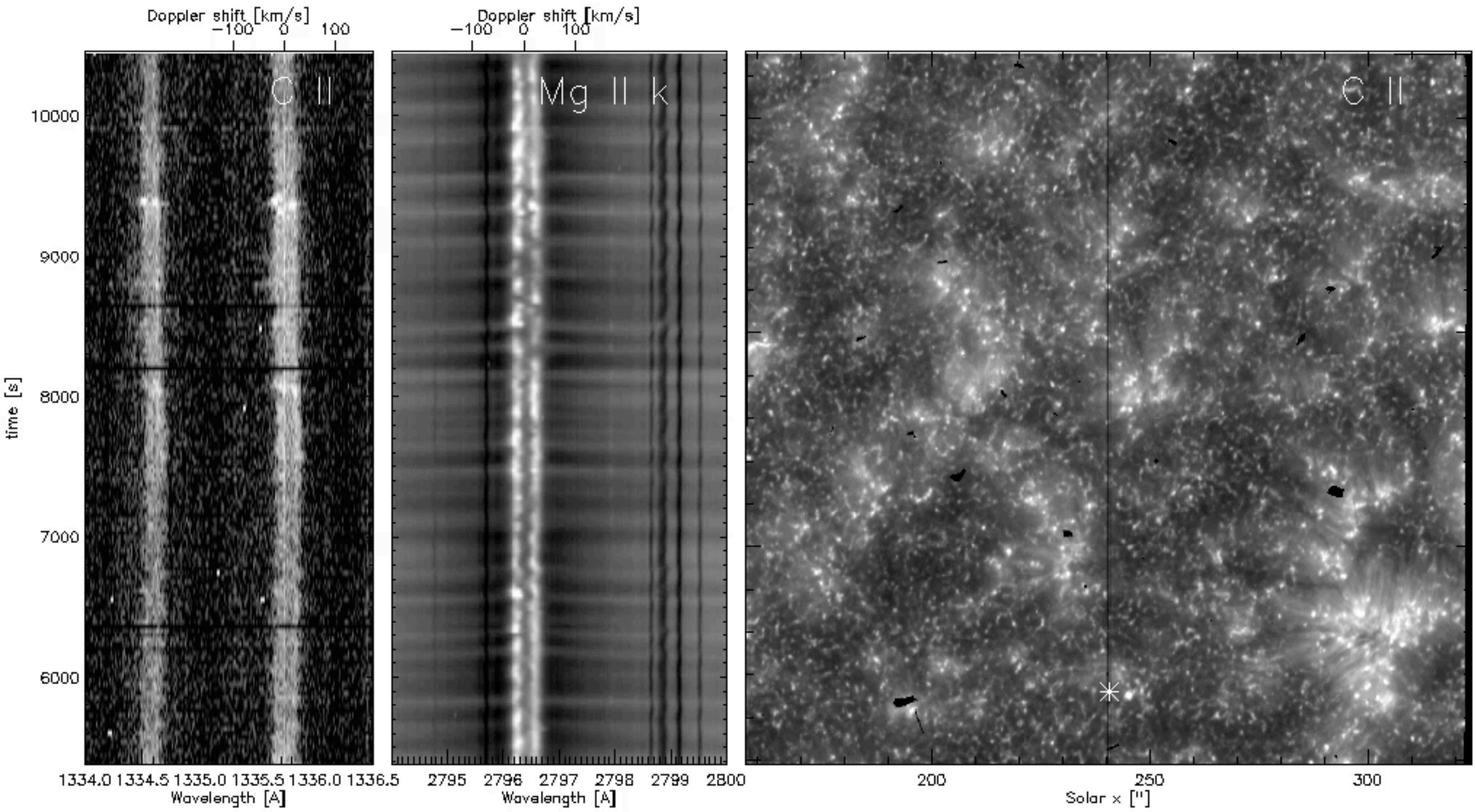

20131008_195658_3820012104

Diagnostics of spicules

8s exposures, 400 step raster, 9s between raster steps

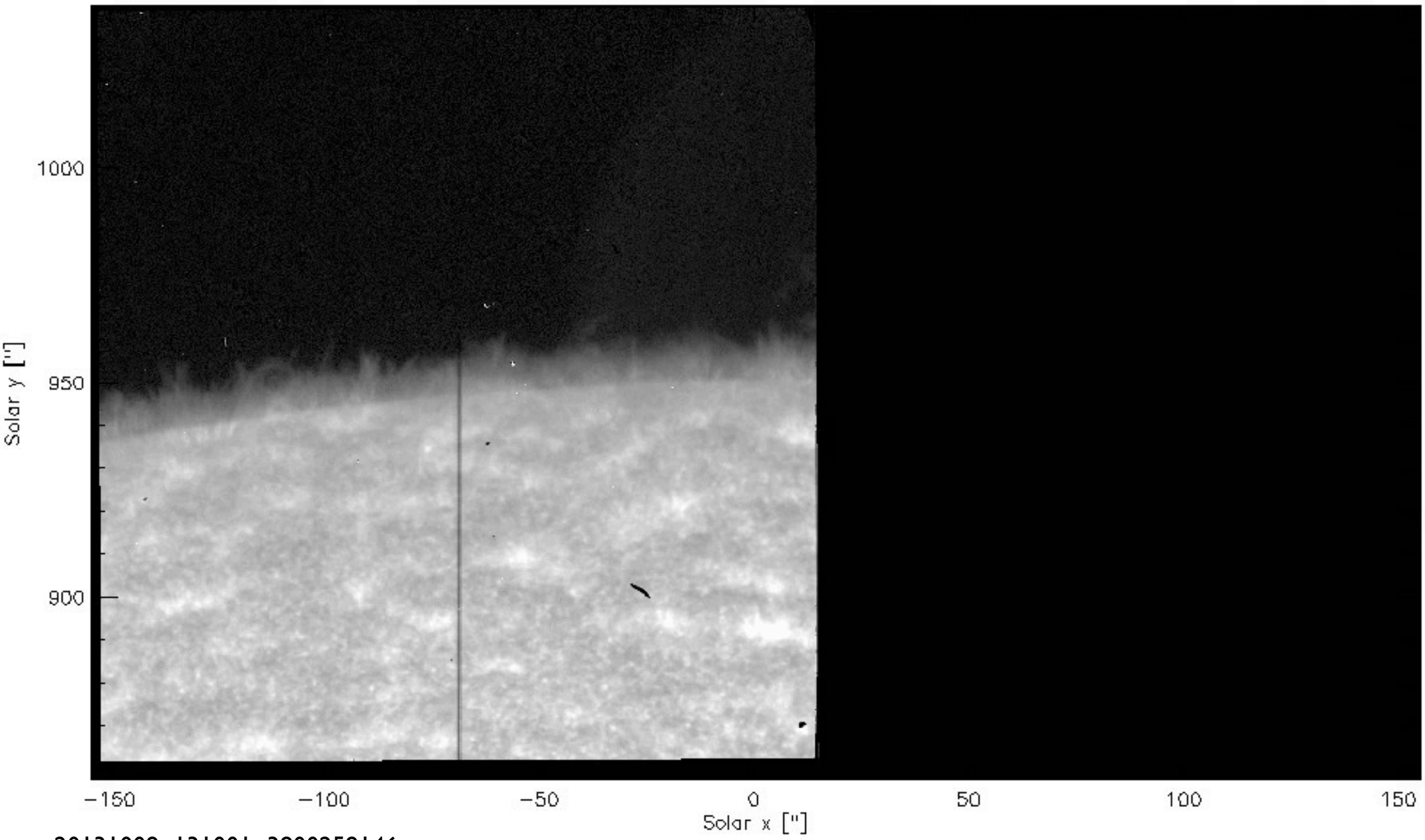

20131009_131001_3800259146

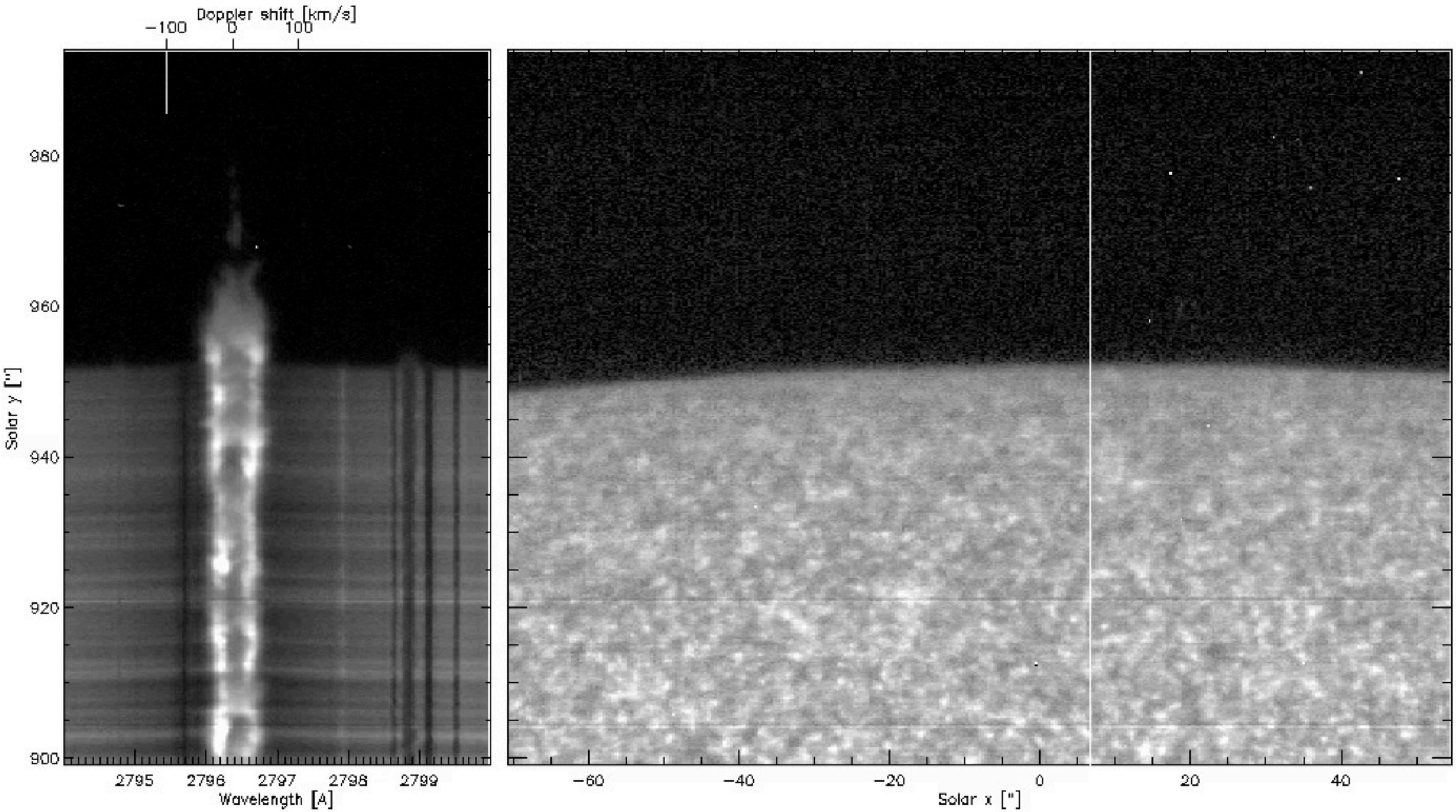

20131009_131001_3800259146

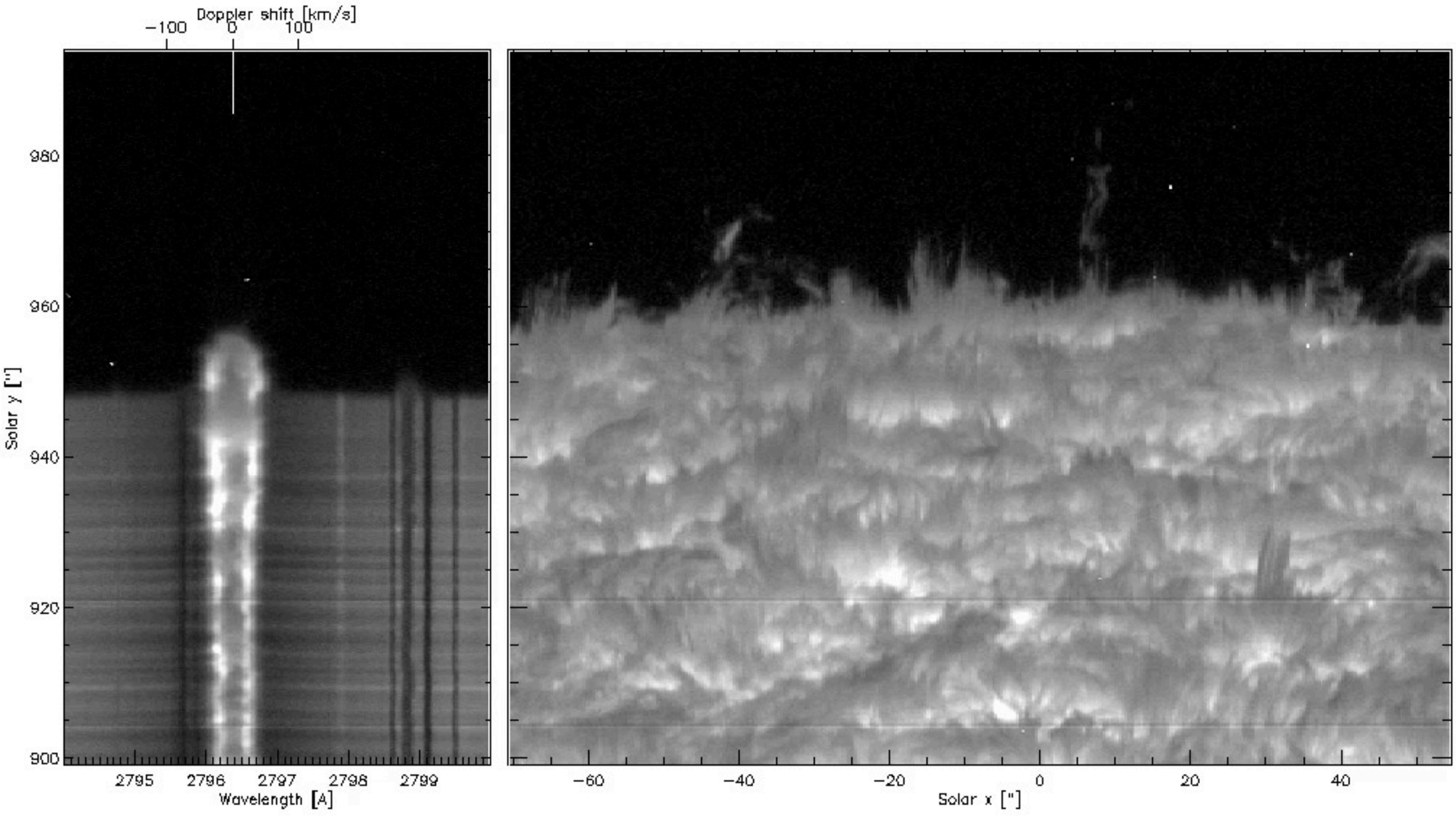

20131009_131001_3800259146

Mg II 280nm diagnostics

Recent papers (2013)

Leenaarts, Pereira, Carlsson, Uitenbroek, De Pontieu (in various permutations):

The Formation of IRIS Diagnostics:

I. A Quintessential Model Atom of Mg II and General FormationProperties of the Mg II h&k Lines

II. The Formation of the Mg II h&k Lines in the Solar Atmosphere

III. NUV Spectra and Images

Mg II h & k lines

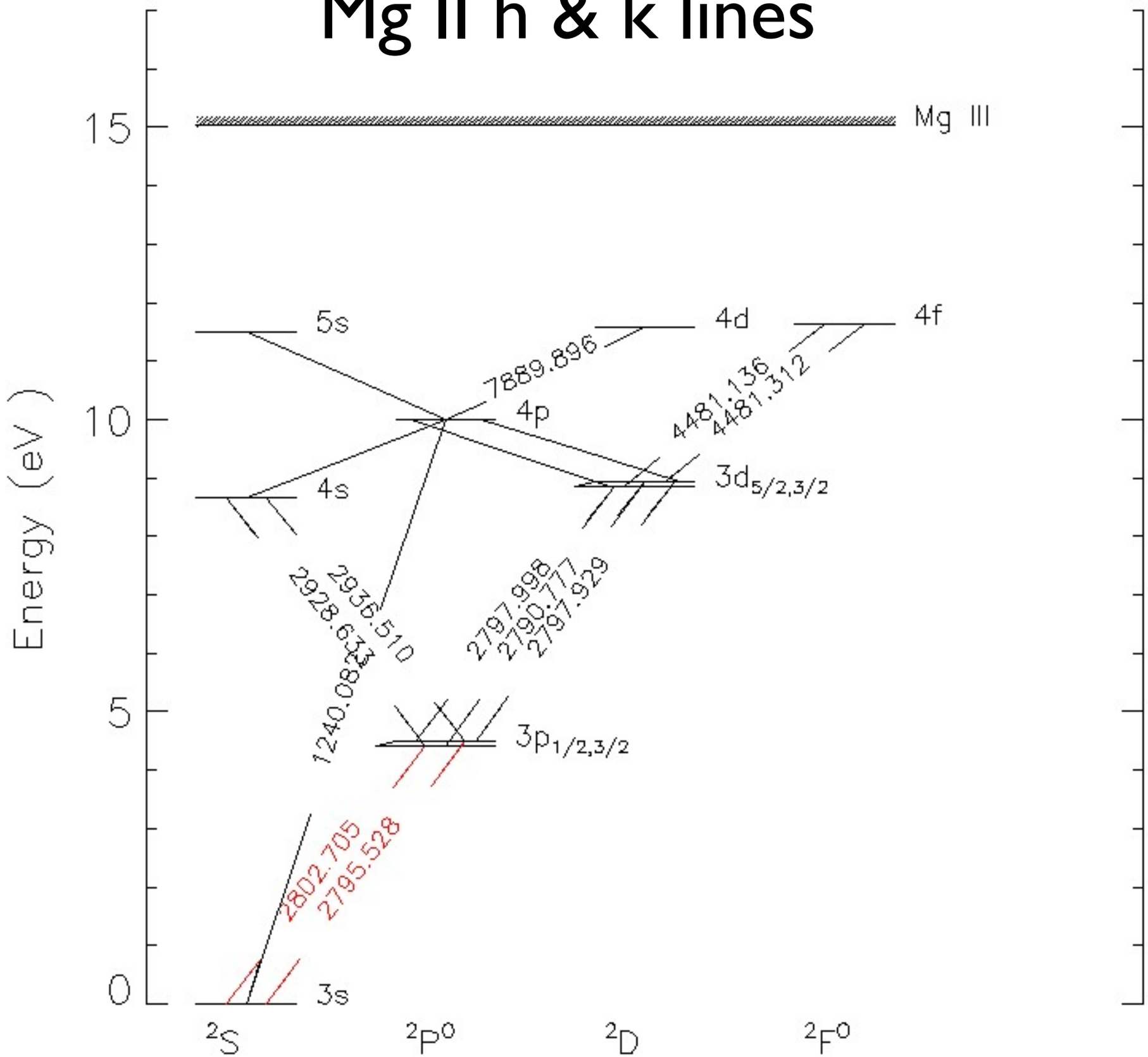

Mg has 18 times the abundance of Ca formed 3 scale-heights higher up

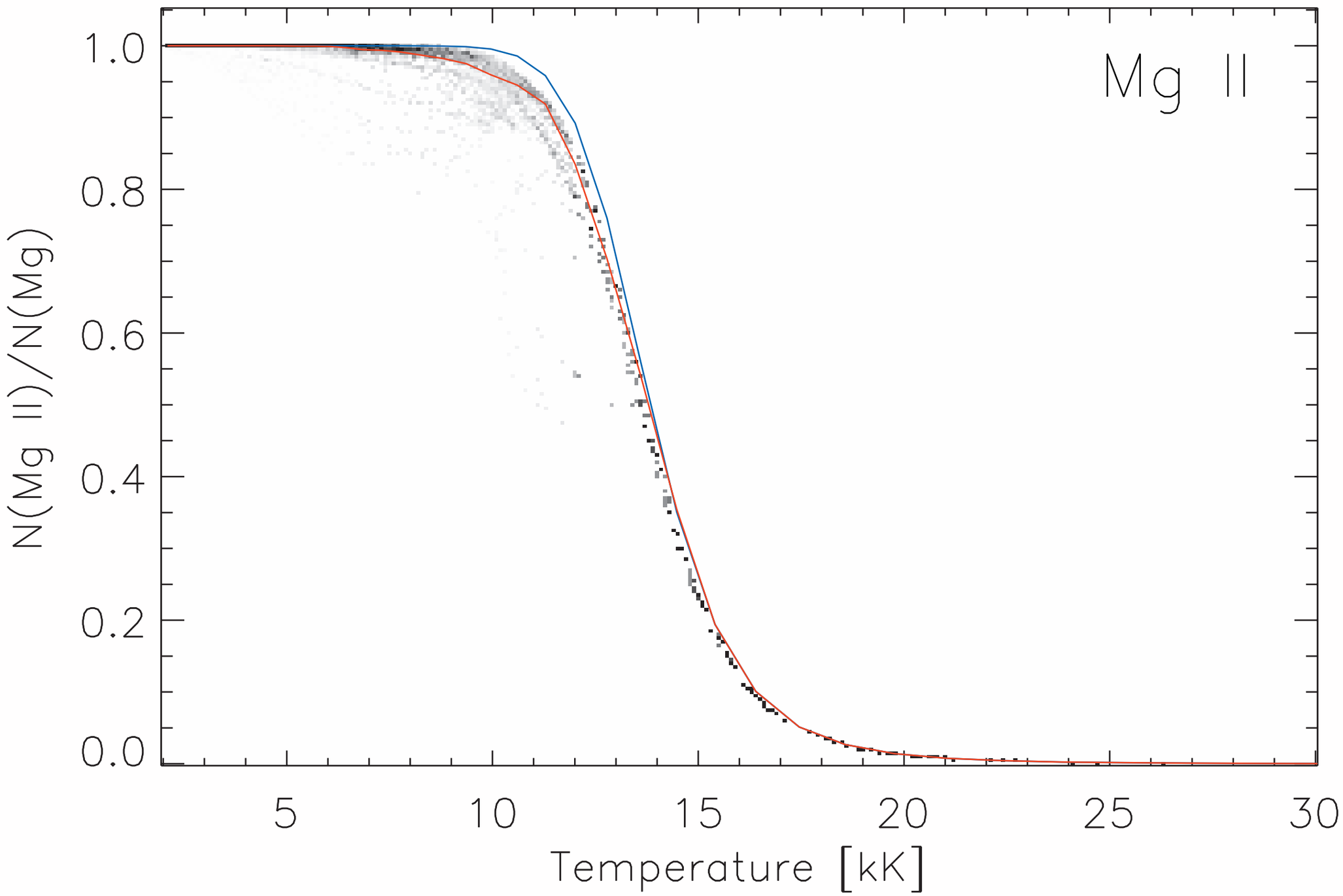

Bifrost model

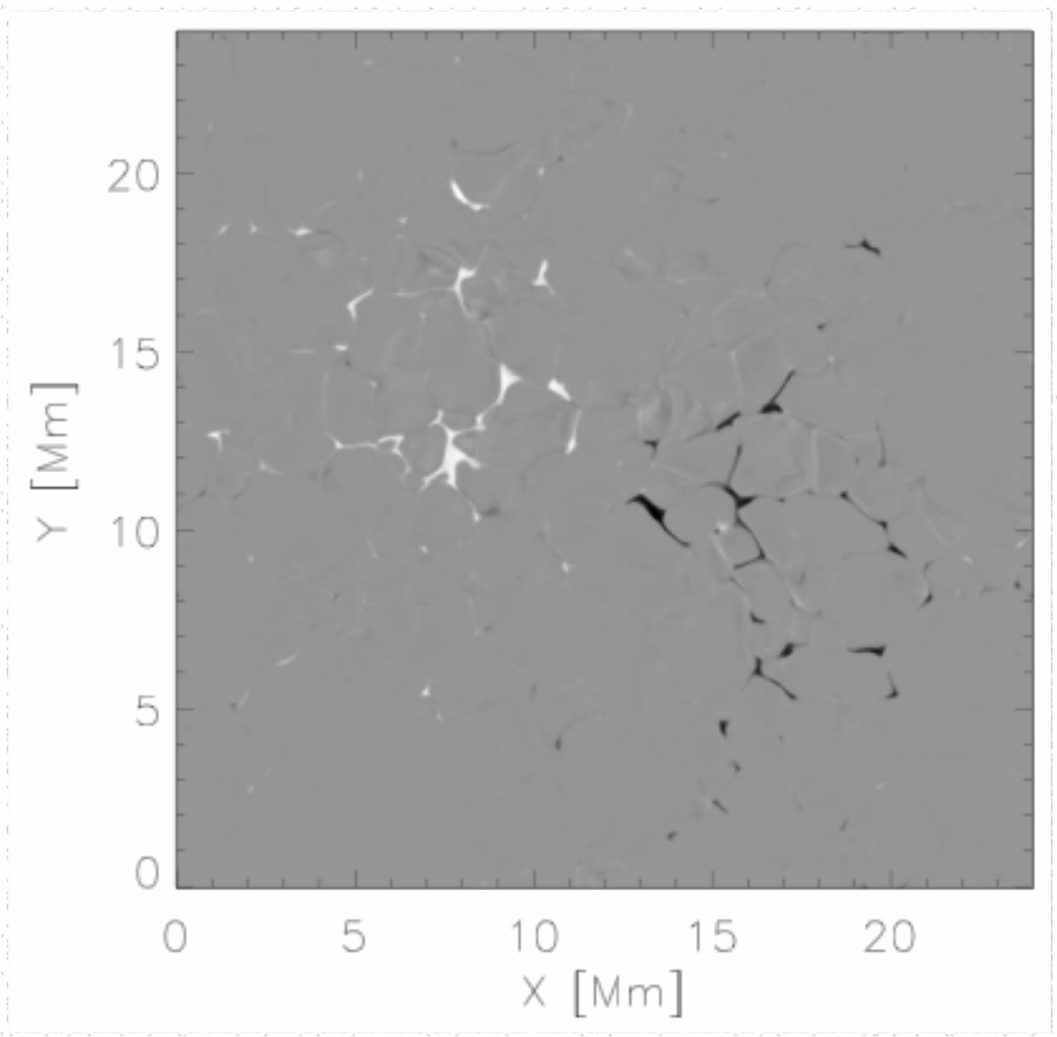

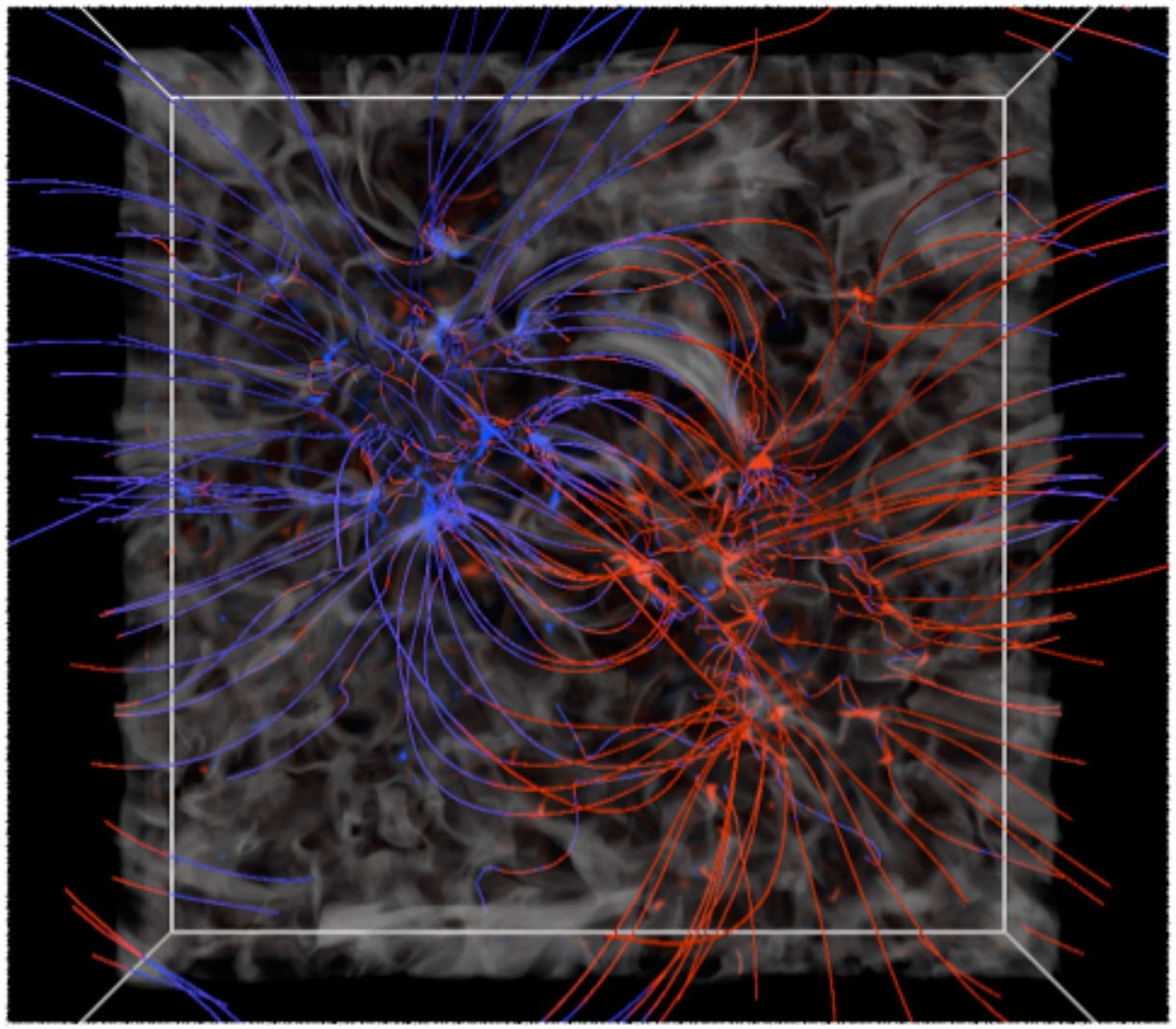

Made available at http://sdc.uio.no/search/simulations

Observables: intensity and Doppler-shift of features

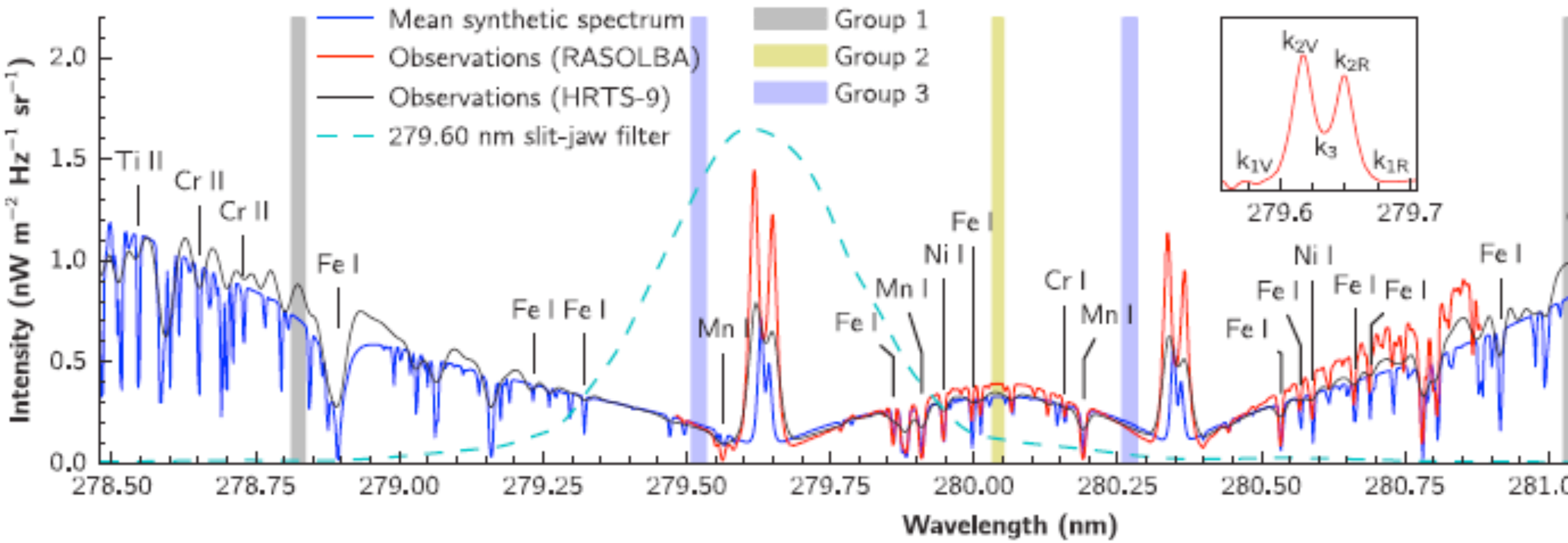

Mg II h&k: line core forms 200 km below the TR

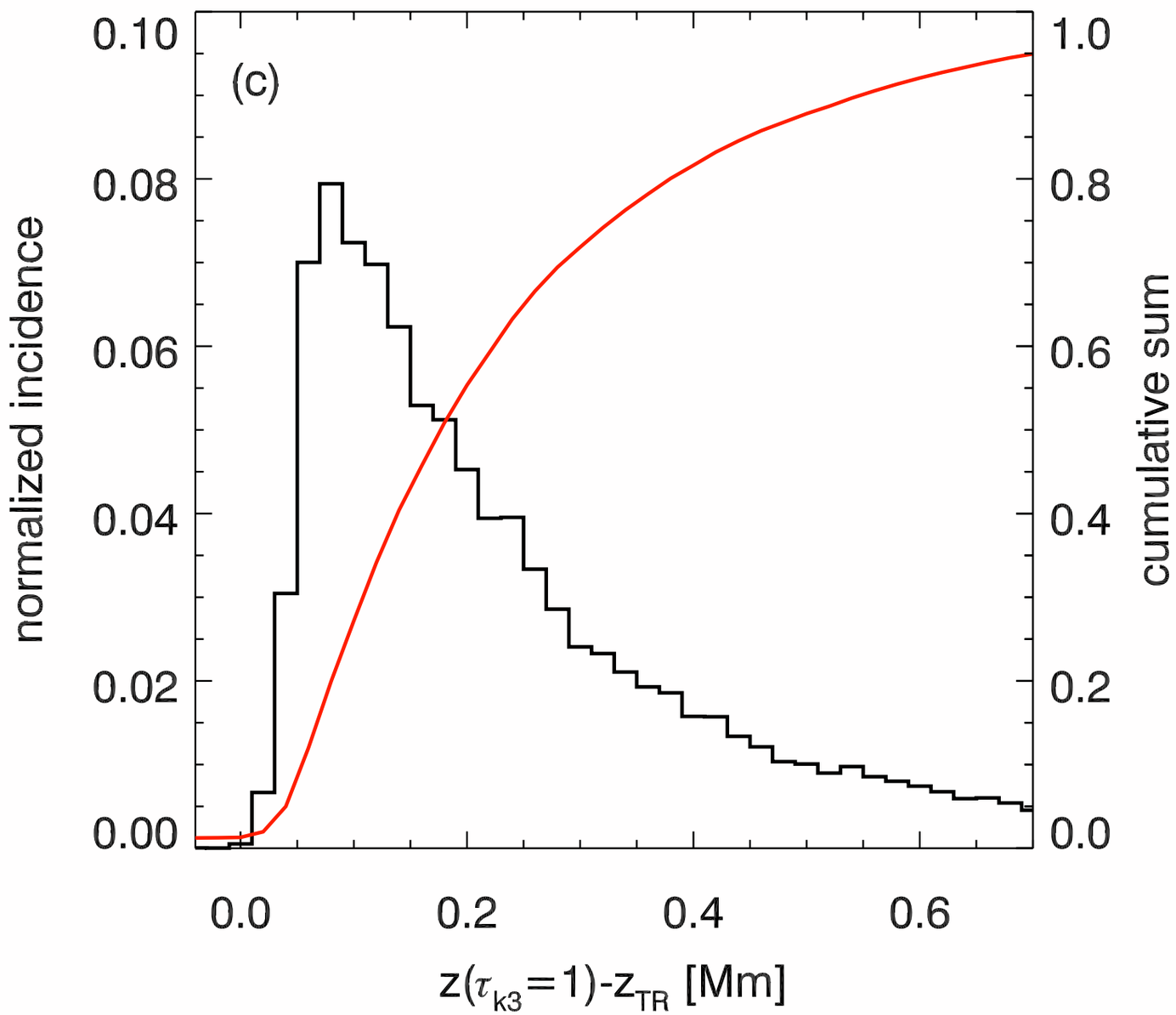

Mg II h&k: h3/k3 minimum Dopplershift correlates with $v_z(\tau=1)$

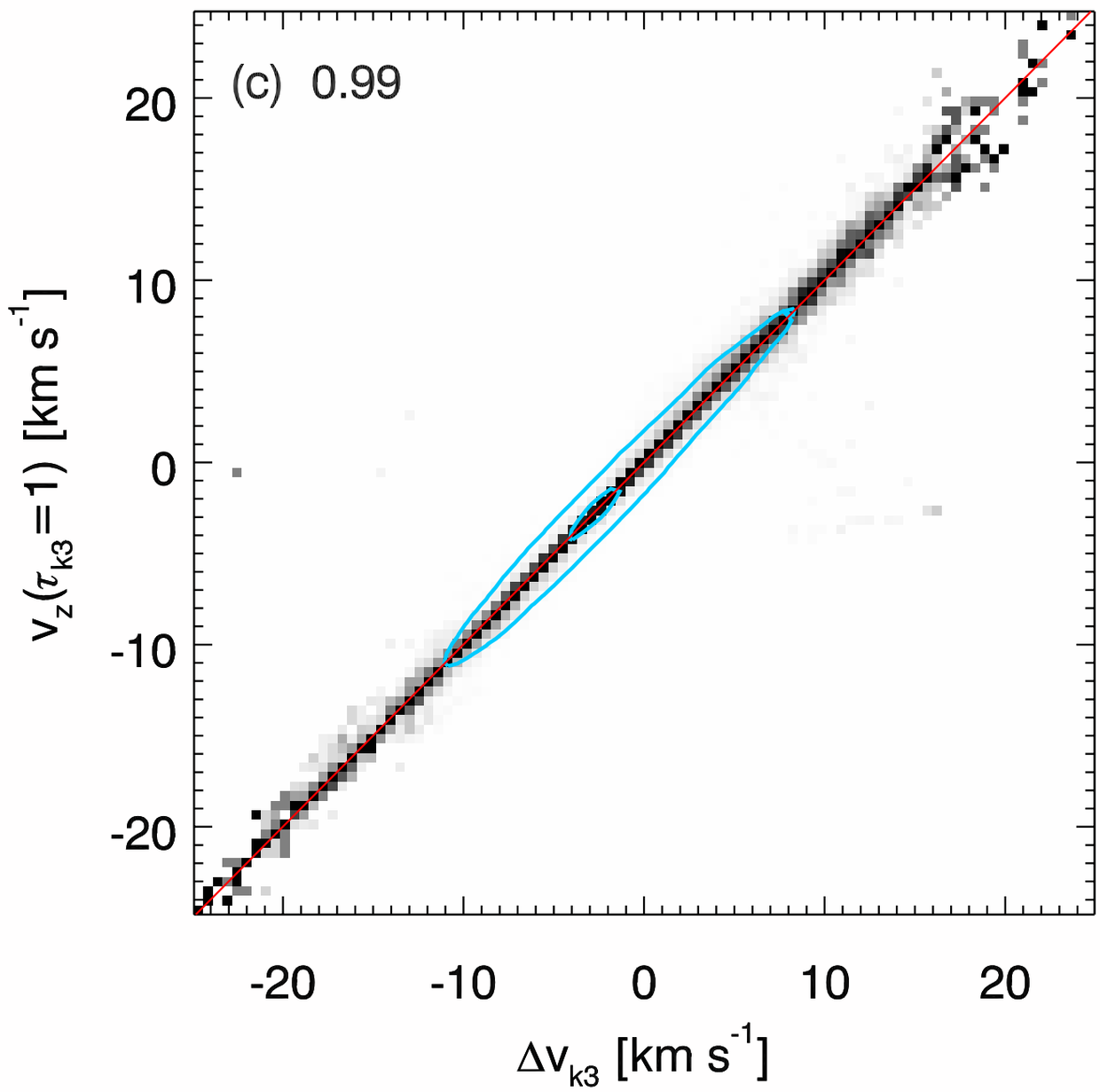

Mg II h&k: h3-k3 Dopplershift measures velocity gradient

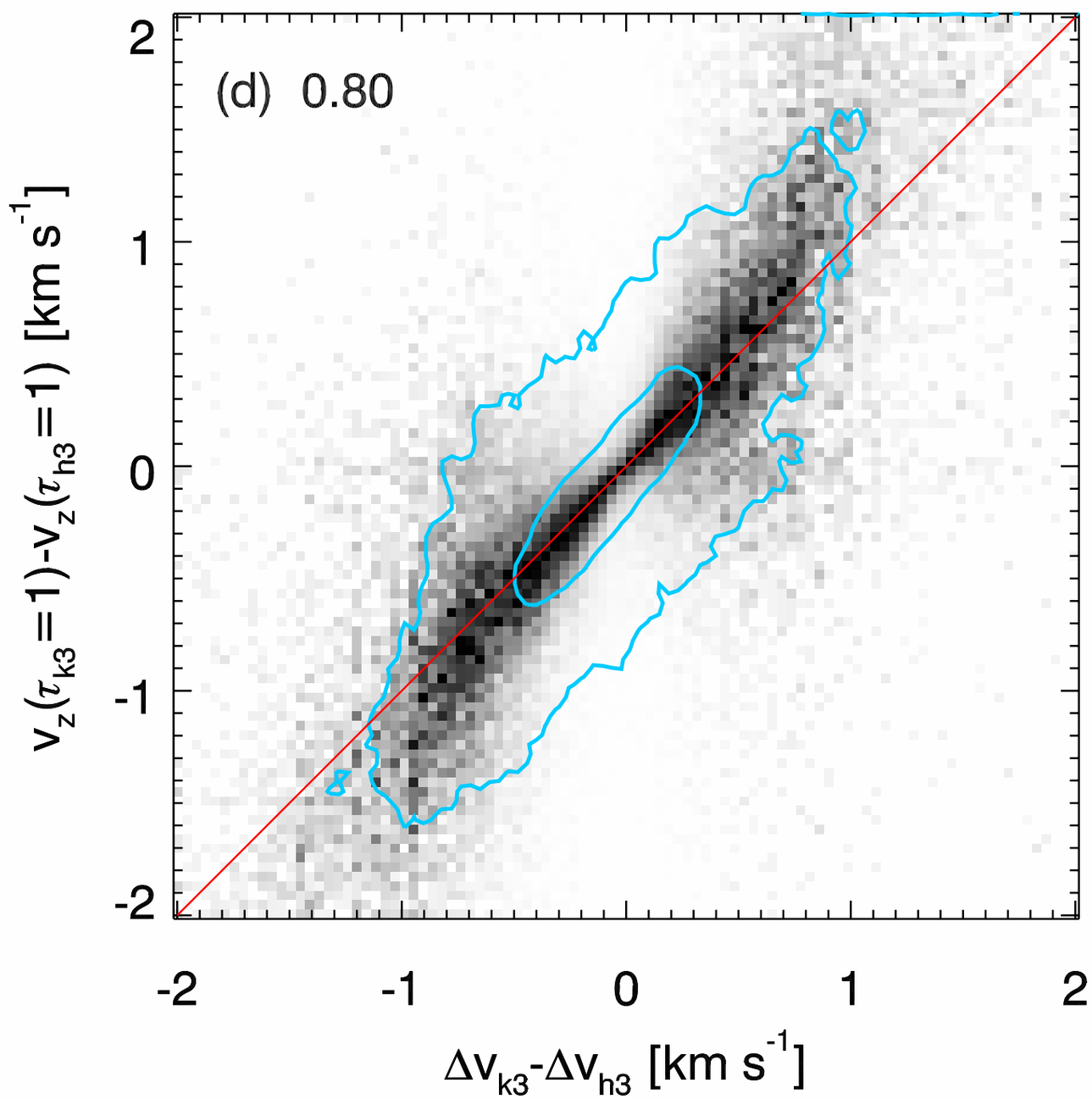

Mg II h&k: peak separation measures velocity extremes

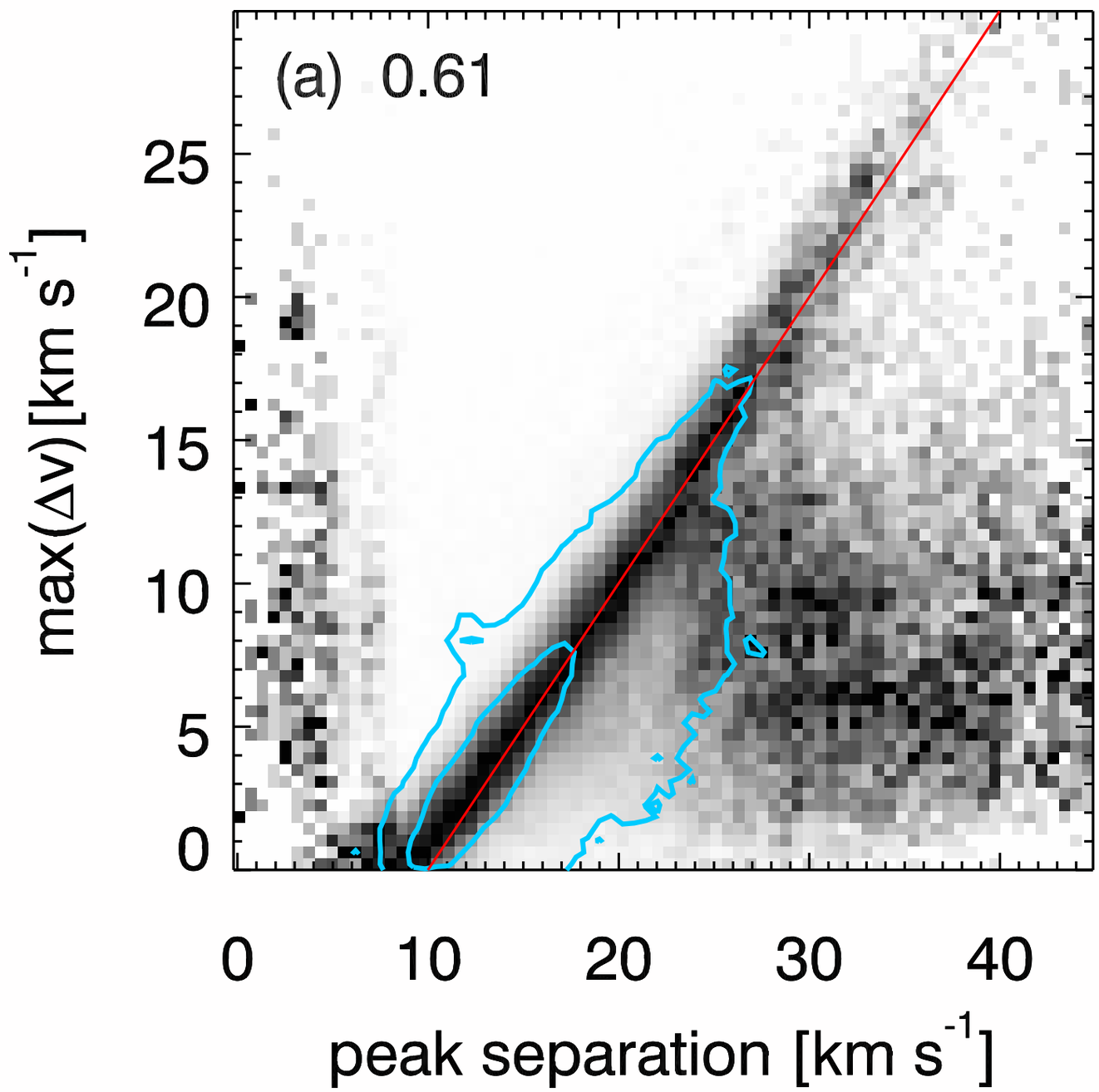

Mg II h&k: peak intensity measures temperature

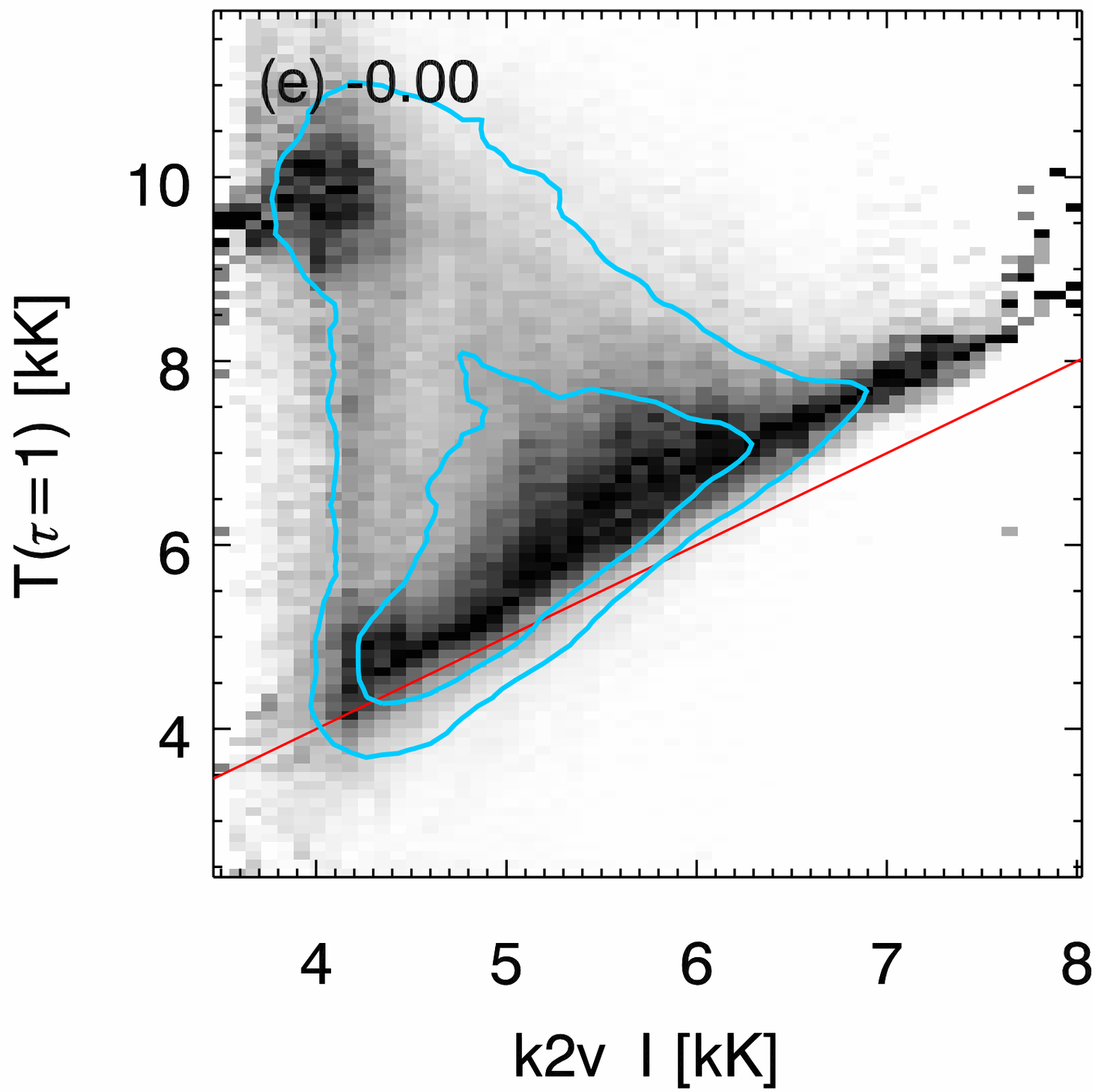

Wide band filters

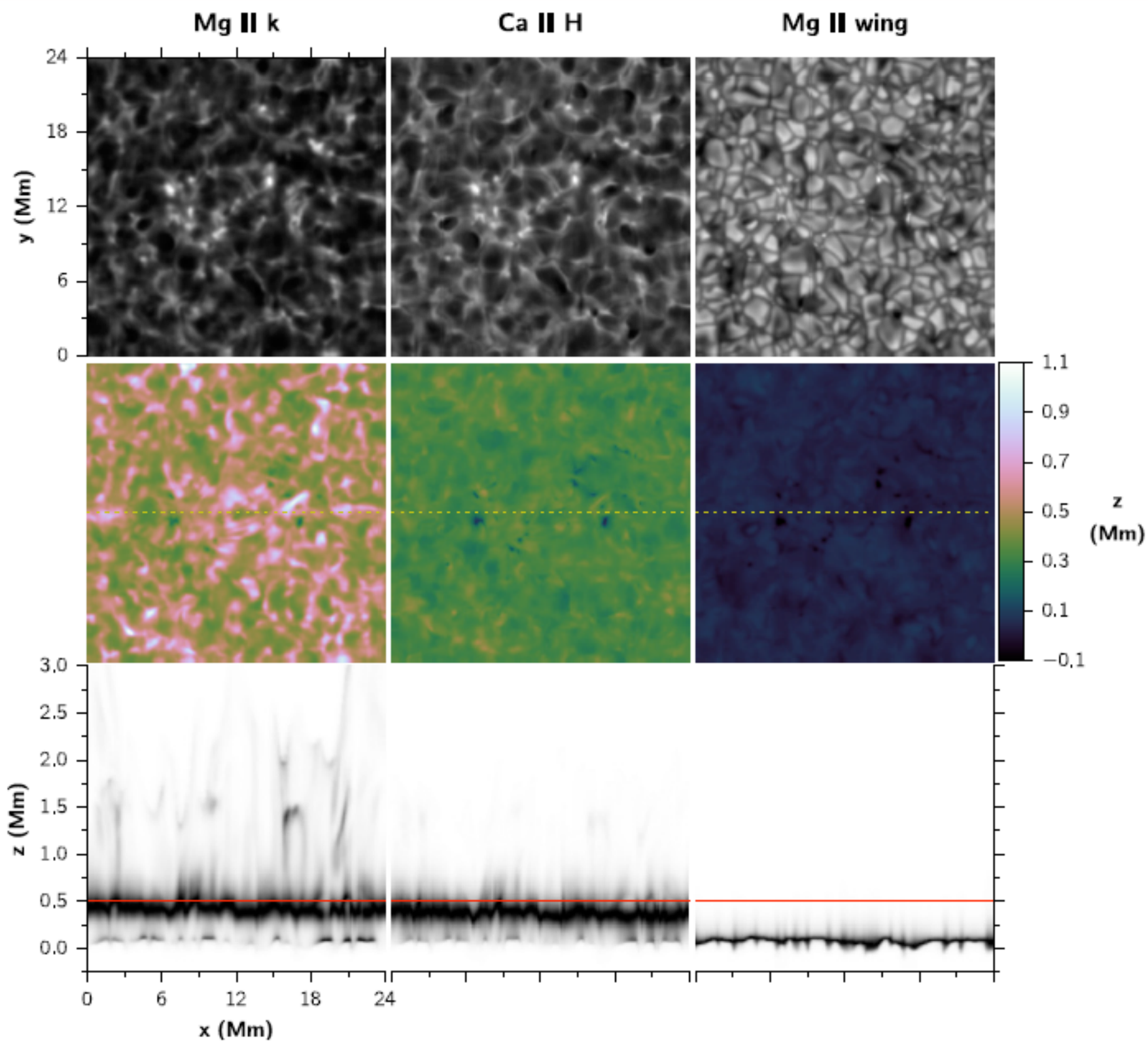

First Comparison between IRIS Data and Numerical Models

There are many low lying, short lived, presumably cool, loops in the C II '1330' and Si IV '1400' slit jaw images.

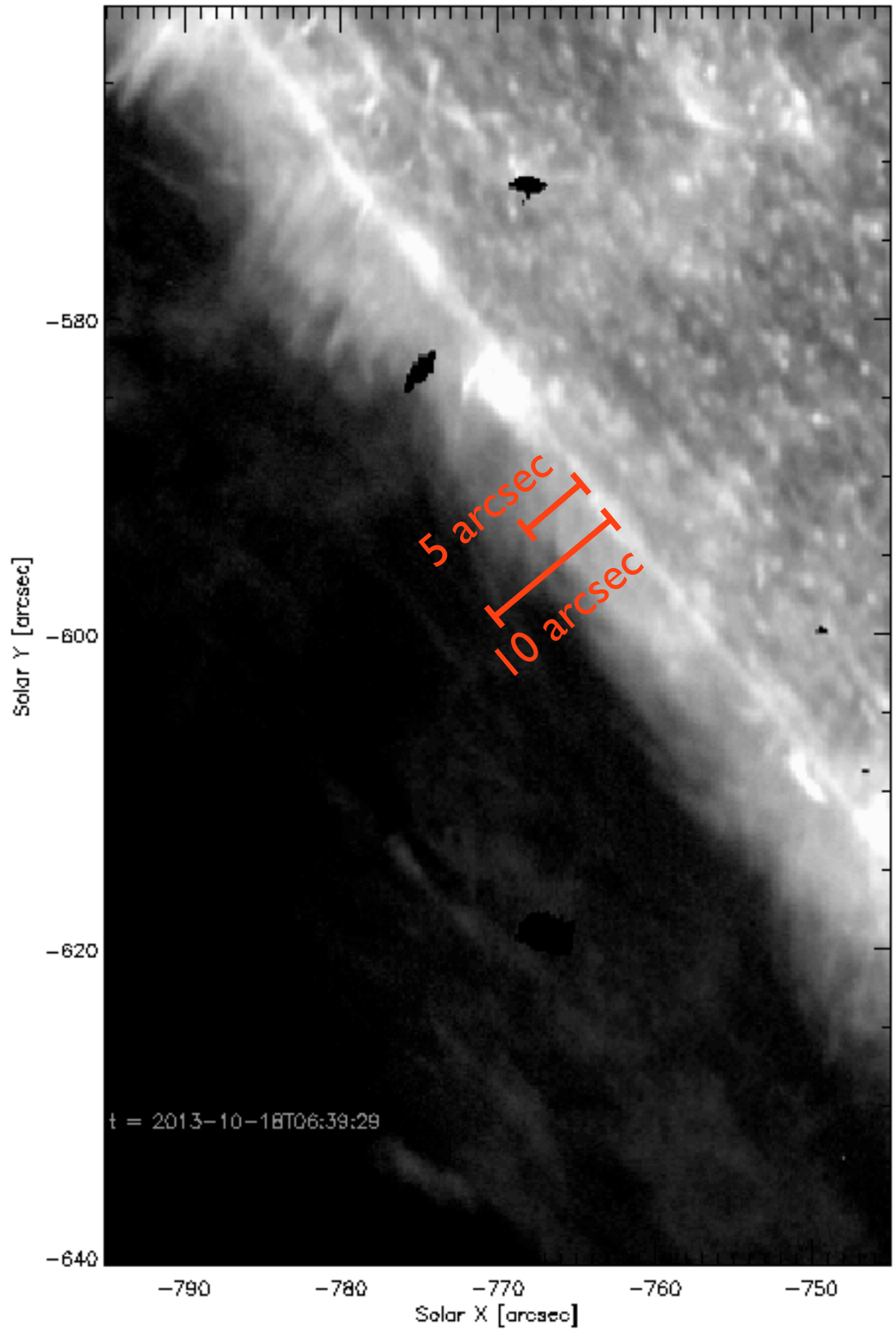

UFS

Viggo Hansteen et al (in prep)

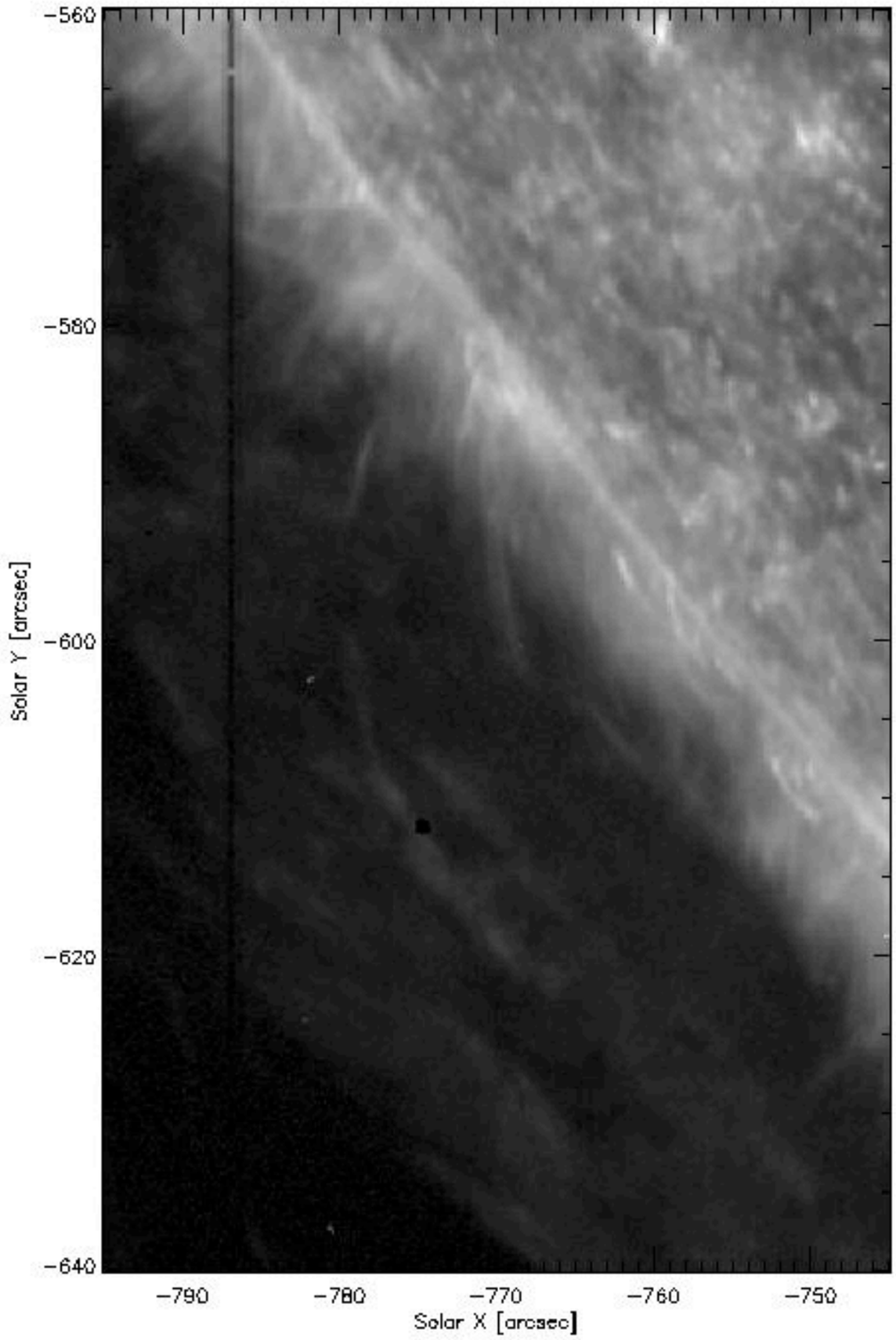
-560
-580
-600
-620
-640
Solar Y [arcsec]
-790
-780
-770
-760
-750
Solar X [arcsec]

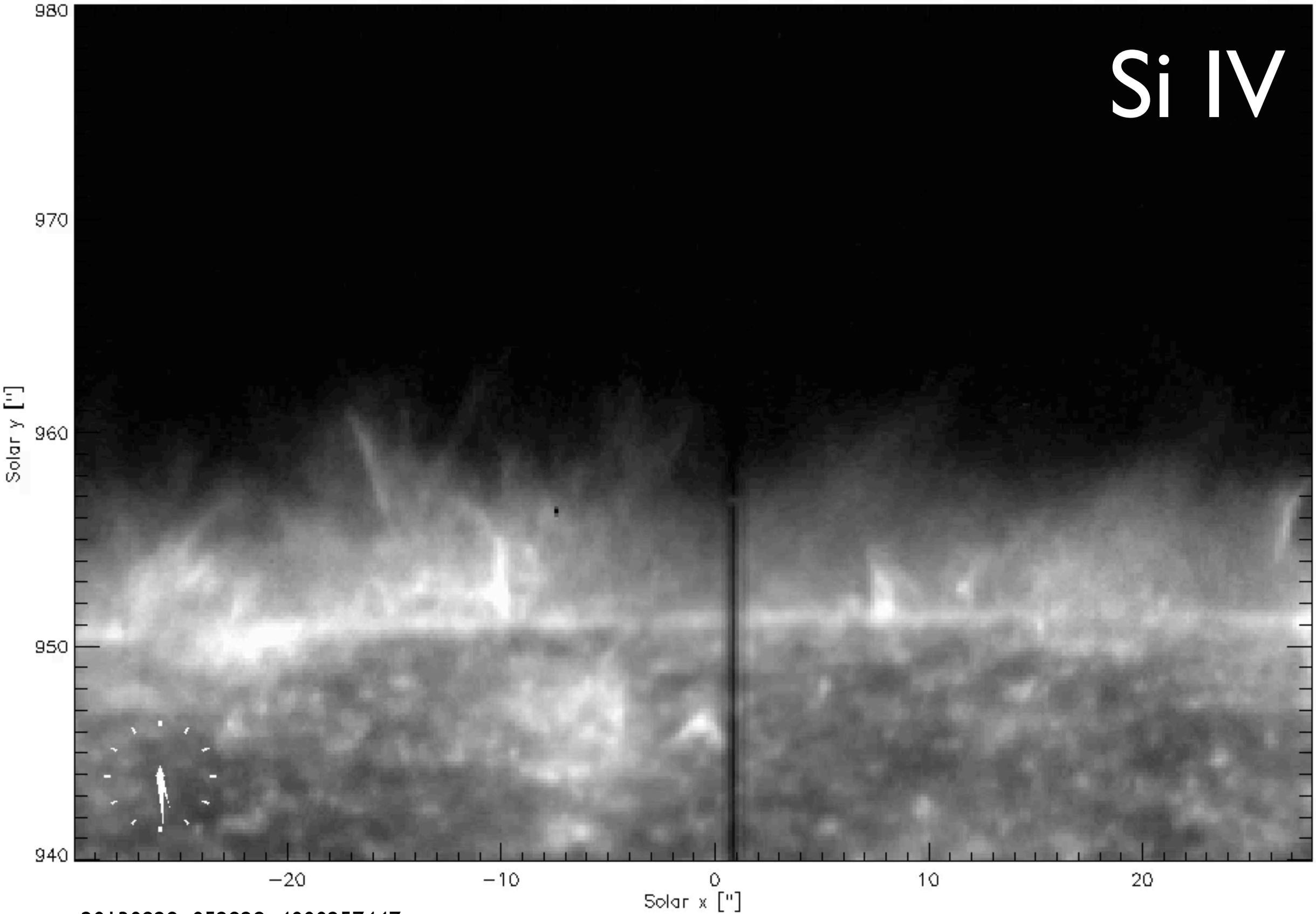

20130929_052928_4000257447

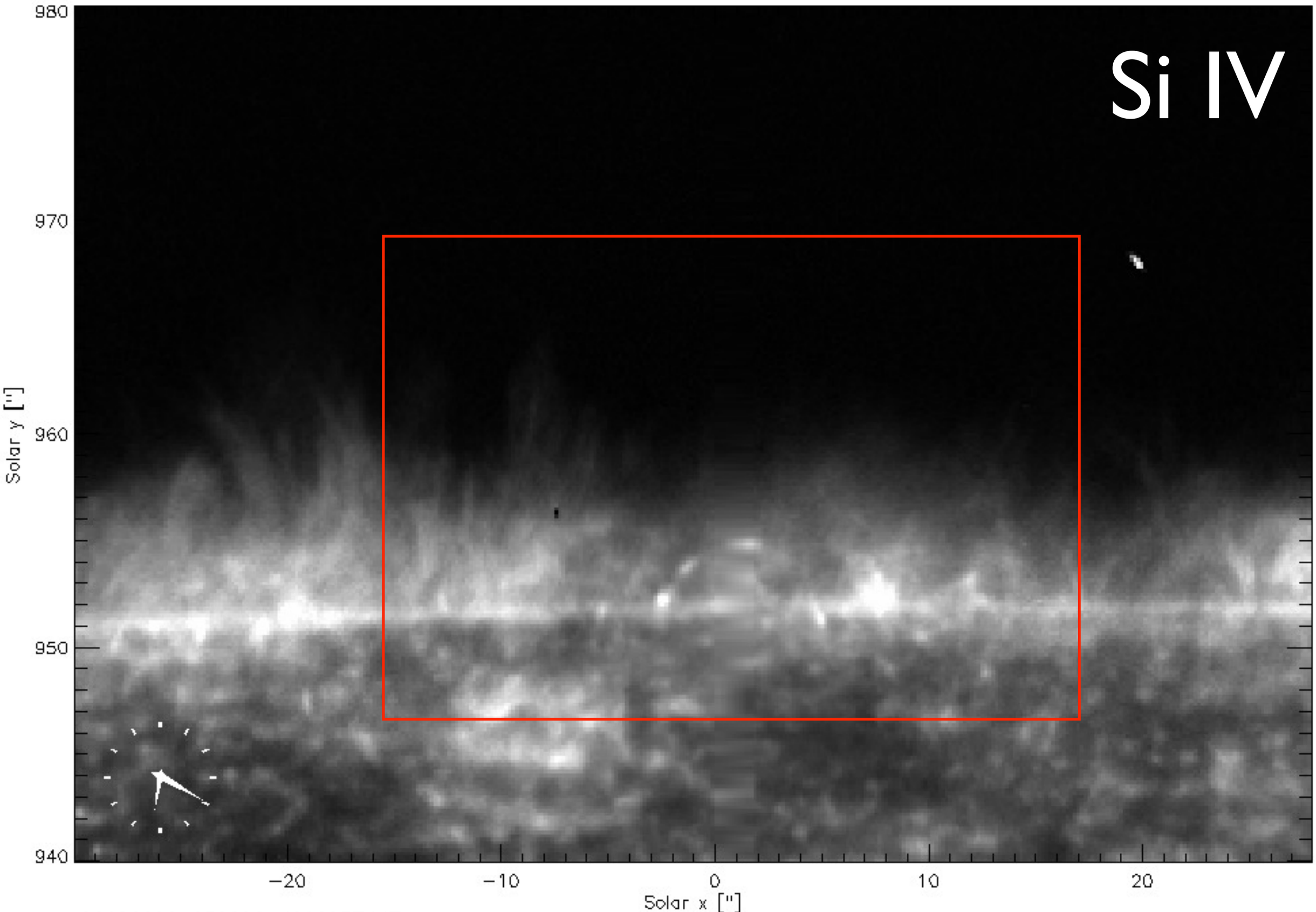

20130929_052928_4000257447

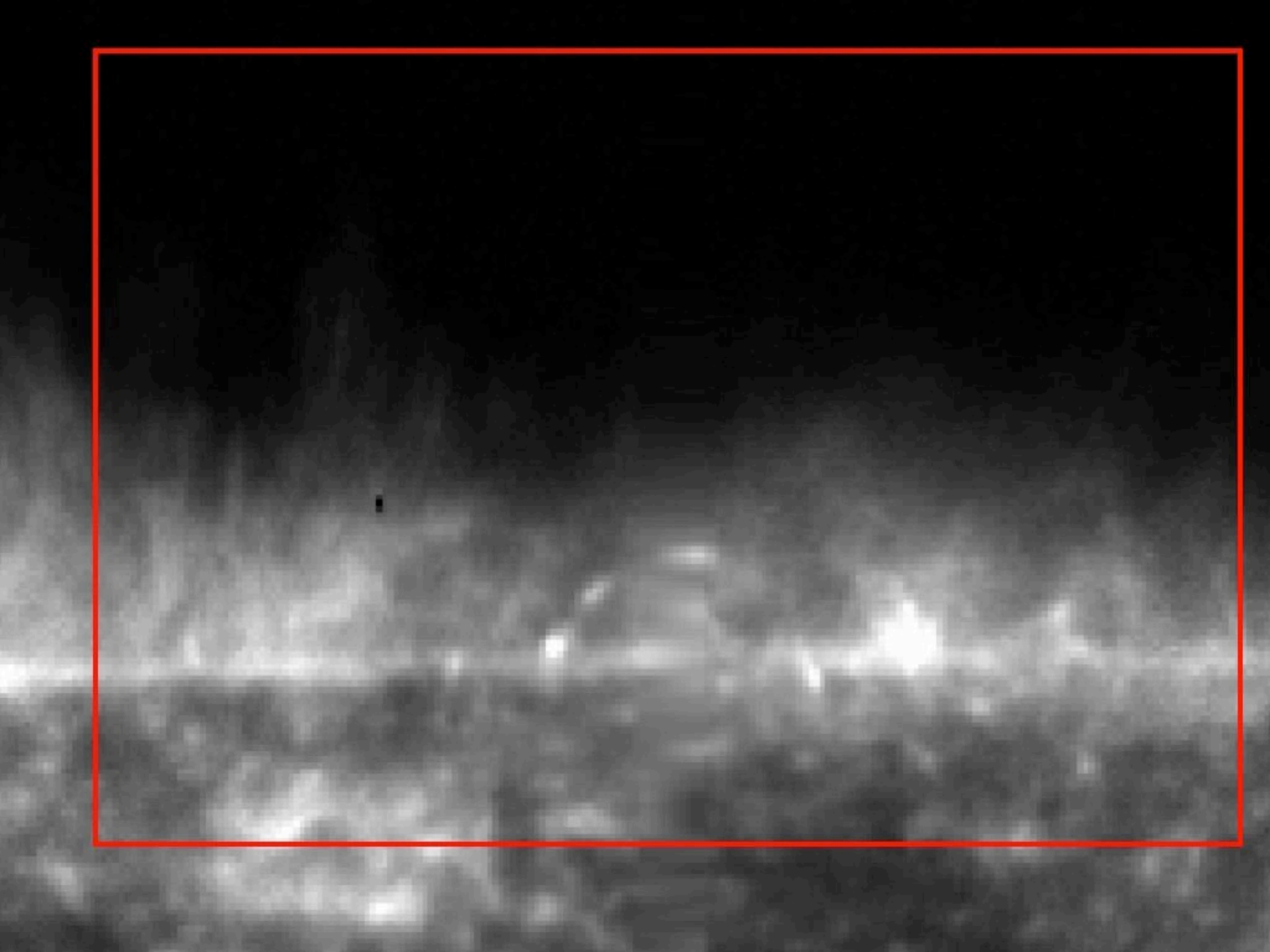

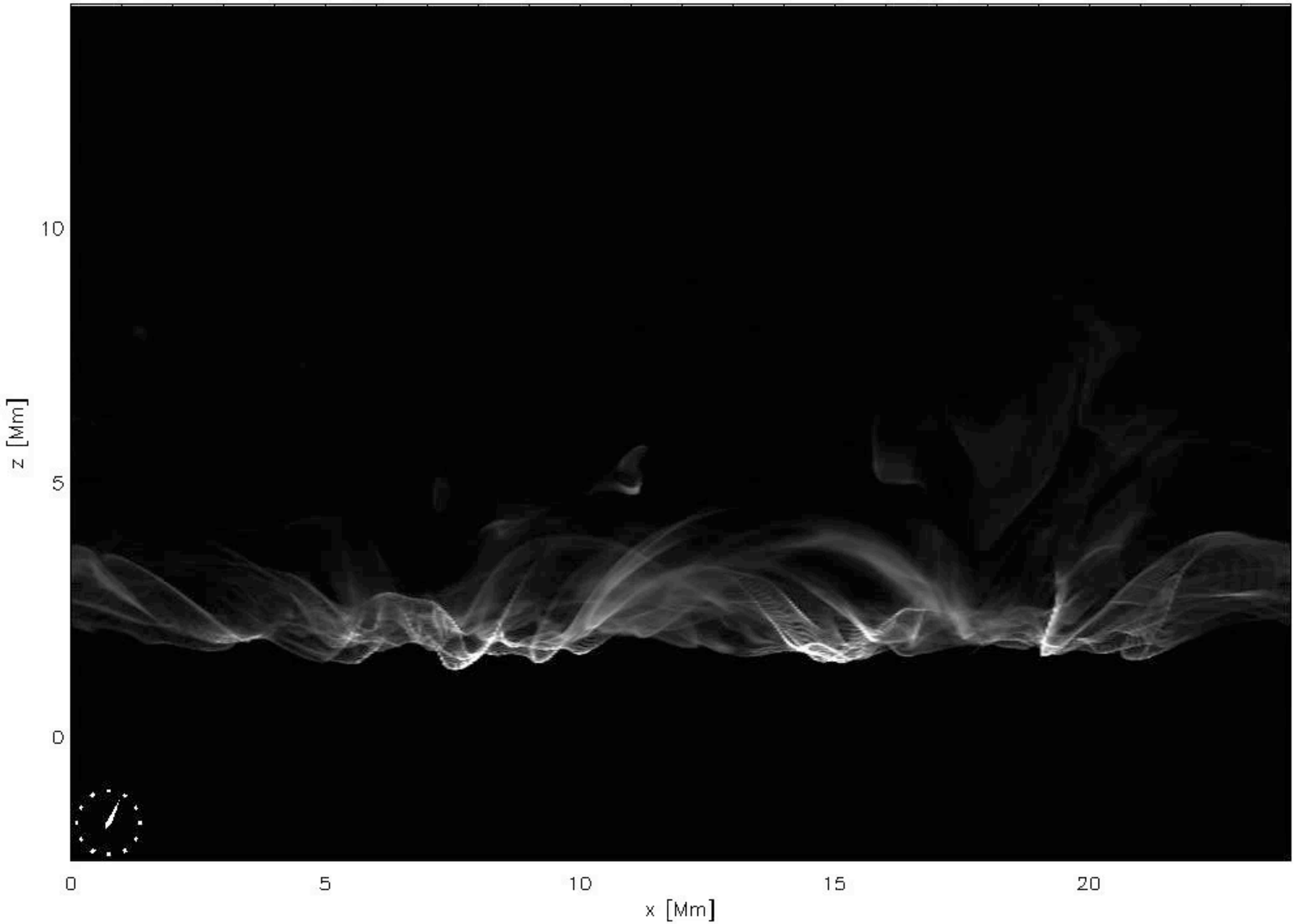
10
5
0
z [Mm]
0
5
10
15
20
x [Mm]

BIFROST simulated Si IV 1393 Å emission

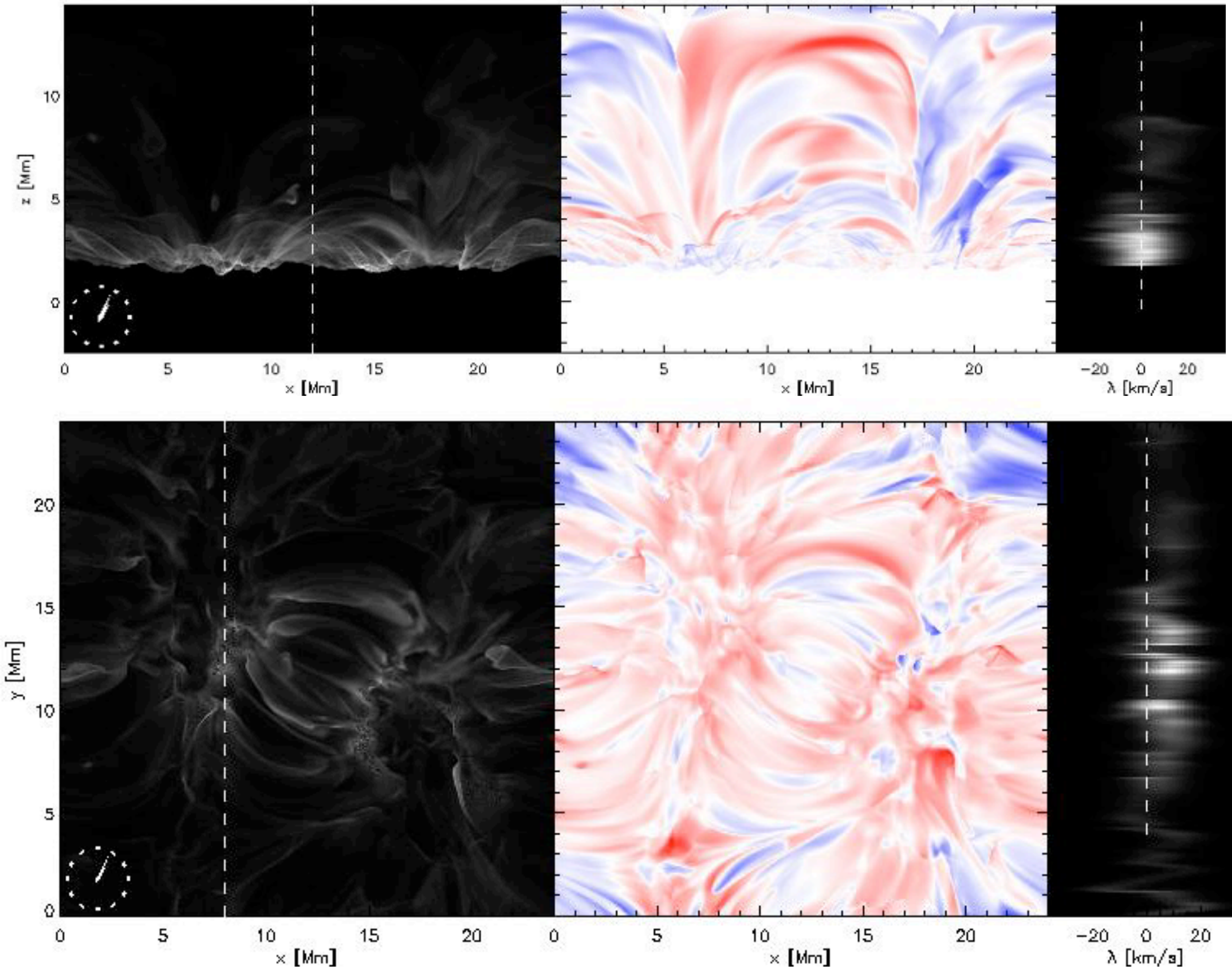

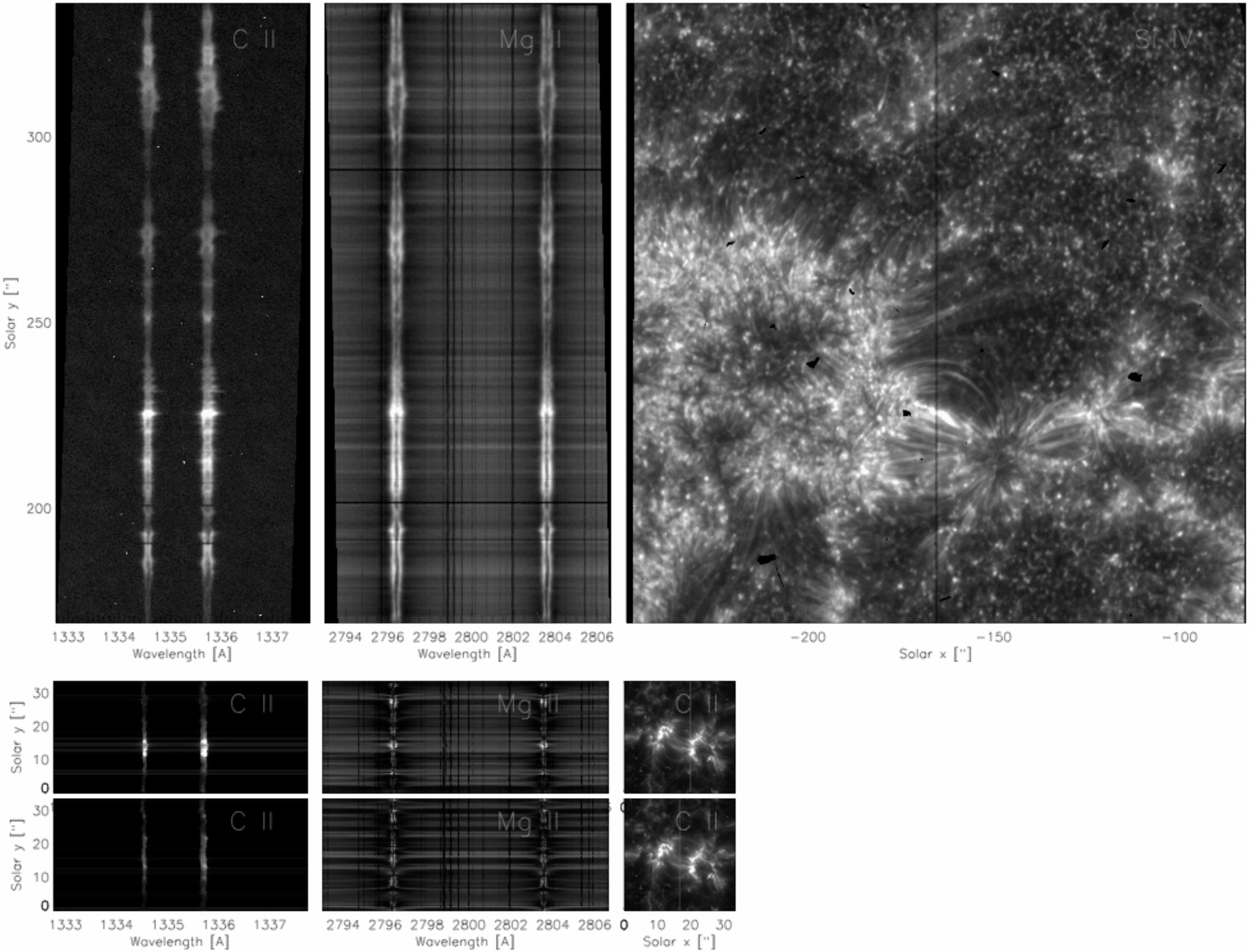
C II
Mg II
Si IV
Solar y ["]
300
250
200
1333 1334 1335 1336 1337
Wavelength [A]
2794 2796 2798 2800 2802 2804 2806
Wavelength [A]
−200
−150
−100
Solar x ["]
C II
Mg II
C II
Solar y ["]
30
20
10
0
C II
Mg II
C II
Solar y ["]
30
20
10
0
1333 1334 1335 1336 1337
Wavelength [A]
2794 2796 2798 2800 2802 2804 2806
Wavelength [A]
0 10 20 30
Solar x ["]

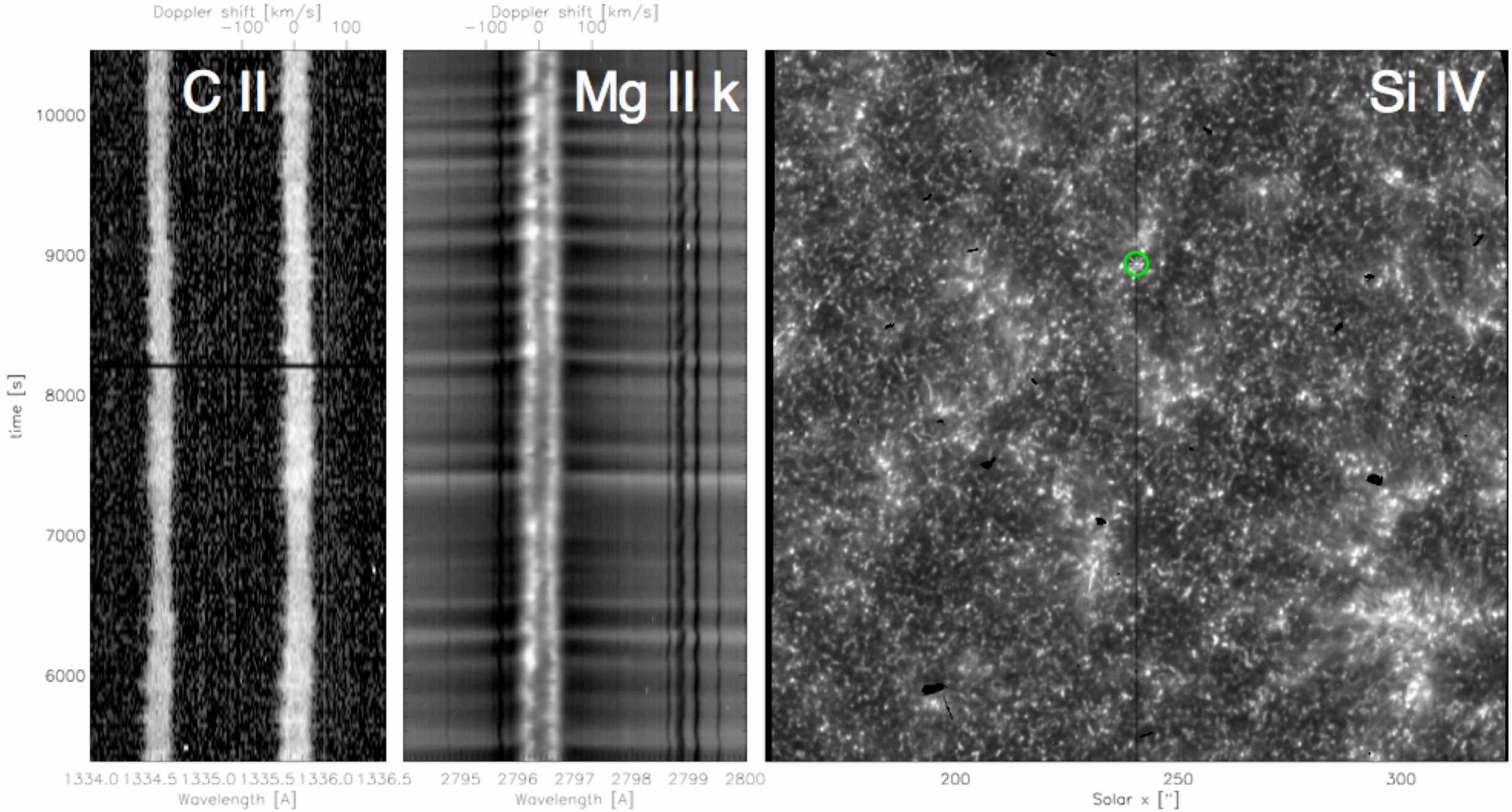
Doppler shift [km/s]
−100 0 100
C II
Mg II k
Si IV
time [s]
10000
9000
8000
7000
6000
1334.0 1334.5 1335.0 1335.5 1336.0 1336.5
Wavelength [A]
2795 2796 2797 2798 2799 2800
Wavelength [A]
200
250
300
Solar x ["]

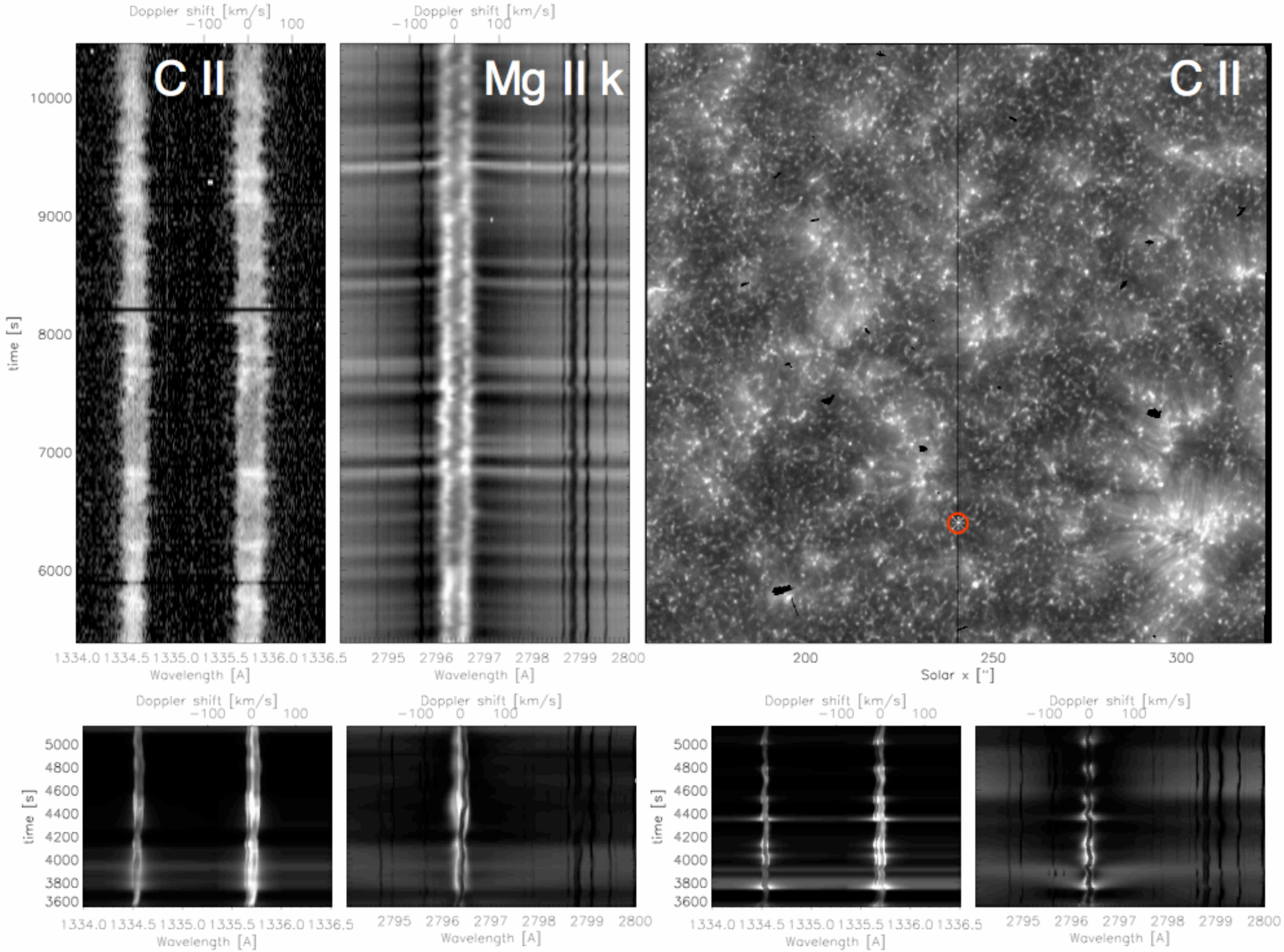
C II
Mg II k
C II
Doppler shift [km/s]
−100 0 100
time [s]
10000
9000
8000
7000
6000
5000
4800
4600
4400
4200
4000
3800
3600
1334.0 1334.5 1335.0 1335.5 1336.0 1336.5
2795 2796 2797 2798 2799 2800
Wavelength [A]
200
250
300
Solar x ["]

Differences simulations/reality

- simulations show narrower profiles and too little emission on average
- not enough small scale dynamics in simulations - need higher resolution + ion-neutral effects + ?
- not enough chromospheric heating - lacking small scale magnetic field + ion-neutral effects + ?

MULTI

MULTI

http://folk.uio.no/matsc/mul23

- 1D
- Statistical equilibrium
- given atmosphere {T, Ne, Vz, Vmic}(x)
- one element at a time
- continuum opacity in LTE
- Complete Redistribution
- Hydrostatic equilibrium can be solved for

MULTI documentation

in http://folk.uio.no/matsc/mul23

multi_manual.pdf	quick start manual
report33.pdf	version 1.0 documentation
mul23.pdf	version 2.3 documentation
idldoc.pdf	IDL routines documentation
multi_exercises.pdf	exercises

MULTI

Input files

ATMOS	atmospheric structure
DSCALE	depth discretization
ABUND	abundances
ABSDAT	background opacities
ATOM	atomic data
INPUT	switches, run-parameters

Output

IDL files
JOBLOG
OUT

ATMOS

```
  VAL3C
  MASS SCALE
*
* LG G
  4.44
*
* NDEP
  52
*
*LG CMASS          TEMPERATURE        NE              V               VTURB
  -5.279262E+00   4.470000E+05   1.205000E+09   0.              1.128000E+01
  -5.270430E+00   1.410000E+05   3.839000E+09   0.              9.870000E+00
  -5.269783E+00   8.910000E+04   5.961000E+09   0.              9.820000E+00
  -5.268492E+00   5.000000E+04   9.993000E+09   0.              9.760000E+00
...
*
*  HYDROGEN POPULATIONS
*  NH(1)         NH(2)         NH(3)         NH(4)         NH(5)         NP
   2.3841E+03   7.9839E-04   2.0919E-04   2.3110E-04   2.9470E-04   1.0030E+09
   5.3401E+04   1.8790E-02   7.4560E-03   8.1751E-03   1.0430E-02   3.1990E+09
   2.4030E+05   7.5740E-02   2.9400E-02   3.1550E-02   4.0101E-02   5.0310E+09
...
```

DSCALE

```
* DEPTH SCALE FROM DSCAL2
 DSCAL2 ON equidistant
 MASS SCALE
* NDEP     lg(Tau_500[1])
  80       -6.672232
      -5.225000
      -5.213486
```

...

ABUND

```
H    1.000E+00
HE   1.000E-01
SI   3.548E-05        from Grevesse 1989
MG   3.802E-05        from Grevesse 1989
AL   2.951E-06        from Grevesse 1989
FE   4.677E-05        from Grevesse 1989
C    3.631E-04        from Grevesse 1989
NA   1.514E-06
S    1.622E-05
K    1.122E-07
CA   2.138E-06
NI   1.202E-07
CR   2.951E-07
N    8.511E-05
O    5.888E-04
NE   3.236E-04
SC   1.259e-09        from Grevesse 1989
TI   9.772e-08        from Grevesse 1989
V    1.000e-08        from Grevesse 1989
MN   2.455e-07        from Grevesse 1989
CO   8.318e-08        from Grevesse 1989
```

ABUND

```
H    12.00     abundances from
HE   10.93     Asplund, Grevesse, Sauval, Scott 2009, ARAA 47, 481
SI    7.51
MG    7.60
AL    6.45
FE    7.50
C     8.43
NA    6.24
S     7.12
K     5.03
CA    6.34
NI    6.22
CR    5.64
N     7.83
O     8.69
NE    7.93
SC    3.15
TI    4.95
V     3.93
MN    5.43
CO    4.99
```

ABSDAT

```
         21
H   HE C   N   O   NE NA MG AL SI S   K   CA SC TI V   CR MN FE CO NI
      1.008      4.003      12.01      14.01      16.00      20.18
      23.00      24.32      26.97      28.06      32.06      39.10
      40.08      45.0       47.9       50.9       52.01      54.9
      55.85      58.9       58.69
     2     3     4     4     4     4     4     4     4     4     4     4
     4     4     4     4     4     4     4     4     4
     2     1
H I
13.595   2 11.0    2
H I
...
/CA II 3P6 4S 2SE       CA III GROUND TERM   P.JUDGE / COMPILATION
 2             0.000    2.0
   ILOGL=1   KVADL=0   MINEX=0   MAXEX=0  NLATB= 11
      510.      600.      750.      850.      950.      1000.
     1020.     1026.     1030.     1035.     1045.
   ILOGT=0   KVADT=0   MINET=0   MAXET=0  NTETB=  1   ITETA=0
 1.557E-19 1.836E-19 2.101E-19 2.183E-19 2.142E-19 2.122E-19
 2.101E-19 2.081E-19 2.060E-19 2.060E-19 2.040E-19
...
```

ATOM

```
CA II
* ABUND   AWGT
  6.36   40.08
*NK NLINE NCONT NRFIX
  6   5    5     0
*   E          G        LABEL                    ION
   0.00000   2.00000   'CA II 3P6 4S 2SE    '   2
 13650.248   4.00000   'CA II 3P6 3D 2DE 3/2'   2
 13710.900   6.00000   'CA II 3P6 3D 2DE 5/2'   2
 25191.535   2.00000   'CA II 3P6 4P 2PO 1/2'   2
 25414.465   4.00000   'CA II 3P6 4P 2PO 3/2'   2
 95785.470   1.00000   'CA III GROUND TERM  '   3
* J  I      F       NQ  QMAX  Q0 IW    GA       GVW      GS
  4  1  3.1600E-01 101  300.  3. 0  1.42E08  234.223  3.0E-06
  5  1  6.3700E-01 101  300.  3. 0  1.46E08  234.223  3.0E-06
  4  2  4.7300E-02 101  150.  1. 0  1.42E08    2.04   3.0E-06
  5  2  9.6000E-03 101  150.  1. 0  1.46E08    2.01   3.0E-06
  5  3  5.7400E-02 101  150.  1. 0  1.46E08    2.01   3.0E-06
* UP  LO   F       NQ   QMAX    Q0
   6  1  2.036E-19  5   -1.     0.0
  1044.2   2.0360E-19
   911.7   2.1400E-19
   850.0   2.1720E-19
   750.0   2.1030E-19
   600.0   1.8200E-19
*
...
 GENCOL
 TEMP
  7     2000.     3000.     6000.    12000.    24000.    48000.    96000.
OHMEGA
  2  1  5.60e+00  5.60e+00  5.60e+00  5.60e+00  5.60e+00  5.60e+00  5.60e+00
OHMEGA
...
```

INPUT

```
DIFF=2.0,ELIM1=0.1,ELIM2=0.001,QNORM=12.85,THIN=0.1,
IATOM2=0,ICONV=1,IHSE=0,ILAMBD=2,IOPAC=1,ISTART=1,ISUM=0,
ITMAX=40,ITRAN=0,NMU=5,
IWABND=0,IWATMS=0,IWATOM=0,IWCHAN=0,IWDAMP=0,IWEMAX=1,IWEQW=0,
IWEVEC=0,IWHEAD=0,IWHSE=0,IWLGMX=1,IWLINE=0,IWLTE=0,IWN=0,IWNIIT=0,
IWOPAC=0,IWRAD=0,IWRATE=0,IWSTRT=0,IWTAUQ=0,IWTEST=0,IWWMAT=0,
IWJFIX=0,IWARN=0,IOPACL=0,ISCAT=0,INCRAD=0,INGACC=0,ICRSW=0,
IOSMET=0,EOSMET=0.5,
IDL1=1,IDLNY=1,IDLCNT=1,IDLOPC=1
```

Working with IRIS data

http://iris.lmsal.com

INTERFACE REGION IMAGING SPECTROGRAPH

Current News

- **9 December 2013:** IRIS-related numerical models (Bifrost) now available
- **2 December 2013:** IRIS mission/instrument paper now available
- **31 October 2013:** Calibrated level 2 data now available:
  - See our Press page for details.
  - Find the data at LMSAL or at University of Oslo
  - Technical documentation updated and available
  - IRIS Today page available

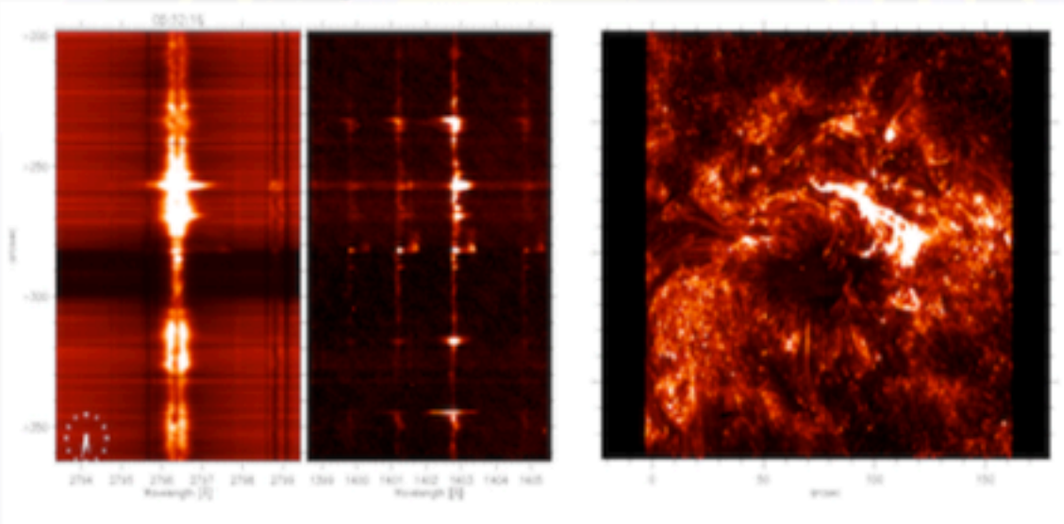

Previous IRIS News

- **1 October 2013:** Quicklook slit-jaw movies available
- **24 July 2013:** First Light Press Release

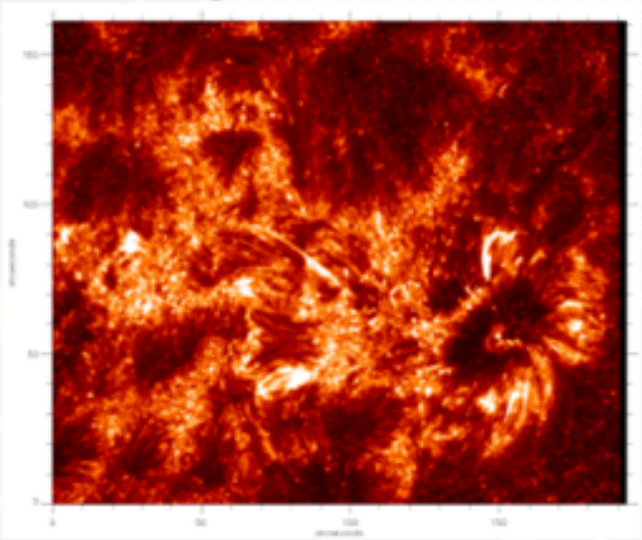

- 27 June 2013: IRIS launched

- 19 June 2009: NASA announces selection of IRIS.

IRIS mission/instrument paper

Operations/Planning

ITN 1 - IRIS Operations Overview
ITN 2 - Manual for Table Creator
ITN 3 - Manual for Timeline Tool
ITN 4 - Manual for Synthetic Observations Tool
ITN 5 - Operations Under Roll Conditions
ITN 6 - AEC Operations
ITN 7 - Compression Approach
ITN 8 - Checklist for IRIS planner
ITN 9 - Periodic Calibration Activities

Data Flow

ITN 10 - General Approach to Data Flow and Archiving
ITN 11 - Definition of Data Levels
ITN 12 - Definition of Keywords
ITN 13 - VSO and IRIS

Calibration

ITN 14 - Dark Current/Offset
ITN 15 - Despiking
ITN 16 - Flat-field
ITN 19 - Geometric Calibration
ITN 20 - Wavelength Calibration
ITN 21 - Recasting into Level 2/3 Data
ITN 22 - Co-alignment, Plate Scale Analysis
ITN 23 - MTF/PSF Determination
ITN 24 - Stellar Calibration
ITN 25 - Gain Determination

Data Analysis

ITN 26 - User Guide To Data Analysis
ITN 27 - Quicklook Tools Manual
ITN 28 - IRIS IDL Data Structure
ITN 29 - Deconvolution Approach
ITN 30 - 60 Day Observing Plan
ITN 31 - IRIS science planning: tables, linelists, targets
SolarSoft Tree and UVSP Database

Numerical Modeling

ITN 33 - General Overview of Numerical Simulations
ITN 34 - Numerical Simulations Quicklook Tools
ITN 35 - Numerical Simulations Synthetic Observables
ITN 36 - RH 1.5 D Manual
ITN 37 - How to Derive Physical Information from Mg II h/k

IRIS Technical Notes List (ITN)

Talks & Posters

Invited Talks at the SDO-4/IRIS/Hinode Workshop - March 2012
IRIS Talk Hinode 5 Meeting Keynote (430 MB) PDF (36 MB)
IRIS Poster
FUV Camera View
NUV Camera View

Concept Study Report

Executive Summary
Science Goals
Instrument Description

Operations

Table Creator
Timeline

Simulator

- IDL code
- Data (large)
- Data (small)

Calibration / Data production

Level 1.5: iris_prep.pro
Level 2: iris_level1to2.pro
Level 3: iris_make_fits_level3.pro

Quicklook

Level 2: iris_xfiles.pro
Level 3: crispex.pro

Simulations

Quicklook: br_xmhd.pro
Radiative Transfer: Multi3d
Radiative Transfer: RH 1.5d (please acknowledge Han Uitenbroek and Tiago Pereira)

Documentation

ITN 33 - General Overview of Numerical Simulations
ITN 34 - Numerical Simulations Quicklook Tools
ITN 35 - Numerical Simulations Synthetic Observables
ITN 36 - RH 1.5 D Manual
ITN 37 - How to Derive Physical Information from Mg II h/k

Bug Tracking

LMSAL DAI Tool (IRIS team only)

A User's Guide To IRIS Data Retrieval, Reduction & Analysis

Tuesday, February 25, 2014

Scott W. McIntosh
(mscott@ucar.edu)

Bart De Pontieu
(bdp@lmsal.com)

Viggo Hansteen
(viggo.hansteen@astro.uio.no)

Mats Carlsson
(mats.carlsson@astro.uio.no)

Paul Boerner
(boerner@lmsal.com)

This guide will evolve and be frequently updated, especially during the early phases of the mission. Please visit IRIS Technical Note 26 frequently for updated PDF files. Email Scott McIntosh with questions and changes and we will respond as fast as possible.

The IRIS solarsoft tree is frequently updated by the science team. We strongly recommend that the user keeps a current version of the software tree on their local machine (or systemwide installation). Execute the following command from inside the solarsoft IDL session:

```
IDL> ssw_upgrade, /spawn, /passive, /iris
```

10/15/2013 - see the IRIS known data issues section.

Public release of Bifrost simulations

“enhanced network” simulation

http://sdc.uio.no/search/simulations

IRIS Technical Note 33; Carlsson et al 2014

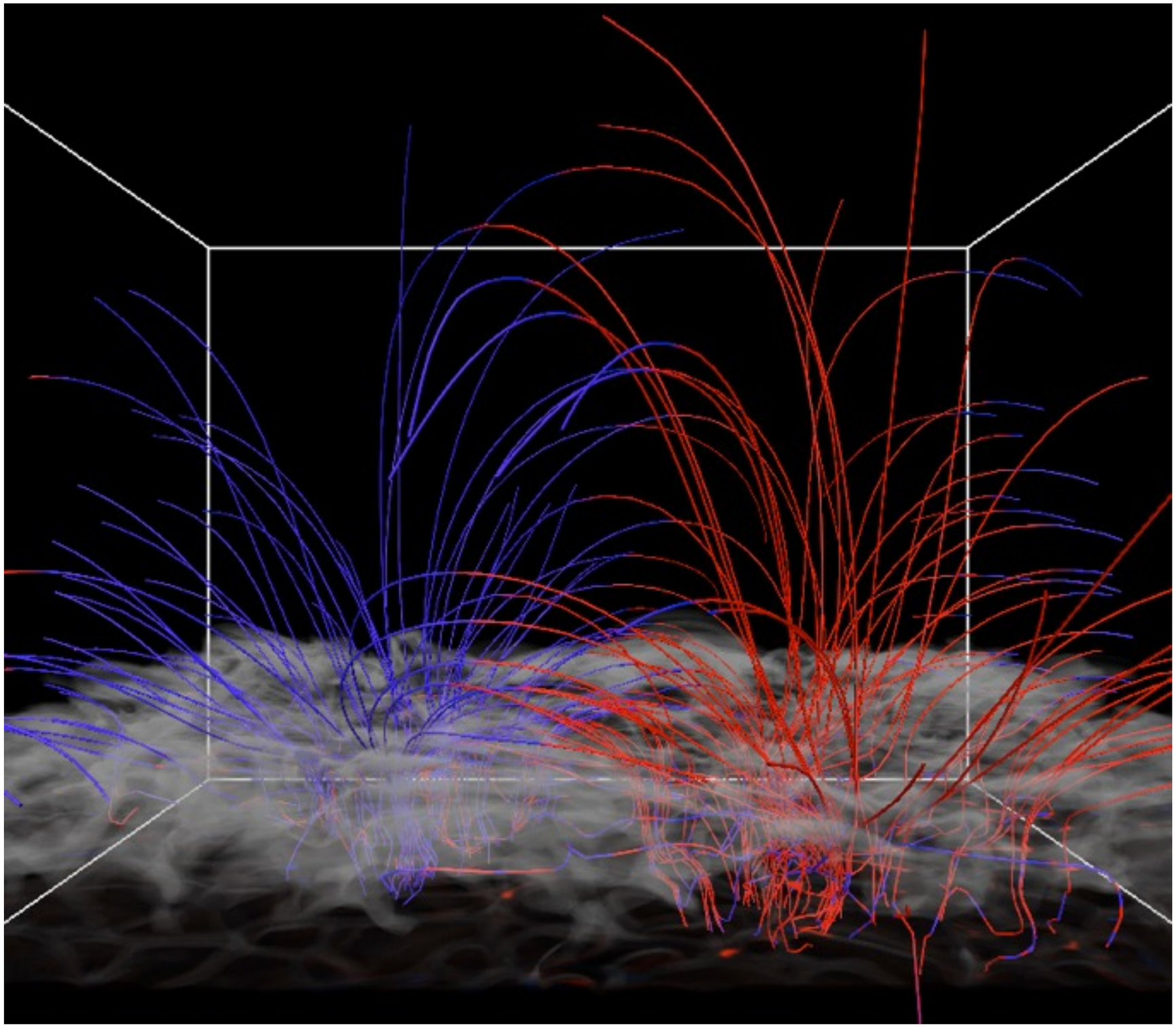

Corona

Transition region

Chromosphere

Photosphere

Convection zone

Bifrost coordinate system

Variables on staggered grid

Internal units (Mm, hs, 10^{-7} g cm^{-3}, Mm/hs etc)

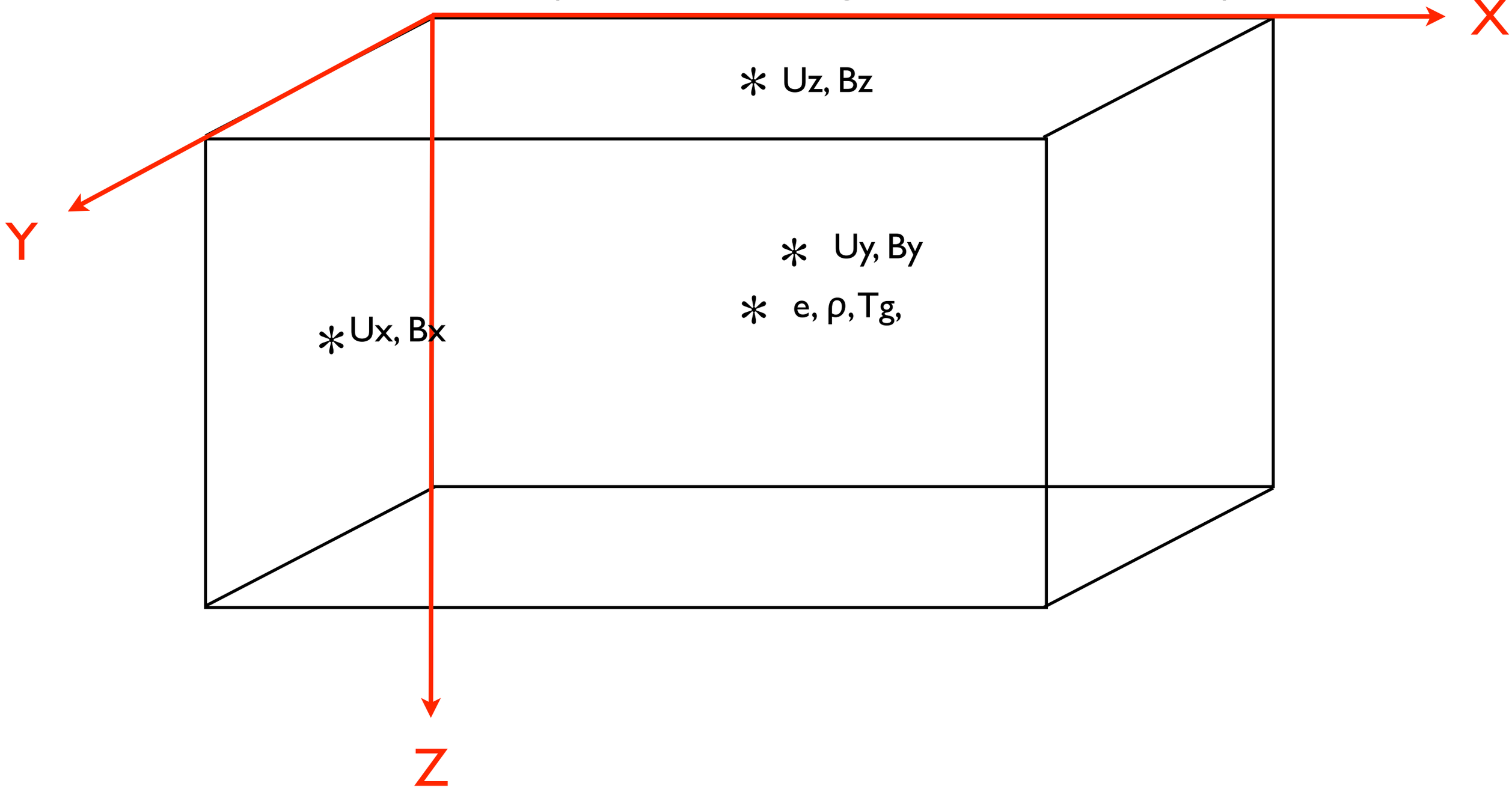

FITS files

Variables all cell centered

SI units (Mm, s, kg m^{-3}, m/s, T, etc)

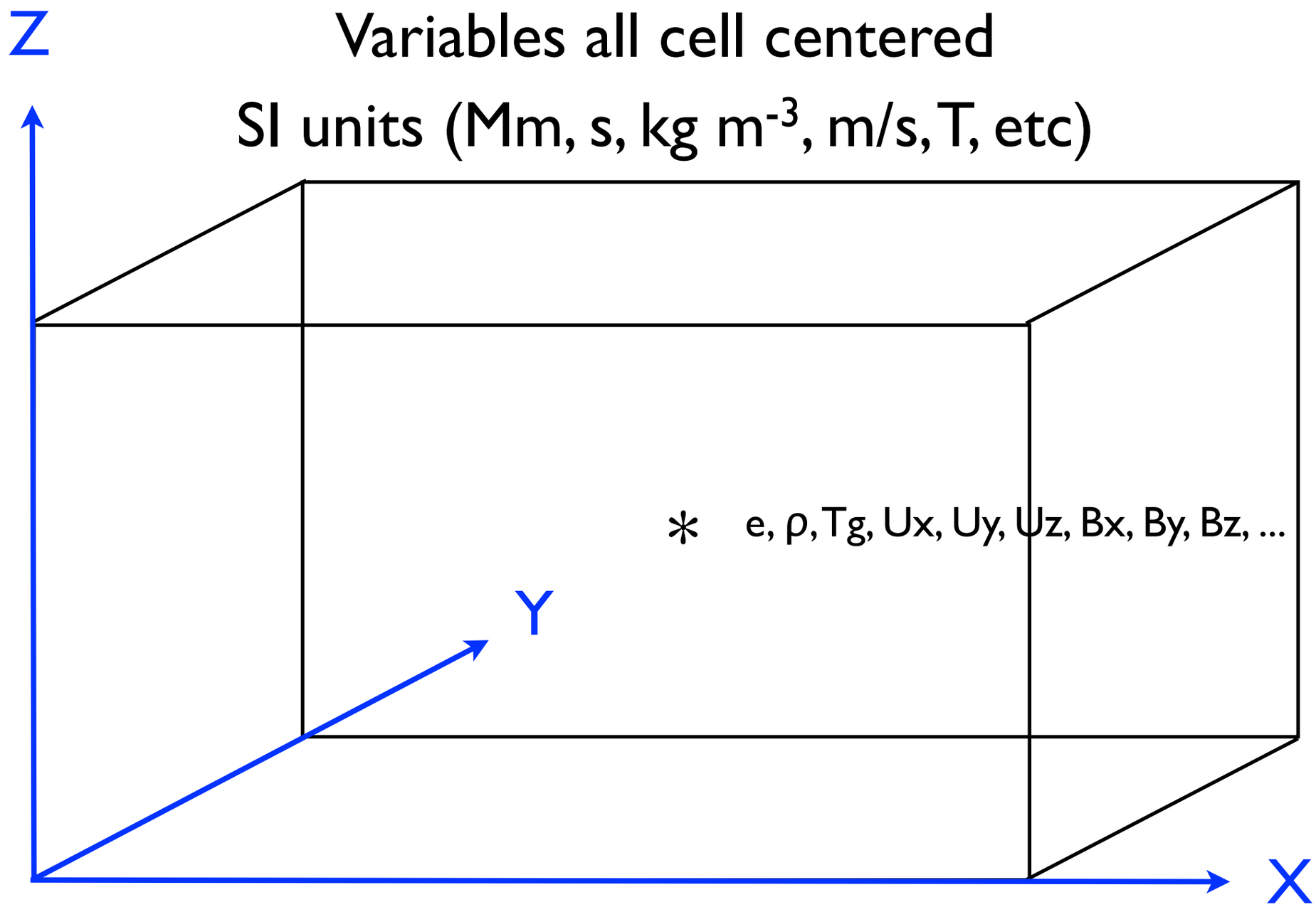

Format

- Level 2: D(x,y,z) one file per variable per timestep (481 MB)
- Level 3: D(x,y,z,t) one file per variable (76 GB)
- Level 2 → Level 3 with provided SW
- Level 3 transpose (D(z,t,x,y)) with provided SW

```
it=385+indgen(157)
br_make_fits_level3,‘en024048_hion’,it,‘lgtg’
br_transpose_fits_level3,‘BIFROST_en024048_hion_lgtg_im.fits’
```

Variables

- e, Ux, Uy, Uz, ρ, Bx, By, Bz
- Tg, Pg, Ne

en024048_hion: 831 GB

FITS

BIFROST_en024048_hion_lgtg_385.fits

```
SIMPLE  =                    T / Written by IDL:  Fri Jul 12 22:13:21 2013
BITPIX  =                  -32 / Number of bits per data pixel
NAXIS   =                    3 / Number of data axes
NAXIS1  =                  504 /
NAXIS2  =                  504 /
NAXIS3  =                  496 /
EXTEND  =                    T / FITS data may contain extensions
INSTRUME= 'Bifrost '           / Data generated by the Bifrost code
OBJECT  = 'en024048_hion'      / Bifrost run name
BTYPE   = 'lg(tg)  '           / Data variable
BUNIT   = 'K       '           / Data unit
CDELT1  =            0.0476190 / [Mm] x-coordinate increment
CDELT2  =            0.0476190 / [Mm] y-coordinate increment
CDELT3  =            0.0971498 / [Mm] (non-uniform) z-coordinate increment
CRPIX1  =                    1 / Reference pixel x-coordinate
CRPIX2  =                    1 / Reference pixel y-coordinate
CRPIX3  =                    1 / Reference pixel z-coordinate
CRVAL1  =              0.00000 / [Mm] Position ref-pixel x-coordinate
CRVAL2  =              0.00000 / [Mm] Position ref-pixel y-coordinate
CRVAL3  =             -2.44401 / [Mm] Position ref-pixel z-coordinate
CTYPE1  = 'x       '           / [Mm] Label for x-coordinate
CTYPE2  = 'y       '           / [Mm] Label for y-coordinate
CTYPE3  = 'z       '           / [Mm] Label for z-coordinate
CUNIT1  = 'Mm      '           / Unit for x-coordinate
CUNIT2  = 'Mm      '           / Unit for y-coordinate
CUNIT3  = 'Mm      '           / Unit for z-coordinate
RUNID   = 'Bifrost_cb24bih'    / Run ID for identification of input files
ELAPSED =              3850.00 / [s] Time of snapshot
DATA_LEV=                    2 / Data level
ZTAU51  =            0.0613866 / [Mm] Average height of tau(500nm)=1
ORIGIN  = ' ITA/Oslo'          / Origin of data
COMMENT Variables from .idl file:
...
```

Documents

- Paper describing simulation characteristics (in prep)
- ITN 33 giving technical details
  - format, keywords, auxiliary software

Enhanced network

en024048_hion (1600s)

- 24x24x17 Mm (2.5 Mm below, 14.5 Mm above z=0)
- 504x504x496 grid
- 48 km horizontal, 19-97 km vertical
- polarities separated by 8 Mm
- <|B|>=30-50 G

http:sdc.uio.no/search/simulations

Radiative transfer products

- NUV passband
  - Mg II h&k + background lines
  - 252 x 252 grid, vertical rays
  - FITS files
    - intensity as function of wavelength
    - $z(\tau_\nu=1)$ as function of wavelength

- ITN 35 describes format, approximations etc

New models

- Higher resolution: 48, 31, 16 km
- Coronal hole at 31 km resolution
- Salt-and-pepper field
- flux emergence
- generalized Ohm's law
- larger Box, small active region